A framework for modelling the interactions between biochemical reactions and inorganic ionic reactions in aqueous systems

Christopher John Brouckaert

BSc (Chemical Engineering) University of Natal

Submitted in fulfilment of the academic requirements
for the PhD degree in Chemical Engineering
in the School of Engineering at the University of KwaZulu-Natal.

May 2022

DEDICATION

This work is dedicated to my friends and colleagues
who made it possible through their support over many years:

Chris Buckley and George Ekama

and to my co-authors:

George Ekama (again)
Barbara Brouckaert
David Ikumi.

ACKNOWLEDGMENTS

DECLARATION - PLAGIARISM

I, Christopher John Brouckaert, declare that:

1. The research reported in this dissertation, except where otherwise indicated, is my original research.
2. This dissertation has not been submitted for any degree or examination at any other university.
3. This dissertation does not contain other persons' data, pictures, graphs or other information, unless specifically acknowledged as being sourced from other persons.
4. 4. This dissertation does not contain other persons' writing, unless specifically acknowledged as being sourced from other researchers. Where other written sources have been quoted, then:
   a. Their words have been re-written, but the general information attributed to them has been referenced
   b. Where their exact words have been used, then their writing has been placed in italics
   c. and inside quotation marks and referenced.
5. This dissertation does not contain text, graphics or tables copied and pasted from the Internet, unless specifically acknowledged, and the source being detailed in the dissertation and in the References sections.
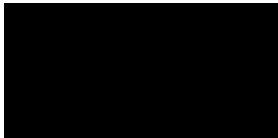
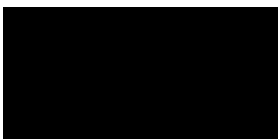Signed: ███████████   Date: 7 May 2022

COLLEGE OF AGRICULTURE, ENGINEERING AND SCIENCE

DECLARATION

The research described in this thesis was conducted at the University of KwaZulu-Natal under the supervision of Prof. David Lokhat.
I hereby declare that all the materials incorporated in this thesis are my own original work except where acknowledgement is made by name or in the form of a reference. The work contained herein has not been submitted in part or whole for a degree at any other university.
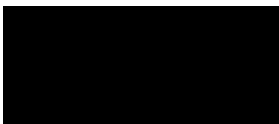
Signed: ▮▮▮▮▮▮▮   Date: 7 May 2022

As the candidate's Supervisor I have approved this dissertation for submission

Signed: ▮▮▮▮▮▮▮   Date: 10/05/2022

Abstract

Bio-processes interact with the aqueous environment in which they take place. Integrated bio-process and three-phase (aqueous–gas–solid) multiple strong and weak acid/base system models are being developed for a range of wastewater treatment applications, including anaerobic digestion, biological sulphate reduction, autotrophic denitrification, biological desulphurization and plant-wide wastewater treatment systems. In order to model, measure and control such integrated systems, a thorough understanding of the interaction between the bio-processes and aqueous-phase multiple strong and weak acid/bases is required.

This thesis is based on a series of five papers that were published in Water SA during 2021 and 2022. Chapter 2 (Part 1 of the series) sets out a conceptual framework and a methodology for deriving bio-process stoichiometric equations. It also introduces the relationship between alkalinity changes in bioprocesses and the underlying reaction stoichiometry, which is a key theme of the series.

Chapter 3 (part 2 of the series) presents the stoichiometric equations of the major biological processes and shows how their structure can be analysed to provide insight into how bioprocesses interact with the aqueous environment. Such insight is essential for confident, effective and reliable use of model development protocols and algorithms.

Where aqueous ionic chemistry is combined with biological chemistry in a bioprocess model, it is advantageous to deal with the very fast ionic reactions in an equilibrium sub-model. Chapter 4 (part 5 of the series) presents details of how of such an equilibrium speciation sub-model can be implemented, based on well-known open-source aqueous chemistry models. Specific characteristics of the speciation calculations which can be exploited to reduce the computational burden are highlighted. The approach is illustrated using the ionic equilibrium sub-model of a plant-wide wastewater treatment model as an example.

Provided that the correct measurements are made that can quantify the material content of the bioprocess products (outputs), the material content of the bioprocess reactants (inputs) can be determined from the bioprocess products via stoichiometry. The links between the modelling and measurement frameworks, which use summary measures such as chemical oxygen demand (COD) and alkalinity, are described in parts 3 and 4 of the series, which are included as appendices to the thesis.

An additional paper, presenting case study on modelling an auto-thermal aerobic bio-reactor, is included as a third appendix, as it demonstrates the application of some of the principles developed in the series of papers.

TABLE OF CONTENTS

Chapter 3: Integration of complete elemental mass balanced stoichiometry and aqueous phase chemistry for bioprocess modelling of liquid and solid waste treatment systems – Part 2: Bioprocess stoichiometry ……………………………………………………………………33

Chapter 1: Introduction

The use of a consistent and comprehensive physicochemical framework for models simulating bio-processes was emphasised by Batstone et. al (2012). This is true for the initial development of such a model, and becomes even more important when the model is maintained and extended by multiple contributors, such as research students. This kind of evolutionary development is prone to introducing subtle, and sometimes not so subtle, inconsistencies, as each new extension tends to focus narrowly on a specific phenomenon.

The dissertation is based on series of 5 papers, published in Water SA, issues 47(3) (2021) and 48(1) (2022) (see https://www.watersa.net/), that set out a framework and methodology for the mathematical modelling of bio-processes that have significant interactions with inorganic aqueous physicochemical processes. The papers represent a distillation of modelling experience of the Water Research Group (WRG) at the University of Cape Town and the Pollution Research Group (now the WASH R&D Centre) at the University of KwaZulu-Natal, over some 15 years of collaboration. Wastewater treatment modelling was pioneered by the WRG much earlier; for example, see Dold et al. (1980). The principle outcome of this work has been the so-called PWM_SA model (Plant Wide Model – South Africa), and the 5 papers were conceived to document the underlying principles of the model, and of the laboratory methods that support its practical application. The PWM_SA model continues to have a major role in publications and theses, e.g. Botha (2015), Brouckaert et al. (2016), De Ketele et al. (2018), Gaszynski (2021), Ghoor (2019), Ikumi (2020), Ikumi et al. (2014), Ikumi et al. (2015a, 2015b), Logan (2015) and Tanyanyiwa (2020).

Part 1 outlines the general framework for constructing a bio-process/aquatic chemistry model, and introduces the fundamental building blocks: kinetics, equilibria, components, species, stoichiometry and alkalinity.

Part 2 considers how these concepts apply to most of the major reaction systems that are encountered in wastewater treatment processes.

Part 3 deals with methods for characterising complex organic material in a way that is compatible with a model.

Part 4 deals with measurement methods for characterising inorganic aqueous solutions for modelling purposes.

Part 5 deals with computational algorithms used by the models for equilibrium speciation of ionic solutions.

The academic dissertation is based on parts 1, 2 and 5, with parts 3 and 4 as appendices. This because the primary author of parts 3 and 4 was Prof George Ekama from UCT. He would have been the supervisor of this PhD, had he not suffered a stroke in December 2019 that ended his academic activities, and left his co-authors to complete the series of papers.

An earlier paper (Kay et al., 2019), on temperature transitions in an autothermal bio-reactor, is included as a third appendix, as it presents a case study demonstrating the application of the concepts developed in the main series of papers.

CONTRIBUTIONS OF THE AUTHORS

George Ekama conceived the idea of writing a series of papers to provide a comprehensive guide on developing and implementing simulation models of wastewater treatment processes in about 2012. At that time, he was guiding the research of a large group of students, mostly at UCT, but also at UKZN and other universities around the world, notably Hong Kong. Much of this work was based on the PWM_SA model, which was primarily developed for conventional wastewater treatment plants, with activated sludge and methanogenic anaerobic digestion, but was being extended to other processes such as sulphidogenic digestion.

David Ikumi was a member of the group of UCT students (now leader of the WRG), and was largely responsible for the coding and calibration of the biological aspects PWM_SA model, together with **Chris Brouckaert**, who was largely responsible for the aquatic chemistry aspects. The latter had become involved in the research after the retirement of Professor Richard Loewenthal from UCT, which left the WRG with significant gap in aquatic chemistry expertise.

The original plan was for a trilogy of papers, covering the aspects of bio-process stoichiometry, laboratory methods and aquatic chemistry speciation. However, as the writing progressed, with research continuing in parallel, the scope grew. A significant expansion resulted from a project funded by Water Research Commission (WRC) on *Integration of Aquatic Chemistry with Bio-process models*, with Chris Brouckaert and **Barbara Brouckaert** as principal researchers. This proposed a comprehensive conceptual framework for bio-process models, which became the basis for part 1; however, its thinking also propagated though all the subsequent papers. It also became clear that the laboratory techniques, which were also being extended by new research, fell into two distinct categories, addressing organic and inorganic characterisation. Thus, the trilogy grew into a "quintilogy".

This re-structuring was accompanied by a significant shift in conceptual perspective. The WRG is based in the Civil Engineering Department at UCT, and its members are predominantly civil engineers. Through long experience, they have become eminent experts in a specialised field of chemical reaction engineering and reactor design. However, with the exception of a few post-graduate students over the years, none has had the benefit of training in the fundamentals of reaction engineering, as taught in undergraduate chemical engineering courses. As a result, many of their very deep insights into biological treatment processes have been expressed in idiosyncratic terms, which have much more compact, systematic and elegant counterparts in classical reaction engineering.

Barbara Brouckaert acted as the scientific editor of the series, although she also contributed summaries of case studies that she had undertaken in previous projects. She was largely responsible for checking the distribution and linking of material between the five papers. A conceptual framework has many forward and backward links between its elements, which are difficult to capture in a purely sequential

narrative. In many places a reader needs at least a rudimentary understanding of a topic, described fully elsewhere in the sequence.

Chris Brouckaert was the primary author of parts 1 and 5. The origin of part 2 was more involved. Its first version (March 2016) was written by George Ekama, in a monumental form that could not be published in a journal. It consisted of 62 pages of text, plus a further 22 pages containing 29 tables of stoichiometric reactions: 84 pages in all. This was the prime example of a chemical engineering topic conceived without the benefit of basic chemical reaction engineering. The final version, rewritten by Chris Brouckaert and published in 2021, has 20 pages in total, including 4 tables and 5 figures. No conceptual material was sacrificed to achieve this compression; the 4 tables contain the same essential information as the original 29. Indeed, an additional modelling case-study was carried out and included in the paper, to illustrate the application of the principles expounded in the text, as recommended by a reviewer. The approach to reaction stoichiometry was re-structured, and equations were re-derived in terms of the more compact set of *standard aquatic chemistry components*.

The treatment made extensive use of a novel concept, namely *alkalinity change of reaction*, which is useful for understanding and quantifying the effect of chemical and biological reactions on solution properties. The concept is novel in that, to the knowledge of the authors (and of Google), it does not appear in any previous literature. However, it is simply an instance of the standard stoichiometric concept of a *property change of reaction*. A related term, *exchanged electrons of reaction*, was also a novelty, but only in name. The same quantity was used, in the same way, by McCarty (1975), who called it *exchangeable electrons*, which conveys a less precise idea of its significance.

Chris Brouckaert was also the sole author of all the computational tools used in the preparation of the papers and related simulation models: the stoichiometry generator, the ionic speciation subroutines and the ionic speciation spreadsheet.

REFERENCES

BATSTONE DJ, AMERLINCK Y, EKAMA G, GOEL R, GRAU P, JOHNSON B, KAYA I, STEYER J-P, TAIT S, TAKÁCS I, VANROLLEGHEM PA, BROUCKAERT CJ and VOLKE E (2012) Towards a generalized physicochemical framework. *Water Science and Technology* 66 (6) 1147–1161. https://doi.org/10.2166/wst.2012.300

BOTHA RF (2015) Characterization of organics for anaerobic digestion by modelling augmented biological methane potential test results, MSc Thesis, University of Cape Town.

BROUCKAERT CJ, BROUCKAERT BM, SINGH A and WU W (2016) Wastewater treatment plant modelling for capacity estimation and risk assessment. *WRC Report TT678/16*. Water Research Commission, Pretoria, South Africa.

DE KETELE J, DAVISTER D and IKUMI DS (2018) Applying performance indices in plantwide for a comparative study of wastewater treatment plant operational strategies. *Water SA* 44(4) 539-550. http://dx.doi.org/10.4314/wsa.v44i4.03

DOLD PL, EKAMA GA and MARAIS GvR (1980) A general model for the activated sludge process. *Progress in Water Technology* 12 (6) 47–77. https://doi.org/10.1016/B978-1-4832-8438-5.50010-8

GASZYNSKI C (2021) Identification of wastewater primary sludge composition using augmented batch tests and mathematical models. PhD Thesis, University of Cape Town, South Africa.

GHOOR, T (2019) Developments in anaerobic digestion modelling. PhD Thesis, University of Cape Town, South Africa.

IKUMI DS (2020) Sensitivity analysis on a three-phase plant-wide water and resource recovery facility model for identification of significant parameters. *Water SA* 46(3) 476–492. https://doi.org.10.17159/wsa/2020.v46.i3.8658

IKUMI DS, HARDING TH and EKAMA GA (2014) Biodegradability of wastewater and activated sludge organics in anaerobic digestion. *Water Research* 56 267-279. https://doi.org/10.1016/j.watres.2014.02.008

IKUMI DS, HARDING TH, VOGTS M, LAKAY MT, MAFUNGWA HZ, BROUCKAERT CJ and EKAMA GA (2015a) Mass balances modelling over wastewater treatment plants III. *WRC Report No. 1822/1/14*. Water Research Commission, Pretoria, South Africa.

IKUMI DS, VOGTS M, EKAMA GA and BROUCKAERT CJ (2015b) Plant-wide modelling of N and P removal with aerobic and anoxic-aerobic digestion of waste sludge. Proc. IWA Watermatex 2015, Gold Coast, Australia, 14–17 June 2015.

KAY LG, BROUCKAERT CJ and SINDALL RC (2019) Modelling mesophilic-thermophilic temperature transitions experienced by an aerobic membrane bioreactor treating furfural plant effluent. *Water SA* 45(3) 317- 328. https://doi.org/10.17159/wsa/2019.v45.i3.6711

KAY LG, BROUCKAERT CJ and SINDALL RC (2019) Modelling mesophilic-thermophilic temperature transitions experienced by an aerobic membrane bioreactor treating furfural plant effluent. *Water SA* 45(3) 317- 328. https://doi.org/10.17159/wsa/2019.v45.i3.6711

LOGAN DH (2015) Co-digestion of Municipal Sewage Sludge with High Strength Industrial Effluents. MScEng Thesis. University of KwaZulu-Natal, Durban, South Africa.

MCCARTY PL (1975) Stoichiometry of biological reactions. *Progress in Water Technology* 7 (1) 157–172.

TANYANYIWA IT (2020) Co-digestion of industrial and domestic wastewater. MScEng Thesis. University of KwaZulu-Natal, Durban, South Africa.

Chapter 2: Integration of complete elemental mass-balanced stoichiometry and aqueous-phase chemistry for bio-process modelling of liquid and solid waste treatment systems – Part 1: The physico-chemical framework

CJ Brouckaert[1], BM Brouckaert[1] and GA Ekama[2]

[1]Water, Sanitation and Health Research and Development Centre, School of Engineering, University of KwaZulu-Natal, Durban, 4041, South Africa

[2]Water Research Group, Department of Civil Engineering, University of Cape Town, Rondebosch, 7700, South Africa

ABSTRACT
Bio-processes interact with the aqueous environment in which they take place. Currently integrated bio-process and three-phase (aqueous–gas–solid) multiple strong and weak acid/base system models are being developed for a range of wastewater treatment applications, including anaerobic digestion, biological sulphate reduction, autotrophic denitrification, biological desulphurization and plant-wide wastewater treatment systems. In order to model, measure and control such integrated systems, a thorough understanding of the interaction between the bio-processes and aqueous-phase multiple strong and weak acid/bases is required. This first in a series of five papers sets out a conceptual framework and methodology for deriving bio-process stoichiometric equations. It also introduces the relationship between alkalinity changes in bioprocesses and the underlying reaction stoichiometry, which is a key theme of the series. The second paper develops the stoichiometric equations for the main biological transformations that are important in wastewater treatment. The link between the modelling and measurement frameworks, which uses summary measures such as chemical oxygen demand (COD) and alkalinity, is described in the third and fourth papers. The fifth paper describes an equilibrium aquatic speciation algorithm which can be combined with bio-process stoichiometry to provide integrated models of wastewater treatment processes.

ABBREVIATIONS

AD	anaerobic digestion
ADM1	Anaerobic Digestion Model 1
AS	activated sludge
ASM	activated sludge models
COD	chemical oxygen demand
OP	ortho phosphate

SYMBOLS

Alk_{ed}	direct alkalinity of the electron donor component
Alk_p	persistent alkalinity of the electron donor component (Alk_{ed} + ΔAlk_T)
Alk_T	total alkalinity in solution
ΔAlk_T	total alkalinity change of reaction
a	molar content of nitrogen in $C_xH_yO_zN_aP_bS_c{}^{ch}$ electron donor
b	molar content of phosphorus in $C_xH_yO_zN_aP_bS_c{}^{ch}$ electron donor
c	molar content of sulphur in $C_xH_yO_zN_aP_bS_c{}^{ch}$ electron donor
ch	charge of $C_xH_yO_zN_aP_bS_c{}^{ch}$ electron donor
$C_xH_yO_zN_aP_bS_c{}^{ch}$	generalized electron donor formula
$C_kH_lO_mN_nP_pS_s$	generalized biomass formula
E	elemental content matrix
EA	augmented elemental content matrix
l	molar content of hydrogen in $C_kH_lO_mN_nP_pS_s$ biomass
m	molar content of oxygen in $C_kH_lO_mN_nP_pS_s$ biomass
n	molar content of nitrogen in $C_kH_lO_mN_nP_pS_s$ biomass
p	molar content of phosphorus in $C_kH_lO_mN_nP_pS_s$ biomass
s	molar content of sulphur in $C_kH_lO_mN_nP_pS_s$ biomass
x	molar content of carbon in $C_xH_yO_zN_aP_bS_c{}^{ch}$ electron donor
y	molar content of hydrogen in $C_xH_yO_zN_aP_bS_c{}^{ch}$ electron donor
Y	biomass yield coefficient
z	molar content of oxygen in $C_kH_lO_mN_nP_pS_s$ electron donor
γ_b	exchangeable electrons of biomass
γ_s	exchangeable electrons of the electron donor
v	stoichiometric coefficient vector
ρ	vector of right-hand-side terms of the element balance equations

INTRODUCTION

This is the first in a series of five papers that aim to set out a consistent approach to modelling biological processes involved in wastewater treatment.

The governing relationships of steady state and dynamic kinetic models of aerobic or anaerobic biological treatment systems fall into three major categories, viz.

- Continuity (mass, energy and momentum balances)
- Equilibria
- Kinetics

Although every reaction process is governed by all these relationships, models often do not explicitly take non-limiting factors into account. Thus, mass balances must always be included, but momentum and energy balances can often be left out (as in this series of papers). The situation with respect to kinetic and equilibrium relationships is more complex, because biochemical models usually represent a network of transformation processes, some of which may be kinetically limited, others equilibrium limited, and others mass-balance limited. Representing a biochemical reaction always involves a stoichiometric equation (mass balance) which may need to be coupled with a kinetic equation and/or equilibrium relationships. A number of models in the literature reflect a clear divide between kinetically controlled biological reactions (e.g. methanogenesis) that are far from equilibrium, and very fast acid/base reactions that are assumed to be at equilibrium (e.g. the dissociation of carbonic acid).

Early dynamic and steady-state models for the activated sludge (AS) system (Dold et al., 1980; WRC, 1984) considered only the bio-processes and comprised only the COD mass-balanced kinetically controlled transformations, as well as N (and P) mass balances, but omitted the C, H and O mass balances. The C balance was not included because most of the CO_2 produced is stripped out by the aeration system and it is assumed that its effect on the reactor pH can be neglected. Consequently, this model did not include speciation or pH prediction. Instead, the variable Alk tracked changes in alkalinity due to the removal and production of strong acids by the bio-processes, like nitrification and denitrification. A large decrease in Alk to below 50 mg/L as $CaCO_3$ was a flag that pH problems could arise in the reactor (WRC, 1984; Henze et al., 2008).

The importance of including weak acid/base chemistry in biological process models was discussed by Batstone et al. (2012). In anaerobic digestion (AD) models, the C-balanced stoichiometry and weak acid/base chemistry parts of models need to be included because the AD methanogens are very sensitive to pH, and the CO_2 and CH_4 gas produced establish a CO_2 partial pressure (p_{CO_2}) in the AD head space that, together with the aqueous phase alkalinity, establishes the AD pH (McCarty, 1975; Andrews and Graef, 1971; Speece, 2008; Sötemann et al., 2005a, b, c). Recently these developments in AD modelling have also been applied to activated sludge system models to enable the creation of plant-wide wastewater treatment models with complete CHONPS, charge and COD mass-balanced stoichiometry and three-phase (aqueous–gas–solid) mixed weak (and strong) acid/base chemistry to predict reactor (AD and AS) pH and mineral precipitation (Sötemann et al., 2005c; Takacs and Vanrolleghem, 2006; Grau et al., 2007; Brouckaert et al., 2010; Ikumi et al., 2011, 2014, 2015). How this integration is achieved in

different steady-state and dynamic bio-process aqueous phase models is the subject of this series of papers.

Ekama and co-workers (e.g. Sötemann et al., 2005b; Ekama, 2009; Poinapen and Ekama, 2010a; Lu et al., 2012) have developed a set of steady-state anaerobic digestion models in which the aquatic chemistry aspects are integrated into the model by expressing the stoichiometric biological half-reactions in terms of the dominant weak acid and base species expected to be present under particular conditions. The formulation of these half-reactions is based on the approach of McCarty (1975), and uses prior knowledge of the weak acid/base chemistry of the various biological treatment processes under typical operating conditions to determine which species to include. This results in a much simpler model that can be solved explicitly. Part 2 of this 5-part series develops this approach in detail (Brouckaert et al., 2021).

The disadvantage of this approach to predicting speciation is that it makes assumptions about the distribution of weak acid/base species that are only valid for a fairly narrow range of conditions (e.g. near-neutral pH). It is therefore not appropriate for dynamic scenarios and deviations from normal operating conditions, e.g., anaerobic digester failure. This is particularly an issue for anaerobic digestion, the performance of which is sensitive to pH fluctuations. Nevertheless, the steady-state models developed using this approach have important practical applications in design and capacity estimation, and understanding the chemistry on which they are based is critical in understanding the role of alkalinity in the design and control of biological processes. Therefore, it is important to understand both how these models work and their limitations.

These limitations have been addressed by various researchers in two different ways:

1. Musvoto et al. (2000a,b; Sötemann et al., 2005a,c; Poinapen and Ekama, 2010b) included dynamic equilibrium speciation equations (very fast forward and reverse reactions) as part of the kinetic structure of their anaerobic digestion model.
2. More recent models have tended to use algebraic algorithms to solve the weak acid/base chemistry and calculate the pH external to the kinetic model (IWA ADM1, Batstone et al., 2002; Serralta et al., 2004; Barat et al., 2011; Lizzaralde et al., 2015; Solon et al., 2015).

DEVELOPING A GENERALIZED APPROACH TO MODEL INTEGRATION

Batstone et al. (2012) argued that an incremental approach to incorporating aquatic chemistry into biochemical process models is inefficient. Modelling the interactions of inorganic aqueous components is a well-established discipline, with a comprehensive conceptual framework. They concluded that a similar framework should be developed for bio-process modelling that encompasses both the biochemical and inorganic aspects. However, the existing biological and inorganic modelling frameworks have different characters, which are shaped by their respective subject matter. An integrated framework obviously needs to reflect both.

Broadly speaking, inorganic aquatic chemistry models (e.g. MINTEQA2, PHREEQC, etc.) tend to be based on precise stoichiometry and thermodynamic data, whereas current biochemical models (e.g. ASM

series models, Henze et al., 2000) tend to be based on summary chemical characteristics (such as chemical oxygen demand: COD), and kinetic formulations. This reflects the fact that biochemistry is concerned with enormously complex organic molecules, that are maintained in states very far from chemical equilibrium by kinetic factors. Conversely, most aquatic chemistry models provide comprehensive support for reaction equilibria, but no special support for kinetically limited processes. Thus, for example, redox reactions are frequently not at equilibrium in aquatic systems, and the kinetic factors governing them have to be established experimentally on a case-by-case basis, just as with biochemical processes. Indeed, some are even catalysed by biochemical processes, such as sulphate to sulphide reduction or ammonia to nitrate oxidation.

These considerations suggest that it would be impractical for an integrated modelling framework to have a uniform approach to all transformation processes and their components, at least for the foreseeable future. A hybrid approach is needed, for which the main new consideration is establishing the links between biological and inorganic processes. There are two major issues to be addressed:

- Precise stoichiometry for biological processes to match that for inorganic processes
- The simultaneous representation of kinetically limited processes and equilibrium limited processes

These papers are chiefly about the stoichiometry, which needs to take account of the requirements of equilibrium and kinetic formulations. Part 2 deals with the development of precise stoichiometry in detail (Ekama et al., 2019). Part 1 makes two further contributions:

- Expressing the stoichiometric balances in terms of components used by the equilibrium speciation model in order to facilitate the integration of the two models
- Using a convenient matrix method to solve the stoichiometric balances

The general methodology adopted here can be summarised as follows (section headings are shown in parentheses):

- Determine which processes will be represented by which type of model (Kinetic and equilibrium models)
- Select a set of model components which are used to describe the material content of the system which are the inputs to the speciation model (Components and species in aquatic process models)
- Express the biological reaction stoichiometry in terms of the speciation model components (Stoichiometry of biological components and reactions); this section also presents a compact matrix method for solving for the stoichiometric reaction coefficients

The algorithm used to calculate the equilibrium speciation is presented in Part 5 of the series. A more detailed discussion and practical demonstration of the principles and tools presented in this paper can also be found in a set of open access course materials on the integration of aquatic chemistry with bio-process models developed under South African Water Research Commission Project K5/2125. The entire

course is available at https://washcentre.ukzn.ac.za/bio-process-models/ Practical implementations of models using these principles are presented by Ikumi et al. (2015).

A simulation model must capture detailed physical knowledge about a system. This paper, Part 1, presents a framework for organising such knowledge about a biochemical system rather than any specific model. The specific information required to build an integrated biochemical model includes which sub-processes are limiting, which transformations need to be explicitly represented in the model, and what reactants and products are involved. The tools presented in this section are applicable to any biochemical system. However, because of the importance of pH in maintaining stable digester operation, many of the examples presented relate to anaerobic digestion.

It is a characteristic of a conceptual framework that there are forward and backward linkages between its parts, and that it needs to be understood in its entirety to be fully useful. A written account is necessarily sequential, and cannot convey this integrated understanding directly – it has to be synthesized by the reader. This means that the relevance of some aspects may not immediately evident when they are first introduced, and earlier sections may need to be revisited to fully grasp their connections with later sections.

CLASSIFICATION OF MODELS

The simulation of chemical and biochemical processes involves two basic kinds of calculations: determining what material will be present at a particular location and time (**mass balancing**), and determining the physical state that it will take on at that point (**speciation**).

Stumm and Morgan (1996) classify aquatic models into two basic kinds:

Continuous open systems, which exchange material with their surroundings, and consequently vary their composition through both flows and reactions

Closed systems, with fixed material content, so that composition can only vary with reactions and internal processes

Chemical and biochemical process simulators almost always employ continuous open system models. A typical model configuration has a set of unit modules which represent control volumes linked by flows. A unit module balances inflows, outflows and internal reactions to determine the composition and characteristics of the material in its control volume, either as a function of time or at steady state.

KINETIC AND EQUILIBRIUM MODELS

Particularly for biochemical models, the internal processes are most often represented as rate-limited reactions, requiring kinetic information for their simulation. However, where process kinetics are not limiting, it is appropriate to use an equilibrium model. This occurs as an asymptotic approximation, when the time scale of the internal transformations becomes very short compared to the time scale of the external flow. In this asymptotic limit, the model becomes one of a closed system. When the rates of aquatic reactions making up the model vary enormously, it becomes appropriate to model some processes using a kinetic formulation, and others using an equilibrium formulation in the same unit

module. This means that the same control volume will be treated simultaneously as an open system for some processes, and a closed system for others. For the equilibrium sub-system, the material content is 'frozen in time' in order to calculate its state. The practical consequence is that the equilibrium speciation only takes account of the instantaneous material content of the system, ignoring time derivatives and material flows across its boundaries.

To illustrate the concepts of kinetic and equilibrium limited processes, consider the hydrolysis of urea:

$$CO(NH_2)_2 + H_2O \rightarrow 2NH_4^+ + CO_3^= \tag{1}$$

The overall reaction could be considered as kinetically limited or mass-balance limited, depending on the time scale of interest. Urea hydrolysis is typically kinetically limited by bio-catalysis, but, given sufficient time, proceeds to completion. Therefore, depending on the time scale of the model, the concentrations of reactants/products over relatively short time scales may be described by reaction kinetics, and over relatively long time scales by mass balance.

However, the products of the hydrolysis reaction (NH_4^+ and $CO_3^=$) are also involved in a parallel set of aqueous phase ionic reactions, of which the following are a sample:

$$NH_4^+ \leftrightarrow NH_3 + H^+ \qquad CO_3^= + H^+ \leftrightarrow HCO_3^- ; H^+ + HCO_3^- \leftrightarrow H_2CO_3 \tag{2}$$
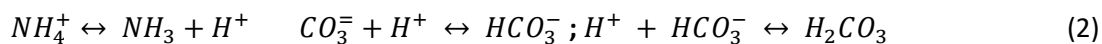
The ionic reactions in Reaction 2 are very rapid compared to urea hydrolysis, and reach equilibrium almost instantaneously. Furthermore, at equilibrium these reactions can have significant reagent concentrations remaining, which are determined by a set of equilibrium relationships. The equilibrium speciation represented by Reaction 2 establishes the pH which affects the kinetics of urea hydrolysis (Fidaleo and Lavecchia, 2003). Therefore, if the hydrolysis process is kinetically limited, an iterative procedure is required to establish both the solution pH and extent of the hydrolysis reaction. Finally, it is important to note that considering a reaction as either equilibrium limited or kinetically limited is a modelling approximation which depends on the model context.

COMPONENTS AND SPECIES IN AQUATIC PROCESS MODELS

A number of different conventions are used to represent aqueous composition in the various models that are currently in use. This section aims to provide a general perspective on the problem of choosing a set of compositional variables for a model.

The term **components** will be used to describe those model entities which collectively **define the overall material content of a system.** This is the same definition of model components which is used in the chemical equilibrium speciation package MINTEQA2 (Allison et al., 2009), and is also equivalent to the meaning of the term components used in biochemical models such as ASM1 (Henze at al., 1987). In the framework presented here, stoichiometric material balances for biochemical transformations are formulated in terms of components (for example, Reaction 1 in the urea hydrolysis example is the stoichiometric balance for the biological transformation part of the model and has been expressed in terms of the model components selected for this system). **Species** are those molecular entities which are required to **describe the actual physical state of the material**. The speciated composition of the aqueous phase is used to calculate characteristic solution properties, such as pH and reaction rates,

since these generally depend on the actual species present. In the urea hydrolysis example, Eq. 2 describes the formation of the species actually present.

The distinction between components and species as defined here is key to the set-up and solution of the equilibrium speciation models. As discussed earlier, this paper presents a framework for organizing the information required to model a bio-chemical system. Perhaps the most critical part of this knowledge consists of understanding what species and components are relevant for a particular system. Since we focus on the tools for organising the knowledge, we work with an assumption that **the biochemical knowledge is already in place.** Our theme is that, **once we understand the species and components of a system***,* the framework and its tools will take us a considerable way towards completing the system description.

General note on terminology and notation for components and species
The terms 'component' and 'species' are widely used in the chemistry and modelling literature with meanings that are closely related, but not necessarily identical to the ones used here. For our purposes, they are variables in a computational model, and their characteristics are purely related to the calculations that are performed on them.

Standard chemical notation does not distinguish between components and species; therefore, one has to infer what is meant from the context. For example, if the symbol NH_3 appears in a balanced stoichiometric reaction equation, it usually indicates a component, since the equation represents a mass balance, nothing more. A symbol such as $NH_{3(aq)}$ or $NH_{3(g)}$ usually (but not inevitably) refers to a molecular species. There is a move to adopt an unambiguous notation in the specialised modelling literature, but it has not been widely accepted yet. In this series of papers we have elected to follow standard chemical notation, which corresponds to the bulk of the literature. In this Part 1, a chemical formula refers to a component unless explicitly stated otherwise. For clarity, species are in italic font to distinguish them from components.

Components
Most equilibrium speciation algorithms are based on what is referred to as 'Duhem's Theorem' in thermodynamics. In fact, this is not strictly a theorem, as it cannot be proven – rather it is a very abstract and general observation about the behaviour of matter. Smith and Van Ness (2005) state it as follows: 'For any closed system formed initially from given masses of prescribed chemical species, the equilibrium state is completely determined when any two independent variables are fixed.' Note that their use of the word 'species' corresponds to the meaning that has been assigned to 'components' in this series of papers. The 'two independent variables' are commonly taken to refer to temperature and pressure, although any other two independent thermodynamic state variables can be substituted.

Hence, the first task of any equilibrium model is to specify the material content of the system being analysed. **Components** are the variables used in this specification. There is no necessity for model components to correspond to chemical constituents as they actually exist in the system; they only have to account correctly for the atoms present.

The use of ionic components requires special consideration. Since macroscopic charge imbalances are not possible, ions cannot be independent elements of the system composition. However, electrons within a system re-distribute themselves at the molecular level to form ions. Since ions are persistent features of aqueous solutions, it is convenient to treat them as components. Databases of ionic component properties are readily available which allow modular representations of aquatic systems in terms of these components.

However, because of the overall electro-neutrality requirement, they are not quite independent components. Where a composition is expressed in terms of ionic components, a charge balance has to be imposed as an additional constraint. Since there is only one overall charge balance, it tends to have less and less impact on the model formulation as the number of ionic components in the system increases.

An ionic component is formally a collection of elements with a net charge. Relative to their neutral reference state, each element may have either gained or lost electrons. An element which gains an electron is said to be **reduced**, and one that loses an electron to be **oxidised**. The net charge of the ion reflects the net gain or loss of electrons by its elements to other (oppositely charged) ions in the solution. So, the charge can be accounted for by considering electrons as part of the stoichiometric content of the ion. Because the electron content is expressed as relative to the neutral elemental state, it can be either a positive or negative quantity, leading to a negative or positive ionic charge, respectively.

To illustrate these concepts, consider carbon dioxide dissolved in otherwise pure water. The species that are believed to be present are water (H_2O), dissolved carbon dioxide (CO_2), carbonic acid (H_2CO_3), carbonate (CO_3^{2-}), bicarbonate (HCO_3^-), hydrogen ion (H^+) and hydroxide ion (OH^-). The solution contains 3 elements: C, H and O. From consideration of the elements alone, its composition has 2 degrees of freedom, which could be regarded as the C:O and H:O ratios. However, the constraint that it was formed from H_2O and CO_2 leaves only 1 degree of freedom. These considerations show that the material content of the system can be expressed in terms of masses of H_2O and CO_2: in other words, using H_2O and CO_2 as the system components. In this respect, the formulae H_2O and CO_2 do not represent molecular entities (species), but just combinations of atoms in fixed ratios (in mathematical terms: basis vectors spanning the model's compositional space).

However, the components standardly used in aquatic chemistry models to represent this kind of system are H_2O, H^+ and CO_3^{2-}. This representation apparently has an extra degree of freedom (3 components instead of 2); however, this is taken up by the charge balance constraint (i.e. every possible composition must have 2 moles of H^+ for every mole of CO_3^{2-}). Considering the electrons: relative to its elemental state, each O in CO_3^{2-} has gained 2 electrons (6 electrons per mole in all). 4 of these were lost by C, and 2 came from H, resulting in a net −2 charge on the CO_3^{2-} and +1 on each H^+. The oxidation states of the elements reflect the electrons transferred – C: +4, O: −2 and H: +1. The number of transferable electrons attributed to each element comes from consideration of their orbital structures. This information can be used in formulating reaction stoichiometry (e.g. McCarty, 1975), but, as the above example shows, the information is also implicit in the stoichiometric formula of the ionic component.

To summarize: components are the variables used to specify the material content of a system. For this purpose, they do not need to correspond to molecular species, and so their choice is not unique. Ionic components are constructed by specifying their content in terms of elements plus or minus electrons, with the understanding that a charge balance constraint will be added to complete the system description. The charge balance and the electron balance are identical, apart from reversal of signs, and once the elements and electrons are balanced, oxidation and reduction will also be balanced.

Species

To represent the physical state of the material in the system, it is important to consider the actual molecular configurations of these atoms. Hence model **species** should correspond to molecular reality as far as possible.

In the equilibrium sub-model, species are related to components by **formation reactions** as described in Part 5. In some cases, components can correspond to the dominant species present, and this can be used to simplify the model and/or equilibrium speciation calculations. However, in other cases, the component chosen will not correspond to the species expected to be present. For example, total sulphate SO_4^{2-} and phosphate PO_4^{3-} present in the system are typical choices for components because they correspond to the quantities measured in a water quality analysis. The sulphate ion SO_4^{2-} is also the dominant sulphate species present at neutral conditions. However, phosphate occurs predominantly as the species $H_2PO_4^-$ and HPO_4^{2-} under the same conditions. In general, **speciation** is the calculation process by which the composition, ultimately reflecting the collection of atoms that make up the system, but usually expressed in terms of component masses, is transformed into one expressed in terms of species masses.

In general, speciation refers to all species, irrespective of whether they take part in equilibrium processes or kinetically limited processes. However, the term is often used as an abbreviation for **equilibrium speciation**, that is, the distribution of species produced by equilibrium processes.

It important to note that that the distinction between components and species (as defined in this paper) is only useful for equilibrium speciation, since the equilibrium state is determined by the material content of the system only. As discussed above, in an equilibrium system at a given temperature and pressure, Duhem's theorem implies that the state depends only on the material present, therefore the speciated composition at equilibrium does not depend on the choice of model components, provided that the mass of each element and associated electrons present is correctly accounted for. However, Duhem's theorem only applies to the equilibrium sub-system and not to the kinetically controlled part of the model. In the kinetic sub-model, the physical state of the system and how it evolves with time do depend on what molecular species are present.   Consequently, the mass balance cannot be decoupled from the speciation for kinetically controlled species. The modelling framework must therefore distinguish between species which are formed by kinetically limited processes, and those that are approximated as formed by equilibrium processes. Examples of the former might be acetate or molecular hydrogen formed as intermediates in anaerobic digestion, while an example of the latter is free hydrogen ion concentration, or equivalently pH.

The presence of kinetically controlled species introduces additional degrees of freedom to the mass balance calculations, which require additional information to specify the composition of the system at any point in time. In the urea hydrolysis example (Eq. 1), the kinetically controlled species urea ($CO(NH_2)_2$) is treated as a component in mass balance calculations, and as a species in kinetic expressions, and the same model variable can be used to hold its concentration for both purposes. However, it is not directly involved in any equilibrium speciation reactions and therefore does not appear in the equilibrium sub-model at all.

However, some kinetically limited species, in particular organic acid and bases, can be simultaneously involved in both kinetically and equilibrium limited processes. For example, acetic acid is not an equilibrium species under the conditions normally encountered in wastewater treatment. Given sufficient time, it will break down to carbonate, methane and water, as indeed takes place through biological action. However, the dissociation of acetic acid into acetate and hydrogen ion is extremely rapid, and can be modelled as being at equilibrium. As in the urea example, acetate will be treated as a component in the bioprocess stoichiometric balance and as a species in the kinetic sub-model. However, unlike urea, acetate is also included in the equilibrium sub-model. The total acetate present in the system will be a component or input to the equilibrium speciation calculations.

This kind of component requires a modification to the application of Duhem's theorem, in which the kinetically maintained component (e.g. acetate) is treated as though it were a separate element for the purpose of specifying the material content of the equilibrium system. This is because, although acetate consists of C, H and O atoms, which are already present in other system components, we do not include conversion to these components in the equilibrium sub-model, because it does not take place instantaneously. Since most redox reactions are kinetically limited, different redox states of the same element, e.g., sulphate and sulphide, nitrate and nitrite, acetate, propionate, carbonate and methane, are typically represented by separate components.

On the other hand, species such as the free H^+ ion cannot be independently added or removed from a physical system in practice, so should not be modelled as components, but rather be determined from the components present by a speciation calculation.

It is worth noting that such issues tend to be addressed automatically for aquatic systems by the choice of standard components included in the databases of aquatic chemistry modelling packages such as MINTEQA2 (Allison et al., 2009) and PHREEQC (Parkhurst and Appelo, 2013).

Formulating components for a model
Fundamental considerations place only a few restrictions on how the components should be chosen. Once one has decided what range of compositions should be represented in a model, what strategies could be used to select from the infinite range of possible formulations? The question of alternative choices of components arises primarily for those involved in equilibrium speciation, not for those components governed by kinetics, which have no reason to be different from the species, as in the urea hydrolysis example.

There are two main issues that will influence the choice, and there will usually be some compromise between them:

(a) To make the model as compact and efficient as possible, one would try to reuse as many as possible of the kinetically important species as components. The remaining components required to span the model's compositional space would be chosen purely for their linear independence. (In the H_2O/CO_2 illustrative example above, this corresponds to using CO_2 and H_2O as the components.)

(b) The alternative strategy is to use, or select from, sets of components from established models (observing the requirements for completeness and independence), thereby tapping into the accumulated experience that they represent. This has advantages when it comes to validating the model, in that comparison with previous models is made easier. (In the H_2O/CO_2 illustrative example, this corresponds to using CO_3^{2-}, H^+ and H_2O as the components).

Strategy (a) will tend to produce models that are compact and efficient, but will be more difficult to compare or integrate with each other.

Strategy (b) will tend to produce models that are more widely understood and compatible with each other, at the possible expense of some computational efficiency.

Aquatic chemistry models such as MINTEQA2 and PHREEQC make use of a highly developed system of components and species, supported by extensive thermodynamic databases. These are referred to here as the **standard aquatic chemistry components** (see Appendix). The component list is carefully designed so that all the components are stoichiometrically independent. This means that any desired system within their scope can be represented simply by including the appropriate set of components. A modeller following strategy (b) need only adopt their system for the inorganic part of the model. This is the approach that is followed in this series of 5 papers. However, examples of the alternative approach will be presented in Part 2 (Brouckaert et al., 2021).

STOICHIOMETRY OF BIOLOGICAL COMPONENTS AND REACTIONS

Note that, since stoichiometric biological reaction equations only express element and charge balances, all the chemical symbols in this section (such as CO_2 or CH_3COO^-) represent components, not species.

The approach that we propose for setting up the biological reaction stoichiometric balances is based on, and equivalent to, McCarty's (1975) general method for deriving the stoichiometry of biologically mediated reactions. McCarty's method involves setting up a **catabolic** (energy providing) reaction and an **anabolic** (biomass growth) reaction from electron-donating and electron-accepting half-reactions. For example, consider the anaerobic utilization of acetate using ammonium as the nitrogen source: Assuming the molecular formula for biomass, $C_5H_7O_2N$, the anabolic half-reactions are:

Electron donor: $\frac{1}{8}CH_3COO^- + \frac{3}{8}H_2O \rightarrow \frac{1}{8}CO_2 + \frac{1}{8}HCO_3^- + H^+ + e^-$ (3a)

Electron acceptor: $\frac{1}{5}CO_2 + \frac{1}{20}HCO_3^- + \frac{1}{20}NH_4^+ + H^+ + e^- \rightarrow \frac{1}{20}C_5H_7O_2N + \frac{9}{20}H_2O$ (3b)
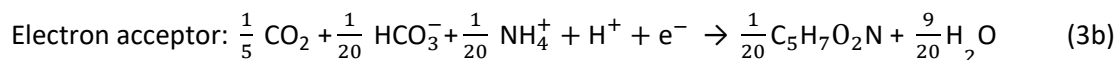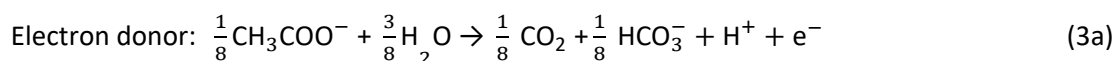
The overall stoichiometric reaction for cell synthesis with acetate as the carbon source is:

Synthesis: $CH_3COO^- + \frac{6}{10} CO_2 + \frac{2}{5} NH_4^+ \rightarrow \frac{2}{5} C_5H_7O_2N + \frac{6}{10} HCO_3^- + \frac{6}{10} H_2O$ (3c)
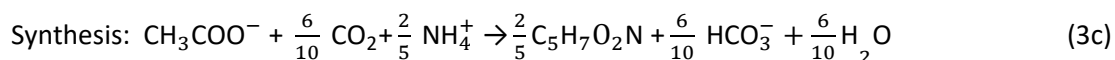
The catabolic half reactions are:

Electron donor: $\frac{1}{8} CH_3COO^- + \frac{3}{8} H_2O \rightarrow \frac{1}{8} CO_2 + \frac{1}{8} HCO_3^- + H^+ + e^-$ (4a)

Electron acceptor: $\frac{1}{8} CO_2 + H^+ + e^- \rightarrow \frac{1}{8} CH_4 + \frac{1}{4} H_2O$ (4b)
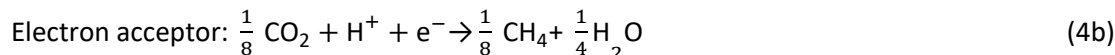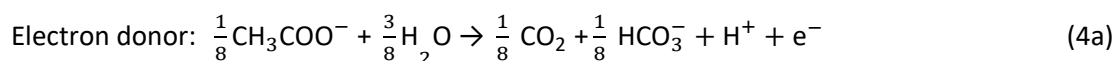
The overall stoichiometric reaction for catabolism with acetate as the energy source is:

Energy: $CH_3COO^- + H_2O \rightarrow CH_4 + HCO_3^-$ (4c)

Equations 1a, 1b, 2a and 2b are taken from tables of half-reactions for various biological transformations provided by McCarty (1975) and Henze et al. (2008). Each half-reaction is normalized to the 'exchangeable' redox electrons to facilitate the construction of the overall balances.

The anabolic and catabolic reactions are then combined as a linear combination into an overall reaction in proportions set by an empirical **yield coefficient** which expresses the fraction of substrate chemical oxygen demand (COD) that becomes biomass COD.

Overall substrate utilisation reaction = $Y \cdot$ anabolic+ $(1-Y) \cdot$ catabolic (5)

The result is a stoichiometric reaction equation which satisfies the complete set of elemental balances and the electron balance.

Assigning the empirical stoichiometric formula ($C_5H_7O_2N$) to represent the biomass is a key step in this development, as it provides the link to the precise stoichiometry of the inorganic components. Part 2 (Brouckaert et al., 2021) extends the concept to all organic wastewater components, and to additional elements using the empirical formulae $C_xH_yO_zN_aP_bS_c^{ch}$ for the electron donor and $C_kH_lO_mN_nP_pS_s$ for the biomass. It is also demonstrated how all the relevant summary characteristics like COD can be calculated from such a formula.

This general approach has been followed in many bio-process models, notably those developed by Ekama and co-authors (e.g. Sötemann et al., 2005a, c; Poinapen and Ekama, 2010a, b; Lu et al., 2012; Brouckaert et al., 2010). For our present purpose we modify the approach in two respects:

- The stoichiometric balances are written in terms of the inorganic speciation model components in order to facilitate the integration of the biological and inorganic sub-models.
- Instead of building the stoichiometric balances by hand from the relevant redox half-reactions, matrix methods are used to solve for the coefficients of the overall balances.

Reaction stoichiometry
A stoichiometric reaction equation represents a set of charge and element balances. In the integrated approach, the stoichiometric balances are expressed in terms of the pre-determined model components. Thus, with one qualification, the only information required to find the coefficients of a stoichiometric reaction equation are:

- The list of components involved in the reaction

- The elemental content and the charge of each component

The qualification concerns the degrees of freedom in the set of balances. The standard case is that if a system involves n balances (e.g. $n - 1$ elements plus charge), it will involve $n + 1$ components, and have 1 degree of freedom. The degree of freedom is conventionally taken up by arbitrarily setting the value of one of the stoichiometric coefficients.

For example, consider the degradation of acetic acid to carbon dioxide and methane:

$$CH_3COOH + H_2O \rightarrow CO_2 + CH_4 \tag{6a}$$

In terms of standard aquatic chemistry components, this is equivalently expressed as:

$$CH_3COO^- + H_2O \rightarrow CO_3^= + H^+ + CH_4 \tag{6b}$$

This list of components has 5 entries: CH_3COO^-, H_2O, $CO_3^=$, H^+ and CH_4.

There are 3 element balances (C, H, and O) and a charge balance (or, equivalently an e^- balance).

So there is 1 degree of freedom, which is taken up by fixing the value of any one of the coefficients, e.g., pre-setting the coefficient of CH_4 in Eq. 4b to 1, after which all the remaining coefficients are found by solving the four balance equations.

However, consider the reaction equation for acetogenesis (from Sötemann et al., 2005a):

$$CH_3CH_2COOH + 2H_2O \rightarrow CH_3COOH + CO_2 + 3H_2 \tag{7a}$$
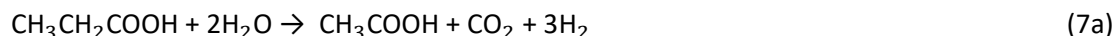
In terms of standard aquatic chemistry components this is expressed as:

$$CH_3CH_2COO^- + 3H_2O \rightarrow CH_3COO^- + CO_3^= + 2H^+ + 3H_2 \tag{7b}$$
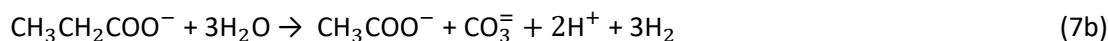
Equation 7b involves 6 components and only 4 balances, and therefore has an extra degree of freedom. For this to be a valid stoichiometric reaction (since stoichiometric equations simply represent degrees of freedom in the compositional space), there must be some prior knowledge of the system which takes up the extra degree of freedom. In this case, the ratio of H_2 to CH_3COO^- produced by the reaction was fixed at 3:1. This may have been based on experimental experience, or a characteristic of the biological pathway, or it may merely have been a simplifying assumption – combining two reactions into one. Whatever the reason, the balances cannot be solved without pre-setting an additional coefficient value. In Eq. 7a, the coefficient of CH_3COO^- was set to 1, and that of H_2 to 3, after which all the remaining coefficients were found by solving the balance equations.

Reaction 7 will be used to illustrate the general method of deriving reaction stoichiometry. The **elemental content matrix E** for the components involved is shown in Table 1-1.

Table 1-1. *Elemental content of the components in Reaction 7b (Refer to Eq. 9)*

	$CH_3CH_2COO^-$	CH_3COO^-	H_2O	$CO_3^=$	H^+	H_2	ρ
C	3	2	0	1	0	0	0
H	5	3	2	0	1	2	0
O	2	2	1	3	0	0	0
e^-	1	1	0	2	−1	0	0

The last row of Table 1-1 contains the electron balance. This could have been equivalently expressed as a charge balance by simply changing the signs of the entries, e.g., the +2 under the $CO_3^=$ means the presence of two e^- and the −1 below the H^+ means the absence of an e^-.

The coefficients of each component in the reaction that need to be found are placed in a **stoichiometric coefficient vector v.** Positive coefficient values indicate products (right-hand-side entries) of the reaction, and negative values indicate reactants (left-hand-side entries). Thus for Reaction 7b:

$$\boldsymbol{v} = [v_{CH3CH2COO^-} \quad v_{CH3COO^-} \quad v_{H2O} \quad v_{CO3=} \quad v_{H+} \quad v_{H2}]^T \tag{8}$$

The superscript T in Eq. 6 indicates the transpose of the vector (i.e. $\boldsymbol{v}$ is a column vector)

Then, the stoichiometric balance equations are expressed as the matrix equation:

$$E \cdot v = \boldsymbol{\rho} \tag{9}$$

where ρ signifies the right-hand-side column vector of the equation (a zero vector at this point – the right-most column in Table 1-1).

Equation 9 has no solution because $\boldsymbol{E}$ is not square (its dimensions are 4 x 6). To obtain a unique solution for the vector $\boldsymbol{v}$, it has to be augmented by adding 2 rows, corresponding to pre-setting two of the stoichiometric coefficients. For instance, if v_{CH3COO^-} is set to 1 and v_{H2} is set to 3, the augmented matrix $\boldsymbol{E_A}$ is shown in Table 1-2, in which the last row is equivalent to $v_{H2} = 3$.

Table 1-2. *Augmented stoichiometric matrix for Reaction 7b (refer to Eq. 10)*

	$CH_3CH_2COO^-$	CH_3COO^-	H_2O	$CO_3^=$	H^+	H_2	ρ_A
C	3	2	0	1	0	0	0
H	5	3	2	0	1	2	0
O	2	2	1	3	0	0	0
e^-	1	1	0	2	−1	0	0
$v_{CH3COO-}$	0	1	0	0	0	0	1
v_{H2}	0	0	0	0	0	1	3

The equation to be solved is then:

$$E_A \cdot v = \rho_A \tag{10}$$

Solving this matrix equation gives $\quad v = [-1 \ 1 \ -3 \ 1 \ 2 \ 3]^T$ (11)

Anabolic and catabolic reactions

The distinguishing characteristic of biological reactions is the coupling between anabolic and catabolic reactions. This is usually modelled by introducing a **yield coefficient**, which represents the fraction of substrate that is consumed by the anabolic reaction. Treating the yield coefficient as an empirical constant is a modelling simplification: in reality it depends on kinetic and equilibrium factors, but in many cases the dependence is not very strong. So, once again, prior knowledge of the system is used to reduce the model's dimensionality, and therefore its complexity.

Obtaining the overall biological reaction stoichiometry is thus simply a matter of obtaining the stoichiometry of the anabolic and catabolic reactions separately according to the method described above, and forming a linear combination in terms of the yield coefficient.

This methodology requires the elemental content of biomass and substrates (electron donors) to be known. It has been common for biochemical models to represent indeterminate organic substances in wastewater purely in terms of their COD, as in ASM1 (Henze et al., 1987). Such a representation is insufficient for modelling physico-chemical processes, and various methods have been used to supply the additional information, such as mass ratios for carbon content (f_C, gC/gCOD), and nitrogen content (f_N, gN/gCOD), which is considered in Part 3 of this series. In the present treatment, we have adopted the use of empirical molecular formulae such as $C_xH_yO_zN_aP_bS_c^{ch}$ to represent complex organics of unknown structure, and $C_kH_lO_mN_nP_pS_s$ for biomass to distinguish it from the electron donor. With this representation, the method outlined in the previous section can be used without modification to determine the stoichiometric coefficients of the separate anabolic and catabolic reactions. The only stipulation is that the substrate coefficient is always pre-set to −1 in both reactions in order to make the application of the yield coefficient straightforward.

The anabolic reaction for biomass growth on propionate is:

$$CH_3CH_2COO^- + v_{CO_3^=}CO_3^= + v_{H^+}H^+ + v_{NH_4^+}NH_4^+ \rightarrow v_{C_5H_7O_2N}C_5H_7O_2N + v_{H_2O}H_2O \qquad (12)$$
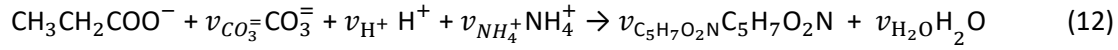
Reworking the derivation according to the matrix method, the augmented stoichiometric matrix is shown in Table 1-3:

Table 1-3. *Augmented stoichiometric matrix for the acetogenic anabolic reaction*

	$CH_3CH_2COO^-$	$C_5H_7O_2N$	H_2O	$CO_3^=$	H^+	NH_4^+	ρ_A
C	3	5	0	1	0	0	0
H	5	7	2	0	1	4	0
O	2	2	1	3	0	0	0
N	0	1	0	0	0	1	0
e^-	1	0	0	2	−1	−1	0
$v_{CH3CH2COO-}$	1	0	0	0	0	0	−1

After solving separately for the anabolic and catabolic stoichiometric coefficient vectors (see Table 1-4), the overall reaction coefficient vector is simply:

$$v_{\text{overall}} = Y \cdot v_{\text{anabolic}} + (1 - Y) \cdot v_{\text{catabolic}} \qquad (13)$$

where *Y* is the yield coefficient.

The set of coefficients obtained according to Eq. 13 are formulated on the basis of 1 mole of substrate consumed. It may be convenient to re-scale it to a different basis to suit the form of its rate expression. A commonly used basis is 1 g of biomass COD produced, as in the ASMs (Henze et al., 2000).

For the acetogenesis example, the catabolic reaction is Reaction 7b. The vector of stoichiometric coefficients needs to be expanded to accommodate both the catabolic and anabolic reactions:

$$v = [v_{\text{CH3CH2COO}-} \quad v_{\text{CH3COO}-} \quad v_{\text{C5H7O2N}} \quad v_{\text{H2O}} \quad v_{\text{CO3}=} \quad v_{\text{H+}} \quad v_{\text{H2}} \quad v_{\text{NH4}}]^{\text{T}} \qquad (14)$$

The results are shown in Table 1-4 using molal units, which depend on the molecular formula used to represent the biomass ($C_5H_7O_2N$). The COD per mol of the biomass formula is 223.986 g O_2/mol, so converting to a basis of 1g COD of biomass produced involves dividing all the terms of v_{overall} by 223.986 × 0.7*Y*.

Table 1-4. *Anabolic, catabolic and overall stoichiometric coefficients for acetogenesis*

	$\nu_{anabolic}$	$\nu_{catabolic}$	$\nu_{overall}$
$CH_3CH_2COO^-$	−1	−1	−1
CH_3COO^-	0	1	$1 - Y$
$C_5H_7O_2N$	0.7	0	$0.7Y$
H_2O	2.1	−3	$5.1Y - 3$
$CO_3^=$	−0.5	1	$1 - 1.5Y$
H^+	−1.3	2	$2 - 3.3Y$
H_2	0	3	$3(1 - Y)$
NH_4^+	−0.7	0	$-0.7Y$

Note that the yield coefficient *Y* in this case has the same numerical value irrespective of the units used, since it is defined as the fraction of substrate consumed which goes to the anabolic reaction. This is the same whether expressed in terms of moles, grams or COD of substrate. This does not apply to all biochemical processes, e.g., for autotrophic nitrification the conventional definition of the yield coefficient expresses biomass COD produced per N removed, and the numerical value does depend on the units used.

This methodology is fundamentally the same as set out by McCarty (1975). However, it does not employ two prominent devices that he presented: the concept of the **exchangeable electrons** of each component, and the division of each reaction into oxidation and reduction **half-reactions***.* In fact, these are not essential features of his method; they are just aids for avoiding errors when determining the coefficients by hand. The use of symbolic algebraic software makes these aids dispensable. However, McCarty's exchangeable electron concept remains an important aid to an understanding of the reaction system.

Exchangeable electrons / electron donating capacity / COD
As pointed out by McCarty (1975), COD expresses the electron donating capacity of a substance as the mass of oxygen which could take up the electrons, i.e., 8g O /mol electrons in the COD test (discussed further in Part 2, Brouckaert et al., 2021). This information is actually inherent in the elemental content matrix. If we consider a generic reaction in which one organic component is transformed into another:

$$C_xH_yO_zN_aP_bS_c^{ch} \rightarrow \nu_1 \cdot C_kH_lO_mN_nP_pS_s + \nu_2 \cdot CO_3^= + \nu_3 \cdot H^+ + \nu_4 \cdot H_2O + \nu_5 \cdot NH_4^+ + \nu_6 \cdot PO_4^{-3} + \nu_7 \cdot SO_4^= \qquad (15)$$
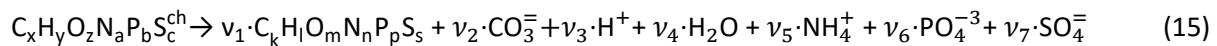
The elemental content matrix for this reaction is shown in Table 1-5:

Table 1-5. *Elemental content matrix for a generic organic reaction*

	$C_xH_yO_zN_aP_bS_c{}^{ch}$	$C_kH_lO_mN_nP_pS_s$	H_2O	$CO_3{}^=$	H^+	$NH_4{}^+$	$PO_4{}^{-3}$	$SO_4{}^=$
C	x	k	0	1	0	0	0	0
H	y	l	2	0	1	4	0	0
O	z	m	1	3	0	0	4	4
N	a	n	0	0	0	1	0	0
P	b	p	0	0	0	0	1	0
S	c	s	0	0	0	0	0	1
e^-	-ch	0	0	2	−1	−1	3	2

This is a 7 x 8 matrix, and consequently has no determinant. If the column for the product biomass $C_kH_lO_mN_nP_pS_s$ is deleted (i.e. only the catabolic reaction is considered), the remaining matrix is 7 x 7, and its determinant is:

$$\gamma_s = (4x + y - 2z - 3a + 5b + 6c - ch) \tag{16}$$

Similarly, if the column for the substrate $C_xH_yO_zN_aP_bS_c{}^{ch}$ is deleted, the determinant of the remaining matrix is:

$$\gamma_b = (4k + l - 2m - 3n + 5p + 6s) \tag{17}$$

The composite stoichiometric factors γ_s and γ_b are identical to the 'exchangeable electrons' of the organic components in the McCarty (1975) treatment. When one solves the matrix equation (Eq. 10) for the stoichiometric coefficients, γ_s and γ_b appear as factors in the solution. One can also derive the forms of γ_s and γ_b by considering the changes taking place in oxidation states of the elements in the organic component during the reaction, which is how McCarty arrived at them.

This demonstrates the equivalence of the elemental matrix and the electron balancing methods for deriving the stoichiometric coefficient values.   However, keeping track of the electrons through a complex set of reactions often provides insight into the mechanisms involved, which is difficult to obtain just by inspecting the elemental matrix. Note that for reasons discussed in Part 2, the term 'exchanged electrons of reaction' is preferred to the term 'exchangeable electrons'. The electrons donated and accepted by the various organic and inorganic components in various biochemical processes are discussed in greater detail in Part 2 (Brouckaert et al., 2021).

Stoichiometric balances and speciation
As discussed in the previous sections, biological stoichiometric reactions are simply material balances which keep track of the elemental and electron content of the products and reactants in biological transformations. They generally do not predict changes in speciation resulting from biological transformations or the distribution of species between phases.

Comparing Eqs 6a with 6b and 4c, and 7a with 7b, it is clear that the same stoichiometric reaction can be written it terms of several different sets of components and still be balanced overall. Our recommendation is that the stoichiometric equations should always be set up in terms of the standard aquatic chemistry modelling components as discussed in the previous sections. However, in other modelling approaches, there is some freedom to choose which components to include in the biological stoichiometric balances.

For example, McCarty (1975) tended to set up his half-reactions in terms of the transfer of one mole of protons plus one mole of electrons ($H^+ + e^-$ in Eqs 3 and 4). In many cases, this leads to half-reactions expressed in terms of two different carbonate species, as, for example, in Eq. 4a:

$$\frac{1}{8}CH_3COO^- + \frac{3}{8}H_2O \rightarrow \frac{1}{8}CO_2 + \frac{1}{8}HCO_3^- + H^+ + e^- \tag{4a}$$
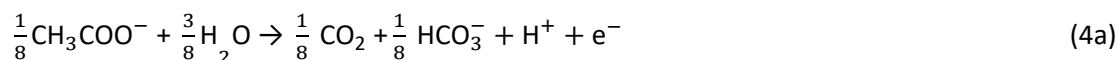
This does not necessarily mean that one mole of acetate will produce one mole of CO_2 and one mole of HCO_3^-. The actual distribution of carbonate species will depend on the entire ionic composition, which also determines properties such as the pH.

In terms of standard aquatic chemistry components, this is equivalent to:

$$\frac{1}{8}CH_3COO^- + \frac{1}{2}H_2O \rightarrow \frac{1}{4}CO_3^= + \frac{11}{8}H^+ + e^- \tag{18}$$

In Eq. 18, the component $CO_3^=$ represents the sum of all the carbonate species produced (including any gaseous CO_2 evolved). Once the composition of the solution has been determined by flow and reaction balances in terms of concentrations of components, the speciation calculation can be employed to determine the concentrations of equilibrium species. So, for example, the total $CO_3^=$ concentration (component concentration, as referred to in Eq. 18) would be calculated by material balance. The carbonate species concentrations, such as $[H_2CO_3]$, $[HCO_3^-]$ and $[CO_3^{2-}]$, are then determined from the speciation calculation. Therefore, standard chemical notation can be confusing, since, apart from the typeface, the same symbol $CO_3^=$ in this paragraph refers to both a component and a species, which are conceptually quite different. However, the context makes it clear whether a component or species is being referred to. In a dynamic model, with kinetic and equilibrium parts, both sets of calculations have to be carried out at each integration time step, because reaction rates and phase separations generally depend on species concentrations rather than component concentrations. So, the stoichiometric mass-balanced time-dependent differential equations part is solved for the changes in component concentrations and the equilibrium speciation algebraic equations part of the model speciates the new component concentrations into species concentrations. These issues will be further discussed in Part 5 of this series.

ALKALINITY

It is usually impractical to define the complete ionic composition of a wastewater aqueous phase, because there are too many possible dissolved components that can be present. Alkalinity, or proton accepting capacity (PAC), is a summary property, easily measured by titration, which provides important information about how biological processes interact with the aqueous environment in which they take place. Part 4 of this series discusses alkalinity further from the measurement point of view, and Part 5

looks at the computational aspects; but for the present purpose, the alkalinity of the aqueous phase is the remaining capacity of the weak-acid anions (e.g. *HCO₃⁻*) present in it to bind protons (e.g. *HCO₃⁻* becoming *H₂CO₃*), thereby reducing the free proton (*H⁺*) concentration, and so acting against a decrease in pH when acid is added (imparting buffer capacity). At the titration end-point, which for the *H₂CO₃* alkalinity is in the vicinity of pH 4.5 (see Part 4 or Loewenthal et al., 1989), the *H₂CO₃* alkalinity is, by definition, zero relative to the selected reference species for the alkalinity, in this case *H₂CO₃*. In 'natural' waters, alkalinity principally is provided by the inorganic carbon (IC) anions. However, in wastewaters additional contributions are made by other weak-acid species such as acetate, ammonia (*NH₃*), propionate, ortho-phosphate (OP) and sulphide (FSS, *HS⁻*). Since biological redox reactions can either take up or produce these anions, as well as protons, they cause changes in the aqueous alkalinity and pH which are important to understand in systems where pH affects the bioprocess rates, such as those of acetoclastic methanogenesis or BSR in AD.

Alkalinity is usually expressed units of mg/L as $CaCO_3$. For the present purpose it is more useful to use units of mol H^+/L, where mol H^+/L x 50 000 yields mg/L as $CaCO_3$ (Loewenthal and Marais, 1976). Alkalinity arises from the formation of protonated species in solution. However, it can also be expressed in terms of component concentrations (Snoeyink and Jenkins, 1980). It is this aspect which is relevant to Parts 1 and 2 of this series.

To illustrate how alkalinity is related to components, consider a solution that is made up of Na_2CO_3, Na_3PO_4, NaAc and NaHS in pure water. These are the sodium salts of the weak-acid anions that commonly contribute to alkalinity, which means that they tend to bind H^+ in aqueous solution to form the protonated species *HCO₃⁻, H₂CO₃, HPO₄²⁻, H₂PO₄⁻, H₃PO₄, HAc, H₂S* and *HS⁻*. The salts that the solution of the example was made from contain no H^+. (The H in NaHS is bound to S as *HS⁻*). When protonated to the maximum extent possible, their weak-acid anions will be entirely converted to *H₂CO₃, H₃PO₄, HAc*, and *H₂S*, which are defined to be the alkalinity reference species.

So the capacity of the initial solution to bind *H⁺* (its alkalinity) is given by:

$$2[CO_3^{2-}] + 3[PO_4^{3-}] + [HS^-] + [Ac^-]$$

where [...] indicates a component concentration in mol/kg.

As [H⁺] is added to the solution by titrating with a strong acid such as HCl, the added *H⁺* progressively reduces the solution's capacity to bind further *H⁺*, that is, it reduces the alkalinity. Hence the alkalinity of the solution during the course of the titration is given by:

$$\text{Alk}_T = 2[CO_3^{2-}] + 3[PO_4^{3-}] + [HS^-] + [Ac^-] - [H^+] \tag{19a}$$

In the measurement context, the alkalinity is defined by the titration with strong acid, which will be affected in various ways by the presence of acid and base species in the original solution. The pH of the example solution is about 11, and if 0.001 M NH_4Cl is added to it, the NH_4^+ will give up most of its H^+ as it dissolves, to bind with the weak-acid anions in the solution, forming *NH₃(aq)*. This exchange will have some effect on the speciation of the solution, and consequently the pH and the distribution of alkalinity among the components, but no effect on the total alkalinity. In terms of measurement, this is

manifested as a change in the shape of the pH titration curve, but no change in the total acid required to reach the titration endpoint, where the $NH_{3(aq)}$ will essentially have been all converted back to NH_4^+. In terms of components, it is explained by saying that NH_4^+ is the reference species for alkalinity, so adding NH_4^+ does not affect Alk_T, so Eq. 19a is unchanged (Loewenthal et al., 1991).

Adding a strong base, such as NaOH (sodium hydroxide), will increase the total acid required to titrate to the endpoint, and therefore the alkalinity, whereas adding a strong acid such H_2SO_4 or HCl will decrease it. In the case of a strong acid, the effect on Eq. 19a can be made explicit by noting that in solution strong acids are present in their fully dissociated forms:

$$HCl \equiv (H^+ + Cl^-); \ H_2SO_4 \equiv (2H^+ + SO_4^{2-}).$$
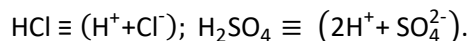
Expressing strong acids in their dissociated form is useful for avoiding confusion in the stoichiometric manipulations that are discussed in Part 2 (Brouckaert et al., 2021). The strong base case is less obvious, as OH^- is not one of the standard aquatic chemistry components: where required, it is represented as $(H_2O - H^+)$. However, H_2O is usually modelled as an invariant background component, and not represented explicitly. Thus OH^- is effectively $(-H^+)$, which means that is already accounted for in Eq. 19a.

Sulphide involves a similar issue. The standard component representing sulphides is HS^-, not S^{2-}, which is considered virtually non-existent as an aqueous solution species. So, if the NaHS in our solution example is replaced by Na_2S, the S^{2-} is represented as $(HS^- - H^+)$. Once again, Eq. 19a is unchanged, but the $[H^+]$ term includes a negative contribution from the sulphide.

So far, the discussion has assumed that the total alkalinity becomes zero when all the relevant acid anions are fully protonated. The limiting species for achieving this condition is H_3PO_4, which is a strong acid, only approaching full protonation at very low pH < 1 (although $H_2PO_4^-$ and HPO_4^{2-} are weak acids). All the other components are fully protonated around pH 4. By a fortunate coincidence, the titration endpoint for $H_2PO_4^-$ is also around pH 4. So for measurement purposes it is convenient to take the reference species for phosphate as $H_2PO_4^-$ rather than H_3PO_4 (Loewenthal et al., 1989). Thus there are two versions of total alkalinity in use, H_2CO_3 / H_3PO_4 / NH_4^+ / H_2S / HAc alkalinity, which we indicate by Alk_T, and H_2CO_3 / $H_2PO_4^-$ / NH_4^+ / H_2S / HAc alkalinity, which we will indicate as Alk_t.

$$Alk_t = 2[CO_3^{2-}] + 2[PO_4^{3-}] + [HS^-] + [Ac^-] - [H^+] \tag{19b}$$

Comparing Eqs 19a and 19b, the difference between the two alkalinity versions is simply:

$$Alk_T - Alk_t = [PO_4^{3-}] = P_T \tag{19c}$$

where P_T is the total ortho-phosphate concentration.

Equations 19a to 19c are written in terms of standard aquatic chemistry components, which is fundamentally an arbitrary choice. There are situations where it is convenient to represent systems in terms of different sets of components. For instance, the composition of our example solution could be expressed in terms of HCO_3^- and HPO_4^{2-}, instead of CO_3^{2-} and PO_4^{3-}. In this case, Eqs 19a and 19b are replaced by:

$$Alk_T = [HCO_3^-] + 2[HPO_4^{2-}] + [HS^-] + [Ac^-] - [H^+] \tag{19d}$$

$$Alk_t = [HCO_3^-] + [HPO_4^{2-}] + [HS^-] + [Ac^-] - [H^+] \tag{19e}$$

In Eqs 19d and 19e, $[HCO_3^-]$ and $[HPO_4^{2-}]$ have the same values as $[CO_3^{2-}]$ and $[PO_4^{3-}]$ in Eq. 19a and 19b, but the value of $[H^+]$ is reduced to account for the H^+ content of the substituted components.

Total alkalinity change of reaction

Since the total alkalinity of a reaction can be expressed as a linear combination of component quantities, it is also a conserved stoichiometric property of the reaction, and so can be used, for example, in mixing calculations (Loewenthal et al., 1989, 1991). Chemical reactions which produce or consume weak acids or bases and protons will change the alkalinity of the aqueous phase, and the change that occurs is a stoichiometric property of the reaction. In the same way that the enthalpy change or exchanged electrons of reaction (Part 2, Brouckaert et al., 2021) are used in energy and electron balances for reacting systems, the concept of **total alkalinity change of reaction** allows alkalinity balances for reacting systems.

The total alkalinity change of reaction is calculated from the difference between the coefficients of the component products and those of the component reactants relevant to the alkalinity, with respect to the selected reference species, i.e.:

$$\Delta Alk_T = \Sigma Alk_{T\text{products}} - \Sigma Alk_{T\text{reactants}} \tag{20}$$

For Eq. 15 the product components contributing to the ΔAlk_T of the reaction are $+v_2CO_3^{2-}$, $+v_6PO_4^{3-}$ and $-v_3 H^+$. If the generic reactant component $C_xH_yO_zN_aP_bS_c{}^{ch}$ is a weak acid/base component itself that contributes to alkalinity, such as NH_3, HS^- or CH_3COO^-, then its consumption by the reaction contributes to the alkalinity change of the reaction. However, if the generic component is a strong acid/base anion or cation such as $S_2O_3^{2-}$, or an insoluble or an uncharged organic, such as particulate starch, urea or dissolved glucose, then it does not contribute. This means that the nature of the generic reactant component needs to be known and the reference species for the alkalinity defined to know whether or not it contributes to the ΔAlk_T of the reaction. Following Eqs 19a and 20 for the ΔAlk_T of Eq. 15 yields Eq. 21, where the alkalinity of the electron donor (Alk_{ed}) is 0 if the generic component does not contribute to the alkalinity of the reactants, or 1, 2 or 3 if it does and is 1, 2 or 3 dissociations away from the reference species.

$$\Delta Alk_T = [\, 2v_2 + 3v_6 \text{ - } v_3] - [Alk_{ed}] \tag{21a}$$

$$\Delta Alk_t = [\, 2v_2 + 2v_6 \text{ - } v_3] - [Alk_{ed}] \tag{21b}$$

These distinctions reduce the utility of the generalized Eq. 21, because one has to know what the generalized component is to select the correct value for Alk_{ed}. The issue is that, although alkalinity is a stoichiometric quantity, unlike all the other stoichiometric quantities considered in this series of papers, the alkalinity contribution of a component is not determined solely by its elemental make-up.

Direct, latent and persistent alkalinity

If sodium acetate (NaAc ≡ NaC$_2$H$_3$O$_2$ ≡ Na$^+$ + C$_2$H$_3$O$_2^-$) is added to a solution, the acetate adds 1 mol of alkalinity per mol acetate to the solution (Alk$_T$ or Alk$_t$). If it is subsequently oxidised to carbonate (C$_2$H$_2$O$_2^-$ + 2O$_2$ → 2CO$_3^{2-}$ + 3H$^+$) the acetate alkalinity is transformed to carbonate alkalinity, to the extent of (2 x 2 – 3 = 1) mol alkalinity per mol acetate that was added. This phenomenon can be described as the electron donor, acetate, having **direct alkalinity** (ΔAlk$_{ed}$) and **persistent alkalinity** (Alk$_p$), which persists in the solution after the acetate is removed by the reaction. Although Alk$_{ed}$ is a true property of the component, the persistent alkalinity depends on the products of the reaction and is therefore a property of the reaction. Nevertheless, in a given redox environment, it can be useful to think of it as a quasi-property of the component.

In the above example, the direct and persistent alkalinities of the acetate both have the same value, since ΔAlk$_T$ for the reaction is zero; however, this is not always the case. Consider the oxidation of urea: (NH$_2$CONH$_2$ + 4O$_2$ → CO$_3^{2-}$ + 4H$^+$ + 2NO$_3^-$). Urea is uncharged, so has no direct alkalinity (Alk$_{ed}$ = 0). However, ΔAlk$_T$ for the reaction is (2 – 4 – 0 – 4 x 0 = –2), so the persistent alkalinity of urea, when its elements are all completely oxidized, is –2 mol/mol; adding urea to the solution will initially have no effect on its alkalinity, but will reduce it as the oxidation reaction proceeds. In a different redox environment, such as an anaerobic reactor, the N reaction product could be NH$_4^+$ rather than NO$_3^-$, in which case the reaction is NH$_2$CONH$_2$ + H$_2$O → CO$_3^{2-}$ + 2NH$_4^+$. In this case ΔAlk$_T$ = 2 + 2 x 0 – 0 – 0 = +2 mol/mol.

From the above, all the alkalinity in the aqueous phase produced by reaction Eq. 15 comes from the electron donor C$_x$H$_y$O$_z$N$_a$P$_b$S$_c$^{ch} relative to the reaction products. So the ΔAlk$_T$ can be described as **latent alkalinity** stored in the electron donor, and released to the aqueous phase during the redox reaction. Thus, the persistent alkalinity of the electron donor is given by:

$$\text{Alk}_p = (\text{Alk}_{ed} + \Delta\text{Alk}_T) \tag{22}$$

The additional alkalinity is therefore not 'created' by the reaction – it is latent in the electron donor, and released to the aqueous phase by the reaction. If the e$^-$ donor is dissolved, then the direct alkalinity of the e$^-$ donor is also in the aqueous phase and the reaction adds the latent alkalinity from the reactant component. Furthermore, a reaction that produces biomass takes up alkalinity and stores it in a particulate form, external to the aqueous phase, although in contact with it. Via this mechanism, alkalinity is commonly transferred from the aqueous phase in an activated sludge reactor, where heterotrophic biomass is produced, to an anaerobic digester, where the alkalinity reappears in the aqueous phase at very high concentration after digestion, because the waste activated sludge (WAS) biomass is thickened before AD (Part 2, Brouckaert et al., 2021). However, since the redox environments are different, the alkalinity released anaerobically may differ from the alkalinity stored aerobically – it depends on the other components involved in the respective reactions.

CONCLUSIONS

The concepts and methods presented are part of a pragmatic framework for modelling wastewater treatment processes that reflects the current state of knowledge. The completely rigorous approach to

chemical reactions involves conservation of matter (stoichiometry), conservation of energy, equilibria and kinetics. Every process is governed by all these factors. However, in many cases models can be simplified by neglecting aspects which are not limiting. Such a simplification applies, not only to the mathematical formulation of models, but also to the experimental methods for obtaining the data required to support the modelling. Thus, most models and measurement techniques associated with wastewater treatment reflect the fact that the biochemical reactions tend to be limited by stoichiometric and kinetic factors. On the other hand, inorganic aqueous models and measurements tend to reflect stoichiometric and equilibrium limitations. When a model needs to represent the interaction between the biochemical reactions and the inorganic reactions, the experimental effort to obtain complete thermodynamic and kinetic data for all the components involved would be enormous, particularly since the exact natures of most organic components are unknown. Retaining the main simplifications that have commonly been applied in both biochemical and inorganic chemistry models makes the task of integrating them manageable.

Nevertheless, it is important to be aware of the rigorous picture, so as to ensure that any simplifications made are appropriate, and to understand their limitations. So, for example, it was pointed out in the section on anabolic and catabolic reactions that a yield coefficient represents a stoichiometric approximation to a thermodynamic limitation. Experience has shown that the approximation is good in many practical circumstances, because yield coefficients do not vary excessively within the range of conditions commonly encountered in wastewater treatment. On the other hand, the speciation of weak acids and bases is much more variable, and for this a stoichiometric approximation will only be appropriate in a very narrow pH range. Fortunately, the modelling tools that we present allow us to construct models that do not resort to such speciation approximations.

REFERENCES

ALLISON JD, BROWN DS and NOVO-GRADAC KJ (2009) MINTEQA2. URL: http://www.epa.gov/ceampubl/mmedia/minteq/ (Accessed 8 Dec 2009).

ANDREWS JF and GRAEF SP (1971) Dynamic modelling of the anaerobic digestion process. Anaerobic Biological Treatment Processes. Advances in Chemistry Series No. 105. American Chemical Society, Washington D.C. 126−162.

BARAT R, MONTOYA T, SECO A and FERRER J (2011) Modelling biological and chemically induced precipitation of calcium phosphate in enhanced biological phosphorus removal systems. *Water Res.* **45** 3744−3752.

BATSTONE DJ, KELLER J, ANGELIDAKI I, KALYUZHNYI SV, PAVLOSTATHIS SG, ROZZI A, SANDERS WTM, SIEGRIST H and VAVILIN VA (2002) Anaerobic digestion model No 1 (ADM1). Scientific and Technical Report No. 13. International Water Association (IWA), London.

BATSTONE DJ, AMERLINCK Y, EKAMA G, GOEL R, GRAU P, JOHNSON B, KAYA I, STEYER J-P, TAIT S, TAKÁCS I, VANROLLEGHEM PA, BROUCKAERT CJ and VOLKE E (2012) Towards a generalized physicochemical framework. *Water Sci. Technol.* **66** (6) 1147−1161. doi: 10.2166/wst.2012.300

BROUCKAERT CJ, IKUMI DS and EKAMA GA (2010) A 3 phase anaerobic digestion model. In: *Proceedings of the 12th IWA Anaerobic Digestion Conference (AD12)*, 1–4 November 2010, Guadalajara, Mexico.

BROUCKAERT CJ, EKAMA GA, BROUCKAERT BM and IKUMI DS (2021) Integration of complete elemental mass balanced stoichiometry and aqueous phase chemistry for bioprocess modelling of liquid and solid waste treatment systems – Part 2: Bioprocess stoichiometry. *Water SA* **47** (3) 287-308. https://doi.org/10.17159/wsa/2021.v47.i3.11858

DOLD PL, EKAMA GA and MARAIS GvR (1980) A general model for the activated sludge process. *Progr. Water Technol.* **12** (6) 47−77.

EKAMA GA (2009) Using bio-process stoichiometry to build a plant-wide mass balance based steady-state WWTP model. *Water Res.* **43** (8) 2101−2120.

FIDALEO M and LAVECCHIA R (2003) Kinetic study of urea hydrolysis in the pH range 4−9. *Chem. Biochem. Eng. Q.* **17** (4) 311−318.

GRAU P, DE GRACIA M, VANROLLEGHEM PA and AYESA E (2007) A new plant wide methodology for WWTPs. *Water Res.* **41** (19) 4357−4372.

HENZE M, GRADY CPL Jnr, GUJER W, MARAIS GVR and MATSUO T (1987) Activated Sludge Model No 1. IWA Scientific and Technical Report No 1. International Water Association (IWA), London.

HENZE M, GUJER W, MINO T and VAN LOOSDRECHT M (2000) Activated Sludge Models ASM1, ASM2, ASM2d, and ASM3. IWA Scientific and Technical Report No 9. International Water Association (IWA), London.

HENZE M, VAN LOOSDRECHT MCM, EKAMA GA and BRDJANOVIC D (2008) *Biological Wastewater Treatment: Principles, Modelling and Design*. IWA Publishing, London. 528 pp.

IKUMI DS, BROUCKAERT CJ and EKAMA GA (2011) A 3 phase anaerobic digestion model. *8th IWA Watermatex conference*, San Sebastian, Spain, 20−22 June 2011.

IKUMI DS, HARDING TH, BROUCKAERT CJ and EKAMA GA (2014) Plant wide integrated biological, chemical and physical processes modelling of wastewater treatment plants in three phases (aqueous-gas-solid).   PhD thesis, Research Report W138, Department of Civil Engineering, University of Cape Town, Rondebosch, 7700, South Africa.

IKUMI DS, HARDING TH, VOGTS M, LAKAY MT, MAFUNGWA HZ, BROUCKAERT CJ and EKAMA GA (2015) Mass balances modelling over wastewater treatment plants III. WRC Report No. 1822/1/14, Water Research Commission, ISBN 978-1-4312-0614-8.

LIZZARALDE I, FERNANDEZ-AREVALO T, BROUCKAERT CJ, VANROLLEGHEM P, IKUMI DS, EKAMA GA, AYESA E and GRAU P (2015) A new general methodology for incorporating physico-chemical transformations into multiphase wastewater treatment process models. *Water Res.* **74** 239−256.

LOEWENTHAL RE and MARAIS GVR (1976) Carbonate chemistry of aquatic systems – theory and application. Ann Arbor Science Publishers, Ann Arbor, MI. Library of Congress 76-24963, ISBN 0-25040141-X.

LOEWENTHAL RE, EKAMA GA and MARAIS GVR (1989) Mixed weak acid/base systems Part I – Mixture characterization. *Water SA* **15** (1) 3–24.

LOEWENTHAL RE, WENTZEL MC, EKAMA GA and MARAIS GVR (1991) Mixed weak acid/base systems Part II: Dosing estimation, aqueous phase. *Water SA* **17** (2) 107–122.

LU H, EKAMA GA, WU D, FENG J, VAN LOOSDRECHT MCM and CHEN GH (2012) SANI process realizes sustainable saline sewage treatment: Steady state model-based evaluation of the pilot-scale trial of the process. *Water Res.* **46** (2) 475–490.

MCCARTY PL (1975) Stoichiometry of biological reactions. *Prog. Water Tech.* **7** (1) 157–172.

MUSVOTO EV, WENTZEL MC, LOEWENTHAL MC and EKAMA GA (2000a) Integrated chemical-physical processes modelling – I. Development of a kinetic-based model for mixed weak acid/base systems. *Water Res.* **34** (6) 1857–1867.

MUSVOTO EV, WENTZEL MC and EKAMA GA (2000b) Integrated chemical-physical processes modelling – II. Simulating aeration treatment of anaerobic digester supernatants. *Water Res.* **34** (6) 1868–1880.

PARKHURST DL and APPELO CAJ (2013) PHREEQC (Version 3). A computer program for speciation, batch-reaction, one-dimensional transport, and inverse geochemical calculations. URL: ftp://brrftp.cr.usgs.gov/pub/charlton/phreeqc/Phreeqc_3_2013_manual.pdf (Accessed 19 November 2013).

POINAPEN J and EKAMA GA (2010a) Biological sulphate reduction with primary sewage sludge in an up flow anaerobic sludge bed reactor – Part 5: Steady-state model. *Water SA* **36** (3) 193–202.

POINAPEN J and EKAMA GA (2010b) Biological sulphate reduction with primary sewage sludge in an up flow anaerobic sludge bed reactor – Part 6: Development of a kinetic model for BSR. *Water SA* **36** (3) 203–214.

SERRALTA J, FERRER J, BORRAS L and SECO A (2004) An extension of ASM2d including pH calculation. *Water Res.* **38** (19) 4029–4038.

SMITH JM and VAN NESS HC (2005) *Introduction to Chemical Engineering Thermodynamics* (7th edn). McGraw Hill, New York.

SNOEYINK VL and JENKINS D (1980) *Water Chemistry.* John Wiley and Sons, New York.

SOLON K, FLORES-ALSINA X, KAZADI MBAMBA C, VOLKE EIP, TAIT S, BATSTONE D, GERNAEY KV and JEPPSON U (2015) Effects of ionic strength and ion pairing on (plant-wide) modelling of anaerobic digestion. *Water Res.* **70** 235–245.

SÖTEMANN SWN, VAN RENSBURG P, RISTOW NE, WENTZEL MC, LOEWENTHAL RE and EKAMA GA (2005a) Integrated chemical/physical and biological processes modelling Part 2 – Anaerobic digestion of sewage sludges. *Water SA* **31** (4) 545–568.

SÖTEMANN SW, RISTOW NE, WENTZEL MC and EKAMA GA (2005b) A steady-state model for anaerobic digestion of sewage sludges. *Water SA* **31** (4) 511–527.

SÖTEMANN SW, MUSVOTO EV, WENTZEL MC and EKAMA GA (2005c) Integrated chemical, physical and biological processes kinetic modelling Part 1 – Anoxic and aerobic processes of carbon and nitrogen removal in the activated sludge system. *Water SA* **31** (4) 529–544.

SPEECE RE (2008) Anaerobic biotechnology and odor/corrosion control for municipalities and industries. Archea Press, Nashville. TN. ISBN 1-57843-052-9. 586 pp.

STUMM W and MORGAN JJ (1996) Aquatic Chemistry: Chemical Equilibria and Rates in Natural Waters. John Wiley and Sons, New York.

TAKÁCS I and VANROLLEGHEM PA (2006) Elemental balances in activated sludge modelling. In*: Proceedings of the IWA World Water Congress*, 10–14 September 2006, Beijing, China.

WRC (Water Research Commission) (1984) Theory, design and operation of nutrient removal activated sludge processes. Wiechers HNS (Ed.) WRC Report No. TT16/84. Water Research Commission. ISBN 0 908356 13 7.

APPENDIX

Standard aquatic chemistry components
Reference is made in several places to the set of **standard aquatic chemistry components***.* These are those used by several freely available and widely used aquatic chemistry models, such as MINTEQA2, PHREEQC and Visual MINTEQ. The following table lists the subset of standard components that feature in the series of papers.

Component	Description	Component	Description
H^+	Hydrogen ion, proton	CO_3^{2-}	Carbonate
K^+	Potassium	NO_3^-	Nitrate
Na^+	Sodium	NO_2^-	Nitrite
Ca^{2+}	Calcium	SO_4^{2-}	Sulphate
Mg^{2+}	Magnesium	SO_3^{2-}	Sulphite
NH_4^+	Ammonium ion	$S_2O_3^{2-}$	Thiosulphate
		HS^-	Hydrosulphide
		Ac^- (CH_3COO^-)	Acetate
		Pr^- ($CH_3CH_2COO^-$)	Propionate

Chapter 3: Integration of complete elemental mass balanced stoichiometry and aqueous phase chemistry for bioprocess modelling of liquid and solid waste treatment systems − Part 2: Bioprocess stoichiometry

CJ Brouckaert[1], GA Ekama[2], BM Brouckaert[1] and DS Ikumi[2]

[1]Water, Sanitation and Health Research and Development Centre, School of Chemical Engineering, University of KwaZulu-Natal, Berea, Durban, KwaZulu-Natal, South Africa

[2]Water Research Group, Dept of Civil Engineering, University of Cape Town, Rondebosch, 7700, South Africa

ABSTRACT

Bioprocesses interact with the aqueous environment in which they take place. Integrated bioprocess and three-phase (aqueous–gas–solid) multiple strong and weak acid/base system models are currently being developed for a range of wastewater treatment applications including anaerobic digestion, biological sulphate reduction, autotrophic denitrification, biological desulphurization and plant-wide water and resource recovery facilities. In order to model, measure and control such integrated systems, a thorough understanding of the interactions between the bioprocesses and aqueous phase multiple strong and weak acid/bases are required. In the first of this series of five papers, the generalized procedure for deriving bioprocess stoichiometric equations was explained. This second paper presents the stoichiometric equations for the major biological processes and shows how their structure can be analysed to provide insight into how bioprocesses interact with the aqueous environment. Such insight is essential for confident, effective and reliable use of model development protocols and algorithms. It shows that the composite parameters, total oxygen demand (TOD, electron donating capacity) and alkalinity (proton accepting capacity), are conserved in bioprocess stoichiometry and their changes in the aqueous phase can be calculated from the bioprocess components. In the third paper, the measurement of the organics composition is presented. The link between the modelling and measurement frameworks of the aqueous phase, which uses the composite parameter alkalinity, is described in the fourth paper. Aqueous ionic speciation modelling is described in detail in the fifth.

KEYWORDS

ABBREVIATIONS

AD	anaerobic digestion
AE	algebraic equation
anammox	anaerobic ammonia oxidation
ASM1	Activated Sludge Model No. 1
BPO	biodegradable particulate organics
BSP	biosulphide potential
BSR	biological sulphate reduction
C	carbon
COD	chemical oxygen demand
DE	differential equation
e^-	electron
EDC	electron donating capacity
Eq.	equation
FBSO	fermentable biodegradable soluble organics
FSA	free and saline ammonia
FSS	free and saline sulphide
H	hydrogen
IC	inorganic carbon
LHS	left hand side
M	molal (mol/kg water)
N	nitrogen
O	oxygen
OP	orthophosphate
P	phosphorus
PAC	proton accepting capacity
pC	negative log (base 10) of the species concertation in molal units (mol/kg)
pH	Negative log (base 10) of the hydrogen ion activity

pK	Negative log (base 10) of the dissociation constant – subscripts a, c1, c2, s1, s2, p1, p2, p3 and n refer to acetate, 1st and 2nd of the IC, 1st and 2nd of the FSS, 1st, 2nd and 3rd of the OP and FSA weak acid base systems, respectively
pK'	negative log of dissociation constant corrected for ionic strength
PWM_SA	Plant Wide Model South Africa
PWMSA_AD	Plant Wide Model South Africa Anaerobic Digestion
redox	reduction oxidation
RHS	right hand side
S	sulphur
SANI	sulphate reduction autotrophic denitrification nitrification integrated system
SRUSB	sulphate reduction upflow sludge bed
TOD	total oxygen demand
UCTSDM1	University of Cape Town Sludge Digestion Model No 1
VSS	volatile suspended solids
WAS	waste activated sludge
WEST	Worldwide Engine for Simulation of wastewater Treatment plants
WRRF	water and resource recovery facility

SYMBOLS

Alk_{ed}	direct alkalinity of the electron donor component
Alk_p	persistent alkalinity of the electron donor component
Alk_T	total alkalinity in solution
ΔAlk_T	total alkalinity change of reaction
γ_B	electron donating capacity of biomass
γ_S	electron donating capacity of the electron donor
γ_{SCOD}	electron donating capacity with respect to chemical oxygen demand (COD)
γ_{STOD}	electron donating capacity with respect to total oxygen demand (TOD)
γ_e	number of e⁻/mol accepted by the electron acceptor reactant to form the product
a	molar content of nitrogen in $C_xH_yO_zN_aP_bS_c{}^{ch}$ electron donor
b	molar content of phosphorus in $C_xH_yO_zN_aP_bS_c{}^{ch}$ electron donor
c	molar content of sulphur in $C_xH_yO_zN_aP_bS_c{}^{ch}$ electron donor
ch	charge of $C_xH_yO_zN_aP_bS_c{}^{ch}$ electron donor
chr	charge of $C_dH_eO_fN_gS_h{}^{chr}$ electron acceptor reactant
chp	charge of $C_rH_tO_uN_vS_w{}^{chp}$ electron acceptor product
d	molar content of carbon in $C_dH_eO_fN_gS_h{}^{chr}$ electron acceptor reactant
E	proportion of the utilized electron donor that becomes biomass and endogenous residue

e molar content of hydrogen in $C_dH_eO_fN_gS_h{}^{chr}$ electron acceptor reactant

e^- electron

f molar content of oxygen in $C_dH_eO_fN_gS_h{}^{chr}$ electron acceptor reactant

f_{hs} fraction of free (H_2S) and saline (HS^-) sulphide (FSS) that is free (H_2S)

f_{op} fraction of the ortho-P (OP), approximated by $H_2PO_4{}^- + HPO_4{}^{2-}$, that is ($H_2PO_4{}^-$)

g molar content of nitrogen in $C_dH_eO_fN_gS_h{}^{chr}$ electron acceptor reactant

h molar content of sulphur in $C_dH_eO_fN_gS_h{}^{chr}$ electron acceptor reactant

j mol/L dissociated VFA (approximated by Ac^-) in AD influent

k molar content of carbon in $C_kH_lO_mN_nP_pS_s$ biomass

l molar content of hydrogen in $C_kH_lO_mN_nP_pS_s$ biomass

m molar content of oxygen in $C_kH_lO_mN_nP_pS_s$ biomass

n molar content of nitrogen in $C_kH_lO_mN_nP_pS_s$ biomass

N_T total free and saline ammonia (FSA) species concentration

p molar content of phosphorus in $C_kH_lO_mN_nP_pS_s$ biomass

P_t total ortho-P (OP) species concentration

q ratio of the carbon (d/r), nitrogen (g/v) or sulphur (h/w) molar content of the electron acceptor reactant and product or 0 if O_2 is electron acceptor.

r molar content of carbon in $C_rH_tO_uN_vS_w{}^{chp}$ electron acceptor product

s molar content of sulphur in $C_kH_lO_mN_nP_pS_s$ biomass

t molar content of hydrogen in $C_rH_tO_uN_vS_w{}^{chp}$ electron acceptor product

u molar content of oxygen in $C_rH_tO_uN_vS_w{}^{chp}$ electron acceptor product

v molar content of nitrogen in $C_rH_tO_uN_vS_w{}^{chp}$ electron acceptor product

w molar content of sulphur in $C_rH_tO_uN_vS_w{}^{chp}$ electron acceptor product

x molar content of carbon in $C_xH_yO_zN_aP_bS_c{}^{ch}$ electron donor

y molar content of hydrogen in $C_xH_yO_zN_aP_bS_c{}^{ch}$ electron donor

Y biomass yield coefficient

z molar content of oxygen in $C_xH_yO_zN_aP_bS_c{}^{ch}$ electron donor

INTRODUCTION

A generalized approach to deriving bioprocess stoichiometry was presented in Part 1 of this series (Brouckaert et al., 2021). Integrating the bioprocess stoichiometry with aqueous phase mixed weak and strong acid/base chemistry for pH prediction is necessary because some bioprocesses or combinations of bioprocesses have a strong influence and/or dependence on pH. Examples of technologically relevant bioprocesses, where accurate pH prediction is important, include methanogenic anaerobic digestion (AD) of (i) high strength low nitrogen (N) industrial organics wastewater which require alkalinity addition to maintain a stable AD pH above 7 (Van Zyl et al., 2008), (ii) co-digestion of sewage sludge and high strength variable N organics such as whey, vinasse or food waste for energy generation, and (iii) co-

digestion of sewage primary sludge and phosphorus (P) rich waste activated sludge at biological N and P removal plants in which significant mineral precipitation can take place (Van Rensburg et al., 2003; Harding et al., 2011). The expression of the stoichiometric balances in terms of a linearly independent set of equilibrium speciation model components, as advocated in Part 1 (Brouckaert et al., 2021), results in a compact and flexible formulation which can be conveniently integrated with speciation models in both steady-state and dynamic models. However, the bioprocess stoichiometric balances derived in this way provide little insight into the weak acid/base chemistry that has an important role in governing the overall system behaviour.

The purpose of this paper, Part 2, is to take a deeper look at the stoichiometry of the major bioprocesses included in wastewater treatment models, as well as their interactions with the multiple strong and weak acid/base systems. Part 2 therefore will contribute the following:

- Derivation of the major bioprocess stoichiometry using the ionic components introduced in Part 1 (Brouckaert et al., 2021)
- Derivation of empirical formulae for complex organic and inorganic components in terms of their carbon (C), hydrogen (H), oxygen (O), nitrogen (N), phosphorus (P), sulphur (S) and charge (ch) content
- Demonstrating how an understanding of the weak acid/base chemistry can be used to construct a simplified speciation model that is appropriate for some steady-state bioprocess models
- Exploring the application of the general principles discussed to two major bioprocesses typically included in water resource and recovery facility (WRRF) models, i.e., methanogenesis and sulphidogenesis

In this paper, the mass-balanced stoichiometry of bioprocess models including P, S and charge, with some of their associated bioprocesses, are derived with the objectives of: (i) demonstrating the general principles of integrated bioprocess and aqueous phase modelling; and (ii) deriving the complete elemental CHONPS, charge and chemical oxygen demand (COD) mass-balanced stoichiometry for some bio-systems, based on the S cycle, such as BSR in acid mine drainage (Poinapen and Ekama, 2010b), the sulphate reduction autotrophic denitrification nitrification integrated system (SANI) process for saline sewage treatment (Lu et al., 2012), leachate treatment and anaerobic and intermittently aerated landfill treatment (Raga et al., 2011) and co-treatment of simplified wet flue gas desulphurization wastewater (Qian et al., 2013, 2015). The procedure is general, and can be applied to any bioprocess, including those not considered in this paper.

BIOPROCESS STOICHIOMETRY AND EXCHANGED ELECTRONS

As noted in Part 1 (Brouckaert et al., 2021), the mass-balanced stoichiometry for bioprocesses can be derived from the procedure of electron (e^-) balance of McCarty (1975). This procedure was advanced by Gujer and Larsen (1995) and Takács and Vanrolleghem (2006), applied to steady-state models by Ekama (2009) and generalized for WRRF models by Grau et al. (2007). This series of papers extends the methodology by adding S and charge and shows the intimate connection between the bioprocesses and

the aqueous phase mixed strong and weak acid/base systems within which they function for both dynamic and steady-state plant-wide WRRF models. This brings the aqueous phase behaviour and pH calculation in bioprocess models from the background to equal importance with the bioprocesses.

The primary purpose of biological WRRFs is usually to reduce the COD of the waste, by breaking down complex organic compounds and/or inorganic pollutants such as ammonia, sulphide, sulphite or thiosulphate, into simpler benign or re-usable molecules and ions, such as CO_2, H_2O, CH_4, N_2, SO_4^{2-} or HS^- Synthesis and maintenance of the active biomass, required to mediate these bioprocesses, also consume some of the influent COD and nutrients. The excess biomass produced is typically separated into a concentrated sludge, which is further reduced in volume and COD content by digestion. All of these biological transformations involve reduction-oxidation (redox) reactions and the key prior system knowledge, required to construct the appropriate bio-chemical stoichiometric balances, concerns which electron donors and electron acceptors are involved in which transformations under which operating conditions, and what the products of these reactions are.

Eight common bioprocesses can take place under anaerobic, anoxic and aerobic conditions, such as in activated sludge, BSR, AD and intermittently aerated (partially aerobic) landfill systems. The electron donors and acceptors for these eight bioprocesses are listed in Table 2-1. The electron (e^-) donor is the substrate for growth of a particular organism mediating a particular bioprocess. The interaction of these bioprocesses in intermittently aerated landfill waste (Raga et al., 2011) is shown in Figure 2-1.
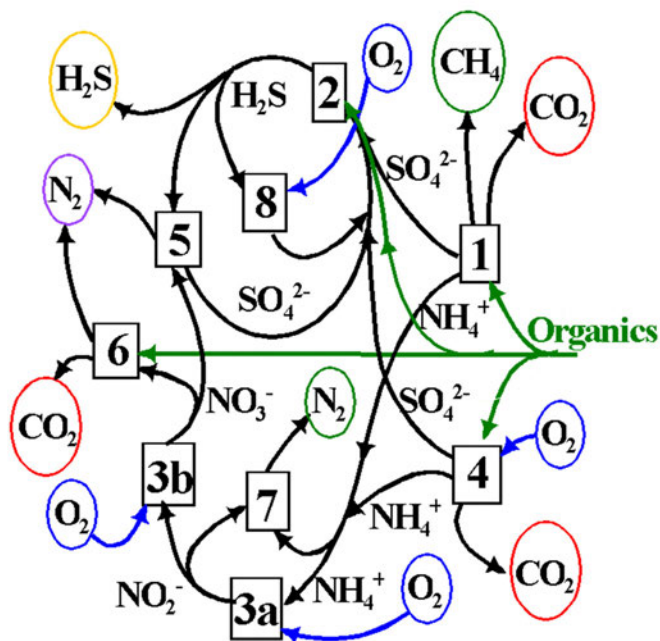
Figure 2-1. *Interaction of the eight bioprocesses listed in Table 2-1 in intermittently aerated landfill solid waste in which products of one bioprocess become reactants for another. The numbers in boxes refer to the bioprocess numbers in Table 2-1, circled components are dissolved or gaseous reactants and products and the ionized reactants and products are in the aqueous phase.*

Table 2-1. *Some bioprocesses that can take place in anaerobic, anoxic and aerobic liquid and solid waste treatment systems. Stoichiometric details of these bioprocesses are given in Table 2-4.*

	Bioprocess	Environment	Electron donor reactant	Electron donor product	Electron acceptor reactant	Electron acceptor product
1	Methanogenesis	Anaerobic	Organics ($C_xH_yO_zN_aP_bS_c^{ch}$)	Carbonate (CO_3^{2-})	Carbonate (CO_3^{2-})	Methane (CH_4)
2a	Sulphidogenesis	Anaerobic	Organics ($C_xH_yO_zN_aP_bS_c^{ch}$)	Carbonate (CO_3^{2-})	Sulphate (SO_4^{2-})	Sulphide (HS^-)
2b	Sulphidogenesis	Anaerobic	Organics ($C_xH_yO_zN_aP_bS_c^{ch}$)	Carbonate (CO_3^{2-})	Sulphite (SO_3^{2-})	Sulphide (HS^-)
2c	Sulphidogenesis	Anaerobic	Organics ($C_xH_yO_zN_aP_bS_c^{ch}$)	Carbonate (CO_3^{2-})	Thiosulphate ($S_2O_3^{2-}$)	Sulphide (HS^-)
2d	Sulphidogenesis	Anaerobic	Organics ($C_xH_yO_zN_aP_bS_c^{ch}$)	Carbonate (CO_3^{2-})	Sulphite (SO_3^{2-})	Thiosulphate ($S_2O_3^{2-}$)
3	Nitrification (NH_4^+ to NO_3^-)	Aerobic	Ammonia (NH_4^+)	Nitrate (NO_3^-)	Oxygen (O_2)	Water (H_2O)
3a	Nitrification (NH_4^+ to NO_2^-)	Aerobic	Ammonia (NH_4^+)	Nitrite (NO_2^-)	Oxygen (O_2)	Water (H_2O)
3b	Nitrification (NO_2^- to NO_3^-)	Aerobic	Nitrite (NO_2^-)	Nitrate (NO_3^-)	Oxygen (O_2)	Water (H_2O)
4	Aerobic hetero Growth	Aerobic	Organics ($C_xH_yO_zN_aP_bS_c^{ch}$)	Carbonate (CO_3^{2-})	Oxygen (O_2)	Water (H_2O)
5a	Autotrophic Denitrification	Anoxic	Sulphide (HS^-)	Sulphate (SO_4^{2-})	Nitrate (NO_3^-)	Nitrogen gas (N_2)
5b	Autotrophic Denitrification	Anoxic	Sulphite (SO_3^{2-})	Sulphate (SO_4^{2-})	Nitrate (NO_3^-)	Nitrogen gas (N_2)
5c	Autotrophic Denitrification	Anoxic	Thiosulphate ($S_2O_3^{2-}$)	Sulphate (SO_4^{2-})	Nitrate (NO_3^-)	Nitrogen gas (N_2)
6	Hetero Denitrification	Anoxic	Organics ($C_xH_yO_zN_aP_bS_c^{ch}$)	Carbonate (CO_3^{2-})	Nitrate (NO_3^-)	Nitrogen gas (N_2)
6a	Hetero Denitrification	Anoxic	Organics ($C_xH_yO_zN_aP_bS_c^{ch}$)	Carbonate (CO_3^{2-})	Nitrate (NO_3^-)	Nitrite (NO_2^-)
6b	Hetero Denitrification	Anoxic	Organics ($C_xH_yO_zN_aP_bS_c^{ch}$)	Carbonate (CO_3^{2-})	Nitrite (NO_2^-)	Nitrogen gas (N_2)
7	[2]Anammox	Anoxic	Ammonia (NH_4^+)	Nitrogen gas (N_2)	Nitrite (NO_2^-)	Nitrogen gas (N_2)
8	Aerobic sulphide oxidation	Aerobic	Sulphide (HS^-)	Sulphate (SO_4^{2-})	Oxygen (O_2)	Water (H_2O)

[2]Anaerobic ammonia oxidation

To illustrate the procedure of formulating biological process stoichiometry, consider the oxidation of a generic organic or inorganic component $C_xH_yO_zN_aP_bS_c^{ch}$ by O_2 under conditions such that the resulting set of reactants and products include CO_3^{2-}, NO_3^-, PO_4^{3-}, SO_4^{2-}, H^+ and H_2O, which are the products of C, N, P, and S. These are products of aerobic heterotrophic growth and nitrification (combined Bioprocess 3 and 4 in Table 2-1). Following the methodology presented in Part 1 (Brouckaert et al., 2021), the reaction equation is derived from the CHONPS element and charge balances.

$$C_xH_yO_zN_aP_bS_c^{ch} + (4x+y-2z+5a+5b+6c-ch)\frac{1}{4}O_2 + (2x-y+a+3b+2c+ch)\frac{1}{2}H_2O$$
$$\rightarrow (2x+a+3b+2c+ch)H^+ + xCO_3^{2-} + aNO_3^- + bPO_4^{3-} + cSO_4^{2-} \tag{1}$$
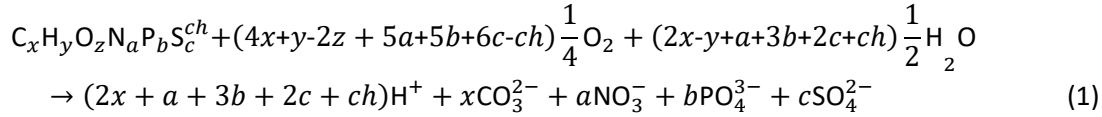
The term $(4x + y - 2z + 5a + 5b + 6c - ch)$ represents the **exchanged electrons** (γ_s, e⁻/mol donor) (Part 1, Brouckaert et al., 2021), for the selected set of electron (e⁻) donor and acceptor reactants and products, i.e:

$$\gamma_s = (4x + y - 2z + 5a + 5b + 6c - ch) \tag{2}$$

So Eq. 1 becomes:

$$C_xH_yO_zN_aP_bS_c^{ch} + \frac{\gamma_s}{4}O_2 + (2x - y + a + 3b + 2c + ch)\frac{1}{2}H_2O \rightarrow (2x + a + 3b + 2c + ch)H^+ +$$
$$xCO_3^{2-} + aNO_3^- + bPO_4^{3-} + cSO_4^{2-} \tag{3}$$
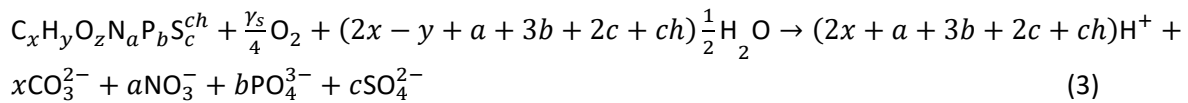
Equations 1 and 3 are given in arrow notation with reactants on the left-hand side (LHS) and products on the right-hand side (RHS) of the arrow. This notation conveys the idea that a stoichiometric equation represents a directional vector of changes in composition that the element balances allow. The equations can also be written in Gujer notation, with reactants −ve and products +ve, summing to zero. This has the advantage that it corresponds to the output of a computational stoichiometry generator (Part 1, Brouckaert et al., 2021) and corresponds with the way in which reaction processes are set up in modelling software. In this paper, the reaction equations use arrow notation, and stoichiometry tables use Gujer notation.

Note that Eqs 1 and 3 are expressed in terms of ionic **components** which, as discussed in Part 1 (Brouckaert et al., 2021), do not necessarily correspond to the actual species present in the aqueous phase. In a dynamic bioprocess model, Eq. 3 gives the change in component amounts over a particular time step governed by a kinetic ordinary differential equation (ODE). The calculation for the integration step can be completed by using the algebraic aqueous-phase speciation model discussed in Parts 1 and 5 (Brouckaert et al., 2021) which calculates the distribution of species actually present (e.g. $H_2PO_4^-$, HPO_4^{2-}, PO_4^{3-}) and corresponding pH, subject to the component mass balances and thermodynamic dissociation equilibrium equations.

 As discussed in Part 1 (Brouckaert et al., 2021), the traditional approach of dividing bioprocesses into electron donor and acceptor half-reactions is not necessary to achieve element- and charge-balanced stoichiometry for the overall reaction. However, breaking the overall reaction into its constituent parts facilitates better understanding of the reaction, and allows combining e⁻ donors with different e⁻ acceptors.

Indeed, since a stoichiometric equation is a linear element and electron balance, all manner of linear transformations can be applied to it to highlight specific issues. The issues which are of most interest for understanding the impacts of the bioprocess on solution properties are the transfers of electrons and protons (H^+ ions) between oxidants, reductants, organic and inorganic components, and the mediating micro-organisms. Thus, the overall reactions can be broken down into electron donor, electron acceptor, anabolic (providing material for micro-organism growth) and catabolic (providing energy to drive the anabolic process) reactions, where the anabolic and catabolic processes are the electron sinks and together form the metabolism of the organism. Furthermore, the reactions can be split into the contributions of each of the CHONP and S elements and charge separately – the overall reaction is then simply the sum of the individual element and charge contributions. These appear in Eq. 5e and more generally in Table 2-2.

The overall bioprocess redox reaction can be formally split into two half-reactions, in which the electrons transferred from the electron donor to the electron acceptor are explicitly shown, i.e.:

$$C_xH_yO_zN_aP_bS_c^{ch} + (3x - z + 3a + 4b + 4c)H_2O \rightarrow (6x + y - 2z + 6a + 8b + 8c)H^+ + xCO_3^{2-} + aNO_3^- + bPO_4^{3-} + cSO_4^{2-} + \gamma_s e^- \qquad (4a)$$
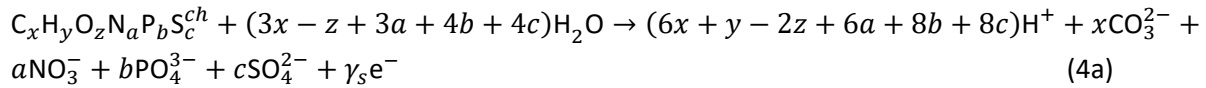
and if oxygen (O_2) is the electron acceptor as in Eq. 1:

$$\gamma_s(H^+ + e^-) + \frac{\gamma_s}{4}O_2 \rightarrow \frac{\gamma_s}{2}H_2O \qquad (4b)$$
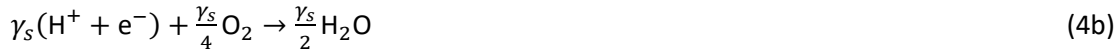
Equation 4b shows oxygen accepting $4e^-$ per mol, or 32/4 = 8 gO/e$^-$. Other electron acceptors can be considered, such as NO_3^- or SO_4^{2-}, yielding different electron acceptor products, such as NO_2^-, N_2, SO_3^{2-}, $S_2O_3^{2-}$ or H_2S, as presented in Table 2-1. To repeat: the selection of the electron acceptor reactants and products is based on knowledge of the bio-process, and needs to be determined beforehand to derive its stoichiometry.

In Eq. 4a, the generic electron donor $C_xH_yO_zN_aP_bS_c^{ch}$ reacts to form particular oxidized products of each of its constituent elements, giving up y_s electrons, which are taken up by the electron acceptor O_2 according to Eq. 4b.

Rearranging Eq. 4a to pair the terms $\gamma_s e^-$ and $\gamma_s H^+$ yields:

$$C_xH_yO_zN_aP_bS_c^{ch} + (3x - z + 3a + 4b + 4c)H_2O \rightarrow (2x + a + 3b + 2c + ch)H^+ + xCO_3^{2-} + aNO_3^- + bPO_4^{3-} + cSO_4^{2-} + \gamma_s(e^- + H^+) \qquad (4c)$$
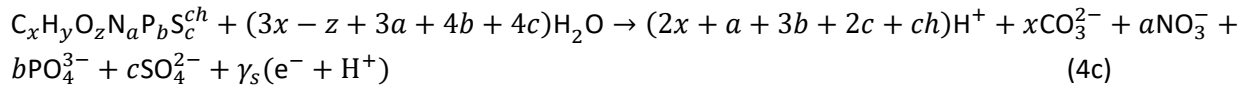
This pairing of some of the protons with electrons in the redox half-reactions, Eq. 4b and Eq. 4c, is discussed further in later sections; suffice to state here that any H^+ **not** paired with an e$^-$ affects the aqueous-phase alkalinity and pH. The next sections discuss the key features that electron donor (source) and electron acceptor (destination) reactions have in common, and demonstrate how the general equations are applied to specific bioprocesses.

ELECTRON (E⁻) DONOR REACTIONS

An electron donor reaction is a half-reaction in which a substrate (electron donor) or other chemical component reactant gives up electrons to produce more oxidized forms of its constituent elements as in Eq. 4a.

Oxidation products

The first important point to note is that the redox state of the oxidation products of the electron donor reaction is determined by the bioprocess. Equation 4a represents the oxidation of the electron donor to H^+, CO_3^{2-}, NO_3^-, PO_4^{3-} and SO_4^{2-} as could occur under aerobic conditions. However, organics degradation and nitrification under aerobic conditions are mediated by different organisms, and so are modelled as separate bioprocesses. Furthermore, under anaerobic conditions, the oxidation products for N and S are expected to be NH_4^+ and HS^-, respectively, noting that NH_4^+ and HS^- are **standard aquatic chemistry components** by convention (Part 5 of this series), and are components, not species. For the NH_4^+ and HS^- components, the general electron donor reaction is:

$$C_xH_yO_zN_aP_bS_c^{ch} + (3x - z + 4b)H_2O$$

$$\rightarrow (6x + y - 2z - 4a + 8b - c)H^+ + xCO_3^{2-} + aNH_4^+ + bPO_4^{3-} + cHS^- + \gamma_s e^- \tag{5a}$$
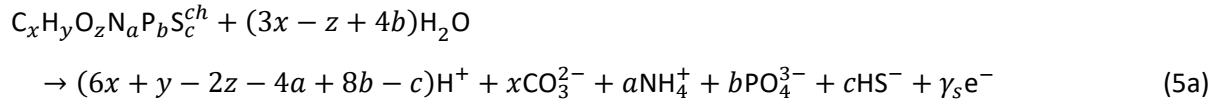
Equation 5a applies to the aerobic degradation of organics when nitrification and sulphide oxidation are modelled as separate reactions; to the anaerobic degradation of organics where the N and S end-products are NH_4^+ and HS^-; and to BSR where the electron acceptor is SO_4^{2-}, SO_3^{2-} or $S_2O_3^{2-}$ (Bioprocesses 2a–2c). Rearranging Eq, 5a so that all bracketed terms have no net charge, and e⁻ is paired with H^+, yields:

$$C_xH_yO_zN_aP_bS_c^{ch} + (3x - z + 4b)H_2O$$
$$\rightarrow x\left(2H^+ + CO_3^{2-}\right) + a(NH_4^+ - H^+) + b\left(3H^+ + PO_4^{3-}\right) + c(H^+ + HS^-)$$
$$+ (\gamma_s + ch)(H^+ + e^-) - ch\, e^- \tag{5b}$$
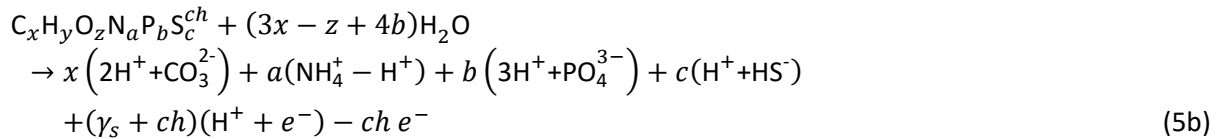
where the **exchanged electrons** γ_s of Eq. 5a is now given by:

$$\gamma_s = (4x + y - 2z - 3a + 5b - 2c) - ch \tag{6}$$

Note that γ_s in Eq. 6 is also referred to as the **electron donating capacity** (EDC) of the electron donor. However, the EDC is not a function of the electron donor only, but also of the reaction products, which, in turn, depend on the conditions under which the reaction takes place (e.g. aerobic, anoxic or anaerobic). When reaction balances are set up in terms of 1 mol of substrate as in Eq. 2, then the exchanged electrons of reaction will equal the EDC of the substrate.

The difference between Eqs 2 and 6 for γ_s is that NH_4^+ and HS^- are the oxidation products of the N and S elements in Eq. 5a instead of NO_3^- and SO_4^{2-} in Eq. 1. Because NH_4^+ and HS^- can each donate 8e⁻ to become NO_3^- and SO_4^{2-}, respectively, the γ_s of Eq. 6 is 8a and 8c e⁻/mol lower than the γ_s of Eq. 2, i.e., the coefficients of the a and c terms in the γ_s equation have changed from +5 and +6 in Eq. 2 to −3 and −2 in Eq. 6. The 8 e⁻/mol electron donating capacity (EDC) of each of the NH_4^+ and HS^- lead to the well-

known 4.57 gO/gN ammonia nitrified to nitrate (from 8 e⁻/mol x 8 gO/e⁻ divided by 14 gN/mol) and 2.0 gO/gS sulphide oxidized to sulphate (from 8 e⁻/mol x 8 gO/e⁻ divided by 32 gS/mol).

Pairing the e⁻ and H⁺ in Eq. 5a yields:

$$C_xH_yO_zN_aP_bS_c^{ch} + (3x - z + 4b)H_2O$$

$$\rightarrow (2x - a + 3b + c + ch)H^+ + xCO_3^{2-} + aNH_4^+ + bPO_4^{3-} + cHS^- + \gamma_s(e^- + H^+) \qquad (5c)$$
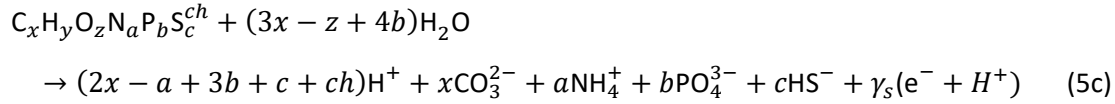
Eq. 5b can also be written as Eq. 5d below, viz.

$$C_xH_yO_zN_aP_bS_c^{ch} + (3x - z + 4b)H_2O \rightarrow xH_2CO_3 + aNH_3 + bH_3PO_4 + cH_2S + (\gamma_s + ch)(H^+ + e^-) - ch\ e^-$$

$$(5d)$$
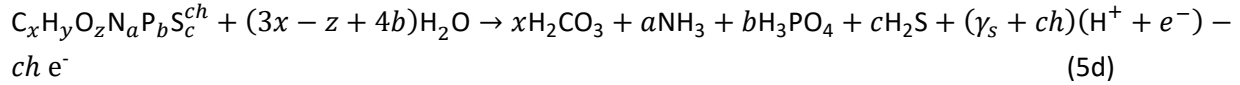
and γ_s remains equal to Eq. 6, showing that the protonated form of the selected reaction product components does not affect the exchanged electrons of the reaction.

Furthermore, as mentioned above, Eq. 5d can be considered the sum of reactions involving individual elements, which are shown in Eq. 5e and more generally in Table 2-2:

$$C_x \quad + 3x\ H_2O \rightarrow x\ H_2CO_3 \quad + 4x\ (H^+ + e^-)$$

$$H_yO_z - z\ H_2O \rightarrow \qquad\qquad (y - 2z)\ (H^+ + e^-)$$

$$N_a \qquad\qquad \rightarrow a\ NH_3 \quad - 3a\ (H^+ + e^-)$$

$$P_b \quad + 4b\ H_2O \rightarrow b\ H_3PO_4 \quad + 5b\ (H^+ + e^-)$$

$$S_c \qquad\qquad \rightarrow c\ H_2S \quad - 2c\ (H^+ + e^-)$$

$$(..)^{ch} \qquad\qquad \rightarrow (-ch)\ e^- \qquad\qquad\qquad\qquad\qquad (5e)$$
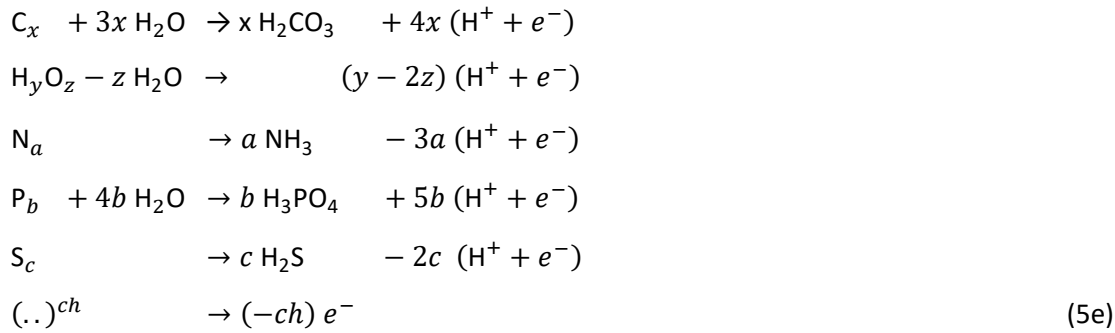
The disaggregation of the reaction stoichiometry in Eq. 5e is the basis of Table 2-2. Equation 5d is reconstructed by adding Rows 1b, 2, 3, 4a, 5b, 6a and 7. The alkalinity with respect to the most protonated species imparted to the aqueous phase by the electron donor is included in Table 2-2. The sum of the relevant rows in Column 7 of Table 2-2 yields the alkalinity of the reaction products $\sum$ Alk$_{Tproducts}$. The overall alkalinity change of reaction depends on the alkalinity of the electron donor Alk$_{ed}$ as discussed in Part 1 (Brouckaert et al., 2021).

The equality of the γ_s of Eqs 5a, 5b, 5c, 5d and 5e confirms that the protonated forms chosen for the reactants and products do not change the EDC of the electron donor reaction, e.g., the EDC (or γ_s) of the H_2CO_3 and CO_3^{2-} are both zero. This can also be shown with the γ_s of Eq. 6 (or 2): For H_2CO_3, γ_s = 4 x 1 + 1 x 2−2 x 3 + 5 x 0 + 5 x 0 + 6 x 0 − 0 = 0 and for CO_3^{2-}, γ_s = 4 x 1 + 1 x 0 − 2 x 3 + 5 x 0 + 5 x 0 + 6 x 0 −(−2) = 0. In general, the γ_s equation can be applied to each part of an electron donor reaction to give the EDC of that part relative to the oxidation state selected for each CHONP and S element.

Table 2-2. *Individual element electron donor reactions in Gujer matrix format with exchanged electrons and protons and alkalinity produced as a function of the oxidation product*

Row	Element	H_2O	Oxidation product	H^+	Exchanged electrons e^-	Mass[a] balance	$Alk_p{}^{[b]}$ contribution
	1	2	3	4	5	6	7
1a	$-C_x$	$-3x$	$+x\ CO_3{}^{2-}$	$+6x$	$+4x$	0	0
1b	$-C_x$	$-3x$	$+x\ H_2CO_3$	$+4x$	$+4x$	0	0
2	$-H_y$	0	0	$+y$	$+y$	0	0
3	$-O_z$	0	$+z\ H_2O$	$-2z$	$-2z$	0	0
4a	$-N_a$	0	$+a\ NH_3$	$-3a$	$-3a$	0	$+a$
4b	$-N_a$	0	$+a\ NH_4$	$-4a$	$-3a$	0	$+a$
4c	$-N_a$	0	$+\dfrac{a}{2}N_2$	0	0	0	0
4d	$-N_a$	$-2a$	$+a\ NO_2{}^-$	$+4a$	$+3a$	0	$-a$
4e	$-N_a$	$-3a$	$+a\ NO_3{}^-$	$+6a$	$+5a$	0	$-a$
5a	$-P_b$	$-4b$	$+b\ PO_4{}^{3-}$	$+8b$	$+5b$	0	0
5b	$-P_b$	$-4b$	$+b\ H_3PO_4$	$+5b$	$+5b$	0	0
6a	$-S_c$	0	$+c\ H_2S$	$-2c$	$-2c$	0	0
6b	$-S_c$	0	$+c\ HS^-$	$-c$	$-2c$	0	0
6c	$-S_c$	$-\dfrac{3}{2}c$	$+\dfrac{c}{2}S_2O_3^{2-}$	$+3c$	$+2c$	0	$-c$
6d	$-S_c$	$-3c$	$+c\ SO_3{}^{2-}$	$+6c$	$+4c$	0	$-2c$
6e	$-S_c$	$-4c$	$+c\ SO_4{}^{2-}$	$+8c$	$+6c$	0	$-2c$
7	$-ch$	0	0	0	$-ch$	0	$-ch$

[a]Reactants (Columns 1 and 2) are given a −ve sign to represent consumption, and products (Columns 3 to 5) are given a +ve sign to represent production, as in a Gujer matrix. Each constituent part of each reaction sums to zero across each row to conform to mass balance as indicated in Row 6. The procedure is general and applies to weak and strong acid/bases, e.g. $NH_4S_2O_3{}^-$

[b]The persistent alkalinity contribution (Column 7) with respect to the most protonated species of the IC, FSA, OP, sulphide and acetate weak-acid/bases is the number of weak-acid anion equivalents produced by the reaction, minus the number of protons produced that can associate with them, i.e., excluding those paired with electrons (Eq. 5c). So the Alk_p in Column 7 is given by (Column 5 − Column 4) + NxColumn 3, where N is the number of H^+ that can be accepted by the weak-acid/base oxidation product to make reference species (strong acids remain fully dissociated), e.g. for Row 5a: $5b - 8b + 3(b) = 0$. For a given electron donor reaction, alkalinity of the reaction products, $\Delta Alk_{Tproducts}$ (Eq. 20, Part 1, Brouckaert et al., 2021) is obtained by adding the alkalinity contributions in Column 7 of the relevant rows; e.g. Alk_p for Eq. 5c is obtained by adding Row 1a, 2, 3, 4b, 5a, 6b and 7 = $0 + 0 + 0 + a + 0 + 0 - ch = a - ch$. Note that H^+ and e^- are always included in the calculation of $\Delta Alk_{Tproducts}$ from Table 2-2 even if they have a negative sign. To calculate the alkalinity change of reaction, subtract the direct alkalinity of the electron donor ($\Delta Alk_T = Alk_p - Alk_{ed}$).

Exchanged electrons (of reaction)

As discussed previously, the McCarty (1975) approach is based on the concept of an electron balance. The advantage of breaking the overall balanced stoichiometry into half-reactions is that it highlights both the source and destination of the **exchanged electrons γ_s** and it allows pairing of electron donor reactions with different electron acceptor reactions. The exchanged electrons in the electron donor reaction are a function of the change in oxidation state of the constituent elements of the electron donor, and are therefore a stoichiometric property of the reaction, depending on both the composition of the electron donor and the oxidation state of the reaction products. Because Eq. 1 is written in terms of the most oxidized products of each constituent element in the electron donor, γ_s in Eq. 2 is the maximum number of exchangeable electrons, whereas γ_s in Eq. 6 is not the maximum possible because the NH_4^+ and HS^- products can still donate electrons. McCarty used the term **exchangeable electrons**, which suggests that they are a property of just the substrate, whereas in fact they depend on all the components participating in the half-reaction. So a more suitable term, **exchanged electrons of reaction**, has been adopted for this series of papers, with **exchanged electrons** as an abbreviation.

Extending the pattern of Eq. 5e, Table 2-2 shows the contribution of each element in the electron donor to the exchanged electrons as a function of the oxidation product of the N and S elements. While the protonated state of the C and P components may be different, their oxidation state is the same in all the bioprocesses considered here. For the purpose of calculating the exchanged electrons, each element in the generic electron donor is treated as having an oxidation state of zero. The true oxidation state of each atom in the electron donor might not actually be zero. However, since the electrons involved are just re-distributed within the molecular structure, the net effect is the same as assuming that their oxidation states are all zero. Consider the contribution of carbon: Because the C in $C_xH_yO_zN_aP_bS_c^{ch}$ all becomes CO_3^{2-} (or H_2CO_3), where it has an oxidation state of +4 (a deficiency of 4 electrons), the electron donor component donates 4 electrons per carbon atom, hence the $4x$ in Eqs 2 and 6. The total exchanged electrons or γ_s for a given reaction is the sum of the contributions from each element in $C_xH_yO_zN_aP_bS_c^{ch}$, as summarized in Table 2-2, Column 5. The terms of the γ_s equation associated with the different oxidation products of N and S are obtained by summing the relevant rows in Column 5. For example, the γ_s term associated with Eq. 5a with NH_4^+ and HS^- as oxidation products is obtained by adding Rows 1a, 2, 3, 4b, 5a, 6b and 7 in Column 5. Similarly, the γ_s terms for Eq. 1 are obtained by adding Rows 1a, 2, 3, 4e, 5a, 6e and 7 in Column 5.

It can be seen from Table 2-2 that only the selection of the oxidation state of the products affects the exchanged electrons (γ_s), not which components are selected to represent the oxidation products. For all the reactions considered here, C, H, O and P always contribute +4, +1, −2 and +5 to γ_s relative to their elemental state. The electron contributions of N and S to the γ_s depend on the specific electron donor product oxidation states involved, and may be positive, zero or negative. If the oxidation state of the N and S are the most oxidized form, i.e., NO_3^- and SO_4^{2-}, their coefficients in the γ_s equation are +5 and +6 because they donate 5 and 6 e^- relative to their elemental N and S state (Eq. 2). If the oxidation state of the N and S are the least oxidized form, i.e., NH_4^+ and H_2S, their coefficients in the γ_s equation are −3 and −2 because now they take up 3 and 2 e^- relative to their elemental state (Eq. 6). The coefficients of the

γ_S equation associated with the oxidation products of CHONP and S elements are shown schematically in Figure 2-2.

Electron state and coefficient in the EDC (γ_S) equation													
e⁻ state, e- donating capacity →						e- state, ← e⁻ accepting capacity							
	-5	-4	-3	-2	-1	0	+1	+2	+3	+4	+5	+6	+7
Coefficient in γ_S equation	-5	-4	-3	-2	-1	0	+1	+2	+3	+4	+5	+6	+7
x	CH_4					C 12				CO_2			
y						H 1	H_2O						
z				H_2O		O 16							
a		NH_4^+				N 14			NO_2^-		NO_3^-		
b						P 31					PO_4^{3-}		
c			H_2S			S 32		$S_2O_3^{2-}$		SO_3^{2-}, SO_2		SO_4^{2-}	
d						B 10			BO_3^{3-}				

Figure 2-2. *Electron (oxidation) state of different components involved in bioprocesses relative to their zero electron state (0, centre column). The EDC (or the electron-accepting capacity EAC = −EDC) is equal to the electron state difference between two components of the same element, EDC from left to right and EAC from right to left; e.g. ammonia's EDC relative to nitrate = +5 − (−3) = +8 e⁻/mol, nitrate's EDC (−EAC) relative to nitrogen gas = 0 − (+5) = −5 e⁻/mol (or EAC = +5 e⁻/mol, so nitrate can accept 5 e⁻/mol), and the EDC of methane relative to CO_2 is 4 − (−4) = +8 e /mol.*

Composition of the electron donor

As discussed in Part 1 (Brouckaert et al., 2021), having precise element and electron balanced bioprocess stoichiometry is key to successfully integrating bioprocess and physico-chemical reaction models. This is a particular challenge for bioprocess models since wastewater typically consists of a diverse mixture of complex organic molecules of unknown composition and structure. The convention adopted in this series of papers, and in the plant-wide WRRF model based on this approach, PWM_SA (Ikumi et al., 2011, 2014, 2015), is to represent each group of complex organic substrates (soluble, particulate, biodegradable, unbiodegradable, settleable, non-settleable) by the generalized empirical formula $C_xH_yO_zN_aP_bS_c^{ch}$, where the stoichiometric coefficients *x, y, z, a, b* and *c* can be calculated from the mass fractions of the various elements determined by wastewater characterization (Part 3 of this series).

Note that the composition of any electron donor containing any combination of CHONPS can be obtained by substituting the appropriate values of the stoichiometric coefficients *x, y, z, a, b, c* and ch into the general formula. This includes simple organics like acetate and inorganic substrates such as thiosulphate and nitrite. Similarly, the exchanged electrons of reaction for complete oxidation of any such electron donor can be derived from Eq. 2, because in Eq. 2 all the elements are in their most oxidized state as far as bioprocesses are concerned. Furthermore, any of the oxidation reactions can also be derived as a linear combination of the oxidation reactions of the constituent elements of the electron donor (Table 2-2). Common examples are listed below.

Ammonia to nitrate: $x = 0$, $y = 4$, $z = 0$, $a = 1$, $b = 0$, $c = 0$, $ch = +1$

$$NH_4^+ + 3H_2O \rightarrow NO_3^- + 2H^+ + 8(H^+ + e^-) \tag{7a}$$

Ammonia to nitrite:

$$NH_4^+ + 2H_2O \rightarrow NO_2^- + 2H^+ + 6(H^+ + e^-) \tag{7b}$$

Nitrite to nitrate: $x = 0$, $y = 0$, $z = 2$, $a = 1$, $b = 0$, $c = 0$, $ch = -1$

$$NO_2^- + H_2O \rightarrow NO_3^- + 2(H^+ + e^-) \tag{7c}$$

Ammonia to nitrogen gas:

$$NH_4^+ \rightarrow N_2 + H^+ + 3(H^+ + e^-) \tag{8}$$

Sulphide to sulphate: $x = 0$, $y = 1$, $z = 0$, $a = 0$, $b = 0$, $c = 1$, $ch = -1$

$$HS^- + 4H_2O \rightarrow SO_4^{2-} + H^+ + 8(H^+ + e^-) \tag{9a}$$

Sulphite to sulphate: $x = 0$, $y = 0$, $z = 3$, $a = 0$, $b = 0$, $c = 1$, $ch = -2$

$$SO_3^{2-} + H_2O \rightarrow SO_4^{2-} + 2(H^+ + e^-) \tag{9b}$$

Thiosulphate to sulphate: $x = 0$, $y = 0$, $z = 3$, $a = 0$, $b = 0$, $c = 2$, $ch = -2$

$$S_2O_3^{2-} + 5H_2O \rightarrow 2SO_4^{2-} + 2H^+ + 8(H^+ + e^-) \tag{9c}$$
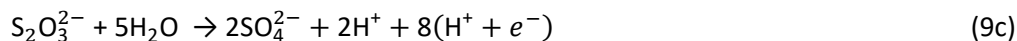
Paired e^- and H^+

Any reaction or half-reaction that starts from a set of reactants that is charge-balanced must produce a charge-balanced set of reaction products (as in Eq. 5e with ch = 0). Thus the electrons in an oxidation or reduction half-reaction must be balanced by positively charged ionic products, of which the most common in biological reactions is H^+. Conversely, every H^+ that is involved in the reaction must be matched by a corresponding negatively charged component. H^+ is of particular interest, because of its role in determining solution pH and alkalinity. However, these properties are not mediated by the H^+ ions alone, but also by the anions with which they are paired. In redox half-reactions, pairings with H^+ ions can be divided into 3 significant categories: with electrons; with anions of strong acids; and with anions of weak acids.

Free electrons cannot accumulate in solution, so they only appear in half-reactions. Therefore, an electron donor half-reaction always has to be combined with an electron acceptor half-reaction, in

which the electron is a reactant, so that the electrons cancel out in the overall reaction (see below). This means that the H⁺ ions that are paired with the electrons in the electron donor half-reaction and the electron destination half-reactions will also cancel out, and consequently have no effect on the solution properties. However, any deficit or surplus of H⁺ after the pairing of H⁺ with e⁻ has to be supplied or absorbed by the aqueous phase with changes of pH and alkalinity. The increase or decrease in H⁺ and other aqueous component products of the bioprocess, such as PO_4^{3-} and CO_3^{2-}, disturb the equilibrium of the aqueous phase, which then re-speciates to re-establish equilibrium. The H⁺ that are paired with strong acid anions, such as sulphate or nitrate, remain virtually completely dissociated, and so have a strong effect on pH. In contrast, the H⁺ that are paired with weak-acid anions, such as acetate, carbonate or phosphate, will tend to remain partially associated with them, and so have no effect on total alkalinity, and a weak and variable effect on pH, depending on the specific pK values of the anions involved relative to the pH of the solution.

Chemical and total oxygen demand (COD and TOD)

COD is the electron-donating capacity (EDC) of components (or groups of components) expressed as oxygen, as if all the electrons donated by the components were accepted by oxygen. The products of the COD test are CO_3^{2-}, NH_4^+, PO_4^{3-}, SO_4^{2-}, H⁺ and H_2O. Note that in the COD test, ammonia is not oxidised, but sulphide is, so the COD measure excludes the EDC of the ammonia but includes the EDC of the sulphide, where the EDC is expressed in terms of mass of oxygen. The **total oxygen demand** (TOD) is the amount of oxygen required to convert the electron donor to the most oxidized forms of its reaction products, including the oxidation of the nitrogen content to NO_3^-, i.e., the products of the TOD reaction are CO_3^{2-}, NO_3^-, PO_4^{3-}, SO_4^{2-}, H⁺ and H_2O (as in Eq. 1). The exchanged electrons of the TOD reaction (Eq. 2) include the maximum possible electrons donated by the N content.

The EDC corresponding to COD of an electron donor can be constructed from Table 2-2 by adding Rows 1a, 2, 3, 4b, 5a, 6e and 7, i.e.:

$$C_xH_yO_zN_aP_bS_c^{ch} + (3x - z + 4b + 4c)H_2O \rightarrow (6x + y - 2z - 4a + 8b + 8c)H^+ + xCO_3^{2-} + aNH_4^+ + bPO_4^{3-} + cSO_4^{2-} + \gamma_s e^-$$ (10a)
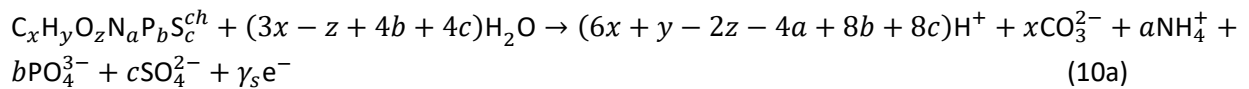
where $\gamma_s = (4x + y - 2z - 3a + 5b + 6c) - ch$ (11)

Pairing the e⁻ with H⁺ in Eq. 10a yields:

$$C_xH_yO_zN_aP_bS_c^{ch} + (3x - z + 4b + 4c)H_2O \rightarrow (2x - a + 3b + 2c + ch)H^+ + xCO_3^{2-} + aNH_4^+ + bPO_4^{3-} + cSO_4^{2-} + \gamma_s(e^- + H^+)$$ (10b)
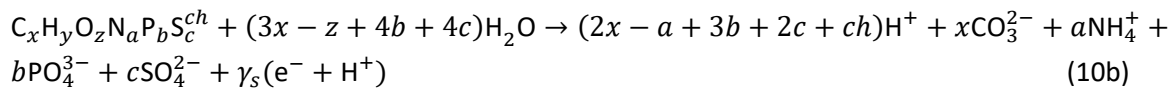
The COD then is 8 γ_s gO₂/mol of $C_xH_yO_zN_aP_bS_c^{ch}$, where the 8 represents 8 gO per e⁻ accepted. The COD as an EDC basis is very convenient for bioprocess modelling because, not only is there an accurate test for its measurement (Standard methods, 2017), it also allows modelling nitrification and BSR bioprocesses separately without correction of the measurement, and therefore is applicable to both aerobic and anaerobic processes. The TOD or COD of a component can be calculated with Eq. 2 or Eq. 11, respectively, from its element and charge composition. It shows, as mentioned before, that the EDC as COD (8 γ_{sCOD}) or TOD (8 γ_{sTOD}) is not affected by the associated protons of the component.

Adding speciation to the electron donor half-reaction

For simplified steady-state bioprocess models with pH estimation (e.g. in spreadsheets) speciation may be added to the electron donor reaction. This requires writing the stoichiometry so that the components match the dominant species within the specified pH range wherein the bioprocess usually operates. For example, in the pH range 6.8 to 8.6, within which most bioprocesses operate, the dominant species of the IC, FSA, OP, sulphide and acetate weak acid/base systems are HCO_3^-, NH_4^+, $H_2PO_4^-$, HPO_4^{2-}, H_2S, HS^- and HAc. The bioprocess stoichiometry is therefore written in terms of the relevant protonated state of these species directly. This is what Sötemann et al. (2005a) and Poinapen and Ekama (2010a) did in their steady-state methanogenic and sulphidogenic models. Whereas only one species is needed for the IC, FSA and acetate systems because their pK values are more than 0.5 pH units outside the 6.8–8.6 pH range, two species of the OP and sulphide systems are needed because these each have a pK value inside the range, which significantly complicates pH calculation when OP and FSS are present in significant quantities. This aspect is considered further below and in Part 5 of this series.

ELECTRON DESTINATION REACTIONS

The electrons donated by the electron donor are used in two sub-bioprocesses by the organisms that mediate a particular bioprocess, (i) anabolism, which is the production of the cell material of the biomass, and (ii) catabolism, which generates energy to transform the electron donor (substrate) to cell material (McCarty, 1975; Ekama, 2009). Both electrons and energy are conserved: The energy associated with the electrons used in anabolism is energy conserved as new cell material and the energy associated with the electrons used in catabolism is transformed to heat. Anabolism and catabolism together form the metabolism of organism growth when mediating a particular bioprocess.

If the electron donor substrate is sufficiently concentrated, the catabolic heat generation will heat the water in which the bioprocesses take place. This is the main heat source in auto-thermal aerobic digestion (Messenger and Ekama, 1993; Pitt and Ekama, 1996). By including the heat of reaction in the breakdown and formation of components in bioprocesses, Fernández-Arévalode et al. (2015) developed a general plant-wide WRRF model that can predict temperature in its different reactors.

Anabolism (biomass growth)

Using the products of the COD reaction (Eq. 10) as the reactants, the biomass formation reaction can be written in terms of standard aquatic chemistry components and with paired H^+ and e^- as follows:

$$k\text{CO}_3^{2-} + n\text{NH}_4^+ + p\text{PO}_4^{3-} + s\text{SO}_4^{2-} + (2k - n + 3p + 2s)\text{H}^+ + \gamma_B(\text{e}^- + H^+) \rightarrow \text{C}_k\text{H}_l\text{O}_m\text{N}_n\text{P}_p\text{S}_s + (3k - m + 4p + 4s)\text{H}_2\text{O} \tag{12}$$
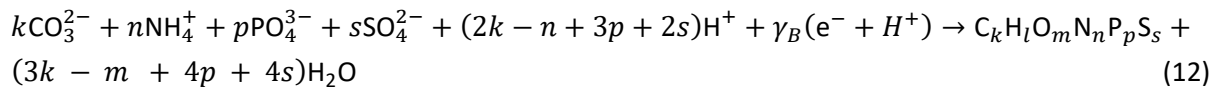
$$\text{where } \gamma_B = (4k + l - 2m - 3n + 5p + 6s) \tag{13}$$

and γ_B is the exchanged electrons of the biomass growth reaction (e⁻/mol).

The COD of the biomass is 8 γ_B gCOD/mol, since Eq. 12 is just the COD reaction (Eq. 10) in reverse.

Rearranging Eq. 12 so that all terms are electro-neutral yields:

$$k\left(2H^+ + CO_3^{2-}\right) + n(NH_4^+ - H^+) + p\left(3H^+ + PO_4^{3-}\right) + s\left(2H^+ + SO_4^{2-}\right) + \gamma_B(H^+ + e^-) \rightarrow$$
$$C_kH_lO_mN_nP_pS_s + (3k - m + 4p + 4s)H_2O \tag{14}$$
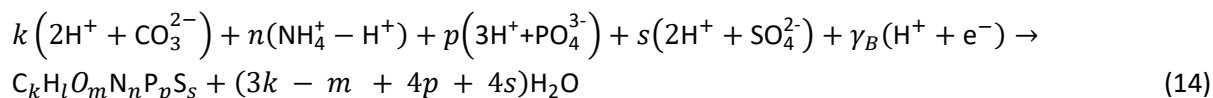
Therefore, Eq. 12 could also be written as:

$$kH_2CO_3 + nNH_3 + pH_3PO_4 + sH_2SO_4 + \gamma_B(H^+ + e^-) \rightarrow C_kH_lO_mN_nP_pS_s + (3k-m+4p+4s)\,H_2O \tag{15}$$
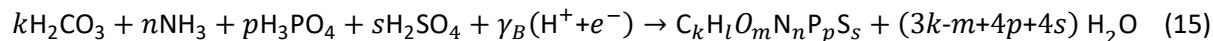
In Eqs 12 and 15, the components retain the same oxidation states – it is only their number of associated protons that have changed. This follows the pattern of Eq. 5e in reverse (with ch = 0), so all the comments made there apply to this anabolic biomass growth process also. Note that while the generic substrate component $C_xH_yO_zN_aP_bS_c{}^{ch}$ includes a stoichiometric coefficient ch for charge, the generic stoichiometric formula for biomass $C_kH_lO_mN_nP_pS_s$ does not because it is generally assumed that biomass is uncharged.

For the purposes of setting up the stoichiometric biotransformation model equations, it fundamentally does not matter whether either the substrate or biomass is represented as charged or neutral, as the charge will be balanced overall by either adding or subtracting protons as illustrated in Eq. 15. However, when a component is also involved in the ionic speciation model, it is more convenient to use a charged representation. For example, it would be awkward and inconvenient for a speciation model to include separate reaction equations for all the possible neutral ion-pairs involving acetate that could be present in solution [HAc, NaAc, KAc, Mg(Ac)$_2$ etc.], so it is convenient to use the charged form (Ac$^-$) as the component, and account for the cations separately.

However, while available experimental evidence (Westergreen et al., 2012) indicates that biomass does include functional groups that can participate in protonation/deprotonation reactions, the overall protonation state does not vary significantly in the pH range 6.8–8.6 in which most of the bioprocesses of interest occur. Therefore, biomass is not included in the ionic speciation model and can be conveniently modelled as an uncharged component.

In the same way as the general electron donor reaction can be generated by adding the oxidation reactions of the individual elements making up the electron donor (Table 2-2), so also can the general biomass formation reaction be generated by adding the biomass anabolic reactions of the individual CHONP and S elements that make up the biomass $C_kH_lO_mN_nP_pS_s$. This is shown in Table 2-3 for the same components of the CHONP and S elements that can be taken up from the aqueous phase to form biomass as electron donor products released to the aqueous phase in Table 2-2, and are also written as mass-balanced reactions summed across the rows to zero. Because anabolism is the reverse of the electron donor reaction, Table 2-3 is essentially the reverse form of Table 2-2 and all the comments on Table 2-2 also apply to Table 2-3.

Note that it is not necessary to include all six elements in the biomass composition. If appropriate, the biomass can be simplified to $C_kH_lO_mN_n$ by assigning zero to the *p* and *s* molar composition values of P and S. Table 2-3 shows that different oxidation states of the components of the N and S elements can also be selected to synthesize the biomass.

In bioprocess model stoichiometry it is most convenient (but not necessary) to generate biomass from the electron donor reactant or product components of the N and S elements (as in Eq. 10 paired with Eq. 12), rather than some other component of these elements, not present as an electron donor reactant or product. For example, with biological sulphite and thiosulphate reduction to sulphide (Bioprocesses 2b and 2c in Tables 1, 4c and 4d), the electron donor reactants sulphite or thiosulphate are selected as the S components for biomass synthesis, rather than another S component like sulphate. Similarly, for autotrophic denitrification with sulphide, sulphite or thiosulphate as electron donor and nitrate or nitrite as electron acceptor (Bioprocesses 5a, 5b and 5c in Tables 1, 4e and 4f), sulphate is selected as the S element component for biomass synthesis because it is present in the stoichiometry as electron donor product. So from a stoichiometric perspective, the choice of N or S element component that is taken up for biomass synthesis is usually governed by whether or not it is available as an electron donor reactant or product, unless there is compelling evidence that a particular species is used for biomass synthesis (as for anammox bacteria, see below). In this regard, the oxidation state of the reaction products aligned with the COD test (CO_3^{2-}, NH_4^+, PO_4^{3-}, SO_4^{2-}, Eq. 10) are usually best suited for modelling bioprocesses because nitrification of ammonia and BSR are modelled with their own bioprocesses (Bioprocesses 2, 3 and 5 in in Tables 1 and 4).

As mentioned above for the electron donor reactions, the selection of the species of the C, N, P and S elements that are to be the components and formed as bioprocess products depends on the purpose of the model for which the bioprocess stoichiometry is derived. The same applies to anabolism (and catabolism – see below). For a steady-state model, some simplifying assumptions can be made, and the components selected to simplify pH calculation from the products (e.g. the AD model of Sötemann et al., 2005a). For a dynamic model or a steady state model with speciation and calculation of pH, it is preferable to select components from the standard aquatic chemistry set (see Part 5 of this series).

Table 2-3. *Individual component anabolism reactions in Gujer matrix format with exchanged electrons and protons and alkalinity change as a function of the anabolic reactant*

Row	Anabolic Reactant	H⁺	Exchanged electrons e⁻	H₂O product	Biomass product	Mass[a] balance	Alkalinity[b] change
	1	2	3	4	5	6	7
1a	$-kCO_3^{2-}$	$-6k$	$-4k$	$+3k$	$+C_k$	0	0
1b	$-kH_2CO_3$	$-4k$	$-4k$	$+3k$	$+C_k$	0	0
2	0	$-l$	$-l$	0	$+H_l$	0	0
3	$-mH_2O$	$+2m$	$+2m$	0	$+O_m$	0	0
4a	$-nNH_3$	$+3n$	$+3n$	0	$+N_n$	0	$-n$
4b	$-nNH_4^+$	$+4n$	$+3n$	0	$+N_n$	0	$-n$
4c	$-\dfrac{n}{2}N_2$	0	0	0	$+N_n$	0	0
4d	$-nNO_2^-$	$-4n$	$-3n$	$+2n$	$+N_n$	0	$+n$
4e	$-nNO_3^-$	$-6n$	$-5n$	$+3n$	$+N_n$	0	$+n$
5a	$-pPO_4^{3-}$	$-8p$	$-5p$	$+4p$	$+P_p$	0	0
5b	$-pH_3PO_4$	$-5p$	$-5p$	$+4p$	$+P_p$	0	0
6a	$-pH_2S$	$+2p$	$+2p$	0	$+S_p$	0	0
6b	$-sHS^-$	$+s$	$+2s$	0	$+S_s$	0	0
6c	$-\dfrac{s}{2}S_2O_3^{2-}$	$-3s$	$-2s$	$+\dfrac{3}{2}s$	$+S_s$	0	$+s$
6d	$-sSO_3^{2-}$	$-6s$	$-4s$	$+s$	$+S_s$	0	$+2s$
6e	$-sSO_4^{2-}$	$-8s$	$-6s$	$+4s$	$+S_s$	0	$+2s$

[a]Reactant coefficients (Columns 1 to 3) have a −ve signs to represent consumption and products (Columns 4 and 5) are given a +ve sign to represent production. The coefficients sum to zero across each row to conform to mass balance (Column 6).

[b]The alkalinity change (ΔAlk_T, Column 7) with respect to the most protonated species of the IC, FSA, OP, sulphide and acetate weak acid/bases is the number of weak acid anion equivalents produced by the reaction minus the number of protons produced that can associate with them, i.e., excluding those paired with electrons (Eq. 12). So the ΔAlk_T in Column 7 is given by N · Column 1 − (Column 2 − Column 3), where N is the number of H⁺ that can be accepted by the weak acid/base oxidation product to make reference species (strong acids remain fully dissociated), e.g. for Row 5a: $-3p -[-8p -(-5p)] = 0$. The ΔAlk_T of the whole anabolism reaction is obtained by adding the alkalinities in Column 7 of the relevant rows, e.g., ΔAlk_T for Eq. 12 is obtained by adding Row 1a, 2, 3, 4b, 5a, and 6e $= 0 + 0 + 0 − n + 0 + 2s = − n + 2s$.

Catabolism

The catabolic electron acceptor reaction is built on the bioprocess's terminal electron acceptor and the species (specifically the redox state) of the particular element that is formed when it accepts the electrons. For example, if SO_3^{2-} is the electron acceptor, then $S_2O_3^{2-}$, S or HS⁻ can be formed (not SO_4^{2-} because that would constitute SO_3^{2-} **donating** electrons, Figure 2-2). Experimental observation is

required to know which specific species of the electron acceptor element are formed. If two species are formed, e.g. $S_2O_3^{2-}$ **and** HS^- (Qian et al., 2015) or SO_3^{2-} **and** S from $S_2O_3^{2-}$ (Deng et al., 2019), then two separate bioprocesses are required to model the system.

The electron acceptor reactions of the most common electron acceptor species of the C, O, N and S elements (components of P are not usually electron acceptors and H_2 is an electron donor) involved in the bioprocesses listed in Table 2-1 can be written in general form with paired e^- and H^+ as:

$$C_dH_eO_fN_gS_h^{chr} + (q \cdot chp - chr)H^+ + \gamma_e(H^+ + e^-) \rightarrow qC_rH_tO_uN_vS_w^{chp} + (f - q \cdot u)H_2O \quad (16a)$$
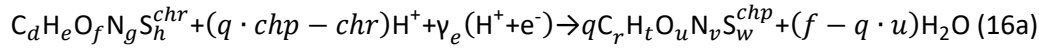
where:

$C_dH_eO_fN_gS_h^{chr}$ and $C_rH_tO_uN_vS_w^{chp}$ represent the electron acceptor reactant and product;

$\gamma_e = q(t - 2u - chp) - (e - 2f - chr)$ is the number of accepted electrons; $\qquad$ (16b)

The coefficient q depends on the element being oxidized (accepting electrons):

C: $q = d/r$; N: $q = g/v$; S: $q = h/w$; if O_2 is the electron acceptor, $q = 0$ $\qquad$ (16c)

Equation 16 applies to all electron acceptor half-reactions involved in the bioprocesses listed in Table 2-1. By assigning the appropriate values to d, e, f, g, h and chr for the electron acceptor reactant and to r, t, u, v, w and chp for the electron acceptor product in Eq. 16, the electron-accepting reactions for 8 electron acceptor species (CO_3^{2-}, SO_4^{2-}, SO_3^{2-}, $S_2O_3^{2-}$, S, O_2, NO_2^-, NO_3^-) of the C, S, O and N elements in the bioprocesses of Table 2-1 can be generated as listed in Eqs 17 to 20. Four additional electron acceptor half-reactions for the S components intermediate between HS^- and SO_4^{2-} are also shown.

$CO_3^{2-} + 2H^+ + 8(H^+ + e^-) \rightarrow CH_4 + 3H_2O$ $\qquad$ Bioprocess 1 $\qquad$ (17)

$SO_4^{2-} + H^+ + 8(H^+ + e^-) \rightarrow HS^- + 4H_2O$ $\qquad$ Bioprocess 2a $\qquad$ (18a)

$SO_3^{2-} + H^+ + 6(H^+ + e^-) \rightarrow HS^- + 3H_2O$ $\qquad$ Bioprocess 2b $\qquad$ (18b)

$S_2O_3^{2-} + 8(H^+ + e^-) \rightarrow 2HS^- + 3H_2O$ $\qquad$ Bioprocess 2c $\qquad$ (18c)

$SO_3^{2-} + H^+ + 2(H^+ + e^-) \rightarrow \frac{1}{2}S_2O_3^{2-} + \frac{3}{2}H_2O$ $\qquad$ Bioprocess 2d $\qquad$ (18d)

$SO_4^{2-} + H^+ + 4(H^+ + e^-) \rightarrow \frac{1}{2}S_2O_3^{2-} + \frac{5}{2}H_2O$ $\qquad$ (18e)

$SO_4^{2-} + 2(H^+ + e^-) \rightarrow SO_3^{2-} + H_2O$ $\qquad$ (18f)

$SO_4^{2-} + 2H^+ + 6(H^+ + e^-) \rightarrow S + 4H_2O$ $\qquad$ (18g)

$S + 2(H^+ + e^-) \rightarrow HS^- + H^+$ $\qquad$ (18h)

$O_2 + 4(H^+ + e^-) \rightarrow 2H_2O$ $\qquad$ Bio 3,3a,3b,4,8 $\qquad$ (19)

$NO_3^- + H^+ + 5(H^+ + e^-) \rightarrow \frac{1}{2}N_2 + 3H_2O$ $\qquad$ Bioprocess 5a,5b,5c,6 $\qquad$ (20a)

$NO_3^- + 2(H^+ + e^-) \rightarrow NO_2^- + H_2O$ $\qquad$ Bioprocess 6a $\qquad$ (20b)

$NO_2^- + H^+ + 3(H^+ + e^-) \rightarrow \frac{1}{2}N_2 + 2H_2O$ $\qquad$ Bioprocess 6b, 7 $\qquad$ (20c)

ELECTRON BALANCE AND OVERALL STOICHIOMETRY

The overall electron balance

The previous sections presented purely stoichiometric descriptions of the three parts of a bioprocess reaction: the electron donor reaction, the anabolic electron destination reaction, and the catabolic electron acceptor reaction. By 'purely stoichiometric' it is meant that the only information contained in the reaction equation is the set of chemical components involved and their embedded element mass and electron (charge) balances.

The overall bioprocess reaction involves the combined set of components for each part, and is subject to the same material balance constraints. Thus, the overall bioprocess reaction stoichiometry can be constructed as a linear combination of the three sub-reactions. In geometric terms, the sub-reactions are basis vectors of the compositional space; i.e., directions along which the composition is allowed to change by the material balance constraints. The overall reaction is a vector, which is a linear combination of the basis vectors. The way this combination is constructed is commonly understood in terms of an overall electron balance in which the electrons donated by the donor (substrate) are divided between the anabolic and catabolic destination reactions, i.e.:

$$\Delta e^-_{donor} = E \cdot \Delta e^-_{anabolic} + (1 - E) \cdot \Delta e^-_{catabolic} \tag{21}$$

However, it is not just the exchanged electrons that are combined in this way, but the entire electron donor, anabolic and catabolic stoichiometric equations, as shown schematically in Figure 2-3.
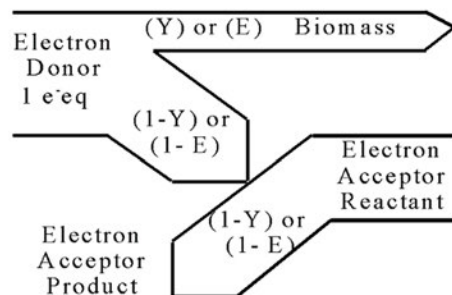
Figure 2-3. *Electron source (donor) and electron destination reactions (biomass – anabolism) and electron acceptor reduction from reactant to product (catabolism). For dynamic models, the proportion of the donor e⁻ to biomass is the specific biomass yield (Y, gCOD biomass produced per gCOD substrate donor utilized). For steady-state models, the proportion of the donor e⁻ to biomass is the net specific biomass and endogenous residue produced (E, gCOD biomass and endogenous residue produced per day per gCOD substrate donor utilized per day: Ekama, 2009).*

The overall reaction equation for the bioprocess is no longer purely stoichiometric, because the coefficient *E* depends on non-stoichiometric factors, such as thermodynamic constraints and details of micro-organism metabolism. The most common approach has been to treat *E* as an empirical parameter; however, deriving its value from a metabolic model is also possible (Smolders et al., 1995; Rittman and McCarty, 2001). In dynamic models, E is the biomass yield coefficient (*Y*) expressed as gCOD biomass synthesized/gCOD substrate utilized. Because endogenous respiration is modelled with a

bioprocess of its own in dynamic models, $E = Y$ for heterotrophic bioprocesses, where the electron donor and biomass are both expressed as COD. However, in fully mass-balanced plant-wide models which express components in terms of mass (Ikumi et el., 2015, Solon et al., 2015), the E value has to be converted to Y in mass units (g biomass/g substrate), i.e.:

$Y= E\frac{\gamma_S M_B}{\gamma_B M_S}$ g biomass/ g substrate; where M_B = (12k + l + 16m + 14n + 31p + 32s) g biomass/mol and M_S = (12x + y + 16z + 14a + 31b + 32c) g substrate/mol

In steady-state models, E is the net (observed) yield, which is a combination of the growth and mass loss processes, i.e.:

$E = \frac{Y_H(1+f_{OHO}b_{OHO}R_S)}{(1+b_{OHO}R_S)}$ for aerobic activated sludge with growth and mass loss modelled as endogenous respiration (Ekama, 2009) and

$E = \frac{Y_{AD}(1+f_{AD}b_{AD}R_S)}{[1+b_{AD}R_S\{1-Y_{AD}(1-f_{AD})\}]}$ for methanogenesis with and mass loss modelled as death regeneration (Sötemann et al., 2005a).

Also, yield coefficients for autotrophic processes (Y_A) are typically expressed in non-COD units, e.g., gVSS/g NH_4-N for nitrification. For the electron balance equation (Eq. 21) to apply, these autotrophic yields must be converted to the ratio of donated electrons taken up by anabolism. For example, consider the case of nitrification where ammonia is aerobically converted to nitrate (Bioprocess 3, electron donor reaction Eq. 7a). From the stoichiometry (Table 2-4a Columns 4 and 9), Y_A g VSS biomass produced per g NH_4-N consumed is:

$Y_A = \frac{M_B}{M_N} \frac{\left(E\frac{\gamma_S}{\gamma_B}\right)}{\left(1+nE\frac{\gamma_S}{\gamma_B}\right)}$ g biomass VSS/g NH_4^+-N

where M_N is the atomic weight of N. Rearranging results in:
$E = \frac{\gamma_B}{\gamma_N} \frac{Y_A M_N}{(M_B - nY_A M_N)}$

which gives E = 0.031 for Y_A = 0.10 g VSS/gNH_4-N for biomass composition of $CH_{1.4}O_{0.4}N_{0.2}P_{0.05}$.

 As an example, consider aerobic growth of heterotrophs on acetate. Aligning the oxidation state of the N and S elements with the products of the COD test (NH_4^+ and SO_4^{2-}) and selecting the protonated forms of components aligned with the standard aquatic chemistry convention, the components involved in the bioprocess are: $C_2H_3O_2^-$ (substrate), $C_kH_lO_mN_nP_pS_s$ (biomass), O_2 (electron acceptor), CO_3^{2-}, NH_4^+, PO_4^{3-}, SO_4^{2-}, H^+, H_2O (oxidation products).

The electron donor reaction can be constructed from Eq. 10a or Table 2-2.

$$C_2H_3O_2^- + 4H_2O \rightarrow 3H^+ + 2CO_3^{2-} + 8(H^+ + e^-) \tag{22a}$$
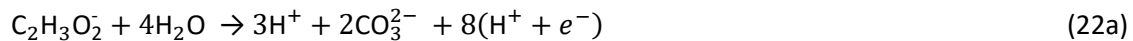
$$\Delta Alk_T = a - 2s - ch = 0\text{-}0\text{-}(\text{-}1)=1 \tag{22b}$$

The anabolic reaction is given by Eq. 12:

$$kCO_3^{2-} + nNH_4^+ + pPO_4^{3-} + sSO_4^{2-} + (2k - n + 3p + 2s)H^+ + \gamma_B(H^+ + e^-)$$
$$\rightarrow C_kH_lO_mN_nP_pS_s + (3k - m + 4p + 4s)H_2O \qquad \Delta Alk_T = (2s - n) \qquad (12)$$
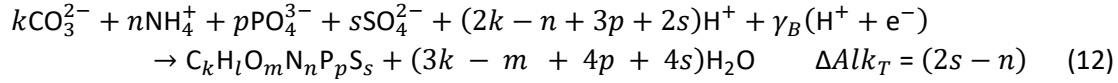
and the electron acceptor (catabolic) reaction is given by Eq. 19:

$$O_2 + 4(H^+ + e^-) \rightarrow 2H_2O \; ; \qquad\qquad\qquad \Delta Alk_T = 0 \qquad (19)$$
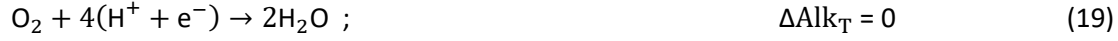
The exchanged electrons for the three half-reactions are y_s = 8, y_B and y_e = 4, respectively, so the reactions are combined as:

$$\langle Eq\ 22a \rangle \rightarrow \frac{8E}{\gamma_B}\langle Eq\ 12 \rangle + \frac{8(1-E)}{4}\langle Eq\ 19 \rangle \qquad (23a)$$

which, after combining like terms and simplifying, gives:

$$C_2H_3O_2^- + \frac{8(1-E)}{4}O_2 + \frac{8nE}{\gamma_B}NH_4^+ + \frac{8pE}{\gamma_B}PO_4^{3-} + \frac{8sE}{\gamma_B}SO_4^{2-} \rightarrow \frac{8E}{\gamma_B}C_kH_lO_mN_nP_pS_s + \left(2 - \frac{8kE}{\gamma_B}\right)CO_3^{2-} +$$
$$\left[\frac{8E}{\gamma_B}(3k - m + 4p + 4s) - 4E\right]H_2O + \left[3 - \frac{8E}{\gamma_B}(2k - n + 3p + 2s)\right]H^+ \qquad (23b)$$
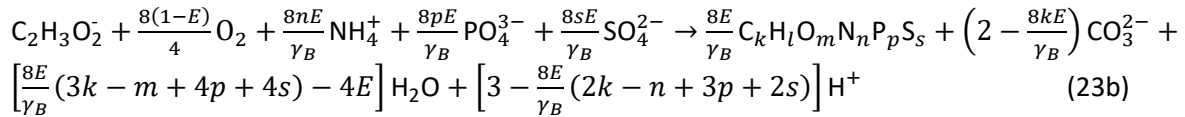
ΔAlk_T of the complete bioprocess Eq. 23b is obtained by similarly combining the ΔAlk_T of the three half-reactions according to Eq. 23c,

$$\Delta Alk_T = \langle \Delta Alk_T\ of\ Eq\ 22b \rangle + \frac{8E}{\gamma_B}\langle \Delta Alk_T\ of\ Eq\ 12 \rangle + \frac{8(1-E)}{4}\langle Eq\ 19 \rangle \qquad (23c)$$

$$\Delta Alk_T = 1 + \frac{8E}{\gamma_B}(-n + 2s) + 0 \qquad (23d)$$

Combining, as per Eq. 21, the general electron donor (Eq. 10a), anabolism (Eq. 12) and electron acceptor (Eq. 16a) equations, with oxidation states of the N and S elements aligned with the products of the COD test (NH_4^+ and SO_4^{2-}), and selecting the protonated forms of the components aligned with the standard aquatic chemistry convention (Part 1, Brouckaert et al., 2021), i.e.:

$$\langle Eq.\ 10a \rangle \rightarrow \frac{\gamma_S E}{\gamma_B}\langle Eq.\ 12 \rangle + \frac{\gamma_S(1-E)}{\gamma_e}\langle Eq.\ 16a \rangle \qquad (24a)$$

yields a generalized stoichiometric bioprocess reaction Eq. 24b in terms of a generic electron acceptor reactant $C_dH_eO_fN_gS_h^{chr}$ and product $C_rH_tO_uN_vS_w^{chp}$.

$$C_xH_yO_zN_aP_bS_c^{ch} + (1 - E)\frac{\gamma_S}{\gamma_e}C_dH_eO_fN_gS_h^{chr}$$
$$\rightarrow q(1 - E)\frac{\gamma_S}{\gamma_e}C_rH_tO_uN_vS_w^{chp} + \left(x - kE\frac{\gamma_S}{\gamma_B}\right)CO_3^{2-} + \left(a - nE\frac{\gamma_S}{\gamma_B}\right)NH_4^+$$
$$+ \left(b - pE\frac{\gamma_S}{\gamma_B}\right)PO_4^{3-} + \left(c - sE\frac{\gamma_S}{\gamma_B}\right)SO_4^{2-} + E\frac{\gamma_S}{\gamma_B}C_kH_lO_mN_nP_pS_s$$
$$+ \begin{bmatrix} (6x + y - 2z - 4a + 8b + 8c) - E\frac{\gamma_S}{\gamma_B}(6k + l - 2m - 4n + 8p + 8s) \\ -(1 - E)\frac{\gamma_S}{\gamma_e}\{q(t - 2u) - (e - 2f)\} \end{bmatrix}H^+$$
$$+ \left[-(3x - z + 4b + 4c) + E\frac{\gamma_S}{\gamma_B}(3k - m + 4p + 4s) + (1 - E)\frac{\gamma_S}{\gamma_e}(f - qu)\right]H_2O$$

$$(24b)$$
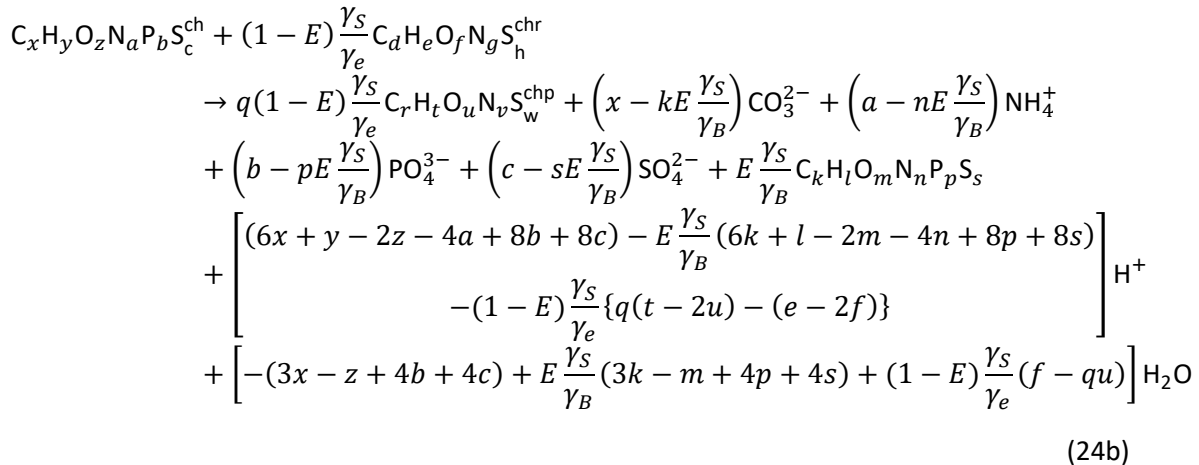
Equation 24b applies to all the bioprocesses in Table 2-1, except 2b, 2c, 2d, (sulphidogenesis with a sulphur reactant other than SO_4^{2-}), 3, 3a, 3b for nitrification and 7 for anammox. Equation 24b does not apply to BSR when the e^- acceptor reactant is not SO_4^{2-}. However, it can be modified to obtain bioprocess stoichiometry for BSR with e^- acceptor reactants other than SO_4^{2-}, such as SO_3^{2-} (Bioprocesses 2b and 2d) and $S_2O_3^{2-}$ (Bioprocess 2c) as described in Table 2-5. For example, for Bioprocess 2c with thiosulphate as the electron acceptor reactant, sulphate is replaced by thiosulphate (Eqs 10a and 24b) and the terms 6c and 6s in Eqs 11 and 13 are replaced by 2c and 2s, respectively (Rows 6c in Tables 2 and 3, respectively). Equation 24b does not apply to nitrification (3, 3a, 3b) because it does not include the appropriate electron donor products for nitrogen (NO_3^- or NO_2^-). However, an analogous overall reaction can be constructed by substituting the appropriate electron donor equation for Eq. 10a in Eq. 24a. The resulting stoichiometric coefficients are listed in Tables A1 and A2 (Appendix). The stoichiometric coefficients for sulphidogenesis are listed in Tables A3. For Bioprocesses 2b–2d, both the electron donor sulphur product and sulphur source for anabolism were made the same as the electron acceptor reactant. The electron donor balance approach illustrated in Figure 2-3 has to be further modified in the case of anammox (Bioprocess 7) because anammox has the peculiarity that it uses different e^- donors for anabolism and catabolism. Anammox is discussed in greater detail below.

The revisions made to obtain the stoichiometry in Tables A1–A4 are listed in Table 2-4. Note that changing the products and reactants in the electron donor and anabolic reactions results in changes in the formulae for y_S and y_B. As discussed previously, y_S and y_B can be calculated for different oxidations of the products and reactants by summing the appropriate rows in Column 5 of Table 2-2 and Column 3 of Table 2-3, respectively. The required changes are noted in Table 2-4.

Table 2-4. *Application of the general stoichiometric Eq. 24b to the bioprocesses in Table 2-1. Electron donor products of the C, N, P and S are standard aquatic chemistry components: CO_3^{2-}, NH_4^+, PO_4^{3-} and SO_4^{2-}*

Bio-process	Electron donor reactant	Electron donor N product	Electron acceptor reactant	Electron acceptor product	Is Eq. 24b valid?
1	Organics	NH_4^+	CO_3^{2-}	CH_4	Yes
2a	Organics	NH_4^+	SO_4^{2-}	H_2S	Yes
2b	Organics	NH_4^+	SO_3^{2-}	H_2S	No. Change e⁻ donor Eq. 10a and associated γ_S
2c	Organics	NH_4^+	$S_2O_3^{2-}$	H_2S	Eq. 11 and anabolism Eq. 12 and associated γ_B
2d	Organics	NH_4^+	SO_3^{2-}	$S_2O_3^{2-}$	Eq. 13 to produce and use SO_3^{2-} , $S_2O_3^{2-}$ and SO_3^{2-}, instead of SO_4^{2-} in bioprocesses 2b, 2c and 2d respectively. This changes the c and s terms in the γ_S Eq. 11 and γ_B Eq. 13 from 6c and 6s to 4c, 2c and 4c and 4s, 2s and 4s respectively.
3	NH_4^+	NO_3^-	O_2	H_2O	No; $\gamma_S = 0$ in Eq. 11; change e⁻ donor reaction to Eq. 4c for TOD.
3a	NH_4^+	NO_2^-	O_2	H_2O	
3b	NO_2^-	NO_3^-	O_2	H_2O	
4	Organics	NH_4^+	O_2	H_2O	Yes
5a	H_2S	-----	NO_3^-	N_2	Yes
5b	$SO_3^=$	-----	NO_3^-	N_2	Yes
5c	$S_2O_3^=$	-----	NO_3^-	N_2	Yes
6	Organics	NH_4^+	NO_3^-	N_2	Yes
6a	Organics	NH_4^+	NO_3^-	NO_2^-	Yes
6b	Organics	NH_4^+	NO_3^-	N_2	Yes
7	NH_4^+	N_2	NO_2^-	N_2	No; N_2 is donor product, NO_2^- oxidized to NO_3^- for anabolism
8	H_2S	-----	O_2	H_2O	Yes

The Gujer matrix

The Gujer matrix format is the standard and systematic way of writing bioprocess stoichiometry of WRRF models. It is an easy-to-read fingerprint of a bioprocess model (Gujer, 2008). The matrix (like Tables A1–A4) lists the bioprocesses in rows and the components in columns. Usually, the matrix is completed by adding the kinetic rate expressions of the bioprocesses in a column on the right (Gujer, 2008). When water is included, as is done here with complete element mass balancing, all the elements CHONPS, e⁻ (or COD = $8\gamma_S$) and charge are balanced across the rows (bioprocesses). In ASM1 (Henze et al., 1987) for example, this is not the case – only COD and N are mass balanced across the rows, not CHOPS and charge. When water is added as in Tables A1–A3, the bioprocess produced or consumed
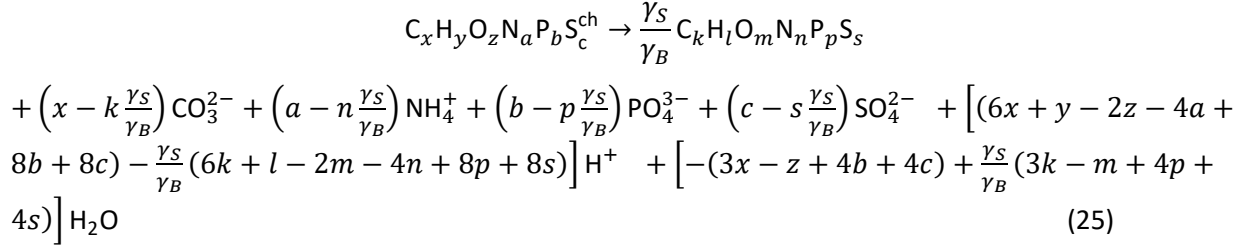
water has to be accounted for separately from the water in the bioreactor. If this is not done, then, with time, models of aerobic and anaerobic reactors increase and decrease in water volume.

Gujer matrices of bioprocess models comprising multiple bioprocesses can be verified for mass balance by summing the product of the CHONPS and ch content of each component and its stoichiometric term across each row (Gujer, 2008; Hauduc et al., 2010) – the elements in the bioprocess are balanced if the sums are all zero. The COD and TOD mass balances can also be checked this way by summing the products of component COD or TOD ($8\gamma_{COD}$ and TOD $8\gamma_{TOD}$, respectively), and the stoichiometric term for each bioprocess (Columns 1 – 19 in Tables A1 – A4). γ_{COD} and γ_{TOD}, are calculated from Eqs 11 and 1, respectively. However, if the CHONPS and ch are balanced, then the COD and TOD must also be balanced because, as Eqs 11 and 1 show, the COD and TOD are properties of the component composition. Note that for Bioprocesses 2b, 2c and 2d in Table 2-A2, the coefficients of the S (c and s) in the γ_S (Eq. 11) and γ_B (Eq. 13) equations have changed to 4, 2 and 4, respectively, because the electron acceptor reactant is SO_3^{2-}, $S_2O_3^{2-}$ and SO_3^{2-} (see Figure 2-2).

Bioprocess stoichiometry is entered into the WRRF simulator WEST (MikebyDHI, 2021) in Gujer matrix format and the software has a facility for automatically checking the elemental mass balances of the bioprocesses entered. We have developed a MATLAB code that can generate the general bioprocess stoichiometry for selected electron donor and acceptor reactants and products (available from https://washcentre.ukzn.ac.za/research/publications). The output of the MATLAB code includes the generalized stoichiometric terms of the reactants and products in the same format as the WEST model code, so that it can be pasted directly into the WEST conversion model editor. The 3-phase (aqueous–gas–solid) plant-wide WRRF model including P and S, PWM_SA in WEST (Ikumi et al., 2014, 2015; Ghoor, 2019) was originally coded this way. This procedure eliminates transcription errors when coding new bio-processes into simulation models and saves much time in model debugging and mass balance verification.

Conversion of one organic component to another
The stoichiometry in Table 2-4 assumes that all the e^- from the donor are passed to the terminal electron acceptor, and conserved in biomass. In the intermediate bioprocesses (which are used in dynamic models, but not steady-state models) this does not always happen. In the University of Cape Town Sludge Digestion Model (UCTSDM1) (Sötemann et al., 2005b) and its successor PWMSA_AD (Ikumi et al., 2011, 2014, 2015), hydrolysis of complex organics produces the intermediate component glucose, which is acidified by acidogens to acetate and hydrogen, both of which have non-zero COD. Eqs 1 to 11 for complete oxidation of the electron donor do not apply in these cases. Furthermore, in the dynamic models, the intermediate organic compounds are not typically represented as being utilized in biomass production. Nevertheless, the principle of transferable e^- and mass balance is still applied in the derivation of the relevant stoichiometric balances. Instead of liberating all the e^- relative to COD, (or TOD) end products and producing e^- donor products that have zero COD, the e^- are conserved in reaction products that have COD (or TOD). The transformation of the general organics component $C_xH_yO_zN_aP_bS_c{}^{ch}$ from one form to another $C_kH_lO_mN_nP_pS_s$ with element, COD and charge mass balance, expressed in terms of standard aquatic chemistry components, is obtained from Eq. 24b with $E = 1$, viz.

$$C_xH_yO_zN_aP_bS_c^{ch} \rightarrow \frac{\gamma_S}{\gamma_B}C_kH_lO_mN_nP_pS_s$$

$$+ \left(x - k\frac{\gamma_S}{\gamma_B}\right)CO_3^{2-} + \left(a - n\frac{\gamma_S}{\gamma_B}\right)NH_4^+ + \left(b - p\frac{\gamma_S}{\gamma_B}\right)PO_4^{3-} + \left(c - s\frac{\gamma_S}{\gamma_B}\right)SO_4^{2-} + \left[(6x + y - 2z - 4a + 8b + 8c) - \frac{\gamma_S}{\gamma_B}(6k + l - 2m - 4n + 8p + 8s)\right]H^+ + \left[-(3x - z + 4b + 4c) + \frac{\gamma_S}{\gamma_B}(3k - m + 4p + 4s)\right]H_2O \tag{25}$$

Equation 25, which is identical to Eq. 15 in Part 1 (Brouckaert et al., 2021), is used to represent hydrolysis of complex organics of various organic types such as fermentable biodegradable soluble organics (FBSO) and biodegradable particulate organics (BPO), each with their own *x, y, z, a, b, c* composition, to glucose ($C_6H_{12}O_6$) without acidogen biomass growth.

The glucose in turn is acidified by acidogens with biomass growth to acetate and hydrogen via:

$$C_6H_{12}O_6 + nE\frac{\gamma_S}{\gamma_B}NH_4^+ + pE\frac{\gamma_S}{\gamma_B}PO_4^{3-} + sE\frac{\gamma_S}{\gamma_B}SO_4^{2-} \rightarrow (1 - E)\frac{(1-\alpha)\gamma_S}{2}H_2 + \left(\frac{\gamma_S}{4} - kE\frac{\gamma_S}{\gamma_B} - \frac{\gamma_S(1-E)\alpha}{4}\right)CO_3^{2-} + E\frac{\gamma_S}{\gamma_B}C_kH_lO_mN_nP_pS_s + \left[\frac{\gamma_S}{2} - E\frac{\gamma_S}{\gamma_B}(2k - n + 3p + 2s) - (1 - E)\alpha\frac{\gamma_S}{2}\right]H^+ + (1 - E)\frac{\alpha\gamma_S}{8}CH_3COOH + \left[-\frac{\gamma_S}{2} + E\frac{\gamma_S}{\gamma_B}(3k - m + 4p + 4s) + (1 - E)\frac{\alpha\gamma_S}{2}\right]H_2O \tag{26}$$
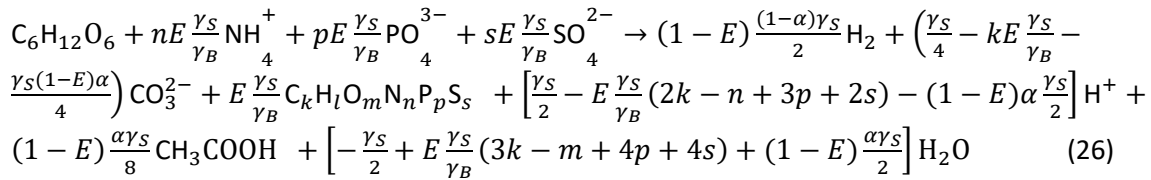
In PWMSA_AD (Ikumi et al., 2011, 2014, 2015), α is set at 2/3, so that two thirds of the glucose EDC (COD) excluding biomass is converted to acetate and one third to H_2. This, again, is imposed on the stoichiometry from prior knowledge of the bioprocess.

The generic product $C_kH_lO_mN_nP_pS_s$ in Eqs 25 and 26 is represented without charge, but this does not reduce their generality, because one can always choose a neutral species to represent the component – e.g. CH_3COOH instead of CH_3COO^-.

Anaerobic ammonia oxidation
Usually a proportion of the e^- donor (*Y* or *E*) is converted to biomass and the remainder passed on to the terminal e^- acceptor (Figure 2-3), however, anaerobic ammonia oxidation (anammox) is an exception. Anammox bacteria use ammonia as the nitrogen source for biomass growth and as an electron donor for autotrophic denitrification (the catabolic reaction is $NH_4^+ + NO_2^- \rightarrow N_{2(g)} + H_2O$). However, nitrite is the electron donor for anabolism where it is oxidized to nitrate, and also the electron acceptor in the denitrification reaction as illustrated in Figure 2-4) (Van Niftrik et al., 2004). The e^- donor equation is obtained by taking Eq. 8 for NH_4^+ and N_2 as e^- donor reactant and product and the e^- acceptor Eq. 20 for NO_2^- and N_2 as e^- acceptor reactant and product. The anabolism equation is obtained from Eq. 12 where the ($e^- + H^+$) pair is supplied by the oxidization of NO_2^- to NO_3^-, Eq. 7c ÷ 2, to give the stoichiometry in Table 2-A1, Bioprocess 7. The net biomass yield $E = 0.1173$ in Figure 2-4 was obtained from Chen et al. (2013) who observed yields of 0.14 gVSS/gNH$_4^+$-N and 0.12 gVSS/gNO$_2$-N.
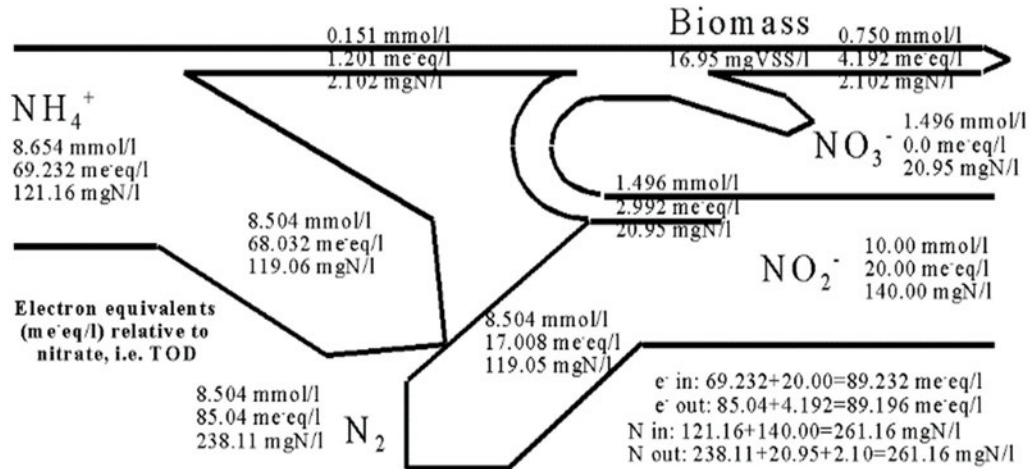
Figure 2-4. *Electron donor* (NH_4^+) *and electron* (e^-) *destination reactions for anammox bacteria showing the flow of* e^- *and nitrogen for E = 0.1173 obtained by calibrating their growth stoichiometry to match the net specific yields of Chen et al. (2013) for a biomass composition of* $CH_{1.4}O_{0.4}N_{0.2}P_0S_0$.

READING BIOPROCESS BEHAVIOUR FROM THE STOICHIOMETRY

Mass-balanced bioprocess stoichiometry ensures that the fluxes of elements CHONPS and charge which exit a biological system are equal to the fluxes entering it. For example, for an AD, the CH_4 and CO_2 gas flows and aqueous-phase pH are entirely defined and dependent on the CHONPS and charge composition of the biodegradable organics degraded in it. In the interests of brevity, only some insights into the very common methanogenic and increasingly exploited sulphidogenic bioprocesses that can be read from their stoichiometry are presented below. It needs to be understood that bioprocess stoichiometry connected to external speciation routines implicitly models the steps described below. In steady-state models, some aqueous-phase speciation reactions and simplifications are explicitly included in the bioprocess stoichiometry described above, so that pH can be calculated directly from the relevant bioprocess products.

Simplified speciation model for methanogenesis

Assuming that (i) the methanogenic AD system remains at near-neutral pH (6.8–8.6) during the reaction; and (ii) BSR does not take place; and (iii) VFA are present at low enough concentration to not significantly influence pH, then based on the pK values of the remaining weak acid/base systems, the dominant species for the FSA is NH_4^+, for the OP are HPO_4^{2-} and $H_2PO_4^-$ and for the IC are HCO_3^- and dissolved CO_2 (often represented as carbonic acid: $H_2CO_3 \leftrightarrow CO_2 + H_2O$). Accordingly, the CO_3^{2-}, PO_4^{3-} and H^+ component terms in the general methanogenic stoichiometric equation in Table 2-A1 (Bioprocess 1) are replaced by the substitutions shown in Eqs 27a to 27c which include only the dominant species expected to be present.

$$[CO_3^{2-}] \equiv (2[HCO_3^-] - [H_2O] - [CO_2]) \tag{27a}$$

$$[H^+] \equiv ([H_2O] + [CO_2] - [HCO_3^-]) \tag{27b}$$

$$[PO_4^{3-}] \equiv \{f_{op}[H_2PO_4^-] + (1 - f_{op})[HPO_4^{2-}] - (1 + f_{op})([H_2O] + [CO_2] - [HCO_3^-])\} \quad (27c)$$

In Eq. 27 it is assumed that any H^+ excess or deficit (i.e., not paired with an e^-) will be supplied or absorbed by the IC system. Also, in Eq. 27c, f_{op} is a parameter with a value between 0 and 1 that increases with solution pH, which is fixed by the requirements of both the IC and OP systems. For the IC system this is via the H_2CO_3 alkalinity (represented by the HCO_3^- concentration), and CO_2 liquid-gas equilibrium via the partial pressure of the CO_2 in the head space (Henry's law, Sötemann et al., 2005a). For the OP system this is via the $H_2PO_4^-$ and HPO_4^{2-} dissociation with its pK'_{p2} value near 7, i.e. $(H^+)[HPO_4^-]/[H_2PO_4^{2-}] = 10^{-pH}(1-f_{op})/f_{op} = 10^{-pK'p2})$. Selecting the stoichiometry for methanogenic AD for which CO_2 and CH_4 are the electron acceptor reactant and product, (i.e. $d = 1$, $e = 0$, $f = 2$, $g = 0$, $h = 0$, chr = 0, $r = 1$, $t = 4$, $u = 0$, $v = 0$, $w = 0$, chp = 0 and $\gamma_e = 8$ e^-/mol in $C_dH_eO_fN_gS_h{}^{chr}$ and $C_rH_tO_uN_vS_w{}^{chp}$), substituting Eqs 27a to c yields a more general steady-state model stoichiometry for methanogenic AD (Eq. 28) than that of Sötemann et al. (2005a). Coupled with the aqueous-gas phase CO_2 equilibrium calculated using Henry's law, the products of this stoichiometry can be used to calculate the AD pH, provided it is between 6.8 and 8.6.

$$C_xH_yO_zN_aP_bS_C^{ch} + \left\{[2x - z + a + b(2 + f_{op}) + 2c - ch] - E\frac{\gamma_S}{\gamma_B}[2k - m + n + p(2 + f_{op}) + 2s] - \frac{2(1-E)\gamma_S}{8}\right\}H_2O \rightarrow \frac{E\gamma_S}{\gamma_B}C_kH_lO_mN_nP_pS_s + \frac{\gamma_S(1-E)}{8}CH_4 + \left[a - nE\frac{\gamma_S}{\gamma_B}\right]NH_4^+ + \left[c - sE\frac{\gamma_S}{\gamma_B}\right]SO_4^{2-} + f_{op}\left[b - pE\frac{\gamma_S}{\gamma_B}\right]H_2PO_4^- + (1 - f_{op})\left[b - pE\frac{\gamma_S}{\gamma_B}\right]HPO_4^{2-} + \left\{[x - a + b(2 - f_{op}) + 2c + ch] - E\frac{\gamma_S}{\gamma_B}[k - n + p(2 - f_{op}) + 2s] - \frac{(1-E)\gamma_S}{8}\right\}CO_2 + \left\{[a - b(2 - f_{op}) - 2c - ch] - E\frac{\gamma_S}{\gamma_B}[n - p(2 - f_{op}) - 2s]\right\}HCO_3^-$$

$$(28)$$

The total alkalinity change (ΔAlk_T) of Eq. 28 is obtained by subtracting the contributions of the weak acid/base reactant species from the contributions of the weak acid/base product species. The contribution of a weak acid/base species to the alkalinity is its deficit of protons relative to its reference species, i.e., HCO_3^- contributes one equivalent of alkalinity whereas $H_2PO_4^-$ and HPO_4^{2-} contribute one and two equivalents, respectively, if the reference species is H_3PO_4. For Eq. 28 ΔAlk_T is:

$$\Delta Alk_T = \left[a - nE\frac{\gamma_S}{\gamma_B}\right] - 2\left[c - sE\frac{\gamma_S}{\gamma_B}\right] - ch \quad (29)$$

From the stoichiometry of Eq. 28 for 1 mol/L biodegradable organics digested [from (gCOD/L)/($8\gamma_S$)]:

(1) The only product terms that have non-zero EDC (COD) are the methane and biomass. Therefore, the COD of the CH_4 is equal to the COD of the biodegradable organics degraded (minus the very small amount, 2–5% of COD, in the AD biomass produced and residual VFA). CH_4 is the main (>95%) AD product from the biodegradable organics that has EDC.

(2) Ignoring the small amount of C in the biomass and residual VFA, the C content of the organics digested exits the AD via three routes – CH4 and CO2 gas and dissolved CO2 (as HCO3-). So the C not converted to CH4 gas becomes dissolved CO2 (HCO3-) and gaseous CO2.

(3) The N content of the biodegradable organics (minus the very small amount of N in AD biomass) represents the electron donor's persistent alkalinity. (In Eq. 29, the S content also affects ΔAlk_T but

in most cases $c << a$). In the breakdown of the organics this alkalinity is transferred to the aqueous phase and so the total alkalinity of the aqueous phase increases by a mol/L, minus (i) the very small amount in N taken up into the AD biomass produced ($nE\gamma_S/\gamma_B$) and (ii) any alkalinity in the residual VFA (not included in Eqs 28 and 29). So in the 6.8–8.6 pH range of ADs, the organic component's latent alkalinity is transferred to the HCO_3^- of the IC system. In fact, in plant-wide models, the alkalinity taken up from the aqueous phase in the form of N into activated sludge biomass in anabolism (Eq. 12) in the AS reactor is transferred to the AD in the biomass of the thickened WAS and released to the aqueous phase in its breakdown at high concentration. Similarly, in the AD of industrial, food or agricultural wastes containing proteins, the alkalinity taken up in the formation of the proteins (external to the AD) is released to the aqueous phase in the AD in their breakdown and adds alkalinity and buffer capacity to the aqueous phase for pH control. Therefore, to keep pH above 7 in AD without alkalinity dosing, the feed to ADs should include proteinaceous material.

(4) When organic P is released to the aqueous phase from the breakdown of organics, the ΔAlk_T does not change (as can be seen in Eq. 29) but the addition of orthophosphate results in the re-speciation of all the weak acid/base systems present (as can be seen in Eq. 28). This re-speciation transfers alkalinity from the HCO_3^- of the IC system to the $H_2PO_4^-$ and HPO_4^{2-} species of the OP system. So the release of P from the breakdown of organics increases the alk H_3PO_4 but decreases the alk H_2CO_3 (using the Loewenthal et al., 1989, 1991 terminology) by the same amount. This increases the CO_2 that leaves the AD as gas (by $b\{2-f_{op}\}$ in the CO_2 term of Eq. 28), which increases the p_{CO2} of the gas phase. The decrease in HCO_3^- causes the pH of the digester to decrease, but now the requirement of the OP system, via its $H_2PO_4^-/HPO_4^=$ dissociation, also has to be met to establish the pH – the f_{op} value at which dissociation requirements of both the OP and IC systems is met establishes the AD pH. The effect on the AD pH of the hydrolysis of polyphosphate from phosphorus accumulating organisms (PAOs), which is different to that of the release of P in the e$^-$ donor organics, and its precipitation as struvite, is presented by Harding et al. (2011) and Ikumi et al. (2014), who show that these processes also cause digester pH to decrease and may stimulate struvite and other mineral precipitation in the digester.

(5) If an organic substrate contains organically bound S (not poly-sulphide or other S granules), this decreases its latent alkalinity, since the release of this S as SO_4^{2-} in the breakdown of the organics decreases the Alk_T of the aqueous phase. This decrease is due to the 2 H$^+$ paired with SO_4^{2-}, and decreases the HCO_3^- concentration by 2c mol/L (Eq. 29). The decreased HCO_3^- increases the CO_2 that exits the digester as gas, similar to the release of organic P (5 above), and so also increases the p_{CO2} of the AD gas, which, together with the decrease in HCO_3^-, decreases the AD pH. However, in the AD the SO_4^{2-} may be reduced to sulphide. This BSR is best modelled by its own bioprocess(es) (2a in Tables 1 and 4). If SO_4^{2-} is reduced to sulphide, the 2c mol/L alkalinity decrease will be (partially) restored by the uptake of H$^+$ in BSR, i.e. $SO_4^{2-} + (f_{os} + 1)H^+ + 8(e^- +H^+) = f_{os}H_2S + (1-f_{os})HS^- + 4H2O$, where the 8(e$^-$ +H$^+$) is supplied by the organics e$^-$ donor. If the free (H_2S) and saline (HS$^-$) sulphide (FSS) is significant, the H_2S/HS$^-$ dissociation also needs to be taken into account to determine the pH in the pH range 6.8–8.6. Dealing with multiple weak acid/base systems in bioprocess stoichiometry

with added speciation to calculate pH, such as Eq. 29, is complex (Harding et al., 2011), which makes using external speciation routines for pH calculation, such as the one described in Part 5 of this series, attractive even for steady-state models.

(6) Based on Eq. 32, and as discussed in Part 1 (Brouckaert et al., 2021), $\Delta Alk_T = 0$ for the conversion of acetate to bicarbonate. Thus, the VFA's persistent alkalinity is transferred to the IC system, which tends to increase the pH since the IC system has a higher pK than the VFA system.

So, from (3) and (6) above, AD aqueous alkalinity is increased only by the alkalinity fed to it, which comes from the release of N from the influent organics, and utilization of dissociated VFA in the feed, i.e. $Alk_T = a + j$ mol/L. Also, from (4) and (5), with the release of P and S from the organics, the CO_2 from the organics that remains dissolved as HCO_3^- decreases while the CO_2 exiting as gas increases. Because the methane gas is fixed by the EDC (COD) of the degraded organics, the increased CO_2 gas increases the partial pressure of CO_2 (p_{CO2}) in the AD headspace and decreases the aqueous phase pH. However, as the OP and sulphide concentrations increase, so the OP and sulphide weak acid/base systems have an increasing effect on establishing the AD pH, because the equilibrium requirements of all weak acid/bases present have to be met, which establish the pH. The influent alkalinity (and pH), the two aqueous alkalinity-increasing processes ((3) and (6) above) and the two aqueous alkalinity-consuming processes ((5) and anabolism), establish the Alk_T and p_{CO2} in the AD and hence the AD pH. The other processes, like the release of OP from the breakdown of organic P ((5) above), do not change the Alk_T but only the speciation. So the net aqueous Alk_T increase (= $a - 2s + j$ mol/L, ignoring AD biomass formation) is completely defined by the composition of the influent organics digested and the type of bioprocess, in this case methanogenesis, which itself does not increase the aqueous alkalinity, as BSR does (Poinapen and Ekama, 2010a).

Some of these considerations are illustrated in Figure 2-5, prepared using a steady-state methanogenic model based on Sötemann et al. (2005a). Table 2 from that paper includes experimental data for anaerobic digestion of a sludge substrate in a mixed laboratory digester with a retention time of 20 days. An elemental composition of $C_{3.5}H_7O_2N_{0.196}$ was used to represent the sludge, calculated from laboratory measurements. This gives a substrate N/COD ratio of 0.0259 g N/g COD. Figure 2-5 shows the model predictions of pH and alkalinity as N/COD is varied by changing the coefficient of N in the substrate formula. (Note that this model did not consider pH inhibition of methanogenesis, and so did not indicate at what point digestion would fail.)
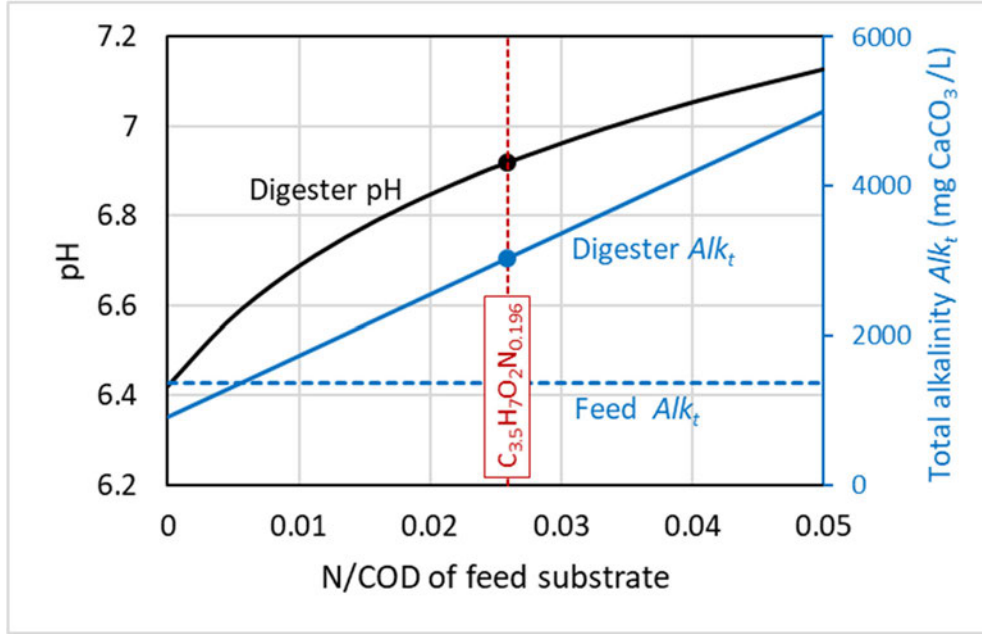
Figure 2-5. *The variation of digester pH and alkalinity with N/COD of the substrate calculated using the steady-state methanogenic model and experimental data from Sötemann et al. (2005a). The point symbols correspond to results from the original paper (although that reports carbonate alkalinities, not total alkalinities).*

Simplified speciation model for sulphidogenesis (Bioprocess 2 – BSR of sulphate to sulphide)

The general stoichiometry (Eq. 24b) tailored to BSR of sulphate to sulphide, with sulphide represented by HS⁻ (Bioprocess 2a in Table 2-1), is given in Table 2-A2. Assuming (i) the BSR reactor pH is between 6.8 and 8.6; (ii) the VFA present is insufficient to affect pH; and (iii) any H^+ excess or deficit (i.e. not paired with e^-) will be supplied or absorbed by the IC and sulphide systems: then the dominant species are NH_4^+ for the FSA, H_2S and HS^- for the sulphide system (pK_{s1} ~7.0) , HPO_4^{2-} and $H_2PO_4^-$ for the OP system (pK_{p2}~ 7.2) and HCO_3^- for the IC system (pK_{c1}~6.4).

Note that unlike for methanogenesis, CO_2 is not included as a product, based on the empirical observation that gas evolution from BSR is negligible. This is because (i) due to the toxicity of sulphide, BSR systems are limited to treating much lower concentrations of waste than methanogenic digesters; therefore less carbonate is released; and (ii) the sulphide released by BSR buffers the pH near pK_{s1}~7.0. Based on the understanding of the dominant species present in the system at near-neutral conditions, a simplified speciation model of BSR can be formulated by replacing the CO_3^{2-}, H^+ and PO_4^{3-} terms in Bioprocess 2a in Table 2-A3 by the substitutions shown in Eqs 30a–30c:

$$[CO_3^{2-}] \equiv ([HCO_3^-] - [H_2S] + [HS^-]) \tag{30a}$$

$$[H^+] \equiv ([H_2S] - [HS^-]) \tag{30b}$$

$$[PO_4^{3-}] \equiv \{f_{op}[H_2PO_4^-] + (1 - f_{op})[HPO_4^{2-}] - (1 + f_{op})([H_2S] - [HS^-])\} \tag{30c}$$

Substituting Eq. 30 into the BSR stoichiometry (Process 2a in Table 2-A2) yields:

$$C_xH_yO_zN_aP_bS_c^{ch} + \left\{[3x - z + 4b + 4c] - E\frac{\gamma_S}{\gamma_B}[3k - m + 4p + 4s] - \frac{4(1-E)\gamma_S}{8}\right\}H_2O +$$

$$\left[\frac{\gamma_S(1-E)}{8} - \left(c - sE\frac{\gamma_S}{\gamma_B}\right)\right]SO_4^{2-} \rightarrow \frac{E\gamma_S}{\gamma_B}C_kH_lO_mN_nP_pS_s + \left[a - nE\frac{\gamma_S}{\gamma_B}\right]NH_4^+ + \left[x - kE\frac{\gamma_S}{\gamma_B}\right]HCO_3^- +$$

$$f_{op}\left[b - pE\frac{\gamma_S}{\gamma_B}\right]H_2PO_4^- + (1 - f_{op})\left[b - pE\frac{\gamma_S}{\gamma_B}\right]HPO_4^{2-} + \left\{[x - a + b(2 - f_{op}) + 2c + ch] - \right.$$

$$\left. E\frac{\gamma_S}{\gamma_B}[k - n + p(2 - f_{op}) + 2s] - \frac{(1-E)\gamma_S}{8}\right\}H_2S + \left\{-[x - a + b(2 - f_{op}) + 2c + ch] + \frac{2(1-E)\gamma_S}{8} + \right.$$

$$\left. E\frac{\gamma_S}{\gamma_B}[k - n + p(2 - f_{op}) + 2s]\right\}HS^- \tag{31}$$

$$\Delta Alk_T = \left[a - nE\frac{\gamma_S}{\gamma_B}\right] - 2\left[c - sE\frac{\gamma_S}{\gamma_B}\right] - ch + \frac{2\gamma_S(1-E)}{8} \tag{32}$$

Equation 31 is the overall stoichiometric balance used in Poinapen and Ekama's (2010a) steady-state biological sulphate reduction model extended to include S in the substrate and biomass terms. Poinapen and Ekama (2010a) explained the lack of CO_2 production in terms of the organic substrate being 'carbon deficient', by which they meant that alkalinity change of reaction (Eq. 32) is greater than the alkalinity of the carbonate species (HCO_3^- at pH ~ 7) released due to the oxidation of the substrate.

This can be understood in contrast to what happens in methanogenesis. It can be shown that ΔAlk_T for methanogenesis (Eq. 29) is approximately equal to the coefficient of HCO_3^- in Eq. 28 (assuming E, b, $c \approx$ 0). This means that under steady-state conditions, any carbonate produced in excess of ΔAlk_T has to be released from solution as CO_2 gas for the pH to remain constant. In BSR, the alkalinity change due to the degradation of the substrate is the same as in methanogenesis (first two terms of Eqs 29 and 32); however, additional alkalinity (third term of Eq. 32) is produced from the reduction of sulphate to sulphide (Eq. 18a). In this case it can be shown that Eq. 32 is approximately equal to the sum of the coefficients of HCO_3^- and HS^- in Eq. 31.

Note that the amount of sulphide produced in BSR is a function of the substrate COD or y_s. It is this additional sulphide alkalinity which buffers the pH near 7 without the loss of CO_2. In Poinapen and Ekama's (2010a) model, the pH is estimated from the HS^- and H_2S concentration ratio, i.e., pH = pK'_{s1}+log{[HS^-]/[H_2S]}. The lack of gas evolution in BSR points to a biosulphide potential (BSP) test in which gas measurements are not necessary and the aqueous concentrations are sufficient for characterizing the biodegradable organics (Chen et al., 2018; Part 3 of this series; Gaszynski et al., 2018).

Note that the assumption of zero CO_2 gas production is not strictly true, because if there is any dissolved carbonate in the system the corresponding equilibrium partial pressure of CO_2 will be non-zero, and there will be the potential for CO_2 gas to diffuse out of solution into the reactor headspace, or to accumulate in sludge granules. A steady-state BSR model including a speciation subroutine (Brouckaert and Brouckaert, 2014) was used to simulate the BSR in the sulphate reduction upflow sludge bed (SRUSB) reactor of Lu et al. (2012). The equilibrium partial pressure of CO_2 (p_{CO2}) was calculated to be very low (at ~0.00050 atm). However, assuming that 10% of the dissolved CO_2 diffused into the headspace resulted in the pH increasing from 7.2 to 7.6 (Lu et al., 2012 measured the pH at 7.8), then, while the loss of CO_2 from solution had a small effect on the C mass balance, it had a noticeable effect on the pH. Furthermore, this shows why it is important that the biosulphide potential (BSP) is conducted in a sealed reactor with no headspace (Part 3 of this series, Gaszynski et al., 2018).

CONCLUSIONS

Complete element mass balance stoichiometry, fully integrated with three-phase (aqueous–gas–solid) physico-chemical processes, is required to predict biosystem pH because the bioprocesses take up from, as reactants, and add to, as products, the aqueous phase ionic mix in which they operate. The aqueous phase in turn exchanges material with the gas phase, and ions with the solid phase in mineral precipitation processes, combining to govern the bioprocess reactor pH. The principles and procedures for the derivation of complete element mass balance stoichiometry were presented in this paper. The remarkable structured order of this, demonstrated in this paper, allows the derivation to be automated and performed computationally, which was set out in Part 1 of this series (Brouckaert et al., 2021). This may give a false impression that stoichiometry provides all that is required to model a process. However, the required prior information is, in fact, largely covered by knowing what components and species are involved in the process; once these are known, the systematic approach explained in this Part 2 of the series will go a long way towards completing the process description. The prior information imposed on the bioprocess stoichiometry required for different modelling purposes, is made explicit in this Part 2.

Dynamic models usually have to take account of intermediate components and species of a process, and so generally require more detailed knowledge than steady-state models, as input to the stoichiometry. The extra complexity that this entails makes it more important to align components and species with the well-established and systematic framework of the standard aquatic chemistry components, and associated speciation models.

With complete element mass-balanced stoichiometry, all the material of the bioprocess reactants – inter alia, influent substrate(s) – are conserved in the bioprocess products, most of which are dissolved aqueous species. Not only are the elements CHONPS and charge conserved but also alkalinity, which is an integral part of the bioprocess stoichiometry. The aqueous species all engage with the physico-chemical processes, most particularly aqueous (re)speciation, gas exchange and mineral precipitation. This intimate interconnection between the bioprocesses and the aqueous phase in which they operate means that the behaviour and progression of bioprocesses can be measured and monitored by changes in the aqueous phase species, which includes the alkalinity. To exploit this interconnection for the purpose of gaining insight into bioprocess behaviour and provide a means for their control, requires two transformation interfaces – one for the organic substrate and one for the aqueous inorganic material – which translate the model variables (components) to measurable parameters and vice versa. For the organic substrate, measurements need to be made to define the composition of the biodegradable organics (if these are not known) and a procedure is developed to determine the composition values (*x, y, z, a, b, c* and ch) in $C_xH_yO_zN_aP_bS_c^{ch}$ from measurements in Part 3. To characterize the aqueous phase, the alkalinity is often used to quantify the inorganic system. Alkalinity is a summary parameter representing many aqueous species, and so an aqueous speciation procedure is required to disaggregate the measured alkalinity into its subsystem species and model components. This is considered in Part 4. The last paper, Part 5, describes the aqueous phase speciation routine mentioned in this paper.

REFERENCES

ALLISON JD, BROWN DS and NOVO-GRADAC KJ (1991) MINTEQA2/PRODEFA2. A geochemical assessment model for environmental systems: Version 3.0. EPA/600/3-91/021. United States Environmental Protection Agency, Washington, D.C.

BAYARD R, BENBELKACEM H, GOURDON R and GOURC J-P (2011) Mass balance on water and dry solids from pilot-scale landfill bioreactor studies. 13th International waste management and landfill symposuim, S. Margherita di Pula, Cagliari, Italy, 3–7 Oct.

BROUCKAERT CJ, BROUCKAERT BM and EKAMA GA (2021) Integration of complete elemental mass balanced stoichiometry and aqueous phase chemistry for bioprocess modelling of liquid and solid waste treatment systems – Part 1: The physico-chemical framework. *Water SA* **47** (3) 276-288. https://doi.org/10.17159/wsa/2021.v47.i3.11857

CHEN TT, ZHENG P and SHEN LD (2013) Growth and metabolism characteristics of anaerobic ammonium oxidizing bacteria aggregates. *Appl. Microbiol. Biotechnol*. **97** (12) 5575–5583. https://doi.org/10.1007/s00253-012-4346-z

CHEN L, TSUI T-H, EKAMA GA, MACKEY HR, HAO T-W and CHEN GH (2018) Development of biochemical sulfide potential (BSP) test for sulfidogenic biotechnology application. *Water Res.* **135** 231–240. https://doi.org/10.1016/j.watres.2018.02.009

DENG Y-F, EKAMA GA, CUI YX, TANG CJ, VAN LOOSDRECHT MCM, CHEN GH and WU D (2019) Coupling of sulfur(thiosulfate)-driven denitratation and anammox process to treat nitrate and ammonium contained wastewater. *Water Res.* **163** 114854. https://doi.org/10.1016/j.watres.2019.114854

EKAMA GA (2009) Using bioprocess stoichiometry to build a steady state plant wide wastewater treatment plant model. *Water Res.* **43** (8) 2101–2120. https://doi.org/10.1016/j.watres.2009.01.036

FERNÁNDEZ-ARÉVALO T, LIZARRALDE I, GRAU P and AYESA E (2015) New systematic methodology for incorporating dynamic heat transfer modelling in multi-phase biochemical reactors. *Water Res.* **60** 141–155. https://doi.org/10.1016/j.watres.2014.04.034

GASZYNSKI CE, IKUMI DS and EKAMA GA (2018) Getting the most out wastewater treatment plants and anaerobic digesters with biodegradability tests: Deliverable 4: Results of the ABMP and ABSP tests. Interim Report to the Water Research Commission on Project K5/2595. University of Cape Town, South Africa.

GHOOR T (2019) Developments in anaerobic digestion modelling, PhD thesis, Water Research Group, Department of Civil Engineering, University of Cape Town.

GRAU P, DE GRACIA M, VANROLLEGHEM PA and AYESA E (2007) A new plant wide methodology for WWTPs. *Water Res.* **41** 4357–4372. https://doi.org/10.1016/j.watres.2007.06.019

GUJER W and LARSEN TA (1995) The implementation of biokinetics and conservation principles in ASIM. *Water Sci. Technol.* **31** (2) 257–266. https://doi.org/10.2166/wst.1995.0114

GUJER W (2008) *System Analysis for Water Technology.* Springer, New York. ISBN 978-3-540-77278-1.

HARDING TH, IKUMI DS and EKAMA GA (2011) Incorporating phosphorus into plant wide wastewater treatment plant modelling - Anaerobic digestion. *8th IWA Watermatex Conference*, 20-22 June 2011, San Sebastian, Spain.

HAUDUC H, RIEGER L, TAKÁCS I, HÉDUIT A, VANROLLEGHEM PA and GILLOT S (2010). A systematic approach for model verification: Application on seven published activated sludge models. *Water Sci. Technol*. **61** (4) 825–839. https://doi.org/10.2166/wst.2010.898

HENZE M, GRADY, CPL (JNR), GUJER W, MARAIS, GVR and MATSUO T (1987) Activated sludge model No 1. IWA Scientific and Technical Report No 1. IWA, London. ISSN 1010-707X. 33 pp.

HENZE M, VAN LOOSDRECHT MCM, EKAMA GA and BRDJANOVIC D (2008) Biological wastewater treatment: Principles, modelling and design. IWA Publishing, London. 528 pp. https://doi.org/10.2166/9781780401867

IKUMI DS, BROUCKAERT CJ and EKAMA GA (2011) A 3 phase anaerobic digestion model. *8th IWA Watermatex Conference*, 20–22 June 2011, San Sebastian, Spain.

IKUMI DS, HARDING TH, BROUCKAERT CJ and EKAMA GA (2014) Plant wide integrated biological, chemical and physical processes modelling of wastewater treatment plants in three phases (aqueous-gas-solid). Research Report W138, Department of Civil Engineering, University of Cape Town, South Africa.

IKUMI DS, HARDING TH, VOGTS M, LAKAY MT, MAFUNGWA HZ, BROUCKAERT CJ and EKAMA GA (2015) Mass balances modelling over wastewater treatment plants III. Final Report to WRC on Contract K5/1822. WRC Report No. 1822/1/14, Water Research Commission, Pretoria. ISBN 978-1-4312-0614-8.

LOEWENTHAL RE and MARAIS GVR (1976) Carbonate chemistry of aquatic systems – theory and application. Ann Arbor Science Publishers, Ann Arbor, MI. Library of Congress 76-24963, ISBN 0-25040141-X.

LOEWENTHAL RE, EKAMA GA and MARAIS GVR (1989) Mixed weak acid/base systems Part I: Mixture characterization. *Water SA* **15** (1) 3–24.

LOEWENTHAL RE, WENTZEL MC, EKAMA GA and MARAIS GVR (1991) Mixed weak acid/base systems Part II: Dosing estimation, aqueous phase. *Water SA* **17** (2) 107–122.

LU H, EKAMA GA, WU D, FENG J, VAN LOOSDRECHT MCM and CHEN G-H (2012) SANI process realizes sustainable saline sewage treatment: Steady state model based evaluation of pilot-scale trial of the process. *Water Res.* **46** (2) 475–490.   https://doi.org/10.1016/j.watres.2011.11.031

MCCARTY PL (1975) Stoichiometry of biological reactions. *Progr. Water Technol.* **7** (1) 157-172.

MIKEBYDHI (2021) WEST2016. Modelling and simulation of wastewater treatment plants. URL: www.mikebydhi.com/products/west (Accessed 9 July 2021).

MESSENGER JR and EKAMA GA (1993) Evaluation of the dual digestion system: Part 3 - Considerations in the process design of the aerobic reactor. *Water SA* **19** (3) 201–208.

PARKHURST DL and APPELO CAJ (2013) Description of input and examples for PHREEQC version 3 – a computer program for speciation, batch-reaction, one-dimensional transport, and inverse geochemical calculations: United States Geological Survey Techniques and Methods, Book 6, Chapter A43. 497 pp. https://doi.org/10.3133/tm6A43

PITT AJ and EKAMA GA (1996) Dual digestion of sewage sludge with air and pure oxygen. *Proc. 69th Water Environment Federation Annual Conference and Exhibition*, Dallas TX. Vol 2. 69–82.

POINAPEN J, EKAMA GA and WENTZEL MC (2009) Biological sulphate reduction using primary sewage sludge in a upflow anaerobic sludge bed reactor – Part 2: Modification of simple wet chemistry analytical procedures to achieve COD and S mass balances. *Water SA* **35** (5) 535–542. https://doi.org/10.4314/wsa.v35i5.49179

POINAPEN J and EKAMA GA (2010a) Biological sulphate reduction using primary sewage sludge in a upflow anaerobic sludge bed reactor – Part 5: Development of a steady state model. *Water SA* **36** (3) 193–202.

POINAPEN J and EKAMA GA (2010b) Biological sulphate reduction using primary sewage sludge in a upflow anaerobic sludge bed reactor – Part 6: Development of a dynamic simulation model. *Water SA* **36** (3) 203–214.

QIAN J, FENG J, CHUI HK, LU H, VAN LOOSDRECHT MCM and CHEN GH (2013) Industrial flue gas desulphurization waste may offer an opportunity to facilitate SANI application for significant sludge minimization in fresh water treatment. *Water Sci. Technol*. **67** (12) 2822–2826. https://doi.org/10.2166/wst.2013.187

QIAN J, LU H, FENG J, EKAMA GA and CHEN G-H (2015) Beneficial co-treatment of simple wet flue gas desulphurization wastes with fresh water sewage through development of mixed denitrification SANI Process. *Chem. Eng. J.* (01/2015) **262** 109–118. https://doi.org/10.1016/j.cej.2014.09.066

RAGA R and COSSU R (2011) Lab scale tests before in situ aerobic stabilization of an old landfill. *13th International Waste Management and Landfill Symposium*, 3–7 October 2011, S. Margherita di Pula, Cagliari, Italy.

RITTMANN BE and MCCARTY PL (2001) *Environmental Biotechnology: Principles and Applications.* McGraw-Hill, New York. ISBN13- 978-0071181846.

SMOLDERS GJF, VAN DER MEIJ J, VAN LOOSDRECHT MCM and HEIJNEN JJ (1995) A structured model for anaerobic and aerobic stoichiometry and kinetics of the biological phosphorus removal process. *Biotechnol. Bioeng.* **47** (3) 227–287. https://doi.org/10.1002/bit.260470302

SOLON K, FLORES-ALSINA X, KAZADI MBAMBA C, VOLKE EIP, TAIT S, BATSTONE D, GERNAEY KV and JEPPSON U (2015) Effects of ionic strength and ion pairing on (plant-wide) modelling of anaerobic digestion. *Water Res.* **70** 235–245. https://doi.org/10.1016/j.watres.2014.11.035

SÖTEMANN SW, RISTOW NE, WENTZEL MC and EKAMA GA (2005a) A steady-state model for anaerobic digestion of sewage sludges. *Water SA* **31** (4) 511–527. https://doi.org/10.4314/wsa.v31i4.5143

SÖTEMANN SW, MUSVOTO EV, WENTZEL MC and EKAMA GA (2005b) Integrated chemical, physical and biological processes kinetic modelling Part 2 - Anaerobic digestion of sewage sludge. *Water SA* 31 (4) 545–568. https://doi.org/10.4314/wsa.v31i4.5145

STANDARD METHODS (2017) *Standard Methods for the Examination of Water and Wastewater* (23rd edn) Eds: Rice EB, Baird RB and Eaton AD. American Water Works Association (AWWA), American Public Works Association (APWA), Water Environment Federation (WEF), Alexandria, VA. ISBN 9781625762405.

TAKÁCS I and VANROLLEGHEM PA (2006) Elemental balances in activated sludge modelling. *Proc. IWA World Water Congress*, 10–14 Sept 2006, Beijing, China.

TAIT S, SOLON K, VOLCKE EIP and BATSTONE DJ (2012) A unified approach to modelling wastewater Chemistry: Model Corrections. *Proc. WWTmod2012 Conference*, 26–28 February 2012. Mont-Sainte-Anne, Québec, Canada.

TAKÁCS I and VANROLLEGHEM PA (2006) Elemental balances in activated sludge modelling. *Proc. IWA World Water Congress*, 10–14 September 2006, Beijing, China.

VAN NIFTRIK LA, FUERST JA, SINNINGHE DAMST JS, KUENEN JG, JETTEN MSM and STROUS M (2004) The anammoxosome: an intracytoplasmic compartment in anammox bacteria. *FEMS Microbiol. Lett.* **233** 7–13. https://doi.org/10.1016/j.femsle.2004.01.044

VAN RENSBURG P, MUSVOTO EV, WENTZEL MC AND EKAMA GA (2003) Modelling multiple mineral precipitation in anaerobic digester liquor. *Water Res.* **37** (13) 3078–3097. https://doi.org/10.1016/S0043-1354(03)00173-8

VAN ZYL PJ, WENTZEL MC, EKAMA GA AND RIEDEL K-H (2008) Design and start up of a high rate anaerobic membrane bio-reactor for the treatment of a low pH, high strength dissolved organic wastewater. *Water Sci. Technol.* **57** (2) 291–295. https://doi.org/10.2166/wst.2008.083

WANG B, WU D, EKAMA GA, TSUI T-H, FENG J and CHEN G-H (2018) Characterization of a new continuous gas-mixing sulfidogenic anaerobic bioreactor: Hydrodynamics and sludge granulation. *Water Res.* **135** 251–261. https://doi.org/10.1016/j.watres.2018.02.013

WESTERGREEN S, BROUCKAERT CJ AND FOXON KM (2012) Modelling of ionic interactions with wastewater treatment biomass. *Water Sci. Technol.* **65** (6) 1014–1020. https://doi.org/10.2166/wst.2012.922

APPENDIX

General bioprocess stoichiometry tables

Note that all the coefficients in these tables can be obtained using the stoichiometry generator program. However, the more complex coefficients look quite different, since the generator does not collect terms neatly, as in the tables.

Tables A1–A4 uses a common set of components (columns), numbered 1 to 19. Columns with no entries in a particular table are omitted.

Table 2-A1. *General bioprocesses stoichiometry for Bioprocesses 1, 3, 4 and 6–8 in Table 2-1*

Components / Bio-process	1 Organics	3 HS⁻	4 Biomass	5 PO_4^{3-}	7 CH_4	8 O_2	9 NH_4^+	10 SO_4^{2-}
1 Methanogenesis	$-C_xH_yO_zN_aP_bS_c^{ch}$		$E\frac{\gamma_S}{\gamma_B}C_kH_lO_mN_nP_pS_s$	$b\text{-}pE\frac{\gamma_S}{\gamma_B}$	$\frac{\gamma_S}{8}(1\text{-}E)$		$\left(a\text{-}nE\frac{\gamma_S}{\gamma_B}\right)$	$\left(c\text{-}sE\frac{\gamma_S}{\gamma_B}\right)$
3 Nitrification (NH_4^+ to NO_3^-)			$E\frac{\gamma_S}{\gamma_B}C_kH_lO_mN_nP_pS_s$	$\text{-}pE\frac{\gamma_S}{\gamma_B}$		$-\frac{\gamma_S}{4}(1\text{-}E)$	$-\left(1+nE\frac{\gamma_S}{\gamma_B}\right)$	$\text{-}sE\frac{\gamma_S}{\gamma_B}$
3a Nitrification (NH_4^+ to NO_2^-)			$E\frac{\gamma_S}{\gamma_B}C_kH_lO_mN_nP_pS_s$	$\text{-}pE\frac{\gamma_S}{\gamma_B}$		$-\frac{\gamma_S}{4}(1\text{-}E)$	$-\left(1+nE\frac{\gamma_S}{\gamma_B}\right)$	$\text{-}sE\frac{\gamma_S}{\gamma_B}$
3b Nitrification (NO_2^- to NO_3^-)			$E\frac{\gamma_S}{\gamma_B}C_kH_lO_mN_nP_pS_s$	$\text{-}pE\frac{\gamma_S}{\gamma_B}$		$-\frac{\gamma_S}{4}(1\text{-}E)$	$\text{-}nE\frac{\gamma_S}{\gamma_B}$	$\text{-}sE\frac{\gamma_S}{\gamma_B}$
4 Aerobic Heterotrophic	$-C_xH_yO_zN_aP_bS_c^{ch}$		$E\frac{\gamma_S}{\gamma_B}C_kH_lO_mN_nP_pS_s$	$b\text{-}pE\frac{\gamma_S}{\gamma_B}$		$-\frac{2\gamma_S}{8}(1\text{-}E)$	$\left(a\text{-}nE\frac{\gamma_S}{\gamma_B}\right)$	$\left(c\text{-}sE\frac{\gamma_S}{\gamma_B}\right)$
6 Heterotrophic Denitrification	$-C_xH_yO_zN_aP_bS_c^{ch}$		$E\frac{\gamma_S}{\gamma_B}C_kH_lO_mN_nP_pS_s$	$b\text{-}pE\frac{\gamma_S}{\gamma_B}$			$\left(a\text{-}nE\frac{\gamma_S}{\gamma_B}\right)$	$\left(c\text{-}sE\frac{\gamma_S}{\gamma_B}\right)$
6a Heterotrophic Denitrification	$-C_xH_yO_zN_aP_bS_c^{ch}$		$E\frac{\gamma_S}{\gamma_B}C_kH_lO_mN_nP_pS_s$	$b\text{-}pE\frac{\gamma_S}{\gamma_B}$			$\left(a\text{-}nE\frac{\gamma_S}{\gamma_B}\right)$	$\left(c\text{-}sE\frac{\gamma_S}{\gamma_B}\right)$
6b Heterotrophic Denitrification	$-C_xH_yO_zN_aP_bS_c^{ch}$		$E\frac{\gamma_S}{\gamma_B}C_kH_lO_mN_nP_pS_s$	$b\text{-}pE\frac{\gamma_S}{\gamma_B}$			$\left(a\text{-}nE\frac{\gamma_S}{\gamma_B}\right)$	$\left(c\text{-}sE\frac{\gamma_S}{\gamma_B}\right)$
7 Anammox			$\frac{E}{\gamma_B}C_kH_lO_mN_nP_pS_s$	$\text{-}p\frac{E}{\gamma_B}$			$-\left(\frac{1}{3}+n\frac{E}{\gamma_B}\right)$	$\text{-}s\frac{E}{\gamma_B}$
8 Aerobic sulphide oxidation		-1	$\frac{E\gamma_S}{\gamma_B}C_kH_lO_mN_nP_pS_s$	$\text{-}p\frac{E\gamma_S}{\gamma_B}$		$-\frac{\gamma_S}{4}(1\text{-}E)$	$\text{-}n\frac{E\gamma_S}{\gamma_B}$	$\left(1\text{-}s\frac{E\gamma_S}{\gamma_B}\right)$

Table 2-A1 continued: *General bioprocesses stoichiometry for the bioprocesses 1,3,4 and 6-8 in Table 2-1*

Components / Bio-process	13 NO_3^-	14 NO_2^-	15 N_2	16 H_2O	17 H^+	CO_3^{2-}
1 Methanogenesis				$E\frac{\gamma_S}{\gamma_B}(3k\text{-}m+4p+4s)+\frac{3\gamma_S}{8}(1\text{-}E) - (3x\text{-}z+4b+4c)$	$(2x-a+3b+2c + ch)-\frac{2\gamma_S}{8}(1\text{-}E)-E\frac{\gamma_S}{\gamma_B}(2k\text{-}n+3p+2s)$	$x\text{-}kE\frac{\gamma_S}{\gamma_B}-\frac{\gamma_S}{8}(1\text{-}E)$
3 Nitrification (NH_4^+ to NO_3^-)	+1			$\left(-3+\frac{\gamma_S(1-E)}{2}+E\frac{\gamma_S}{\gamma_B}[3k\text{-}m+4p+4s]\right)$	$2-E\frac{\gamma_S}{\gamma_B}[2k\text{-}n+3p+2s]$	$-kE\frac{\gamma_S}{\gamma_B}$
3a Nitrification (NH_4^+ to NO_2^-)		+1		$\left(-2+\frac{\gamma_S(1-E)}{2}+\frac{E\gamma_S}{\gamma_B}[3k\text{-}m+4p+4s]\right)$	$2-E\frac{\gamma_S}{\gamma_B}[2k\text{-}n+3p+2s]$	$-kE\frac{\gamma_S}{\gamma_B}$
3b Nitrification (NO_2^- to NO_3^-)	+1	-1		$\left(-1+\frac{\gamma_S(1-E)}{2}+\frac{E\gamma_S}{\gamma_B}[3k\text{-}m+4p+4s]\right)$	$-E\frac{\gamma_S}{\gamma_B}[2k\text{-}n+3p+2s]$	$-kE\frac{\gamma_S}{\gamma_B}$
4 Aerobic Heterotrophic				$\frac{\gamma_S}{2}(1\text{-}E)\text{-}[3x\text{-}z+4b+4c]+E\frac{\gamma_S}{\gamma_B}[3k\text{-}m+4p+4s]$	$(2x-a+3b+2c + ch)$ $-E\frac{\gamma_S}{\gamma_B}[2k\text{-}n+3p+2s]$	$x\text{-}kE\frac{\gamma_S}{\gamma_B}$
6 Heterotrophic Denitrification	$-\frac{\gamma_S}{5}(1\text{-}E)$		$\frac{\gamma_S}{10}(1\text{-}E)$	$\frac{3\gamma_S}{5}(1\text{-}E)\text{-}[3x\text{-}z+4b+4c]+E\frac{\gamma_S}{\gamma_B}[3k\text{-}m+4p+4s]$	$(2x-a+3b+2c + ch) -E\frac{\gamma_S}{\gamma_B}(2k\text{-}n+3p+2s)-\frac{\gamma_S}{5}(1\text{-}E)$	$x\text{-}kE\frac{\gamma_S}{\gamma_B}$
6a Heterotrophic Denitrification	$-\frac{\gamma_S}{2}(1\text{-}E)$	$\frac{\gamma_S}{2}(1\text{-}E)$		$\frac{\gamma_S}{2}(1\text{-}E)\text{-}(3x\text{-}z+4b+4c)+E\frac{\gamma_S}{\gamma_B}(3k\text{-}m+4p+4s)$	$(2x-a+3b+2c + ch)-E\frac{\gamma_S}{\gamma_B}(2k\text{-}n+3p+2s)$	$x\text{-}kE\frac{\gamma_S}{\gamma_B}$
6b Heterotrophic Denitrification		$-\frac{\gamma_S}{3}(1\text{-}E)$	$\frac{\gamma_S}{6}(1\text{-}E)$	$\frac{2\gamma_S}{3}(1\text{-}E)\text{-}(3x\text{-}z+4b+4c)+E\frac{\gamma_S}{\gamma_B}(3k\text{-}m+4p+4s)$	$(2x-a+3b+2c + ch)-\frac{\gamma_S}{3}(1\text{-}E)-E\frac{\gamma_S}{\gamma_B}[2k\text{-}n+3p+2s]$	$x\text{-}kE\frac{\gamma_S}{\gamma_B}$
7 Anammox	$+\frac{E}{2}$	$-\left(\frac{1}{3}+\frac{E}{2}\right)$	$+\frac{1}{3}$	$\left(\frac{2}{3}-\frac{E}{2}+\frac{E}{\gamma_B}[3k\text{-}m+4p+4s]\right)$	$-\frac{E}{\gamma_B}[2k\text{-}n+3p+2s]$	$-k\frac{E}{\gamma_B}$
8 Aerobic sulphide oxidation				$-\frac{E\gamma_S}{2}+\left(\frac{E\gamma_S}{\gamma_B}[3k\text{-}m+4p+4s]\right)$	$1-\frac{E\gamma_S}{\gamma_B}[2k-n+3p+2s]$	$-k\frac{E\gamma_S}{\gamma_B}$

Table 2-A2. *General bioprocesses stoichiometry for Bioprocesses 2a to 2d in Table 2-1. The change of alkalinity of reaction (ΔAlk_T) can be calculated from the components which contribute to alkalinity, as per Eq. 19 in Part 1 (Brouckaert et al., 2021).*

Components Bio-process	1 Organics	3 or 12 HS^- or $S_2O_3^{2-}$	4 Biomass	5 PO_4^-	9 NH_4^+	10,11,12 $SO_4^{2-}, SO_3^{2-}, S_2O_3^{2-}$
2a Sulphidogenesis (SO_4^{2-} to HS^-)	$-C_xH_yO_zN_aP_bS_c^{ch}$	$\dfrac{\gamma_S}{8}(1\text{-}E)HS^-$	$E\dfrac{\gamma_S}{\gamma_B}C_kH_lO_mN_nP_pS_s$	$b\text{-}pE\dfrac{\gamma_S}{\gamma_B}$	$a\text{-}nE\dfrac{\gamma_S}{\gamma_B}$	$[-\dfrac{\gamma_S}{8}(1\text{-}E)+c\text{-}sE\dfrac{\gamma_S}{\gamma_B}]SO_4^{2-}$
2b Sulphidogenesis (SO_3^{2-} to HS^-)	$-C_xH_yO_zN_aP_bS_c^{ch}$	$\dfrac{\gamma_S^*}{6}(1\text{-}E)HS^-$	$E\dfrac{\gamma_S^*}{\gamma_B^*}C_kH_lO_mN_nP_pS_s$	$b\text{-}pE\dfrac{\gamma_S^*}{\gamma_B^*}$	$a\text{-}nE\dfrac{\gamma_S^*}{\gamma_B^*}$	$[-\dfrac{\gamma_S^*}{6}(1\text{-}E)+c\text{-}sE\dfrac{\gamma_S^*}{\gamma_B^*}]SO_3^{2-}$
2c Sulphidogenesis ($S_2O_3^{2-}$ to HS^-)	$-C_xH_yO_zN_aP_bS_c^{ch}$	$\dfrac{2\gamma_S^\dagger}{8}(1\text{-}E)\,HS^-$	$E\dfrac{\gamma_S^\dagger}{\gamma_B^\dagger}C_kH_lO_mN_nP_pS_s$	$b\text{-}pE\dfrac{\gamma_S^\dagger}{\gamma_B^\dagger}$	$a\text{-}nE\dfrac{\gamma_S^\dagger}{\gamma_B^\dagger}$	$[-\dfrac{\gamma_S^\dagger}{8}(1\text{-}E)+\dfrac{c}{2}-\dfrac{s}{2}E\dfrac{\gamma_S^\dagger}{\gamma_B^\dagger}]S_2O_3^{2-}$
2d Sulphidogenesis (SO_3^{2-} to $S_2O_3^{2-}$)	$-C_xH_yO_zN_aP_bS_c^{ch}$	$+\dfrac{\gamma_S^*}{4}(1\text{-}E)\,S_2O_3^{2-}$	$E\dfrac{\gamma_S^*}{\gamma_B^*}C_kH_lO_mN_nP_pS_s$	$b\text{-}pE\dfrac{\gamma_S^*}{\gamma_B^*}$	$a\text{-}nE\dfrac{\gamma_S}{\gamma_B}$	$[-\dfrac{\gamma_S^*}{2}(1\text{-}E)+c\text{-}sE\dfrac{\gamma_S^*}{\gamma_B^*}]SO_3^{2-}$

γ_S^* and γ_B^* are based on +4c and +4s in Eqs 11 and 13. SO_3^{2-} is the reference oxidation state for S. So γ_S^* of SO_3^{2-} relative to elemental S=+4c e^-/molS (Fig 2).

$\gamma_S^\dagger$ and $\gamma_B^\dagger$ are based on +2c and +2s in Eqs 11 and 13. $S_2O_3^{2-}$ is the reference oxidation state for S. So $\gamma_S^\dagger$ of $S_2O_3^{2-}$ relative to elemental S=+2c e^-/molS (Fig 2).

Table 2-A2 continued: *General bioprocesses stoichiometry for Bioprocesses 2a–d in Table 2-1*

Components Bio-process	16 H_2O	19 CO_3^{2-}	17 H^+
2a Sulphidogenesis (SO_4^{2-} to HS^-)	$-(3x\text{-}z+4b+4c)+\dfrac{4\gamma_S}{8}(1\text{-}E)+E\dfrac{\gamma_S}{\gamma_B}[3k\text{-}m+4p+4s]$	$x\text{-}kE\dfrac{\gamma_S}{\gamma_B}$	$(2x-a+3b+2c+ch)-\dfrac{\gamma_S}{8}(1\text{-}E)\text{-}E\dfrac{\gamma_S}{\gamma_B}[2k\text{-}n+3p+2s]$
2b Sulphidogenesis (SO_3^{2-} to HS^-)	$-(3x\text{-}z+4b+3c)+\dfrac{3\gamma_S^*}{6}(1\text{-}E)+E\dfrac{\gamma_S^*}{\gamma_B^*}[3k\text{-}m+4p+3s]$	$x\text{-}kE\dfrac{\gamma_S^*}{\gamma_B^*}$	$(2x\text{-}a+3b+2c+ch)-\dfrac{\gamma_S^*}{6}(1\text{-}E)\text{-}E\dfrac{\gamma_S^*}{\gamma_B^*}[2k\text{-}n+3p+2s]$
2c Sulphidogenesis ($S_2O_3^{2-}$ to HS^-)	$-\left(3x\text{-}z+4b+\dfrac{3}{2}c\right)+\dfrac{3\gamma_S^\dagger}{8}(1\text{-}E)+E\dfrac{\gamma_S^\dagger}{\gamma_B^\dagger}\left[3k\text{-}m+4p+\dfrac{3}{2}s\right]$	$x\text{-}kE\dfrac{\gamma_S^\dagger}{\gamma_B^\dagger}$	$(2x\text{-}a+3b+c+ch)-E\dfrac{\gamma_S^\dagger}{\gamma_B^\dagger}[2k\text{-}n+3p+s]$
2d Sulphidogenesis (SO_3^{2-} to $S_2O_3^{2-}$)	$-(3x\text{-}z+4b+3c)+\dfrac{3\gamma_S^*}{4}(1\text{-}E)+E\dfrac{\gamma_S^*}{\gamma_B^*}[3k\text{-}m+4p+3s]$	$x\text{-}kE\dfrac{\gamma_S^*}{\gamma_B^*}$	$(2x\text{-}a+3b+2c+ch)-\dfrac{2\gamma_S^*}{4}(1\text{-}E)\text{-}E\dfrac{\gamma_S^*}{\gamma_B^*}[2k\text{-}n+3p+2s]$

$\gamma_S^*, \gamma_B^*, \gamma_S^\dagger$ and $\gamma_B^\dagger$ – see footnotes on Table 2-4c.

Table 2-A3. *General bioprocesses stoichiometry for the Bioprocesses 5a–c in Table 2-1*

Components / Bio-process	1 Organics	11,12 SO_3^{2-}; $S_2O_3^{2-}$	3 HS$^-$	4 Biomass	5 PO_4^{3-}	9 NH_4^+	10 SO_4^{2-}
5a Autotrophic denitrification (H$_2$S/HS$^-$ and NO$_3^-$)			-1	$\frac{E\gamma_S}{\gamma_B}C_kH_lO_mN_nP_pS_s$	$-p\frac{E\gamma_S}{\gamma_B}$	$-n\frac{E\gamma_S}{\gamma_B}$	$+\gamma_S\left(\frac{1}{8}-s\frac{E}{\gamma_B}\right)$
5b Autotrophic denitrification (SO$_3^{2-}$ and NO$_3^-$)		$-SO_3^{2-}$		$\frac{E\gamma_S}{\gamma_B}C_kH_lO_mN_nP_pS_s$	$-p\frac{E\gamma_S}{\gamma_B}$	$-n\frac{E\gamma_S}{\gamma_B}$	$+\gamma_S\left(\frac{1}{2}-s\frac{E}{\gamma_B}\right)$
5c Autotrophic denitrification (S$_2$O$_3^{2-}$ and NO$_3^-$)		$-S_2O_3^{2-}$		$\frac{E\gamma_S}{\gamma_B}C_kH_lO_mN_nP_pS_s$	$-p\frac{E\gamma_S}{\gamma_B}$	$-n\frac{E\gamma_S}{\gamma_B}$	$+\gamma_S\left(\frac{2}{8}-s\frac{E}{\gamma_B}\right)$

Table 2-A3 continued: *General bioprocesses stoichiometry for the bio-processes 5a, b and c in Table 2-1.*

Components / Bio-process	13 NO$_3^-$	14 NO$_2^-$	15 N$_2$	16 H$_2$O	17 H$^+$	19 CO$_3^{2-}$
5a Autotrophic denitrification (HS$^-$ and NO$_3^-$)	$-\frac{\gamma_S}{5}(1-E)$	†	$+\frac{\gamma_S}{10}(1-E)$	$\left(\frac{3\gamma_S}{5}(1-E)-\frac{4\gamma_S}{8}+\frac{E\gamma_S}{\gamma_B}[3k-m+4p+4s]\right)$	$\left(\frac{\gamma_S}{8}-\frac{\gamma_S}{5}(1-E)-\frac{E\gamma_S}{\gamma_B}[2k-n+3p+2s]\right)$	$-k\frac{E\gamma_S}{\gamma_B}$
5b Autotrophic denitrification (SO$_3^{2-}$ and NO$_3^-$)	$-\frac{\gamma_S}{5}(1-E)$	†	$+\frac{\gamma_S}{10}(1-E)$	$\left(\frac{3\gamma_S}{5}(1-E)-\frac{\gamma_S}{2}+\frac{E\gamma_S}{\gamma_B}[3k-m+4p+4s]\right)$	$\left(-\frac{\gamma_S}{5}(1-E)-\frac{E\gamma_S}{\gamma_B}[2k-n+3p+2s]\right)$	$-k\frac{E\gamma_S}{\gamma_B}$
5c Autotrophic denitrification (S$_2$O$_3^{2-}$ and NO$_3^-$)	$-\frac{\gamma_S}{5}(1-E)$	†	$+\frac{\gamma_S}{10}(1-E)$	$\left(\frac{3\gamma_S}{5}(1-E)-\frac{5\gamma_S}{8}+\frac{E\gamma_S}{\gamma_B}[3k-m+4p+4s]\right)$	$\left(\frac{2\gamma_S}{8}-\frac{\gamma_S}{5}(1-E)-\frac{E\gamma_S}{\gamma_B}[2k-n+3p+2s]\right)$	$-k\frac{E}{\gamma_B}\gamma_S$

†If nitrite were the e$^-$ acceptor denitrified to N$_2$ gas, then the 5 in the NO$_3^-$, H$_2$O and H$^+$ terms becomes 3 in the NO$_2^-$, H$_2$O and H$^+$ terms and the 10 in the N$_2$ term becomes 6

Chapter 4: Integration of complete elemental mass-balanced stoichiometry and aqueous-phase chemistry for bioprocess modelling of liquid and solid waste treatment systems – Part 5: Ionic speciation

CJ Brouckaert[1], BM Brouckaert[1] and GA Ekama[2]

[1]WASH R&D Centre, School of Engineering, University of KwaZulu-Natal, Durban 4041, South Africa

[2]Water Research Group, Department of Civil Engineering, University of Cape Town, Rondebosch 7700, South Africa

ABSTRACT

Where aqueous ionic chemistry is combined with biological chemistry in a bioprocess model, it is advantageous to deal with the very fast ionic reactions in an equilibrium sub-model, as was frequently mentioned in the preceding papers in this series. This last paper in the series presents details of how of such an equilibrium speciation sub-model can be implemented, based on well-known open-source aqueous chemistry models. Specific characteristics of the speciation calculations which can be exploited to reduce the computational burden are highlighted. The approach is illustrated using the ionic equilibrium sub-model of a plant-wide wastewater treatment model as an example.

LIST OF ABBREVIATIONS

ASM   activated sludge models

IWA   International Water Association

PWM_SA_AD   University of Cape Town/University of KwaZulu-Natal Anaerobic Digestion Model , a subset of the plant wide PWM_SA model

LIST OF SYMBOLS

A Debye-Hűckel constant

Alk_t total alkalinity in solution relative to $H_2CO_3/H_2PO_4^-/NH_4^+/H_2S/HAc$

K_i equilibrium constant for the formation reaction for species i

I ionic strength, mol/kg

z_i ionic charge on species i

$[i]$ molal concentration of component i, mol/kg

$[i]$ molal concentration of species i, mol/kg

$\{i\}$ activity of species i, dimensionless

ΔH enthalpy change of reaction, J/mol

γ_i activity coefficient of species i

INTRODUCTION

In the previous papers of this series, numerous references have been made to speciation calculations for reactions which closely approach equilibrium, in particular those involving ionic species. As explained in Part 1 (Brouckaert et al., 2021a), the overall model is divided into a kinetically controlled part, and an equilibrium part. For the equilibrium sub-model, the distinction between components and species is particularly important, because its material balance can be formulated purely in terms of components, leading to a much more compact set of balance equations. Once these balances have determined the material content of the system, the equilibrium calculation determines how this material is distributed among the various species. This separation is particularly advantageous for a dynamic model, because while the balance equations are differential equations, the equilibrium calculation involves algebraic equations only.

Aqueous ionic speciation models such as MINTEQA2 (Allison et al., 2009) and PHREEQC (Parkhurst and Appelo, 2013) have been developed to a high degree of sophistication and reliability, to the extent that in many cases their uncertainties are practically negligible compared to those associated with the biological reactions. This means that the modeller can adopt a complex structure of equilibrium species to ensure accurate results, without the penalty of introducing a large number of adjustable parameters. The required parameter values are available in thermodynamic databases, and very seldom require adjustment. These considerations provide a strong motivation to align a biochemical model with one of the established aquatic speciation models, thus exploiting the accumulated knowledge and experience that they represent. This involves adopting their system of components and species, and their reaction equilibrium parameters.

SETTING UP A SPECIATION MODEL

It is possible to couple the PHREEQC computation engine itself to a biochemical model via its automatic programming interface (API); however, its very generality within the aquatic speciation domain is likely to make this inefficient – the biochemical model would use only a small fraction of its outputs. The approach we have taken is to set up customised speciation models which are limited to the scope of each biochemical model to reduce the computational burden. Lizzaralde et al. (2014) compared a model using customised routine against one using the PHREEQC API, and found the former to be significantly faster.

The customised model approach will be illustrated using the example of the ionic equilibrium sub-model used in the anaerobic digestion model of Brouckaert et al. (2010). Only acid/base and ion-paring reactions were included in the equilibrium speciation model, excluding redox reactions and phase-transfer reactions (gas evolution and precipitation), which are much slower, and often not close to equilibrium. These were represented in the anaerobic digestion model as rate-controlled processes, with the equilibrium speciation providing the degrees of over- or under-saturation that drive the phase transfer reactions (see Appendix A). The C++ code for the ionic speciation routine, together with an Excel spreadsheet implementation, can be downloaded from https://washcentre.ukzn.ac.za/bio-process-models/

Choosing components

The components were chosen according to the set of transformation processes represented in the anaerobic digestion model. An anaerobic digester typically includes the carbonate, phosphate, ammonia, acetate, propionate and water weak acid/base subsystems (Loewenthal et al., 1994). Additionally, sodium, potassium, magnesium, calcium, chloride and sulphate are ubiquitous in municipal wastewaters. The ionic model therefore has 12 ionic components for the mass balances: H^+, Na^+, K^+, Ca^{2+}, Mg^{2+}, NH_4^+, Cl^-, Ac^-, Pr^-, CO_3^{2-}, SO_4^{2-} and PO_4^{3-}. Sulphide, NO_2^-, NO_3^- and iron (Fe^{2+}, Fe^{3+}) were not included in this the model, as partial nitration, and reduction of sulphate to sulphide, was neglected as an approximation in the anaerobic digestion model, and dosing of metal salts for phosphorus removal was not represented. A later model that caters for these additional processes has six additional components (HS^-, NO_2^-, NO_3^-, Fe^{2+}, Fe^{3+}, Al^{3+}), but more than twice the number of species, making the system of equations much larger. However, since no additional principles are involved, we have chosen to present the smaller system as our example.

Choosing species

The source of information was the *minteq.v4.dat* database distributed with PHREEQC. PHREEQC automatically includes all the species in the database that contain the components specified by the user. In most situations, several of these make negligible contributions. The complexity of the model can be reduced by eliminating species that will not contribute significantly anywhere within the range of conditions that will be of interest to the model.

To discover which species could be omitted, a representative composition for an anaerobic digester liquor was set up in PHREEQC, and run for three pH values covering the range that the anaerobic digestion model might be expected to encounter (5, 7 and 9). Species were selected that contributed at least 2% to the inventory of any component in at least one of the model runs. So, for example, the species *NaHCO₃* had to amount to at least 2% of the total Na^+, H^+ or CO_3^{2-} in at least

one of the simulated solutions. The 42 ionic species that were selected in this way were: H^+, Na^+, K^+, Ca^{++}, Mg^{++}, NH_4^+, Cl^-, Ac, Pr^-, HAc, HPr, NH_3, HCO_3^-, SO_4^{2-}, HPO_4^{2-}, OH^-, H_2CO_3, CO_3^{2-}, $CaCO_3$, $MgCO_3$, $CaHCO_3^+$, $MgHCO_3^+$, $H_2PO_4^-$, $MgPO_4^-$, $CaPO_4^-$, $MgHPO_4$, $CaHPO_4$, $CaSO_4$, $MgSO_4$, $CaOH^+$, $MgOH^+$, $NH_4SO_4^-$, $NaHPO_4^-$, $NaCO_3^-$, $NaHCO_3$, $MgH_2PO_4^+$, $CaAc^+$, $NaAc$, $MgAc^+$, $CaPr^+$, $MgPr^+$ and $NaSO_4^-$, where the last 24 in the list are often referred to as *ion pairs*. Note that, as in the previous papers in this series, species are italicized to distinguish them from components.

Table 5-1 presents the reaction scheme in a form known as a **tableau**, which is similar to the Gujer matrix for biological reactions. The matrix contains the stoichiometric coefficients for the formation reaction of each species from its components, and the two right-most columns hold the thermodynamic constants for each species at 25°C or 298.15°K (obtained from the *minteq.v4.dat* database).

This selection of components and species still leads to quite a complex model, requiring the simultaneous solution of 42 non-linear equations. Whether this level of complexity is really required for the anaerobic digestion model is a question that would require a great deal of investigation to answer fully. If alkalinity and pH predictions were the only issues, one could dispense with most of the ion pair species without serious consequences. However, the prediction of whether a precipitate will form or not is quite sensitive to the ion pairs (Solon et al., 2015). As will be discussed in the next section, the extra computational burden of adding species is not great, so we have preferred to err on the side of greater complexity.

Table 5-1. *Tableau representation of the Brouckaert et al. (2010) speciation model*

Species	H⁺	Na⁺	K⁺	Ca⁺⁺	Mg⁺⁺	NH₄⁺	Cl⁻	Ac⁻	Pr⁻	CO₃⁼	SO₄⁼	PO₄⁻³	logK	ΔH (J/mol)
H^+	1												0	0
Na^+		1											0	0
K^+			1										0	0
Ca^{++}				1									0	0
Mg^{++}					1								0	0
NH_4^+						1							0	0
Cl^-							1						0	0
Ac^-								1					0	0
Pr^-									1				0	0
$HCO_3^=$	1									1			10.329	-14600
$SO_4^=$											1		0	0
$HPO_4^=$	1											1	12.375	-15000
OH^-	-1												-13.997	55810
H_2CO_3	2									1			16.681	-23600
$CaCO_3$				1						1			3.2	16000
$MgCO_3$					1					1			2.92	12000
$CaHCO_3^+$	1			1						1			11.599	5400
$MgHCO_3^+$	1				1					1			11.339	-10600
$CO_3^=$										1			0	0
$H_2PO_4^-$	2											1	19.573	-18000
$MgPO_4^-$					1							1	4.654	12970.4
$CaPO_4^-$				1								1	6.46	12970.4
$MgHPO_4$	1				1							1	15.175	-3000
$CaHPO_4$	1			1								1	15.035	-3000
PO_4^{-3}												1	0	0
HAc	1							1					4.757	410
HPr	1								1				4.874	660
NH_3	-1					1							-9.244	-52000
$CaSO_4$				1							1		2.36	7100
$MgSO_4$					1						1		2.26	5800
$CaOH^+$	-1			1									-12.697	64110
$MgOH^+$	-1				1								-11.397	67810
$NH_4SO_4^-$						1					1		1.03	0
$NaHPO_4^-$	1	1										1	13.445	0
$NaCO_3^-$		1								1			1.27	-20350
$NaHCO_3$	1	1								1			10.079	-28330.1
$MgH_2PO_4^+$	2				1							1	21.2561	-4686.1
$CaAc^+$				1				1					1.18	4000
$NaAc$		1						1					-0.18	12000
$MgAc^+$					1			1					1.27	0
$CaPr^+$				1					1				0.9289	3347.2
$MgPr^+$					1				1				0.9689	4267.7
$NaSO_4^-$		1									1		0.73	1000

It should be mentioned that some authors (e.g. Flores-Alsina et al., 2015) prefer a different formulation of the set of speciation equations, in which H⁺ in the tableau is replaced by the charge balance over the remaining set of components. This is simply a linear transformation of the set of variables, and is entirely equivalent. The motivation for using it seems to be that [H⁺] is not measurable, whereas the charge balance is a linear combination of measurable quantities. However, this apparent advantage is only fully realised when dealing with synthetic solutions made up from pure chemicals. Measurements on wastewater samples very seldom cover all the ions present, and, even when they do, measurement errors upset the charge balance. The solution state is very sensitive to the H⁺ concentration, so the measured charge balance cannot be used to infer it

reliably; consequently, further considerations have to be used to establish an appropriate charge balance, exactly parallel to those discussed in relation to [H+] in the later section of this paper, on using speciation with composition measurements.

The speciation algorithm

As mentioned previously, the principles of ionic speciation are well established: they are set out in Stumm and Morgan (1996). The concentrations of the 42 ionic species are related to the concentrations of the 12 components by a set of 12 stoichiometric balances, together with a set of 30 equilibrium relationships which form a set of simultaneous algebraic equations. The equilibrium relationships are formulated in terms of species **activities**, which are related to their concentrations by **activity coefficients**.

In the set of equations that constitute the model, the balance equations are linear, but the equilibrium relationships are non-linear. For example, consider the equations for propionate Pr⁻ (a conveniently simple example, since the model has only four species containing Pr⁻). The balance equation is:

$$[\text{Pr}^-] = [Pr^-] + [HPr] + [CaPr^+] + [MgPr^+] \tag{1}$$

In Eq. 1 the square brackets indicate molal concentrations, italics indicate species, and Roman typeface indicates a component. [Pr⁻] is also referred to as a **total concentration**, as it is the sum of the concentrations of all species present that include Pr⁻.

There is one equilibrium relationship for each of the species formed from more than one component (e.g. *HPr, CaPr⁺*). Take *HPr*, for example. Its entry in Table 5-1 corresponds to the formation reaction *H⁺ + Pr⁻ → HPr*, with the corresponding equilibrium relationship:

$$\{HPr\} = K_{\text{HPr}} \cdot \{H^+\} \cdot \{Pr^-\} \tag{2}$$

In Eq 2, {…} indicates the activity of the species, and K_{HPr} is an equilibrium constant, which is a function of temperature only, and can be calculated from the thermodynamic parameters in Table 5-1.

$$\log_{10}(K_{\text{HPr}}) = 4.874 + \frac{660}{8.314 \times 2.303} \left[\frac{1}{298.15} - \frac{1}{T} \right] \tag{3}$$

The activities are related to molal concentrations by **activity coefficients**, e.g.

$$\{Pr^-\} = \gamma_{Pr} \cdot [Pr^-] \tag{4}$$

Equation 4 can be dimensionally confusing, since {Pr⁻} and γ_{Pr} are dimensionless, whereas [Pr⁻] has dimensions of mol/kg. This is because there is a hidden term – the complete form is:

$$\{i\} = \gamma_i \cdot [i] \Big/ [i_o]$$

where the subscript o indicates the species in a **standard state** which is defined so that [i_o] = 1 mol/kg for all species *i*. This definition effectively sets the value of the equilibrium constant (e.g. K_{HPr} in Eq 2). By convention [i_o] = 1, whatever concentration units are used, so the form of Eq. 4 remains the same if the units are changed; however, the equilibrium constant value changes. So, it is critical to use *K* values that correspond to the concentration units of the model.

Activity coefficients of each species were modelled using the Davies equation (Stumm and Morgan, 1996).

$$\log_{10}(\gamma_i) = -Az_i^2 \cdot \left(\frac{\sqrt{I}}{\sqrt{I}+1} - 0.3I\right) \tag{5}$$

In Eq 4, *I* is the **ionic strength** of the solution $I = \frac{1}{2}\sum_i [i]\, z_i^2$ and z_i is the ionic charge on species *i*. *A* is the **Debye-Hűckel constant**, which is, in fact, not strictly constant, but a function of temperature.

$$A = 1.82 \times 10^6 (\epsilon T)^{-1.5} \tag{6}$$

ϵ is the dielectric constant of water, 78.49 at 25°C, *T is* the absolute temperature.

The Davies equation is considered to be valid for *I* < 0.5 mol/kg (Solon et al., 2015)

The equations similar to Eqs 2 and 4 are substituted into Eq. 1 to eliminate all but one of the species containing Pr⁻, for example:

$$[\text{Pr}]= [Pr^-]+\frac{K_{HPr}\gamma_{Pr}}{\gamma_{HPr}}[H^+][Pr^-]+K_{CaPr}\frac{\gamma_{Ca}\gamma_{Pr}}{\gamma_{CaPr}}[Ca^{2+}][Pr^-]+K_{MgPr}\frac{\gamma_{Mg}\gamma_{Pr}}{\gamma_{MgPr}}[Mg^{2+}][Pr^-]$$

$$\tag{7}$$

The effect of applying this transformation to all the component balances is to reduce the number of simultaneous equations, to be solved numerically, from 42 to 12. The set of species concentrations remaining after the reduction ($[Pr]$, $[H^+]$, $[Ca^{2+}]$, $[Mg^{2+}]$ etc.) is termed the **primary search variables** or **master species** for the numerical solution of the equations. Once these core equations have been solved for the master species concentrations, all the remaining species concentrations can be calculated explicitly from the equilibrium equations similar to Eq. 2. It is always possible to do this reduction of variables, so that the number of equations needing simultaneous solution is the number of components in the model. This means that the computational burden of extra species for a given set of components is relatively small.

Computational considerations

Minimising the computational burden is important, since the speciation calculation is performed at each integration step during the numerical solution of the model balance equations. In fact, when using an integration algorithm with variable time-step control, there are additional trial evaluations within an integration step. There are three particularities of the speciation calculation that can be exploited.

Firstly, because the solution composition evolves with time, the solution obtained at the previous time step provides an excellent initial guess for the following time step. When designing a numerical algorithm, there is generally a trade-off between the number of iterations required for convergence, and the complexity of the calculations within an iteration. So, we kept the solution variables in memory between integration steps as estimates for the next step, and used a relatively unsophisticated solution algorithm, i.e., a secant search for $[H^+]$, and successive substitution for the other 11 search variables. Flores-Alsina et al. (2015) used an alternative algorithm, which we have also implemented in a later version of our speciation routine: a classic multivariate Newton-Raphson (Press et al., 2007) with analytic evaluation of the Jacobian matrix (see Appendix B for details).

There is obviously a problem at the first integration step, since there is no previous solution to use as an initial estimate. The second useful characteristic is that the 12 primary search variables (master species concentrations) must have values between zero and the corresponding component concentration. This makes it relatively easy to generate an adequate starting guess for the variables. Since this happens only once at the beginning of a simulation, it does not matter much that a larger number of iterations is required for convergence during this initial step. Typically, the solution converges in 10 to 30 iterations for the first step, but 3 to 5 iterations during subsequent steps of a simulation.

This leads to the last particularity, the choice of the species concentrations that constitute the primary search variables. The speciation works best, both in terms of the rate of convergence and the accuracy of the solution, if the master species concentrations, that the algorithm solves for, are the dominant ones for their components. For example, under most circumstances carbonate in an anaerobic digester liquor is predominantly in the HCO_3^- form. Similarly, HPO_4^{2-} is usually the dominant species for the phosphate system. Thus, we exploit the fact that the range of conditions under which an anaerobic digester operates is relatively limited, and choose search variables accordingly.

The one component that cannot be handled in this way is H^+. Although most H^+ is usually complexed with weak acid anions (in most wastewaters it is predominantly present as HCO_3^-) an algorithm that chose HCO_3^- as a master species would be unable to deal with a solution that has no carbonate present. Since it comes from the solvent water, H^+ is always present, although its concentration may be very low. The problem of very low concentrations can be circumvented by a logarithmic transformation; however, there would be an undesirable computational penalty in evaluating logarithms and exponentials. Fortunately, the extra computation can be minimised. Evaluating a term in the transformed Jacobian $\frac{\partial y}{\partial lnx} = \frac{x \partial y}{\partial x}$ adds only a single multiplication per term, and when one has to apply the exponential correction, one can use the first-order series approximation exp $(\delta x) \approx 1 + \delta x$, which becomes increasingly accurate as the solution converges, i.e. $\delta x \to 0$.

Thus, the set of master species adopted was H^+, Na^+, K^+, Ca^{++}, Mg^{++}, NH_4^+, Cl^-, Ac^-, Pr^-, HCO_3, SO_4^{2-} and HPO_4^{2-} (highlighted in green in Table 5-1).

Using speciation with composition measurements
Up to this point, the discussion has focused on speciation calculations during a simulation, where component concentrations are established by material-balance calculations. It is also necessary to use speciation calculations to transform measured compositional data into compositions in terms of model components, that can be used as input to the material balances, or to compare with model outputs. Measurement aspects are discussed in Part 4 (Ekama et al., 2022); here we briefly outline the use of the speciation routine to implement the calculations.

A typical set of measurements on a wastewater sample will not provide a complete description of its composition. Leaving aside the complex dissolved and particulate organic content, the inorganic ionic composition will be represented by some measured component concentrations (e.g. phosphate, sulphate, chloride, sodium, calcium), together with pH and alkalinity, which are summary indicators that reflect the presence of a complex of components. Of the components that strongly

affect pH and alkalinity, H^+ cannot be measured directly, and CO_3^{2-} is not commonly measured directly.

The problem that pH measurements pose for modellers is that pH is not a conserved quantity, and so cannot be used directly in material balance calculations. The component H^+ is conserved, but cannot be measured directly. Thus, it is necessary to use a speciation model to convert pH and alkalinity measurements to equivalent H^+ and CO_3^{2-} concentrations, which can then be used in mass balance calculations. This essentially involves a trial-and-error search for the H^+ and CO_3^{2-} component concentrations that match the measured pH and alkalinity. This approach is used by MINTEQA2 (Allison et al., 2009) and PHREEQC (Parkhurst and Appelo, 2013) and was adopted in the PWM_SA model by Ikumi et al. (2015), of which PWM_SA_AD is a sub-model and uses the same ionic speciation routine (Brouckaert et al., 2010).

However, pH and alkalinity are not functions of just $[H^+]$ and $[CO_3^{2-}]$. They depend on the whole composition of the solution, which theoretically requires the measurement of all solute concentrations. This is very seldom feasible. However, the effects of other dissolved ions on pH and alkalinity vary greatly, so some are more important to get right than others. The anions of weak acids such as phosphate, sulphide and acetate, and the cations of weak bases such as ammonia, are critical, because they associate with H^+ and contribute to the measured alkalinity. Anions of strong acids (e.g. chloride and sulphate) and cations of strong bases (e.g. sodium, potassium, calcium and magnesium) have a minor influence on the H^+ activity coefficient via their contributions to the ionic strength of the solution, and are much less critical. Thus, while it is important to have the correct concentrations for the weak acid and base components, it may be adequate, for modelling purposes, to use the ionic strength to summarise the effect of the rest of the inorganic ions. There are empirical correlations to estimate ionic strength from measured electrical conductivity (e.g. Bhuiyan et al., 2009). This kind of approximation is obviously not appropriate when modelling precipitation that involves one or more of the strong acid or base ions, for example Ca^{2+}, in which case it is important to have the speciation of Ca^{2+} right, including ion pairs, such as $CaSO_4$ and $CaPO_4^-$, that reduce the free calcium ion concentration $[Ca^{2+}]$.

ALKALINITY

Alkalinity was introduced in Part 1 (Brouckaert et al., 2021a) and further discussed in Parts 2 (Brouckaert et al., 2021b) and 4 (Ekama et al., 2022); however, a definition of alkalinity for modelling purposes needs to be chosen. The options are:

(a) From a laboratory measurement point of view, alkalinity is the result of a titration with HCl to an endpoint somewhere between pH 3.5 and 4.5 (the **operational** definition, according to Snoeyink and Jenkins, 1980). For modelling purposes, to use this directly as the definition is very awkward, as it effectively involves simulating the titration, i.e., solving for the amount of H^+ and Cl^- to be added to achieve the required pH.

(b) Alkalinity could be defined in terms of species present in the solution in question, by considering all the species that would be protonated at pH 3.5 and calculating the difference between their proton content in the solution and in their fully protonated form.

(c) It could also be calculated from the component concentrations, by subtracting the total H^+ concentration from the weighted sum of total anion component concentrations which represents the H^+ that they would contain when fully protonated.

Snoeyink and Jenkins (1980) call (b) and (c) **analytical** definitions of alkalinity. In the context of a mass-balance model, that works in terms of component concentrations, calculating the alkalinity from the operational definition given in (a) would require one to do speciation calculations for the solution at both its original composition and at the titration endpoint composition (and at a number of other compositions during the search for the end-point); Definition (b) would require speciation of the original composition only; while Definition (c) requires no speciation calculation at all.

A simulation of the titration of a solution with composition as shown in Table 5-2 was used to compare the values of alkalinity calculated according to the three different definitions. Note that the composition is specified in terms of component concentrations, not species concentrations. The water content of the solution is implicit in the mol/kg units.

Table 5-2. *Example solution composition*

Component	Concentration (mol/kg water)	Component	Concentration (mol/kg water)
H^+	0.020578	Mg^{2+}	0.001030566
Na^+	0.034	NH_4+	0.010411719
Cl^-	0.026187307	CO_3^{2-}	0.01278
Ca^{2+}	0.000667442	PO_4^{3-}	0.004794351

The resulting total alkalinity (Alk_t) values are:

Definition (a):   0.016853 M   or   843 mg/L as $CaCO_3$
Definition (b):   0.016874 M   or   844 mg/L
Definition (c):   0.016877 M   or   844 mg/L

The differences between these values are negligible compared to uncertainties in experimental determinations. Thus Definition (c), based purely on component concentrations, is the obvious one to choose for a computational model.

For the solution of Table 5-2, the expression for the alkalinity according to Definition (c) in terms of component concentrations is:

$$Alk_t = 2 \cdot [PO_4^{3-}] + 2 \cdot [CO_3^{2-}] + [Ac^-] + [Pr^-] + [HS^-] - [H^+] \tag{8}$$

where the Alk_t uses the alkalinity of the orthophosphate system expressed with respect to the $H_2PO_4^-$ species. The total alkalinity, according to Definition (c), is simply a linear combination of component concentrations, which shows that it is a purely stoichiometric quantity expressed with respect to a selected set of reference species. Indeed, The IWA ASM series of models (Henze et al., 2000) considers total alkalinity as a component in itself.

The expression for alkalinity of the example solution according to Definition (b), in terms of species concentrations, is:

Alk_t = $[OH^-]$ + $[CaOH^+]$ + $[MgOH^+]$ - $[H^+]$ + $[HCO_3^-]$ + $2[CO_3^{2-}]$ + $2[CaCO_3]$ + $[CaHCO_3^+]$ + $[MgHCO_3^+]$ + $2 \cdot [MgCO_3]$ + $2 \cdot [NaCO_3^-]$ + $[NaHCO_3^-]$ + $[HPO_4^{2-}]$ + $2 \cdot [PO_4^{3-}]$ + $2 \cdot [MgPO_4^-]$ + $2 \cdot [CaPO_4^-]$ + $[MgHPO_4]$ + $[CaHPO_4]$ + $[NaHPO_4^-]$ + $[Ac^-]$ + $[NaAc]$ + $[Pr^-]$ + $[CaPr^+]$ + $[MgPr^+]$ + $[NH_3]$ + $[HS^-]$ + $2 \cdot [S^=]$

(9)

In Eq. 9 $[H^+]$, for instance, represents the concentration of free hydrogen ion (species concentration: 4.899 x 10^{-8} M for this example, corresponding to pH 7.4) rather than [H$^+$], the total hydrogen ion concentration (component concentration: 0.020578 M) as in Eq. 8.

Equation 9 can be simplified by including only the main contributing species, i.e., omitting the ion pairs,

Alk_t ~ $[OH^-]$ − $[H^+]$ + $[HCO_3^-]$ + $2[CO_3^{2-}]$ + $[NH_3]$ + $[HS^-]$ + $[HPO_4^{2-}]$ + $[Ac^-]$ + $[Pr^-]$ (10)

Under the range of conditions encountered in anaerobic digesters, the difference between Eqs 9 and 10 will be less than 1%.

Note that terms involving $[Pr^-]$ and $[HS^-]$ have been included in Eqs 8 to 10 for completeness – they are all zero for the example solution of Table 5-2. $[HS^-]$ is also always zero for the speciation model of Table 5-1, as it does not include HS$^-$ as a component.

CONCLUSIONS

Models of biological processes often need to include interactions with inorganic ionic species, in order to represent phenomena such as acid/base reactions, gas transfer and precipitation. Particularly for the acid/base reactions, an equilibrium sub-model is appropriate, because they have time scales that are orders of magnitude shorter than the biological reactions. The situation is not as clear-cut for redox reaction and phase-transfer reactions which may depart significantly from equilibrium, and so may be more appropriately included in the kinetically limited sub-model. In setting up an equilibrium speciation sub-model, modellers can take advantage of the knowledge and experience contained in freely available modelling software such as MINTEQA2 and PHREEQC. It is possible to couple such software directly to a model: for example, PHREEQC provides a programming interface to access its functions. However, there are computational advantages to customising the speciation algorithm for the range of conditions expected for a given biological system.

The aquatic species and components included in the model must be chosen carefully according to what phenomena the model is required to represent. The established aquatic chemistry models provide useful guides; however, because they are designed to be used in a very wide range of contexts, they tend to suggest model structures that are more complex than necessary for a given process model, but have the advantage of reliability. However, one can reduce the complexity of the model, while using PHREEQC or MINTEQA2 as a reference to check the accuracy of key outputs.

REFERENCES

ALLISON JD, BROWN DS AND NOVO-GRADAC KJ (2009) MINTEQA2. URL: https://www.epa.gov/ceam/minteqa2-equilibrium-speciation-model (Accessed 5 June 2019).

BHUIYAN IH, MAVINIC DS and BECKIE RD (2009) Determination of temperature dependence of electrical conductivity and its relationship with ionic strength of anaerobic digester supernatant, for struvite precipitation. *J. Environ. Eng.* **135** 1221–1226.

BROUCKAERT CJ, IKUMI DS and EKAMA GA (2010) A 3 phase anaerobic digestion model. *Proceedings 12th IWA Anaerobic Digestion Conference (AD12)*, Guadalajara, Mexico, 1–4 Nov 2010.

BROUCKAERT CJ, BROUCKAERT BM and EKAMA GA (2021a) Integration of complete elemental mass-balanced stoichiometry and aqueous-phase chemistry for bioprocess modelling of liquid and solid waste treatment systems – Part 1: The physico-chemical framework. *Water SA* **47** (3) 276–288. https://doi.org/10.17159/wsa/2021.v47.i3.11857

BROUCKAERT CJ, EKAMA GA and BROUCKAERT BM (2021b) Integration of complete elemental mass-balanced stoichiometry and aqueous-phase chemistry for bioprocess modelling of liquid and solid waste treatment systems – Part 2: Bioprocess stoichiometry. *Water SA* **47** (3) 289–308. https://doi.org/10.17159/wsa/2021.v47.i3.11858

EKAMA GA, BROUCKAERT CJ and BROUCKAERT BM (2022) Integration of complete elemental mass-balanced stoichiometry and aqueous-phase chemistry for bioprocess modelling of liquid and solid waste treatment systems – Part 4: Aligning the modelled and measured aqueous phases. *Water SA* 48(1) 21–31. https://doi.org/10.17159/wsa/2022.v48.i1.3322

FLORES-ALSINA X, KAZADI MBAMBA C, SOLON K, VRECKO D, TAIT S, BATSTONE DJ, JEPPSSON U and GERNAEY KV (2015) A plant-wide aqueous phase chemistry module describing pH variations and ion speciation/pairing in wastewater treatment process models. *Water Res.* **85** 255–265.

HENZE M, GUJER W, MINO T and VAN LOOSDRECHT M (2000) Activated sludge models ASM1, ASM2, ASM2d, and ASM3. IWA Scientific and Technical Report. IWA, London.

LOEWENTHAL RE, KORNMULLER URC and VAN HEERDEN EP (1994) Modelling struvite precipitation in anaerobic treatment systems. *Water Sci. Technol.* **30** (12) 107–116.

LIZZERALDE I, BROUCKAERT CJ, VANROLLEGHEM PA, IKUMI DS, EKAMA GA, AYESA E and GRAU P (2014) Incorporating aquatic chemistry into wastewater treatment process models: a critical review of different approaches. In: *Proceedings 4th IWA/WEF Wastewater Treatment Modelling Seminar*. WWTmod2014, Spa, Belgium, 30 March 30–2 April 2014. 227–232.

PARKHURST DL and APPELO CAJ (2013) PHREEQC (Version 3)-- A computer program for speciation, batch-reaction, one-dimensional transport, and inverse geochemical calculations. URL: https://www.usgs.gov/software/phreeqc-version-3 (Accessed 5 June 2019).

PRESS WH, TEUKOLSKY SA, VETTERLING WT and FLANNERY BP (2007) *Numerical Recipes* (3rd edn). Cambridge University Press, Cambridge.

SNOEYINK VL and JENKINS D (1980) *Water Chemistry.* John Wiley and Sons, New York.

SOLON K, FLORES-ALSINA X, KAZADI MBAMBA C, VOLKE EIP, TAIT S, BATSTONE D, GERNAEY KV and JEPPESON U (2015) Effects of ionic strength and ion pairing on (plant wide) modelling of anaerobic digestion. *Water Res.* **70** 235–245.

STUMM W and MORGAN JJ (1996) *Aquatic Chemistry: Chemical Equilibria and Rates in Natural Waters*. John Wiley and Sons, New York.

APPENDIX A

Phase transfer reactions

The anaerobic digestion model of Brouckaert et al. (2010) considered three phases, gas liquid and solid, with phase-transfer reactions distributing material between them. These phase-transfer reactions were represented as kinetically controlled, and so not handled by the equilibrium speciation sub-model, which dealt with the liquid phase only. However, the rate expressions for the phase-transfer reactions involved liquid species concentrations that required the equilibrium speciation sub-model for their evaluation.

Gas transfer

The evolution of CO_2 is used as the example. The transfer reaction is:

$$CO_3^{2-} + 2H^+ \leftrightarrow CO_{2(g)} + H_2O \tag{A1}$$
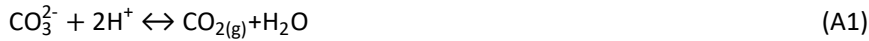
Dissolved carbonate exerts an equilibrium partial pressure P_{CO2_eq} which can be represented as

$$P_{CO2\_eq} = K_H \cdot \{H_2CO_3\} \tag{A2}$$

K_H is the Henry's Law Constant, and can be calculated from thermodynamic data as a function of temperature. The rate of Reaction A1 is then modelled as:

$$R_{CO2\_ev} = k_{CO2} \cdot \left(P_{CO2\_eq} - P_{CO2}\right) \tag{A3}$$

P_{CO2_eq} is calculated from the liquid equilibrium speciation, whereas P_{CO2} is calculated from the gas phase mass balance. The rate constant k_{CO2} is a model parameter.

Precipitation/dissolution

This follows a similar treatment. Consider the precipitation of $CaCO_3$ as the example.

The precipitation/dissolution reaction is:

$$Ca^{2+} + CO_3^{2-} \leftrightarrow CaCO_{3(s)} \tag{A4}$$

The solution is saturated with respect to $CaCO_{3(s)}$ when

$$\{Ca^{2+}\} \cdot \{CO_3^{2-}\} = K_{CaCO3\_sat} \tag{A5}$$

K_{CaCO3_sat} is a **saturation coefficient** and can be calculated from thermodynamic data as a function of temperature. $\{Ca^{2+}\} \cdot \{CO_3^{2-}\}$ is termed an **ion product** IP_{CaCO3}, and is calculated from outputs of the equilibrium speciation sub-model.

When ($IP_{CaCO3} > K_{CaCO3\_sat}$), $CaCO_{3(s)}$ will precipitate, and when ($IP_{CaCO3} < K_{CaCO3\_sat}$) any $CaCO_{3(s)}$ that is present in the reactor will dissolve. So, the rate of Reaction A4 is modelled as proportional to ($IP_{CaCO3} - K_{CaCO3\_sat}$).

It should be noted that this is the most elementary and idealised model of precipitation possible. In reality, precipitation is often very complex, because of the short inter-atomic distances in crystal structures, which lead to strong interactions. However, a model that took these into account, apart

from its intrinsic complexity, would need to be supported by very detailed measurements that would be quite impractical in the context of wastewater treatment.

APPENDIX B

Implemention of the Newton-Raphson algorithm for ionic speciation
The Newton-Raphson algorithm solves a set of non-linear equations $f(x) = 0$ iteratively by linearising the equations at successive trial points. Here F, x, and 0 are vectors – i.e.

$$f = (f_1, f_2, \dots f_n)^T , \; x = (x_1, x_2, \dots x_n)^T, \; 0 = (0, 0, \dots 0)^T \tag{B1}$$

The superscript T indicates that the vectors are transposed – i.e. they are column vectors.

Linearisation at any trial point x is achieved by evaluating the Jacobian matrix

$$J = \frac{\partial f}{\partial x} \tag{B2}$$

For the present problem, x is the vector of 12 master species concentrations, and f is the vector of errors in the 12 component balances. The vector of corrections to x is given by the solution to the set of linear equations (A3), which can be solved numerically using a standard algorithm.

$$f - J \cdot \delta x = 0 \tag{B3}$$

The formulation of the Newton-Raphson scheme for the speciation problem can be illustrated with reference to Eq. 7, which is one of the 12 equations to be solved. We rearrange it as:

$$f_{Pr} = [Pr^-] + K'_{HPr}[H^+][Pr^-] + K'_{CaPr}[Ca^{2+}][Pr^-] + K'_{MgPr}[Mg^{2+}][Pr^-] - [Pr^-] \tag{B4}$$

Here f_{Pr} is the error in the propionate balance, which, together with the 11 other component balance errors, should be driven to zero by a proper choice of values of $[Pr^-]$, $[H^+]$, $[Ca^{2+}]$ and $[Mg^{2+}]$ (and eight other concentrations which appear in the other balance equations). $[Pr^-]$ is a constant, and the K' values, although not strictly constant, can be considered approximately constant during a single iteration.

The terms in the Jacobian matrix are the derivatives of the error equations with respect to the variables. From Eq. B4:

$$\frac{\partial f_{Pr}}{\partial [Pr^-]} = 1 + K'_{HPr}[H^+] + K'_{CaPr}[Ca^{2+}] + K'_{MgPr}[Mg^{2+}]$$

$$\frac{\partial f_{Pr}}{\partial [H^+]} = K'_{HPr}[Pr^-]$$

$$\frac{\partial f_{Pr}}{\partial [Ca^{2+}]} = K'_{CaPr}[Pr^-]$$

$$\frac{\partial f_{Pr}}{\partial [Mg^{2+}]} = K'_{MgPr}[Pr^-]$$

$$\tag{B5}$$

If one chooses to use the logarithmic transformation, Eq. B3 becomes:

$$f - J' \cdot \delta \ln x = 0 \tag{B6}$$

where Eq. A5 becomes

$$\frac{\partial f_{Pr}}{\partial ln[Pr^-]} = [Pr^-]\frac{\partial f_{Pr}}{\partial [Pr^-]} = [Pr^-]\big(1 + K'_{HPr}[H^+]+K'_{CaPr}[Ca^{2+}]+K'_{MgPr}[Mg^{2+}]\big)$$
$$= [Pr^-] + [HPr] + [CaPr] + [MgPr]$$

$$\frac{\partial f_{Pr}}{\partial ln[H^+]} = [H^+]\frac{\partial f_{Pr}}{\partial [H^+]} = K'_{HPr}[H^+][Pr^-] = [HPr]$$

$$\frac{\partial f_{Pr}}{\partial ln[Ca^{2+}]} = [Ca^{2+}]\frac{\partial f_{Pr}}{\partial [Ca^{2+}]} = K'_{CaPr}[Ca^{2+}][Pr^-] = [CaPr]$$

$$\frac{\partial f_{Pr}}{\partial ln[Mg^{2+}]} = [Mg^{2+}]\frac{\partial f_{Pr}}{\partial [Mg^{2+}]} = K'_{MgPr}[Mg^{2+}][Pr^-] = [MgPr]$$

(B7)

In this case, once the vector of values for $\boldsymbol{\delta}$ **ln** $\boldsymbol{x}$ has been obtained from the solution of B6, the correction to the ith variable during the jth iteration is applied as:

$$\ln x_{i,j} = \ln x_{i,j-1} + \delta \ln x_{i,j}$$

which is equivalent to:

$$x_{i,j} = x_{i,j-1} \cdot \exp\big(\delta \ln x_{i,j}\big) \approx x_{i,j-1} \cdot \big(1 + \delta \ln x_{i,j}\big)$$

(B8)

This completely avoids evaluation of the ln and exp functions.

Chapter 5: Conclusions

The papers contained in this thesis have presented a modelling framework for processes where aqueous bio-chemical reactions interact with inorganic ionic reactions, particularly those involved in wastewater treatment. Even the most complex of such models is a highly simplified approximation to physical reality, and the framework presents a pragmatic approach based on current knowledge and computing power. A modeller must constantly be aware of the limitations that such simplifications introduce in representing reality. These limitations also provide focus points for research to advance the art of modelling. For example, precipitation was mentioned only very briefly in Appendix B of part 5. Precipitation reactions are very complex, particularly from complex solutions such as wastewater, as shown by Hauduc et al. (2015). It is not yet feasible for such a complex model to be incorporated into wastewater treatment models, if only because the experimental data required to support it would be far too detailed to measure at a wastewater treatment plant. As resource recovery from wastewater becomes more important, research into precipitation modelling has become a significant trend.

Two major areas of uncertainty that require simplification and approximation in wastewater treatment are: a) the chemical nature of the organic components (including micro-organisms) taking part in the biological reactions; and b) the complete set of all inorganic ionic components (with well-known chemical natures) present in wastewater. Assigning empirical elemental formulae to the organic components allows them to be linked to the inorganic components by element-balanced stoichiometric reactions. Methods are also required for characterising both organic and inorganic components in wastewater in terms that are compatible with a model.

Accordingly, the thesis has explored three main themes: the interactions between aqueous biological and inorganic ionic reactions, the interactions between kinetically-controlled and equilibrium-controlled processes, and the interactions between modelling and measurement. In all cases, each aspect has critical dependencies on the other, for example, models depend on measurements for calibration and validation, while measurements require modelling for interpretation, and for deriving values of critical quantities.

With stoichiometry as the glue holding them together, these three themes combine to form a framework for a class of bioprocess models for which transport processes and energy balances are not critical to the formulation of a model. This is appropriate for simulating many wastewater treatment processes. This does not mean that transport processes and energy are unimportant in wastewater treatment, but their dynamics are little affected by the dynamics of the biochemical reactions.

The paper of appendix 3 (Kay et al. 2019) shows that the framework is readily extended to include energy balances where their dynamic interactions are important. There, the exothermic reaction had a significant effect on the reactor temperature, which in turn affected the reaction rate. In a typical municipal activated sludge reactor, the reactions are also exothermic, but concentrations are too low for the temperature to be affected significantly, and the reactor temperature is almost the same as that of the influent wastewater.

Transport processes can introduce substantial extra complexity, which would also require an extension to the framework of the thesis. A typical municipal activated sludge process is operated with intense mixing to ensure thorough aeration. This high intensity (which is a dominant factor in the energy balance) has a significant effect on the reaction rates, but there is practically no reciprocal effect. So, the energy and mixing intensities are imposed on the process model via parameter values, rather than being computed as dynamic variables. Computational fluid dynamics (CFD) provides the framework for systems where transport processes, physico-chemical processes and energy are intimately interconnected. Most CFD software provides for local physico-chemical transformation models, to be evaluated at each spatial location and at each time step. Such a local physico-chemical model might well be constructed according to the framework outlined in this thesis, since the transport processes are handled by the CFD code.

Another important theme was introduced briefly in Part 1. The thesis presents a framework for organising knowledge: this knowledge must be in place before invoking the framework. The specific information required to build an integrated biochemical model includes which subprocesses are limiting, which transformations need to be explicitly represented in the model, and what reactants and products are involved. Part 2 summarises this prior knowledge for many wastewater treatment processes, based on George Ekama's long experience. Once we understand the species and components of a system, the framework and its tools will take us a considerable way towards completing the system description. These tools are the *stoichiometry generator* (described in principle in part 1, and used extensively for part 2), and the *ionic speciation subroutine* and speciation spreadsheet *VBSpeciation6.1_xlsm* (described in part 5, and used for part 4). These are available for download from [Integration of aquatic chemistry with bio-process models - Washcentre (ukzn.ac.za)](ukzn.ac.za)

A further consistent preoccupation of the papers has been to use, and, where necessary, devise precise terminology. Relevant examples are the careful distinction drawn between components and species, and the new terms *alkalinity change of reaction* (parts 1 and 2) and *exchanged electrons of reaction* (part 2). The 'exchanged electrons' was used (perfectly rigorously) by McCarty (1975), but the term that he used, 'exchangeable electrons', suggests a property of an electron donor component, rather than a property of a stoichiometric reaction. A computational model translates intuitive concepts of physical systems, which are usually somewhat fuzzy, into precise and rigid code. Terminology is used to communicate concepts between individuals, and imprecise terminology runs the risk of conveying a correct, if fuzzy, concept as an incorrect fuzzy concept to be coded into a model. A good example of misleading terminology is alluded to in part 2, where Poinapen and Ekama (2010) described the situation where very little gaseous CO_2 is produced during sulphidogenic anaerobic digestion, as due to 'carbon deficiency' of the electron donor. This suggests that digesting a substance with a high enough carbon content would cause CO_2 to be evolved. However, extending their analysis to the hypothetical digestion of pure carbon showed that CO_2 evolution would still be insignificant, and that the limitation is related to alkalinity production by the reaction.

The conceptual framework presented in this thesis has been the basis for the PWM_SA plant-wide wastewater treatment process model since about 2010. This model has been the focus of research at the universities of Cape Town and KwaZulu-Natal, as well as practical application to wastewater treatment plants in both centres. Developing and maintaining the model has, in turn, led to the

development and refinement of the conceptual framework. The PWM_SA model is widely available to researchers and practitioners as part of the standard installation of the WEST® modelling software from the Danish Hydraulic Institute (DHI).

REFERENCES

HAUDUC H, TAKACS I, SMITH S, SZABO A, MURTHY S, DAIGGER GT and SPERANDIO M (2015) A dynamic physicochemical model for chemical phosphorus removal. *Water Research* 73 157-170. http://dx.doi.org/10.1016/j.watres.2014.12.053

KAY LG, BROUCKAERT CJ and SINDALL RC (2019) Modelling mesophilic-thermophilic temperature transitions experienced by an aerobic membrane bioreactor treating furfural plant effluent. *Water SA* 45(3) 317- 328. https://doi.org/10.17159/wsa/2019.v45.i3.6711

POINAPEN J and EKAMA GA (2010) Biological sulphate reduction using primary sewage sludge in a upflow anaerobic sludge bed reactor – Part 5: Development of a steady state model. *Water SA* 36 (3) 193–202.

Appendix A: Integration of complete elemental mass-balanced stoichiometry and aqueous-phase chemistry for bioprocess modelling of liquid and solid waste treatment systems − Part 3: Measuring the organics composition

GA Ekama[1] and CJ Brouckaert[2]

Water Research Group, Dept of Civil Engineering, University of Cape Town, Rondebosch 7700, Cape Town, South Africa

Pollution Research group, School of Chemical Engineering, University of KwaZulu-Natal, Durban, South Africa

ABSTRACT

Bioprocesses transform the components of the material entering single or multiple reactor systems from one kind to another without a change in total material exiting the system(s) in the solid, aqueous or gas phases. Provided that the correct measurements are made that can quantify the material content of the bioprocess products (outputs), the material content of the bioprocess reactants (inputs) can be determined from the bioprocess products via stoichiometry. Based on this principle of mass conservation, the augmented biomethane (AugBMP) and biosulphide (AugBSP) potential test procedures are proposed, which change the BMP from a stand-alone test to a bio-reactor on which a range of additional tests are made to determine the composition of biodegradable organics. The AugBSP, which is based on biological sulphate reduction, can replace the inaccurate gas measurements in the BMP with the more accurate aqueous sulphate and sulphide measurements. The suitability of these two procedures is evaluated from a theoretical and modelling perspective. The analytical tests required to determine the composition of influent organics, expressed as $C_xH_yO_zN_aP_bS_c$, are identified. Examples of the calculation procedure from the test results are given. It is concluded that the augmented BMP (AugBMP) and BSP (AugBSP) test procedures, supplemented by anaerobic digestion dynamic modelling, are as accurate as the analytical measurements for determining the composition of biodegradable organics, and also allow the hydrolysis rate of the biodegradable organics and the unbiodegradable fraction of the organics to be determined. Knowing these characteristics of organics fed to anaerobic digesters is important to predict the anaerobic digester performance and stability.

KEYWORDS

bioprocess modelling, stoichiometry, anaerobic digestion, biomethane potential, biosulphide potential, integrated modelling

INTRODUCTION

The material content flux of the reactants in the influent for a continuous system, or the initial mass of reactants for a batch system, completely specifies the material content of the bioprocess products in the effluent of a flow process, or at a point in time for a batch process. The bioprocesses transform the components contained in the material entering bioreactor systems from one set of chemical components to another, without a change in total material flux exiting the system(s) in the solid, aqueous or gas phases. Similarly, in a batch reactor system, the bioprocesses transform the components contained in the material content at time zero from one set to another without a change in total material content of the products in the aqueous, gaseous or solid phases with time. This means that, provided that the correct measurements are made so that the material content of the bioprocess products (outputs) can be quantified, the material content of the bioprocess reactants (inputs, e.g., biodegradable organics) can be determined from the bioprocess products via stoichiometry. The paper presents the characterisation of the influent organics using this principle.

MUNICIPAL WASTEWATER CHARACTERIZATION

Municipal influent wastewater can be fractionated into seven organics groups, distinguished by their physical and biodegradable characteristics (Figure 3-1).
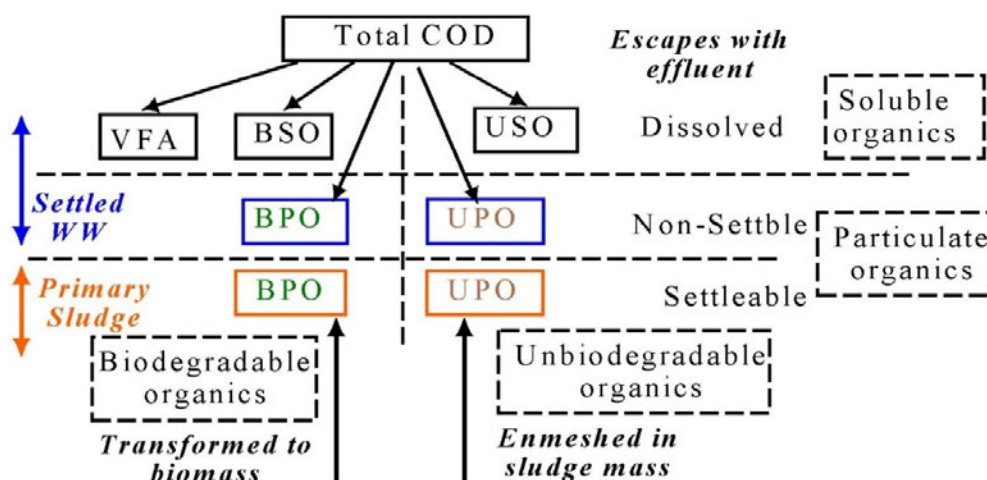
Figure 3-1. *Raw wastewater and settled characterization divides raw wastewater organics into seven organics groups: three physical (dissolved, non-settleable and settleable) and two biological (biodegradable and unbiodegradable), each with a $C_xH_yO_zN_aP_bS_c^{ch}$ composition. While settleable and non-settleable UPO may have different compositions, currently it is not possible to measure if such a difference exists, so in plant-wide models it is assumed that they have the same composition; similarly for BPO.*

There are three dissolved groups: volatile fatty acids (VFA) represented by acetate, fermentable biodegradable soluble organics (FBSO) and unbiodegradable soluble organics (USO); and four particulate groups: biodegradable particulate organics (BPO) and unbiodegradable particulate organics (UPO), each of which are subdivided into non-settleable and settleable fractions. A stoichiometric composition is assigned to each of these seven organics groups, as *x, y, z, a, b* and *c*

values in $C_xH_yO_zN_aP_bS_c$. Adding influent free and saline ammonia (FSA) and ortho phosphate (OP), the elemental contents of which are known, the wastewater constituents are completely characterized for both raw wastewater (all seven constituents), settled wastewater (the three dissolved and two non-settleable constituents) and primary sludge (all 5 non-settleable in the water flow plus the two concentrated settleable constituents). Then, adding elemental compositions for activated sludge (AS) and anaerobic digester (AD) biomass and endogenous residue, as k, l, m, n, p and s values in $C_kH_lO_mN_nP_pS_s$, the seven wastewater organics and FSA and OP, and the products generated from them via the biological processes, can be tracked through the water and resource recovery facility (WRRF) comprising both aerobic and anaerobic unit operations (Ekama, 2009; Ikumi et al., 2015). This approach of characterising the municipal wastewater organics is feasible because Ikumi et al. (2014) showed that the influent and endogenously generated unbiodegradable particulate organics, as defined by aerobic (AS) conditions, and without anaerobic digester (AD) fed sludge pre-treatment, are also unbiodegradable under anaerobic digester (AD) conditions. Details of isolation and composition measurement of these organic components will be considered in a future paper.

This approach to characterising the influent organics can also be applied to stand-alone bioreactors, such as methanogenic ADs and biological sulphate reduction (BSR) systems and can be aligned with that of Anaerobic Digestion Model No 1 (ADM1, Batstone et al., 2002). The proportion and composition of fats, carbohydrates and lipids in each of the FBSO, non-settleable BPO and settleable BPO groups can be assigned such that the chemical oxygen demand (COD), carbon (C), nitrogen (N), phosphorus (P) and sulphur (S) match the $C_xH_yO_zN_aP_bS_c$ composition of the group. We adopt the general approach of assigning a single composition to each group for characterising the influent organics to ADs in plant-wide models or as stand-alone ADs, because (i) it aligns with municipal wastewater characterization, (ii) is sufficiently general to include industrial wastewater, the organic fraction of municipal solid waste (OFMSW) and many other bio-system applications, and (iii) employs as many as possible measurement methods routinely used at municipal and industrial water and resource recovery facilities (WRRF), which are included in Standard Methods (1998).

ELECTRON DONOR ORGANICS COMPOSITION

The general organics composition $C_xH_yO_zN_aP_bS_c{}^{ch}$ can be written in various equivalent forms, e.g.:

$$C_xH_yO_zN_aP_bS_c^{ch} \equiv C_{f_C/12}H_{f_H/1}O_{f_O/16}N_{f_N/14}P_{f_P/31}S_{f_S/32}^{f_{ch}} \tag{1}$$

$$C_xH_yO_zN_aP_bS_c^{ch} \equiv C_1H_{y/x}O_{z/x}N_{a/x}P_{b/x}S_{c/x}^{f_{ch/x}} \tag{2}$$

where f_C, f_H, f_O, f_N, f_P and f_S are the six mass ratios (g element/g component) of the organics (volatile suspended solids, VSS if particulate) and the right-hand-side of Eq. 1 gives the stoichiometric composition of 1 g of the e⁻ donor organics. The organics composition mass balance is given by the sum of its mass ratios, viz.:

$$f_C + f_H + f_O + f_N + f_P + f_S = 1 \text{ g or g VSS if particulate} \tag{3}$$

The mass ratios f_C, f_H, f_O, f_N, f_P and f_S are identical to the $\alpha_{C,i}$, $\alpha_{H,i}$, $\alpha_{O,i}$, $\alpha_{N,i}$ and $\alpha_{P,i}$ of Grau et al. (2007) and Volcke et al. (2006), were the i refers to the different organic groups. While the molar masses of these three different forms of expressing the compositions of each organic group are different, the relative masses of the composition elements are the same in each form.

For many industrial wastewaters, the charge and composition of the e⁻ donor are known because they originate from reasonably well-defined industrial processes and operations, e.g., synthesis reaction product water (Van Zyl et al., 2008). If the influent organics have a charge, this can be detected by pH-titration curves over the 4–10 pH range to see if there are additional weak acid/base systems present to the usual inorganic carbon (IC), volatile fatty acids (VFA), OP, FSA and free (H_2S) and saline (HS^-) sulphide (FSS) (Westergreen et al., 2012).

Aside from the VFA, which are measured separately (by gas chromatography or 5-point titration: Moosbrugger et al., 1993; Vannecke et al., 2015; see also Part 4 of this series – Ekama et al., 2022) and can be represented by acetate, the elemental composition of municipal wastewater organics, the organic fraction of municipal solid waste (OFMSW) and food waste organics are not known and can vary on a daily or feed batch basis. The dynamic response of bioprocess systems, like methanogenesis, biological sulphate reduction (BSR), and even activated sludge (AS), cannot be modelled unless the composition of the various most significant organics groups is known. For aerated AS open to the atmosphere, knowledge of the elemental compositions of the organics groups is not necessary – the mass (VSS), COD, N and P content of each are sufficient because most CO_2 produced from C content of the organics is stripped out to the atmosphere by the aeration system. However, closed bioreactors, such as methanogenic AD, are profoundly affected by varying composition of the feed organics, even where the feed rate is constant because varying organics composition affects the gas and aqueous phases, and hence the aqueous pH (Brouckaert et al., 2021b). So, measurement of the organics elemental composition **before** they are fed to AD systems is very important to predict the system's response, the main reason for which is to avoid bio-system upset or failure. Accordingly, completely mass-balanced, three phase (aqueous–solid–gas) plant-wide bioprocess models are written in a general way, which requires the composition parameters of the various organics groups, including the AD biomass, as inputs to the models (Brouckaert et al., 2010; Ikumi et al., 2011; Brouckaert et al., 2021b).

Accepting that the charge (*ch*) of municipal wastewater organics, the organic fraction of municipal solid waste (OFMSW) and food waste is zero, there are six unknowns in Eqs 1 to 3, either *x*, *y*, *z*, *a*, *b* and *c* or f_C, f_H, f_O, f_N, f_P and f_S. So six measurements are required to define the composition. This paper proposes measurement and calculation methods for determining the composition of the different organics groups.

CALCULATING ORGANICS AND BIOMASS ELEMENTAL COMPOSITIONS

In the bioprocess stoichiometry, the elemental composition of all but two components are known, i.e., the organics and the biomass. Actually, it is the composition of these two components that affect the concentrations of all the other components of known composition in the aqueous and gas phases involved in the bioprocesses. Therefore, the changes in the aqueous and gas phase concentrations caused by these two components can be used to determine their composition. Sometimes, for autotrophic and anaerobic processes, an approximate biomass composition can be assumed (like $C_1H_{1.4}O_{0.4}N_{0.2}$, or the better known $C_5H_7O_2N$, Porges and Hoover, 1952) because the net biomass yield (E) is very low, usually <10% of the electron (e⁻) donating capacity (EDC) utilized, but for aerobic processes where the net yield is high (>40%), reasonably accurate estimates of the biomass composition are required to accurately calculate (with steady state or dynamic models) the bioprocess reactants (nitrate and oxygen consumption) and products (sludge production).

Ideally, the measurements required to define the composition should be the six associated with the six mass ratios because they are directly connected to the molar compositions via Eq. 1, i.e., the volatile suspended solids (VSS), total organic carbon (TOC), total organic hydrogen (TOH), total organic oxygen (TOO), total organic nitrogen (TON), total organic phosphorus (TOP) and total organic sulphur (TOS). However, these are not equally amenable to direct or indirect measurement, and furthermore the different organics groups are difficult to isolate and measure without the interfering presence of some of the other organics groups. So COD is added to the list, where the COD is the electron (e^-) donating capacity (EDC) of the organics expressed as oxygen used if all the donated e^- were accepted by oxygen.

Accepting for the moment that the different organics groups can be isolated and measured independently, then for particulate organics (BPO and UPO), four of the seven parameters can be measured with routine wet chemical analysis, i.e., VSS, COD, TON and TOP, where TON and TOP are obtained from the total Kjeldahl nitrogen (TKN), FSA, total phosphorus (TP) and OP tests, i.e., TON = TKN − FSA and TOP = TP − OP. From these four measurements (actually six, two each for the TON and TOP), the three mass ratios f_{cv} (gCOD/gVSS), f_N (gTON/gVSS) and f_P (gTOP/gVSS) can be determined. The remaining three mass ratios can be obtained by elemental analysis, viz., f_C, f_H and f_S (details below). This leaves the TOO/VSS (f_O), which is replaced by the COD/VSS mass ratio (f_{cv}). Also, sometimes one of the mass ratios is not measured but calculated from the remaining five measured mass ratios and the mass balance (Eq. 3). Therefore, equations are required based on mass balance from which the non-measured mass ratios (e.g. f_O and/or f_H) can be calculated from the five (or four) measured mass ratios. For dissolved organics, it is not possible to do a mass concentration measurement (like VSS for particulate). So one of the mass ratios needs to be assumed, e.g. f_{cv} gCOD/g or f_C gC/g and the mass determined from it and one of the COD or TOC concentration measurements.

MASS RATIO EQUATIONS INCLUDING THE COD/VSS MASS RATIO AND MASS BALANCE

The elemental composition of the e^- donor organics (Eqs 1 or 2) (and biomass k, l, m, n, p, and s in $C_kH_lO_mN_nP_pS_s$ if this is to be determined), requires all six element mass ratios to be known. If, for example, f_O and f_H are not measured and replaced by the COD/VSS ratio (f_{cv}) and mass balance, i.e. $f_H = 1 − f_C + f_O + f_N + f_P + f_S$, then equations for f_O and f_H can be derived in terms of the five measured mass ratios ($f_{cv}, f_C, f_N, f_P, f_S$), by considering the element and charge balances for the overall reaction of the COD test. Selecting the standard aquatic chemistry components that represent the products of the COD test (i.e. CO_3^{2-}, H_2O, NH_4^+, PO_4^{3-}, SO_4^{2-}, which all have an EDC relative to COD of zero as in Eqs 10 and 11 in Brouckaert et al., 2021b (Part 2), yields:

$$f_O = \frac{16}{18}\left[1 - \frac{1}{8}f_{cv} - \frac{8}{12}f_C - \frac{17}{14}f_N - \frac{26}{31}f_P - \frac{26}{32}f_S\right] \qquad \text{gO/gVSS} \qquad (4)$$

$$f_H = \frac{1}{9}\left[1 + f_{cv} - \frac{44}{12}f_C + \frac{10}{14}f_N - \frac{71}{31}f_P - \frac{80}{32}f_S\right] \quad \text{gH/gVSS} \qquad (5)$$

Details of the derivation of Eqs 4 and 5 are given in the Appendix. Equations 4 and 5 have been set up to maintain the mass balance when one or more of the mass ratios are set to zero. With all six mass ratios known (some zero), the molar composition of the organics (or biomass) can be determined from Eq. 1. Then with Eq. 2, this molar composition for 1 g organics can by scaled to any

desired molar mass or composition. For example, the mass ratios f_{cv} = 1.416 gCOD/gVSS, f_C = 0.531 gC/gVSS and f_N = 0.124 gN/gVSS (with f_P and f_S = 0) yield f_O = 0.283 gO/gVSS and f_H = 0.0619 gH/gVSS from Eqs 4 and 5. Then from Eq. 1 the molar composition for 1 gVSS is $C_{0.04425}H_{0.06195}O_{0.01769}N_{0.00886}$. This can be scaled to a C_1 basis by multiplying the molar values by 1/0.004425 = 22.60 gVSS/mol and yields $C_{1.0}H_{1.4}O_{0.4}N_{0.2}$, which is equivalent to the well known $C_5H_7O_2N$ for biomass grown on milk protein (casein) first measured by Porges and Hoover (1952).

Equations 4 and 5 are general and apply not only to organics but also to any uncharged e^- donor, such as H_2S, $H_2S_2O_3$ and CH_3COOH, provided the appropriate mass ratios are substituted into them for the particular e^- donor. For example, taking $H_2S_2O_3$ for which $f_C = f_N = f_P = 0$, f_{cv} = 64/114 gCOD/g, f_S = 64/114 gS/g, then f_O = 16/18{1 − 1/8 x 64/114 − 0 − 0 − 0 − 26/32 x 64/114} = 48/114 and f_H = 1/9{1 + 64/114 − 0 + 0 − 0 − 80/32 x 64/114} = 2/114, which are correct from the known composition of $H_2S_2O_3$.

The coefficients in Eqs 4 and 5 have been retained in fraction form because they conform to specific rules, which are explained in Appendix 1. These rules reveal a remarkably consistent order – there is always much beauty when creation reveals its secrets. This order means that Eqs 4 and 5 apply irrespective of the e^- donor products selected for an e^- donor reaction, such as COD (EDC of ammonia excluded) or total oxygen demand (TOD, EDC of ammonia included) which is demonstrated in Appendix 1.

All of the discussion above on the calculation of the composition of the organics applies equally to the calculation of the composition of the biomass, because in bioprocess stoichiometry the biomass is simply a different type of organic compound.

MEASUREMENT ERROR IN ORGANICS COMPOSITION DETERMINATION

The advantage of basing the f_H and f_O mass ratio equations on the mass balance is that any of the mass ratios can be set to zero if deemed negligibly small (like f_P or f_S) and maintain the mass balance with the remaining non-zero mass ratios. This is useful not only for known e^- donor substrates like acetate, sulphide or ammonia but also for organics. If the P, S or even H content of a substrate or biomass are considered low enough to ignore, these mass ratios can be set to zero and the remaining mass ratios, f_C, f_O and f_N, then represent 100% of the mass of the substrate organics or biomass. If these three mass ratios (f_C, f_O and f_N) were measured with COD, TOC, TKN and VSS tests and they do not add to 1, then the error would need to be spread across all three mass ratios in a way reflecting the uncertainty associated with the measurements required for the different mass ratios to establish the mass balance (Σf_i = 1).

From a measurement perspective, replacing the f_H mass ratio by the mass balance aggregates any error in the measurement of the other mass ratios onto the f_H. Because f_H contributes relatively little (<10%) to the total mass of the organic, even relatively small errors in the large contributors to the mass of the organics (f_C, f_{cv} and f_O) can cause f_H to become −ve. It is therefore better to measure f_H and f_N also and then distribute the error in the mass balance between all the measured mass ratios to establish the mass balance. How much of the error to assign to each mass ratio depends on the uncertainty (standard deviation) associated with the measurements required for the different mass ratios.

MEASUREMENT OF THE ORGANICS COMPOSITION

Biomethane potential (BMP) test procedure

Improved and refined over the years, the biomethane potential (BMP) test procedure has long been used to estimate the methane that can be potentially generated from an organic material when anaerobically digested (Owen et al., 1979; Speece, 1996, 2008). The test is conducted by running two AD batch tests in parallel for around 15 days, one control (hereafter referred to as Control) with AD biomass seed sludge only (and distilled water or filtered effluent in place of the organics volume) and one test (hereafter referred to as Test) with the same volume and concentration of seed sludge plus a measured volume and concentration of organics. Daily, the gas (CH_4 and CO_2) generation by both are measured. The difference in the CH_4 production between the Test and Control is assumed to be due to the utilization of the organics and the COD of this CH_4 as a ratio of the COD of the organics added to the Test is deemed to be the biodegradable fraction of the organics (Lin et al., 1999; Moody et al., 2009; Angelidaki et al., 2009).

Augmented BMP test procedure

In this paper, Augmented BMP (AugBMP) and biosulphide potential (AugBSP) test procedures are proposed. By measurements on samples withdrawn at regular intervals from the Test and Control batch tests of the BMP test, the FSA, OP and *H_2CO_3 alk* (and VFA by 5-point titration, Moosbrugger et al., 1993; Vannecke et al., 2015; Part 4 of this series – Ekama et al., 2022) and the in-situ pH, the composition mass ratios (f_{cv}, f_C, f_N, f_P) of the biomass in the AD sludge seed and the biodegradable organics can be determined. This procedure is essentially an extension of that proposed by Raposo et al. (2006), Batstone et al. (2009) and Jensen et al. (2011). Raposo et al. (2006) proposed adding to the BMP test procedure VFA, pH and partial and total alkalinities analyses. However, these two alkalinities are not related to the *H_2CO_3* alkalinity in mixtures of weak acids/bases and so do not correctly characterize the aqueous phase comprising mixed weak acid/base systems to accurately recover the C in the biodegradable organics. Interestingly, Appels et al. (2011) developed a regression model that includes 19 organics compositional variables (such as COD, proteins, carbohydrates, S, P, pH) measured in triplicate on each of 29 sewage sludge samples from various WRRF and tested in the BMP test procedure. They concluded that their regression model can predict the ultimate methane production potential of a random sludge sample within 1.15%.

From the bioprocess stoichiometry of methanogenesis (Part 2 – Brouckaert et al., 2021b,), in the Control, the C, N and P in the biomass endogenously respired ('lost') becomes part of the gaseous and aqueous products and can be measured there. So from the concentration differences in the Control between start and end ($C_{end} - C_{start}$), the COD, VSS, C, N and P of the biomass endogenously respired ('lost') can be calculated: These calculations from a theoretical AugBMP test procedure are shown in Tables 1 and 2. From the difference in *H_2CO_3 alk* (from which the difference in CO_3^- is determined), CH_4 and CO_2 volumes generated between the end and start of the Control, the C content of the biomass (f_C) can be calculated (Table 3-3). It is important that the *H_2CO_3 alk* (i.e. the alkalinity of the inorganic carbon and water systems only) is correctly identified, which can be done in mixed weak acid/base systems with the 5-point titration (Part 4 of this series – Ekama et al., 2022). Similarly, the N and P content of the biomass (f_N, f_P) can be calculated from the difference between the end and start FSA and OP concentrations. Also, the COD of the biomass 'lost' (f_{cv}) is

given by the difference between the end and start methane COD. Finally, the VSS of the biomass 'lost' is the difference between the end and start VSS concentrations. Provided all the necessary measurements can be made accurately enough (which is not necessarily the case), theoretically it is possible to determine the composition mass ratios of the biomass in the AD sludge seed from the control batch of the AugBMP test procedure.

Table 3-1. *Sludge seed and organics composition used for AugBMP and AugBSP test procedure structural identifiability modelling*

Organics type		Sludge seed				Organics		
		Acidogen biomass	Acidogen end res	Seed UPO	Com- bined	BPO (casein)	Organics UPO	Com- bined
COD	mg/L	500	500	4 000	5 000	4 000	1 000	5 000
%	% of COD	10	10	80	100	80	20	100
VSS	mgVSS/L	338	338	2 580	3 256	690	2875	3 565
ISS	mgISS/L	-	-	-	600	-	-	500
TSS	mgTSS/L	-	-	-	3 856	-	-	4 065
f_{cv}	gCOD/gVSS	1.4810	1.4810	1.5500	1.5357	1.3913	1.4500	1.4027
f_C	gC/Gvss	0.5180	0.5180	0.4800	0.4879	0.5217	0.5000	0.5175
f_N	gN/gVSS	0.1000	0.1000	0.0500	0.0604	0.1522	0.0500	0.1324
f_P	gP/gVSS	0.0250	0.0250	0.0150	0.0171	0.0000	0.0250	0.0048
f_S	gS/Gvss	0.0000	0.0000	0.0000	0.0000	0.0000	0.0000	0.0000

Table 3-2. *AugBMP and AugBSP Test and Control start and end results*

Parameter	Units	Test Start	Test end	End–start	Control start	Control end	Control end–start	Change Test–Control
[1]COD	mg/L	5 000	3 057	−1 943	2 500	2 416	−84	1 859
VSS	mg/L	3 410	2 011	−1 399	1 628	1 572	−56	1 342
ISS	mg/L	550	550	0	300	300	0	-
TSS	mg/L	3 960	2 561	−1 399	1 928	1 872	−56	1 342
Vol	L	2.0	2.0	-	2.0	2.0	-	-
[1]TKN	mgTKN-N/L	354.3	354.3	0	113.3	113.3	0	0
[1]TP	mgTP-P/L	56.4	56.4	0	40.3	40.3	0	0
SolCOD	mgCOD/L	0.0	0.0	0.0	0.0	0.0	0.0	0.0
[2]TKN	mgTKN-N/L	20.0	234.8	214.8	15.0	20.6	5.6	209.1
[2]FSA	mgFSA-N/L	20.0	234.8	214.8	15.0	20.6	5.6	209.1
[2]TP	mgTP-P/L	20.0	19.1	−0.9	12.5	13.9	1.4	−2.33
[2]OP	mgOP-P/L	20.0	19.1	−0.9	12.5	13.9	1.4	−2.33
[3]Alk	mg/L CaCO$_3$	100.0	869.2	769.2	75.0	91.8	16.8	752.4
[4]CH$_4$	mL at 20°C	0.0	1 459.6	1 459.6	0.0	62.9	62.9	1 396.8
[4]CO$_2$	mL at 20°C	0.0	725.4	725.4	0.0	38.3	38.3	687.1
%C	gC/gTSS	43.35	38.52		41.20	40.88		
%H	gH/gTSS	6.37	6.29		7.04	7.06		
%N	gN/gTSS	8.44	4.67		5.10	4.95		
[5]Alk	mg/L CaCO$_3$	100.0	3 141.5	3 041.5	75.0	196.9	121.9	2 919.6
[6]SO$_4$	mgS/L	1 500	528.6	−971.4	1 500	1 458.2	−41.8	−929.6
[6]FSS	mgS/L	0.0	971.4	971.4	0.0	14.8	41.8	929.6
f_{cv}	gCOD/gVSS	1.4662	1.5199		1.5357	1.5377		
f_C	gC/gVSS	0.5034	0.4905		0.4879	0.4868		
f_N	gN/gVSS	0.0980	0.0594		0.0604	0.0589		
f_P	gP/gVSS	0.0107	0.0186		0.0171	0.0168		
f_S	gS/gVSS	0.0000	0.0000		0.0000	0.0000		

[1]Unfiltered samples

[2]Filtered samples

[3]H_2CO_3 *alk* in mg/L as CaCO$_3$ for the BMP test

[4] mL gas at 20°C. COD of CH_4 gas = mL x 273.15/(273.15 + 20)/22.4 x 64

COD balance for BMP: COD_{end} + COD of CH_4 = COD_{start}; 2 x 3 057 + 3 886 = 2 x 5 000

Carbon in gas = (mL CH_4 + mL CO_2)273.15/(273.15 + 20)/22.4 x 12 mgC

Carbon in H_2CO_3 alk = H_2CO_3 alk/50 x 12 x (V_S + V_B), where V_S and V_B are volume of substrate organics and volume of AD sludge mass added to batch test (1 L each)

C balance for BMP: $carbon_{end}$ + C in gas + C in H_2CO_3 alk = $carbon_{start}$

N balance for BMP and BSP: TKN_{end} = TKN_{start}

P balance for BMP and BSP: TP_{end} = TP_{start}

[5]H_2CO_3 alk in mg/L as $CaCO_3$ for the BSP test

[6]FSS and SO_4 results for BSP test procedure

COD balance for BSP:COD_{end} + COD of FSS = COD_{start}; 2 x 3 057 + 2 x 64/32 x 971.4 = 2 x 5 000

C balance for BSP: $carbon_{end}$ +C in H_2CO_3 alk = $carbon_{start}$

S balance for BSP: FSS_{end} + SO_{4end} = FSS_{start} + SO_{4start}

Table 3-3. *Calculation of biomass mass ratios and molar composition from BMP Control results*

	Molar composition	
1: COD in methane: (62.9)273.15/(273.15 + 20)/22.4 x 64 = 167.4 mgCOD		
2: C in gas: (62.9 + 38.3)273.15/(273.15 + 20)/22.4 x 12 = 50.5 mgC		
3: C in H_2CO_3 alk = 16.8/50 x 12 = 4.0 mgC/L		
4: Total C = 50.5 +4.0(1 + 1) = 58.6 mgC		
5: Decrease in VSS mass = 56.5 mgVSS/L x 2 L = 113 mgVSS	Molar composition	
6: COD/VSS mass ratio f_{cv} = 167.4/113 = 1.481 gCOD/gVSS	Measured	Theoretical
7: C mass ratio of organics f_C = 58.6/113 = 0.518 gC/gVSS	k = 1.000	k = 1.000
8: N mass ratio of organics f_N = 5.6/56.5 = 0.100 gN/gVSS	n = 0.166	n = 0.166
9: P mass ratio of organics f_P = 1.4/56.5 = 0.025 gP/gVSS	p = 0.019	p = 0.019
10: H mass ratio from Eq. 5: f_H = 0.0662 gH/gVSS	l = 1.534	l = 1.534
11: O mass ratio from Eq. 4: f_O = 0.2908 gO/gVSS	m = 0.421	m = 0.421

Table 3-4. *Calculation of organics mass ratios and molar composition from BMP results*

	Measured	Theoretical
1: COD in methane: (1 396.8)273.15/(273.15 + 20)/22.4 x 64 = 3 718.6 mgCOD		
2: C in gas: (1 396.8 + 687.1)273.15/(273.15 + 20)/22.4 x 12 = 1 040.2 mgC		
3: C in H_2CO_3 *alk* = 752.4/50 x 12 x (1 + 1) = 361.2 mgC		
4: Total C = 1 040.2 + 361.2 = 1 401.4 mgC		
5: Decrease in VSS mass = 1 343 mgVSS/L x 2L = 2 686 mgVSS	Molar composition	
6: COD/VSS mass ratio f_{cv} = 3 718.6/2 686 = 1.3851 gCOD/gVSS	Measured	Theoretical
7: C mass ratio of organics f_C = 1 401.4/2 686 = 0.5217 gC/gVSS	1.0000	1.000
8: N mass ratio of organics f_N = 209.2/1 343 = 0.1558 gN/gVSS	0.2558	0.250
9: P mass ratio of organics f_P = −2.3/1343 = −0.0017 gP/gVSS	−0.0013	0.00
10: H mass ratio from Eq. 5: f_H = 0.0652 gH/gVSS	1.4977	1.500
11: O mass ratio from Eq. 4: f_O = 0.2588 gO/gVSS	0.3718	0.375

Similarly, in the Test batch, the differences between the end and start ($T_{end} - T_{start}$) concentrations and volumes are products generated by both the biomass endogenous respiration and the utilization of the organics. Then the differences in concentrations between the Test and Control [($T_{end} - T_{start}$) − ($C_{end} - C_{start}$)] are deemed to be products generated by the degraded biodegradable organics. Again, provided all the necessary measurements can be made accurately enough (which is not necessarily the case), theoretically, it is possible to estimate the composition mass ratios of the biodegradable organics from the AugBMP test procedure (Tables 1, 2 and 4). So from the difference [($T_{end}-T_{start}$) - ($C_{end} - C_{start}$)] in H_2CO_3 *alk* (from which the difference in HCO_3^- is determined), and the C in CH_4 and CO_2, the C content of the organics (f_C) can be calculated (Table 3-4). Similarly, the N and P content of the organics (f_N, f_P) can be calculated from the differences of the FSA and OP concentrations [($T_{end} - T_{start}$) − ($C_{end} - C_{start}$)]. Also, the COD of the organics utilized (f_{cv}) is given by the methane COD difference [($T_{end} - T_{start}$) − ($C_{end} - C_{start}$)]. Finally, the VSS of the organics utilized is given by the VSS concentrations difference [($T_{end} - T_{start}$) − ($C_{end} - C_{start}$)]. If the biodegradable organics are dissolved, the calculation procedure remains the same. However, because a mass measurement like VSS for particulate organics cannot be made, one of the mass ratios like COD/mass (f_{cv}) has to be assigned an assumed value.

Measurements most prone to error in the AugBMP test procedure are the biogas ($CH_4 + CO_2$) volume and composition (%CH_4) and the VSS difference. Also, samples taken during the test reduce the liquid volume and decrease the gas production, which is complicated to correct for. Gas volumes are difficult to measure accurately, more so than aqueous concentrations. The VSS difference will be subject to large variation when it is the difference between two large concentrations (end minus start). These errors will affect the accuracy of all the mass ratios.

Augmented biosulphide potential (AugBSP) test procedure

The AugBSP test procedure is proposed to obviate the gas volume measurement error and correction problems. Loewenthal et al. (2005) showed that the hydrolysis rates of organics under methanogenic and sulphidogenic conditions were not significantly different provided the sulphide concentration does not increase above 500 mgH_2S-S/L. As discussed in Part 2 (Brouckaert et al., 2021b), very little gas is produced by BSR, because the sulphide produced buffers the pH at values where the vapour pressures of CO_2 and H_2S are very low (in the absence of a separate source of acidity). The only gas production would be by diffusion into the reactor headspace until the partial pressures of CO_2 and H_2S reach saturation. Minimising the headspace volume will suppress this almost completely.

Figure 3-2. *Augmented biosulphide potential (AugBSP) test equipment*

The AugBSP test procedure follows the same procedure as the AugBMP test procedure, i.e., a Control and a Test batch BSR test are run in parallel. Each is done in a completely sealed glass reactor fitted with a purpose-built sealed lid with a screw-operated plunger and clampable sample withdrawal hose (Figure 3-2). pH has to be measured in situ with a probe directly in the AugBSP reactor, because pH will rise quickly in extracted samples due to loss of H_2S and CO_2. To ensure the AugBSP reactor remains completely full with no head space, when a sample is required the sample withdrawal hose is unclamped and the screw-operated plunger screwed down to force out a sample

from the reactor. Two samples are collected and treated in the manner outlined by Poinapen et al. (2009), viz., one collected in a sample jar with 1 drop 10N NaOH and the other in a sample jar without NaOH. The sample with the NaOH can be membrane vacuum filtered without loss of H_2S (and CO_2) and the organics and FSS determined via the COD or another method. If FSS is measured by another method, then it is still necessary to collect the sample into 10N NaOH to avoid H_2S loss. If inaccurate FSS results are entered into the 5-point titration programme, it will yield inaccurate results for the *H_2CO_3 alk* (Poinapen et al., 2009). The filtered sample is analysed for FSA, FSS and OP. After centrifugation of the sample collected without NaOH, the 5-point titration is done on the supernatant. Moderate loss of CO_2 and H_2S does not affect the *H_2CO_3 alk* result from the 5-point titration test and companion speciation calculation programme. Provided accurate in-situ FSA, FSS and OP concentrations are entered into the 5-point titration companion calculation programme (obtainable from https://washcentre.ukzn.ac.za/bio-process-models/), accurate estimates of the *H_2CO_3 alk* will be obtained (Poinapen et al., 2009; Part 4 of this series – Ekama et al., 2022). An accurate estimate of the *H_2CO_3 alk* allows an accurate estimate to be made of the C composition of the AD biomass (Control) and biodegradable organics (Test).

The results from a theoretical AugBSP test with the identical inputs as the theoretical AugBMP test are given in Tables 1 and 2. From the bioprocess stoichiometry of sulphidogenic AD (Brouckaert et al., 2021b), in the Control, the C in the biomass endogenously respired ('lost') becomes aqueous HCO_3^- only. So from the (C_{end} – C_{start}) difference in *H_2CO_3 alk* (from which the difference in HCO_3^- is determined), the C content of the biomass (f_C) can be calculated (Table 3-5). Similarly, the N and P content of the biomass (f_N, f_P) can be calculated from the (C_{end} – C_{start}) difference in FSA and OP concentrations. Also, the COD of the biomass 'lost' (f_{cv}) is given by the (C_{end} – C_{start}) difference in FSS (converted to COD, i.e. mgFSS-S/L x 64/32) or SO_4^{2-} (converted to COD, i.e. mgSO$_4$-S/L x 64/32) concentrations. Finally, the VSS of the biomass 'lost' is the (C_{end} – C_{start}) difference in VSS concentrations. All these measurements are on aqueous samples which can be measured accurately, except possibly the VSS. Hence, it is theoretically possible to determine the compositional mass ratios of the AD biomass from the AugBSP Control batch (Table 3-5).

Similarly to the AugBMP, the differences in concentrations between the AugBSP Test and Control [(T_{end} – T_{start}) – (C_{end} – C_{start})] are deemed to be products generated by the degraded biodegradable organics. So from the difference [(T_{end} – T_{start}) – (C_{end} – C_{start})] in *H_2CO_3 alk* (from which the difference in C is determined), the C content of the organics (f_C) can be calculated (Table 3-6). Similarly, the N and P content of the organics (f_N, f_P) can be calculated from the differences of the FSA and OP concentrations [(T_{end} – T_{start}) – (C_{end} – C_{start})]. Also, the COD of the organics utilized (f_{cv}) is given by the sulphide COD or sulphate (converted to COD) difference [(T_{end} – T_{start}) – (C_{end} – C_{start})]. Finally, the VSS of the organics utilized is given by the VSS concentration difference [(T_{end} – T_{start}) – (C_{end} – C_{start})]. All these measurements are of aqueous-phase concentrations and can be measured accurately, except possibly the VSS.

Table 3-5. *Calculation of biomass mass ratios and molar composition from BSP Control results*

Calculated results	Molar composition	
	Measured	Theoretical
1: COD in FSS: (41.8)/32 x 64 = 83.6 mgCOD/L		
2: C in gas: 0 mgC/L		
3: C in H_2CO_3 alk = 121.9/50 x 12 = 29.3 mgC/L		
4: Total C = 0 + 29.3 = 29.3 mgC/L		
5: Decrease in VSS mass = 56.5 mgVSS/L		
6: COD/VSS mass ratio f_{cv} = 83.6/56.5 = 1.481 gCOD/gVSS		
7: C mass ratio of organics f_C = 29.3/56.5 = 0.518 gC/gVSS	1.000	1.000
8: N mass ratio of organics f_N = 5.6/56.5 = 0.100 gN/gVSS	0.166	0.166
9: P mass ratio of organics f_P = 1.4/56.5 = 0.025 gP/gVSS	0.019	0.019
10: H mass ratio from Eq. 5: f_H = 0.0662 gH/gVSS	1.534	1.534
11: O mass ratio from Eq. 4: f_O = 0.2908 gO/gVSS	0.421	0.421

Hence, theoretically, it is possible to determine the compositional mass ratios of the biodegradable organics from the AugBSP test procedure (Table 3-6). Practically, because all the required concentrations are measured in the aqueous phase, decreasing the Control and Test volumes due to sampling does not affect the results.

Table 3-6*. Calculation of organics mass ratios and molar composition from BSP results*

Calculated results	Molar composition	
	Measured	Theoretical
1: COD in FSS: 1 160.6/32 x 64 = 2 321.2 mgCOD		
2: C in gas: 0 mgC/L		
3: C in H_2CO_3 *alk* = 3 645.9/50 x 12 = 874.8 mgC/L		
4: Total C = 874.8 mgC/L		
5: Decrease in VSS mass = 1 676 mgVSS/L		
6: COD/VSS mass ratio f_{cv} = 2 321.2/1 676 = 1.3851 gCOD/gVSS		
7: C mass ratio of organics f_C = 874.8/1 676 = 0.5220 gC/gVSS	1.0000	1.0000
8: N mass ratio of organics f_N = 261.2/1 676 = 0.1558 gN/gVSS	0.2558	0.2500
9: P mass ratio of organics f_P = −2.95/1676 = −0.0017 gP/gVSS	−0.0013	0.0000
10: H mass ratio from Eq. 5: f_H = 0.0651 gH/gVSS	1.4977	1.5000
11: O mass ratio from Eq. 4: f_O = 0.2588 gO/gVSS	0.3718	0.3750

STRUCTURAL IDENTIFIABILITY OF THE AugBMP and AugBSP PROCEDURES

The structural ability of the AugBMP and AugBSP test procedures to identify the elemental mass ratios of the biomass and biodegradable organics was checked with two types of methanogenic (MP) and sulphidogenic (BSR) kinetic and stoichiometric models – a simplified model with the hydrolysis/acidogenesis and endogenous respiration bioprocesses yielding final MP and BSR products and a complete two-phase (aqueous–gas) methanogenic and sulphidogenic bioprocess model with fully integrated aqueous-phase modelling (PWM_SA_AD_BMP/BSP, Botha, 2015; Botha et al., 2015), which is an implementation of the PWM_SA_AD anaerobic digestion model used by Ghoor (2019), which in turn is a subset of the PWM_SA plant-wide WRRF model (Ikumi et al, 2015).

Organics composition determination with a simplified AD model

In the simplified model, a spreadsheet was coded with the COD mass-balanced kinetics model based on saturation hydrolysis/acidogenesis kinetics (Sötemann et al., 2005) for batch test conditions and the fully mass balanced CHONPS stoichiometry for methanogenesis, one sheet for the Test, an identical parallel sheet for the Control and a third sheet for the [(T_{end} − T_{start}) − (C_{end} − C_{start})] concentration differences. The methanogenic sludge seed comprised three organics types – acidogen biomass, acidogen endogenous residue and unbiodegradable particulate organics (UPO

seed), and the organics comprised two organics types – biodegradable particulate organics (BPO), represented by Casein ($C_1H_{1.5}O_{0.375}N_{0.250}$, Table 3-1, which yields mass ratios f_{cv} = 1.3913 gCOD/gVSS, f_C = 0.5217 gC/gVSS, f_N = 0.1522 gN/gVSS, f_P = 0.0000 gP/gVSS) and unbiodegradable particulate organics (UPO organics). The COD concentration and mass ratios assigned to each of the three groups in the sludge seed and the two groups in the organics are shown in Table 3-1. The combined concentrations and mass ratios calculated from the individual organics' values are also shown in Table 3-1.

For both the AugBMP and AugBSP test procedures, in the Control batch, 1 L sludge seed was mixed with 1 L distilled water and in the Test batch, 1 L sludge seed was mixed with 1 L organics. In the AugBSP Test and Control batches 1 500 mgSO$_4$-S/L was added. The start (C_{start}, T_{start}), end (C_{end}, T_{end}) and difference ($C_{end} − C_{start}$, $T_{end} − T_{start}$) particulate and aqueous concentrations and gas volumes of the Control and Test batches are shown in Table 3-2 for both the Test and Control batches of the AugBMP and AugBSP procedures. The end particulate and aqueous concentrations and gas volumes are the calculated values after 12 d using the saturation hydrolysis/acidogenesis kinetics of Sötemann et al. (2005), i.e. K_M = 5.27 gCOD/(gCOD.d) and K_S = 7.98 gCOD/gCOD for primary sewage sludge. The acidogen biomass yield (Y_{AD}), endogenous respiration rate (b_{AD}) and endogenous residue fraction (f_{AD}) were 0.10 gCOD/gCOD, 0.041 /d and 0.08, respectively. After 12 d, 99.85% of the biodegradable organics was utilized in the Test batch and 36.36% of the acidogen biomass was endogenously respired in the Control batch. The methane and sulphide COD production rate and cumulative methane and sulphide COD versus time in the AugBMP and AugBSP Test and Control batches are shown in Figure 3-3. The acidogen biomass (Z_{AD}), acidogen endogenous residue (Z_{ED}), organics unbiodegradable particulate COD (S_{upi}) and organics biodegradable particulate COD (S_{bp}) concentrations versus time in the Test and Control AugBMP and AugBSP batches are shown in Figure 3-4. Similarly, the FSA and OP concentrations versus time are shown in Figure 3-5, the H_2S *alkalinity* (alk), H_3PO_4 *alk*, H_2CO_3 *alk* and total *alk* concentrations versus time in Figure 3-6 for the AugBMP and in Figure 3-7 for the AugBSP Test and Control batches. The sulphate and sulphide concentrations versus time in the AugBSP Test and Control are shown in Figure 3-8 and cumulative methane, carbon dioxide and total gas volume in mL (at 20°C) versus time in the AugBMP Test and Control are shown in Figure 3-9. The gradual increase in gas (in BMP) and sulphide (in BSP) production rate over the first 2 days was obtained by including an acidogen activity factor, which increased parabolically from 0 at time 0 to 100% after 2 days.
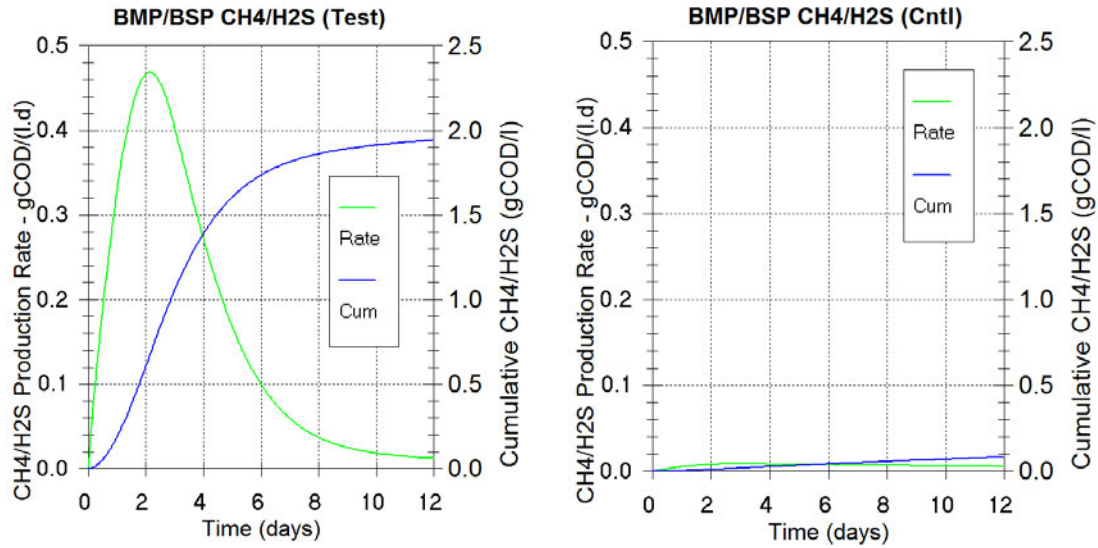
Figure 3-3. *Methane in BMP and FSS in BSP COD production rate and cumulative methane and FSS COD versus time in the Test (Figure 3-3a left) and Control (Cntl; Figure 3-3b right) BMP and BSP batches. BMP methane and BSP sulphide COD concentrations are the same so fall on the same lines.*
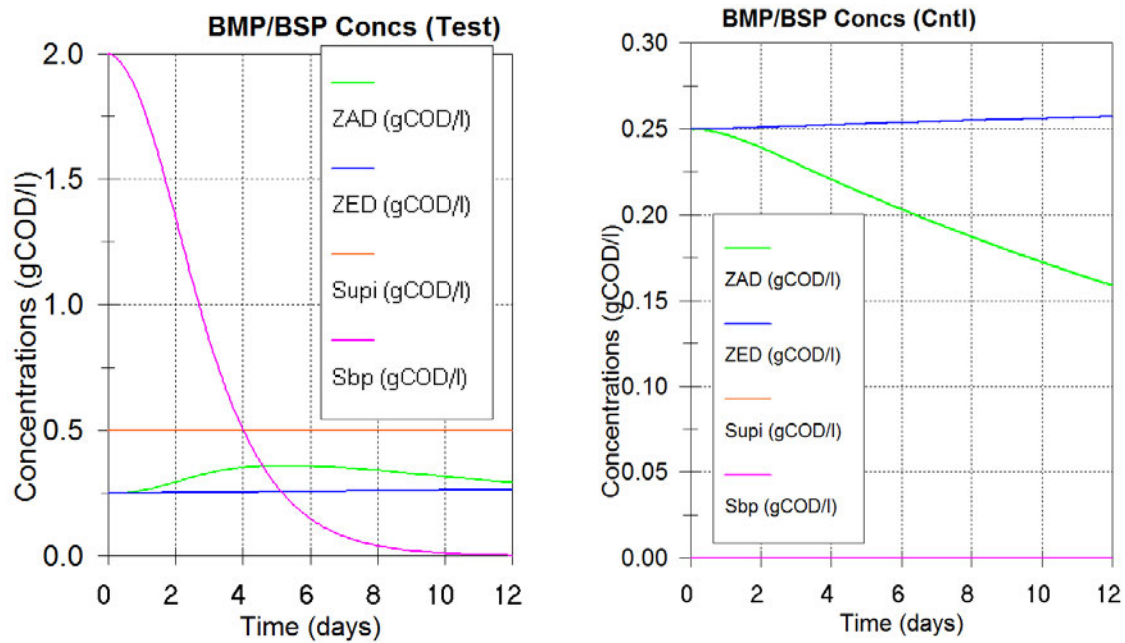

Figure 3-4. *Acidogen biomass (Z_{AD}), acidogen endogenous residue (Z_{ED}), organics unbiodegradable particulate COD (S_{upi}) and organics biodegradable particulate COD (S_{bp}) concentrations versus time in the Test (Figure 3-4a left) and Control (Cntl, Figure 3-4b right) BMP and BSP batches. Note difference in concentration scales between Test and Control. BMP and BSP solids concentrations are the same so fall on the same lines.*
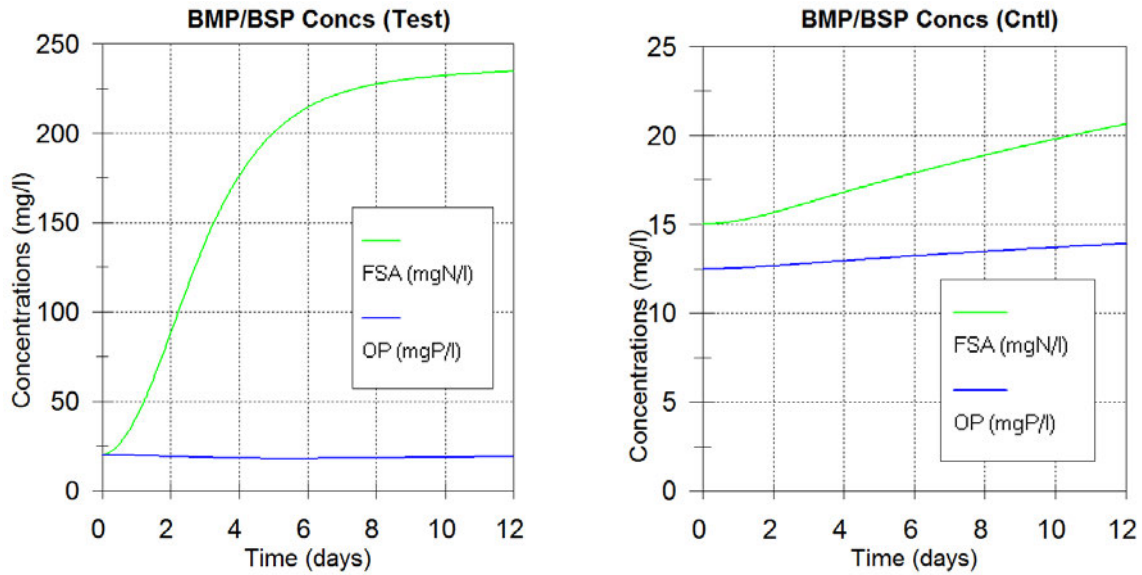
Figure 3-5. *Free and saline ammonia (FSA) and ortho-phosphate (OP) concentrations versus time in the Test (Figure 3-5a left) and Control (Cntl, Figure 3-5b right) BMP and BSP batches. Note difference in concentration scales between Test and Control. BMP and BSP FSA and OP concentrations are the same so fall on the same lines.*
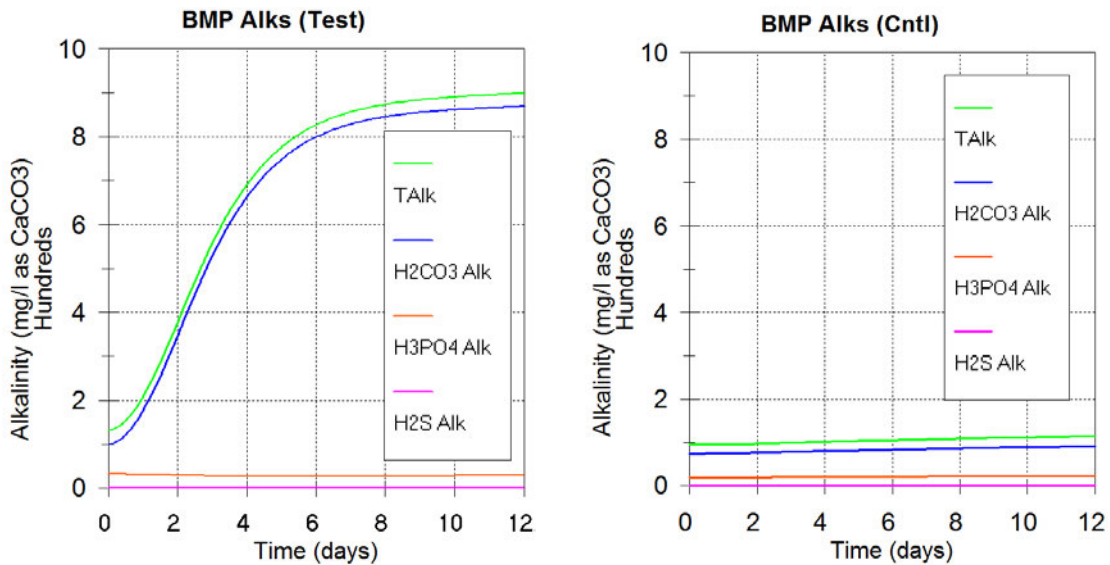

Figure 3-6. *H_2S alk, H_3PO_4 alk, H_2CO_3 alk and total alk concentrations versus time in the Test (Figure 3-6a left) and Control (Cntl, Figure 3-6b right) BMP batches*
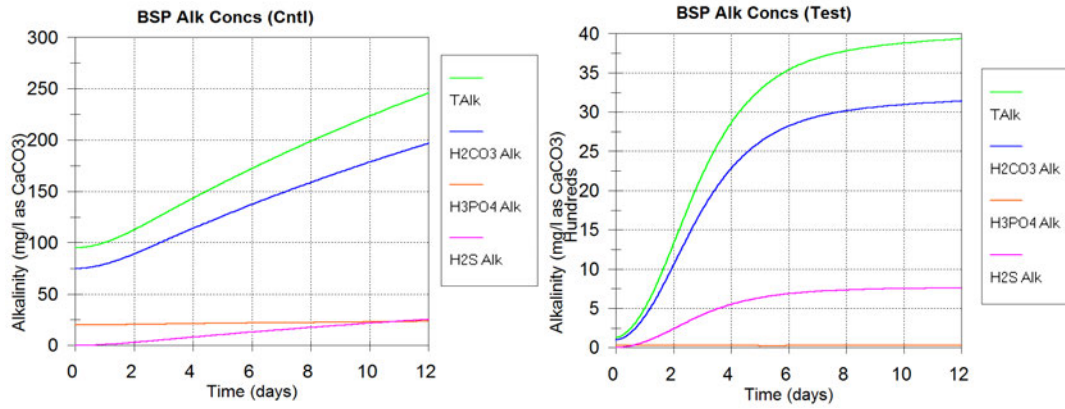
Figure 3-7. *H_2S alk, H_3PO_4 alk, H_2CO_3 alk and total alk concentrations versus time in the Test (Figure 3-7a left) and Control (Cntl, Figure 3-7b right) BSP batches. Note difference in concentration scales between Test and Control)*
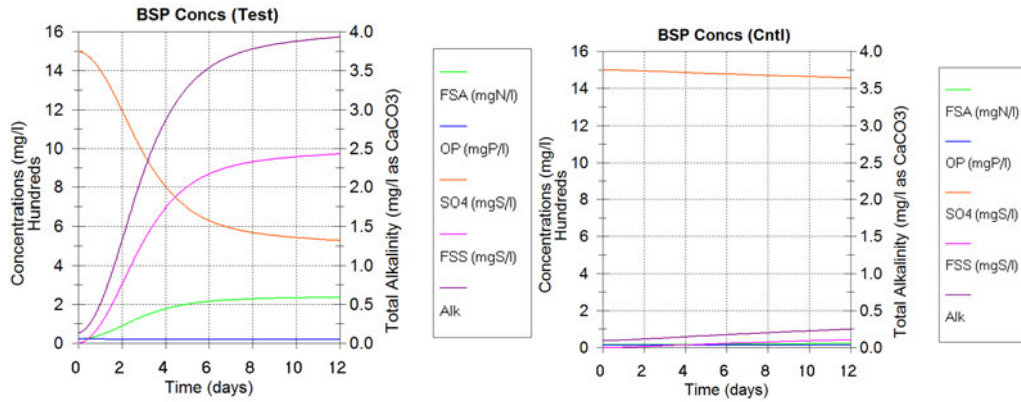

Figure 3-8. *Free and saline ammonia (FSA), ortho-phosphate (OP), sulphate (SO_4), free and saline sulphide (FSS) and total alkalinity (TAlk) concentrations versus time in the BSP Test (Figure 3-8a left) and Control (Cntl, Figure 3-8b right) batches.*
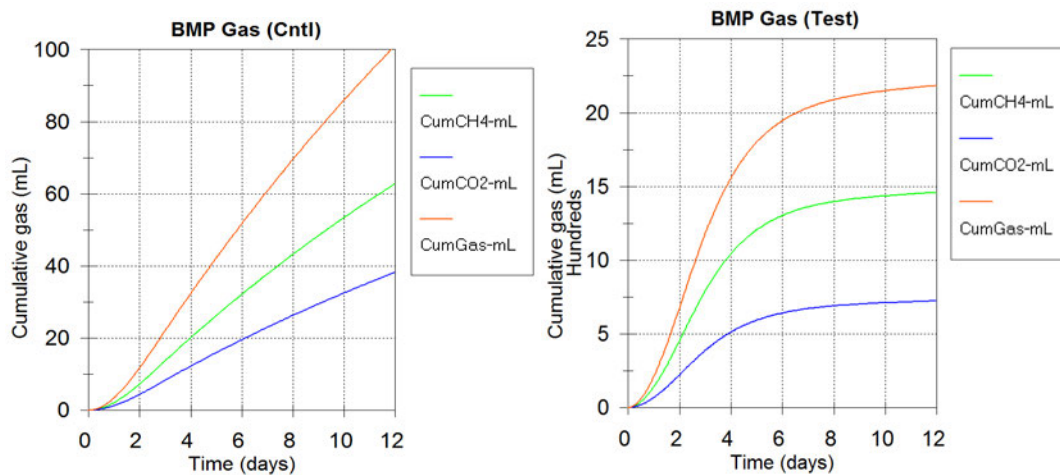

Figure 3-9. *Cumulative methane (CH_4), carbon dioxide (CO_2) and total gas volume in mL versus time in the BMP Test (Figure 3-9a left) and Control (Cntl , Figure 3-9b right) batches (note difference in volume scales between Test and Control)*

Calculating the biomass composition from the AugBMP and AugBSP procedure results

Tables 3 and 4 show the calculation of the biomass composition that was endogenously respired in the AugBMP and AugBSP Control ($C_{end} - C_{start}$) batches. Both AugBMP and AugBSP procedures yield the same composition results for the biomass and are exactly the same as the input biomass composition (Table 3-1). This proves the validity of the approach for the Control batch. The result is exact because only one bioprocess (endogenous respiration) operates in the AugBMP and AugBSP Control batches decreasing the acidogen biomass concentration.

Calculating the organics composition from the AugBMP and AugBSP procedure results

Tables 5 and 6 show the calculation of the example organics casein (milk protein, $C_1H_{1.50}O_{0.375}N_{0.25}$) composition that was utilized in the AugBMP and AugBSP Test [($T_{end} - T_{start}$) − ($C_{end} - C_{start}$)] batches. The determined composition of the casein is very close but not exact. This is because biomass growth and endogenous respiration take place in the Test batch and biomass usually has a different composition to the biodegradable organics. If the acidogen yield is set to zero, then the composition of the organics casein is exact. The calculated mass ratios and composition from the AugBMP and AugBSP test results for casein organics are f_{cv} = 1.385 gCOD/gVSS, f_C = 0.5217 gC/gVSS, f_N = 0.1558 gN/gVSS and f_P = −0.0017 gP/gVSS. If f_P is set to zero (it cannot be negative, f_{ch} and f_S also set to 0) and f_H and f_O calculated from Eqs 5a and 4a, then the determined composition is $C_1H_{1.4875}O_{0.3700}N_{0.2558}P_0$, which is close to the theoretical (Table 3-1). The reason the calculated composition is close to the theoretical and not exact is because the AD biomass yield is low (Y_{AD} = 0.10 gCOD/gCOD). The larger the yield, the larger the error. This indicates that while with a simple kinetic and stoichiometric model it is structurally not possible to determine the exact organics composition with AugBMP and AugBSP tests, the determined composition is very close to the theoretical value. Any experimental error in actual AugBMP and AugBSP test procedures will result in error in the determined organics composition. The significance and magnitude of the error in the measurements required to estimate the different mass ratios is currently being investigated.

Adding elemental analysis to the AugBMP and AugBSP procedures

The organics composition estimate can be improved by adding elemental analysis of the solids of the Test and Control start and end times. Table 3-7 shows the theoretical elemental analysis results of dried solids samples taken from the Test start and Test end conditions taking into account that the %C, %H and %N are with respect to dried total suspended solids (TSS) (not volatile suspended solids, VSS) and therefore include the inorganic suspended solids (ISS). Because the COD-based hydrolysis-acidogenesis and endogenous respiration kinetic constants were the same for the AugBMP and AugBSP Test and Control batches, the particulate concentrations and elemental analysis results are the same for both. Additional wet chemical laboratory measurements, required to determine the composition of the organics utilized in the Test batch and the biomass endogenously respired in the Control batch, are VSS and TSS, unfiltered COD, TKN and TP and filtered COD, TKN, FSA, TP and OP at the start and end times. These additional laboratory results are also shown in Table 3-2. The last column of Table 3-2 shows the difference between the Test and Control batches [($T_{end} - T_{start}$) − ($C_{end} - C_{start}$)]. The calculation of the COD, C, N and P mass balances for the Test and Control batches from the results in Table 3-2 are set out in Table 3-8.

The procedure for calculating the composition of a mixture of organics from elemental analysis and additional laboratory results is shown in Table 3-7a for the Test start results. In Table 3-7a, the %C, %H and %N are converted to mass concentrations by multiplying by the TSS, and the N and P concentrations are given by the difference between the unfiltered and filtered TKN and TP concentrations (Column 1). Assuming a mass balance on the VSS, the O concentration is given by the VSS minus the sum of the C, H, N and P concentrations (Column 1). The f_C, f_H, f_O, f_N and f_P mass ratios are calculated from the C, H, O, N, and VSS concentrations (Column 2). The x, y, z, a and b molar composition values are calculated from the mass ratios with Eqs 1 and 2 (Columns 3 and 4). With the x, y, z, a and b molar composition values for 1 gVSS known (Column 3), the COD concentration and COD/VSS ratio are calculated with Eqs 7 and 8 (Column 1), viz.:

$$\text{COD} = 8\gamma_S = 8(4x + y - 2z - 3a + 5b) \qquad \text{gCOD/mol or} \qquad (7)$$

$$f_{cv} \qquad = 8\left[4\frac{f_C}{12} + 1\frac{f_H}{1} - 2\frac{f_O}{16} - 3\frac{f_N}{14} + 5\frac{f_P}{31}\right] \qquad \text{gCOD for 1 gVSS} \qquad (8)$$

The measured COD/VSS ratio is given by f_{cv} measured = (Unfiltered COD − Filtered COD)/VSS = (5 000 − 0)/3410.3 = 1.4662 gCOD/gVSS (Column 2). Because the 'experimental' results used in this calculation are exact, the calculated COD = f_{cv} x VSS = 1.4662 x 3410.3 = 5 000 mgCOD/L matches exactly the measured COD (also 5 000 mgCOD/L).

Table 3-7a. *Calculation of mixed organics composition from elemental and laboratory analysis results at (a) Test start.*

Calculation of concentrations	Calculation of mass ratios	Comp. for 1 gVSS	Comp. for $x = 1$
(a) Test start			
C = %C/100 x TSS = 43.35/100 x 3 960 = 1 716.7 mgC/L	f_C = C/VSS = 1 716.7/3 410 = 0.5034	$x = f_c/12 = 0.04195$	$x = 1.0000$
H = %H/100 x TSS = 6.37/100 x 3 960 = 252.4 mgH/L	f_H = H/VSS = 252.4/3 410 = 0.0740	$y = f_h/1 = 0.07400$	$y = 1.7641$
N = %N/100 x TSS = 8.44/100 x 3 960 = 334.3 mgN/L	f_N = N/VSS = 334.3/3 410 = 0.0980	$a = f_n/14 = 0.00700$	$a = 0.1669$
N = (UnfiltTKN − FiltTKN) = 354.3 − 20.0 = 334.3 mgN/L	f_N = N/VSS = 334.3/3 410 = 0.0980	$a = f_n/14 = 0.00700$	$a = 0.1669$
P = (UnfiltTP − FiltTP) = 56.4 − 20.0 = 36.4 mgP/L	f_P = P/VSS = 36.4/3 410 = 0.0107	$b = f_p/31 = 0.00034$	$b = 0.0082$
O = VSS − Conc(C + H + N + P) = 3 410.3 − 2 339.7 = 1 070.6 mgO/L	f_O = O/VSS = 1 070.6/3 410 = 0.3139	$z = f_o/16 = 0.01962$	$z = 0.4677$
COD from comp. = $8\gamma_S$ = 8(4x + y − 2z − 3a + 5b) x VSS = 5 000 mgCOD/L	f_{cv} = 5 000/3 410.3 = 1.4662	f_{cv} = 1.4662	$\gamma_S = f_{cv}/8 = 0.1833$
COD from measurement = 5 000 mgCOD/L	Calculated COD = f_{cv} x VSS = 5 000 mgCOD/L		

Table 3-7b. *Calculation of mixed organics composition from elemental and laboratory analysis results at (b) Test end*

Calculation of concentrations	Calculation of mass ratios	Comp. for 1 gVSS	Comp. for $x = 1$
(b) Test end			
C = %C/100 x TSS = 38.52/100 x 2 561.4 = 986.7 mgC/L	f_C = gC/gVSS = 986.7/2 011 = 0.4905	$x = f_c/12 = 0.04088$	$x = 1.0000$
H = %H/100 x TSS = 6.29/100 x 2 561.4 = 161.2 mgH/L	f_H = gH/gVSS = 161.2/2 011 = 0.0801	$y = f_h/1 = 0.08013$	$y = 1.9601$
N = %N/100 x TSS = 4.67/100 x 2 561.4 = 119.5 mgN/L	f_N = gN/gVSS = 119.5/2 011 = 0.0594	$a = f_n/14 = 0.00424$	$a = 0.1038$
N = (UnfiltTKN−FiltTKN) = 354.3−234.8 = 119.5 mgN/L	f_N = gN/gVSS = 119.5/2 011 = 0.0594	$a = f_n/14 = 0.00424$	$a = 0.1038$
P = (UnfiltTP−FiltTP) = 56.4 − 19.1 = 37.3 mgP/L	f_P = gP/gVSS = 37.3/2 011 = 0.0186	$b = f_p/31 = 0.00060$	$b = 0.0146$
O = VSS − Conc(C + H + N + P) = 2 011.4 − 1 304.6 = 706.8 mgO/L	f_O = gO/gVSS = 706.8/2 011 = 0.3514	$z = f_o/16 = 0.01962$	$z = 0.5327$
COD from comp. = $8\gamma_S$ = 8(4x + y − 2z − 3a + 5b) x VSS = 3 057 mgCOD/L	f_{cv} = gCOD/gVSS = 3 057.1/2 011.4 = 1.5199	f_{cv} = 1.5199	$\gamma_S = f_{cv}/8 = 0.1900$
COD from measurement = 3 057 mgCOD/L	Calculated COD = f_{cv} x VSS = 3 057 mgCOD/L		

For actual measurements, the calculated COD will not match exactly the measured COD. The calculation procedure is based on mass balance because the gO was calculated by difference in Table 3-7a. A mismatch between calculated and measured COD means there is error in the measurements from which the composition is calculated. Which of the results to change to match the calculated and measured COD depends on the uncertainty associated with each of the measurements that go into the calculation. Results with high uncertainty (high standard deviation) are the ones to change. The COD is probably one of the most accurate of the measurements and so changing some of the other less accurate measurements to reconcile the calculated COD with that measured is the best approach. Identifying which of the measurements to change to reconcile the calculated COD with that measured is currently being investigated. The same calculation procedure is applied to the Test end results (Table 3-7b) and for the Control start and end results (not shown).

Once the compositions of Test and Control start and end samples have been determined, the composition of the utilized organics is determined by subtracting the end concentrations from the start concentrations. This is $T_{start} - T_{end}$ for the biodegradable organics and $C_{start} - C_{end}$ for the biomass. This calculation is done in Table 3-8, with the calculation method listed below the table. For the biomass, Table 3-8 shows that the determined biomass composition from the Control (Column 6) is exact and the same as that obtained from the AugBMP and AugBSP procedure results. For the organics (Column 3) the determined organics composition from the Test (Column 3) is the same as that obtained from the AugBMP and AugBSP procedure results and therefore close to the theoretical composition of casein. This demonstrates that the analytical and calculation procedure is theoretically valid, and the accuracy of the determined compositions depends on the error in the experimental measurements.

There are more measurements listed in Table 3-2 than required to calculate the organics and biomass compositions from elemental analysis results. As mentioned above, to determine the five composition molar values (x, y, z, a, b in $C_xH_yO_zN_aP_b$) or mass ratios (f_C, f_H, f_O, f_N, f_P), six measurements are required – essentially, the C, H, O, N, P and VSS of the organics and biomass. The C, H and N are obtained from the elemental analysis. Because this analysis is done on dried solids, additionally the TSS mass needs to be measured (which it would be anyway, in the VSS measurement). The O is replaced by COD and the P is obtained from the unfiltered and filtered TP laboratory results. This means that two additional pieces of information are available to reduce error – the laboratory TKN and FSA results for the N content, which duplicates the %N from the elemental analysis, and mass balance, i.e., $f_C + f_H + f_O + f_N + f_P = 1$ ($f_S = 0$). So the error on the N content can be reduced by taking the average of the N content obtained for the laboratory TKN and elemental N analyses in the COD reconciliation calculation (Tables 7a and b). The error can also be reduced by doing the AugBMP or AugBSP tests in duplicate or triplicate, with elemental analysis. While this will increase cost, it will improve the organics composition estimate in actual tests.

 In practice, reconciling the measurements to obtain the best estimate of the organics and biomass compositions also has to take into account the relative experimental uncertainties associated with the various measurements (Gaszynski, 2020).

Table 3-8. *Procedure for calculating the biodegradable organics and biomass compositions from Test start and end and Control start and end elemental and laboratory analysis results*

No.	Parameter	Units	1	2	3	4	5	6
			Test Start	Test End	Differ-ence	Control start	Control end	Differ-ence
1	f_{cv}	gCOD/gVSS	1.4662	1.5199	1.3890	1.5357	1.5377	1.4810
2	f_C	gC/gVSS	0.5034	0.4905	0.5218	0.4879	0.4868	0.5181
3	f_H	gH/gVSS	0.0740	0.0801	0.0652	0.0834	0.0840	0.0662
4	f_O	gO/gVSS	0.3139	0.3514	0.2601	0.3513	0.3534	0.2907
5	f_N	gN/gVSS	0.0980	0.0594	0.1535	0.0604	0.0589	0.1000
6	f_P	gP/gVSS	0.0107	0.0186	−0.0007	0.0171	0.0168	0.0250
7	Mass balance	ΣRows 2–6	1.000	1.000	1.000	1.000	1.000	1.000
8	MeasCOD	mgCOD/L	5 000	3 057	1943	2 500	2 416	84
9	ThVSS	mgVSS/L	3 410	2 011	1 399	1 628	1571	56
10	Carbon	mgC/L	1 717	987	730	794	765	29
11	Hydrogen	mgH/L	252	161	91	136	132	4
12	Oxygen	mgO/L	1 071	707	364	572	557	16
13	OrgN	mgN/L	334	119	215	98	92	6
14	OrgP	mgP/L	36	37	−1	28	26	2
15	Mass balance	ΣRows 10–14	3 410	2 011	1 399	1 628	1 571	57

Columns 1 and 2, Row 1 to 6: Mass ratios from Table 3-2. f_H and f_O calculated from Eqs 5 and 4.

Columns 1 and 2, Row 7: Mass balance: $f_C + f_H + f_O + f_N + f_P = 1.000$

Columns 1 and 2, Row 8 and 9: VSS and COD concentrations from Table 3-2

Columns 1 and 2, Row 10 to 14: Element mass concentrations, e.g., mgC/L = f_C x VSS

Columns 1 and 2, Row 15: Mass balance: mgC/L + mgH/L + mgO/L + mgN/L + mgP/L = mgVSS

Column 3, Row 10 to 14: Test Start minus Test End concentrations

Column 3, Row 8 and 9: Test Start minus Test End VSS and COD concentrations

Column 3, Row 15: Mass balance: mgC/L + mgH/L + mgO/L + mgN/L + mgP/L = mgVSS difference

Column 3, Row 1 to 6: Mass ratios from element concentrations, e.g., f_C = (mgC/L)/(mgVSS/L)

Column 3, Row 7: Mass balance: $f_C + f_H + f_O + f_N + f_P = 1.000$ for Test start minus Test end

Calculation procedure for Control in Columns 4, 5 and 6 is the same as above for Test.

Organics composition determination with a dynamic kinetic AD model

The complete (CHONPS) element mass-balanced bioprocess stoichiometry ensures that the material content of the system input or batch test start is equal to that of the system output or batch test end. For the BMP and BSP tests, this ensures that the material content remains constant with time with the reactant components representing the material content changing with time to product components in the particulate, dissolved and gaseous phases.

The AD unit of the PWM_SA_AD model developed by Brouckaert et al. (2010) and Ikumi et al. (2011, 2015) was adapted to model the BMP test procedure (Botha, 2015; Botha et al., 2015). This model runs on the WEST platform (MikebyDHI, 2021), which includes sensitivity analysis and parameter estimation features. The sensitivity analysis feature allows identification of the bioprocess product components that are most strongly affected by the different feed organic composition parameters. The parameter estimation feature allows determination of the feed organics composition characteristics that best fit a set of measured bioprocess product results.

Adapting PWM_SA_AD to the BMP (and BSP) test procedure required conversion from an influent flow system to a batch test system. Also, for the sensitivity analysis and parameter estimation, the parameters that specify the characteristics of the organics, viz., the composition of the biodegradable organics, the unbiodegradable fraction of the organics and the degradation (hydrolysis) rate of the biodegradable organics, need to be nominated. For the Control batch this is the composition of the AD biomass groups, i.e., k, l, m, n, p and s in $C_kH_lO_mN_nP_pS_s$ (the same for all four biomass groups), the non-active fraction of the AD seed sludge and the endogenous respiration rate of the four biomass groups (the same for each). With these parameters known from the Control batch, for the Test batch, the parameters determined are the composition of the feed organics, i.e., x, y, z, a and b in $C_xH_yO_zN_aP_b$, the unbiodegradable fraction of the feed organics and the hydrolysis rate of the biodegradable organics, i.e., K_m and K_s in the Monod hydrolysis kinetic rate equation.

Ghoor (2019) extended the PWM_SA_AD model to include the biological sulphate reduction (BSR) bioprocess stoichiometry and kinetics, as well as the S content parameters for each organic (c in $C_xH_yO_zN_aP_bS_c$) and biomass (s in $C_kH_lO_mN_nP_pS_s$) group. The sulphidogenic and methanogenic bioprocesses co-exist within the PWM_SA_AD model base, but the interactions between them have not yet been modelled. Thus, either the methanogenic or the sulphidogenic bioprocesses can be selected, while the others remain dormant in the model. The hydrolysis, acidogenesis and acetogenesis bioprocesses are common to both methanogenic and sulphidogenic systems and therefore are always active. This allows the PWM_SA_AD model to be used for the organics characteristics determination from AugBSP tests in the same way as for AugBMP tests. The only difference for the AugBSP test procedure is that aqueous sulphide and sulphate are measured instead of gaseous CO_2 and CH_4.

The PWM_SA_AD_BMP/BSP model was verified by checking that the COD, element (C, H, O, N, P and S) mass and charge balance to 100.000% at every time step of the simulation. Anaerobic bioprocesses consume water, which means that from a complete element mass balance perspective, the AD products which include H and O obtain this H and O not only from the organics but also from the water. This water consumption (or production with aerobic processes) has to be monitored in the model to check the H and O mass balances of the bioprocesses. If the start and end H and O mass balances are checked, including the H and O of the water volume of the batch, errors in the

bioprocess H and O mass balances will not be detected because they are overwhelmed by the vast excess of H and O in the water volume compared to that in the organics and biomass (AD seed sludge) inputs. The PWM_SA, model keeps track of H and O uptake (anaerobic) or release (aerobic) as H_2O from and to the water volume in the bioprocess stoichiometry mass balance continuity checks to avoid this.

To reduce the number of initial concentrations that require measurement, the PWM_SA_AD model calculates the pH using equilibrium speciation (Part 1 – Brouckaert et al., 2021a,; also Part 5 of this series – Brouckaert et al., 2022). This method tracks 14 total ionic component concentrations that are most commonly found in wastewater streams, as well as the pH, *H_2CO_3* alkalinity, ionic strength (total dissolved solids, TDS or conductivity) and temperature. *NaCl* is added to the simulated solution to achieve the measured ionic strength determined from the conductivity. The initial ionic composition is used as a reference state, and any changes in C, H, O, N, P, S components and charge caused by the bioprocesses are tracked and used to calculate the pH as it changes with time (Brouckaert et al., 2021b; see also Parts 4 and 5 of this series).

Determining the organics composition characteristics with parameter estimation (PE)
The PE procedure runs a large number of model simulations which calibrates a set of user-selected model parameters. It uses the variable values measured at each time step of an AugBMP or AugBSP test as a set of variables (selected by the user) and compares them with the corresponding variable values generated by the model. The set of selected parameter values are changed slightly for every simulation until the error between the measured variable values and the model-generated variable values is a minimum. The variable values selected for the AugBMP test procedure (Test and Control batches) are the measured aqueous (e.g. soluble COD, *H_2CO_3 alk*, VFA, OP, FSA, pH) concentrations and CH_4 and CO_2 production rates (Figures 3-3 to 3-6).

In order to optimize the protocol for determining the parameters representing the composition of the organics (Test) and biomass (Control), a number of procedural calibration tests were conducted first. These calibration tests assessed the impact of (i) uncertainty in measured variable values, (ii) errors in initial simulation start parameter values, (iii) changes in statistical PE settings, and (iv) reducing the number of provided variable values on the accuracy of the PE-determined parameters. Because no AugBMP test data was available for this, PWM_SA_AD_BMP/BSP model-generated data was used as a basis (Figures 3-3 to 3-8). This allowed the success of the calibration tests to be compared by determining the percentage error (δ) in each parameter, for which the actual parameter value (P_{act}) was known. Since the data were generated using basis parameters from literature, P_{act} could be used to calculate δ, the relative error between the actual value of the parameter (P_{act}) and the corresponding estimated parameter value (P_{est}) in terms of a percentage for each parameter via $\delta = 100(P_{act} - P_{est})/P_{act}$.

To determine the best variables to include in the AugBMP test procedure, nine variables were selected in the PE calibration tests, i.e., methane (CH_4) and CO_2 gas production rates, OP, FSA, soluble COD, *H_2CO_3* alkalinity and VFA concentrations, the partial pressure of CO_2 (p_{CO2}) and the pH. These variables were selected from literature for their sensitivity to the selected set of parameters and from the simplicity of their measurement procedures. The set of seven selected parameters representing the characteristics of each of the feed organics and biomass were the four elemental

composition values (y, z, a, b in $C_xH_yO_zN_aP_bS_c$ with x set to 1 and the $c = 0$ for the Test batch and l, m, n, p and s in $C_kH_lO_mN_nP_pS_s$ with k set to 1 and the $s = 0$), the unbiodegradable particulate fraction (UPO, f_U_Inf for the organics in the Test batch and the non-biomass part of the AD sludge seed in the Control batch) and the two Monod kinetics hydrolysis kinetic rate constants of the biodegradable organics (kM_BInf and KS_BInf) for the Test batch or the endogenous respiration rate for the biomass.

In the dynamic kinetic model, a biomass activity factor which gradually increased from zero to 100% over the first 1 to 2 days was not required as in the simple spreadsheet model discussed above. This is because the Control batch simulation correctly determines the biomass concentrations to start the Test batch simulation. This eliminates the interference of the activity factor in the determination of the organics hydrolysis kinetic rate constants.

The first calibration runs tested the impact of an error of 5% and 10% in the initial simulation start parameter value inputs (e.g. biomass concentrations), which provides the PE procedure with a starting point for the first simulation, after which the selected parameters are adjusted automatically until optimized. An estimate for the initial parameter values was found to be sufficient as an error of 10% in the initial parameter values only produced an average error of 0.0311% in the estimated parameter values. However, if the initial parameter values can be estimated within a narrow confidence interval so that the size of the range in which the parameters are allowed to vary can be reduced (from ±50% to ±25% of the initial parameter value), then the accuracy of the estimated parameter values, from measured variable values with an uncertainty of up to ±5%, can be improved from an average error of 21.02% to 4.02%.

 An increase in the number of time steps (from 1/d for 4 d to 1/d for 8 d) at which variable values were measured in a BMP test decreased the accuracy of the results from an average error of 4.02% to 10.21%. This is because the degradation of the biodegradable organics was complete within 4 days, so increasing the simulation to 8 days with additional measurements did not add any accuracy to the organics characterization values. The factor which had the largest impact on the accuracy of the estimated parameter values was the uncertainty in the variables (measured) values. An uncertainty of up to ±5% in the experimentally measured variable concentrations resulted in an average error in the estimated parameters of 21.02% and an uncertainty of up to ±10% resulted in average errors of 24.34% and 26.18%. However, as mentioned above, a reduction in the range in which the parameters are allowed to vary can reduce these errors considerably.

Of the nine variables, the OP, FSA and soluble COD values were highlighted as critical measurements because FSA and OP significantly influenced the accuracy of the N and P content of the BPO, respectively (a and b in $C_xH_yO_zN_aP_b$), while soluble COD had a significant influence on the average accuracy across all the parameters. Even though the OP, FSA and soluble COD are the three least practical measurements to include in the BMP test due to their relatively time-consuming protocols, they are worth making because of the increase in accuracy in biodegradable organics composition they provide.

A set of six variables, viz. the OP, FSA, soluble COD, CO_2 rate, CH_4 rate and ρ_{CO2}, was found to be sufficient for estimating the set of seven organics parameters (y, z, a, b, f_U_Inf, kM_BInf and KS_BInf) assuming the variable values are 100% accurate. Since the accuracy of the estimated

parameters decreases with an increase in experimental error of measured variable values, the use of the full set of nine sensitive variables is recommended in the PWM_SA_AD_BMP/BSP model PE protocol.

 The same calibration tests were performed using sulphidogenic bioprocesses in PWM_SA_AD_BMP/BSP. In the AugBSP procedure, the CH_4 and CO_2 production rates and ρ_{CO2} are replaced with aqueous sulphide and sulphate concentrations. The BSP calibration produced the same accuracy levels as the BMP calibration tests. The advantage of the AugBSP test procedure is that aqueous sulphide (and sulphate as an additional variable) production rate can be measured more accurately than gaseous CH_4 and CO_2 production rates.

 In this investigation, PWM_SA_AD_BMP/BSP included a single elemental composition for the influent biodegradable particulate organics (BPO). This assumes that the BPO are homogenous with a single hydrolysis rate. This reduced the number of parameters that needed to be determined by PE to the nine required for just one organic group. In reality, the organics may comprise several groups that have different compositions and hydrolyse at different rates. This may be considered the subject for future extensions of the PWM_SA_AD_BMP/BSP model. If sufficiently accurate compositions for single homogenous organics can be determined with the proposed AugBMP and AugBSP and modelling procedures, further research can be conducted into extending the model to two or three groups of biodegradable organics in the same organic material.

CONCLUSIONS

Bioprocesses transform the components contained in the material content flux entering single or multiple reactor systems from one kind to another without a change in total material content flux exiting the system in the solid, aqueous or gas phases. Based on this principle of mass conservation in bioprocess stoichiometry, the augmented biomethane (AugBMP) and augmented biosulphide (AugBSP) potential test procedures have been evaluated. These two test procedures change the BMP from a stand-alone test to a bio-reactor on which a range of additional tests are made to determine the composition of the biodegradable organics. The analytical tests were identified that need to be made to quantify the material content of the bioprocess products (outputs). This allows the material content of the bioprocess reactants (inputs), expressed as $C_xH_yO_zN_aP_bS_c$, to be determined from the measured bioprocess products and examples of the calculation procedure to do this were given. The AugBMP and AugBSP test procedures, supplemented by anaerobic digestion dynamic modelling, is as accurate as the analytical measurements for determining the composition of biodegradable organics, and also allows the hydrolysis rate of the biodegradable organics and the unbiodegradable fraction of the organics to be determined. Knowing these characteristics of organics before they are fed to anaerobic digesters (AD) is important to predict the AD performance and stability when fed the organics.

The BMP test can be criticized for being similar to the century-old biochemical oxygen demand (BOD) test – except that it is anaerobic, and therefore no better than the BOD. The problems and deficiencies of the BOD as a wastewater-strength measure for modelling aerobic processes such as the activated sludge system have been voiced for decades (for example, see Wentzel et al., 2003). The comparison with the BOD is valid in the sense that both use a sludge seed and rely on bioprocesses as opposed to more consistent and reproducible chemical reactions. However, the

criticism that, as a result, the BMP also cannot be used as a organics strength measurement for mass-balanced modelling, as it yields similarly variable results, is unduly harsh for five reasons:

- Oxygen is not very soluble in water and so the BOD without aeration (as opposed respirometry with aeration) has to be done at high dilutions. The BMP test can be done at much higher seed and organics concentrations so differences are more accurate to measure and this avoids the multiplication of error.
- The yield of biomass and the endogenous respiration rate under anaerobic conditions are very low, so that practically all of the electron-donating capacity of the organics is captured in measurable electron acceptors. In contrast, the yield of biomass and the endogenous respiration rate under aerobic conditions are high, with the result that a significant proportion of the electron-donating capacity of the organics is captured in unmeasurable unbiodegradable material, which precludes the BOD test from being used as an organics strength measure for mass-balanced modelling.
- There is an international drive to standardize the BMP test procedure (Raposo et al., 2011a) and the results from an inter-laboratory evaluation show that the 'influence of inocula and experimental factors was nearly insignificant with respect to the extents of the anaerobic biodegradation' (Raposo et al., 2011b p. 1 088).
- The BOD was regarded a test in itself and not a bio-reactor on which many tests are done. The BMP is also a stand-alone test but the augmented BMP (AugBMP) and augmented BSP (Aug BSP) are not – these are bio-reactors on which a range of tests are conducted to focus the purpose and improve the results.
- Bioprocess stoichiometry and dynamic kinetic modelling techniques have become well developed over the past 40 years and generally these have not been applied to the BOD to improve its reliability – it was not necessary because it was replaced by the much better COD test as a basis for mass-balanced modelling-based operation.

Adding bioprocess stoichiometry and dynamic kinetic modelling techniques, as in the AugBMP and AugBSP, will significantly improve their reliability and reproducibility. It is realized that adding modelling and more analysis will be more costly and require greater levels of competence. Where such additional resources are required in industrial processes, there would be little hesitation to acquire them. With the transition from waste treatment to resource recovery and recycling in bio-refineries, there necessarily will be a need to also adopt new more complex approaches if this transition is to be realized.

ABBREVIATIONS

AD	anaerobic digestion
ADM1	Anaerobic Digestion Model No 1
Alk	alkalinity
AS	activated sludge
AugBMP	augmented biomethane potential test
AugBSP	augmented sulphide potential test
BMP	biomethane potential test
BPO	biodegradable particulate organics
BSP	biosulphide potential test
BSR	biological sulphide reduction
COD	chemical oxygen demand
Cntl	Control
EDC	electron donating capacity
FBSO	fermentable biodegradable soluble organics
FSA	free and saline ammonia
FSS	free and saline sulphide
IC	inorganic carbon
MP	methane producing (methanogenic)
OFMSW	organic fraction of municipal solid waste
OP	ortho phosphate
PE	parameter estimation
TOC	total organic carbon
TOD	total oxygen demand
TOH	total organic hydrogen
TON	total organic nitrogen
TOO	total organic oxygen
TOP	total organic phosphorus
TOS	total organic sulphur
UPO	unbiodegradable particulate organics
USO	unbiodegradable soluble organics
VFA	volatile fatty acids
VSS	volatile suspended solids
WRRF	water and resource recovery facility

SYMBOLS

$\alpha_{C,i}$ carbon to mass ratio of component I (ex Volcke et al. 2006)

$\alpha_{H,i}$ hydrogen carbon to mass ratio of component I (ex Volcke et al. 2006)

$\alpha_{N,i}$ nitrogen to mass ratio of component I (ex Volcke et al. 2006)

$\alpha_{O,i}$ oxygen to mass ratio of component I (ex Volcke et al. 2006)

$\alpha_{P,i}$ phosphorus to mass ratio of component I (ex Volcke et al. 2006)

γ_S electron donating capacity of the electron donor

$\gamma_{S\text{-}COD}$ electron donating capacity with respect to COD

$\gamma_{S\text{-}TOD}$ electron donating capacity with respect to TOD

a molar content of nitrogen in $C_xH_yO_zN_aP_bS_c{}^{ch}$ electron donor

b molar content of phosphorus in $C_xH_yO_zN_aP_bS_c{}^{ch}$ electron donor

B   boron

c molar content of sulphur in $C_xH_yO_zN_aP_bS_c{}^{ch}$ electron donor

C   carbon

ch molar content of carbon in $C_xH_yO_zN_aP_bS_c{}^{ch}$ electron donor

C_i coefficient of element i in the EDC (γ_S) equation.

d molar content of boron in $C_xH_yO_zN_aP_bS_cB_d{}^{ch}$ electron donor if B were included

E net biomass yield gCOD biomass produced/d per gCOD substrate utilized/d, a combined effect of growth and endogenous respiration (Ekama, 2009).

e^- electron

f_B boron to mass ratio (gB/mass, gB/gVSS for particulate organics)

f_C carbon to mass ratio (gC/mass, gC/gVSS for particulate organics)

f_{ch} charge to mass ratio (ch/g molar mass)

f_{cv} COD/mass ratio (COD/VSS mass ratio for particulate organics)

f_H hydrogen to mass ratio (gC/mass, gC/gVSS for particulate organics)

f_i mass ratio of element i

f_N nitrogen to mass ratio (gC/mass, gC/gVSS for particulate organics)

f_O oxygen to mass ratio (gC/mass, gC/gVSS for particulate organics)

f_P phosphorus to mass ratio (gC/mass, gC/gVSS for particulate organics)

f_S sulphur to mass ratio (gC/mass, gC/gVSS for particulate organics)

f_{tv} TOD/mass ratio (TOD/VSS mass ratio for particulate organics)

H   hydrogen

i element i (any of CHONPS)

k molar content of hydrogen in $C_kH_lO_mN_nP_pS_s$ biomass

l	molar content of oxygen in $C_kH_lO_mN_nP_pS_s$ biomass
M_B	atomic mass of the boron (10)
M_C	atomic mass of the carbon (12)
M_{ed}	molar mass of the electron donor
M_H	atomic mass of the hydrogen (1)
M_i	atomic mass of element i
M_O	atomic mass of the oxygen (16)
M_N	atomic mass of the nitrogen (14)
M_P	atomic mass of the phosphorus (31)
M_S	atomic mass of the sulphur (32)
n	molar content of nitrogen in $C_kH_lO_mN_nP_pS_s$ biomass
N	nitrogen
O	oxygen
p	molar content of phosphorus in $C_kH_lO_mN_nP_pS_s$ biomass
P	phosphorus
s	molar content of sulphur in $C_kH_lO_mN_nP_pS_s$ biomass
S	sulphur
V_B	volume of organic substrate added to BMP or BSP batch test
V_S	volume of sludge seed added to BMP or BSP batch test
x	molar content of carbon in $C_xH_yO_zN_aP_bS_c{}^{ch}$ electron donor
y	molar content of hydrogen in $C_xH_yO_zN_aP_bS_c{}^{ch}$ electron donor
z	molar content of oxygen in $C_xH_yO_zN_aP_bS_c{}^{ch}$ electron donor

REFERENCES

APPELS L, LAUWERS J, GINS G, DEGRÈVE J, VAN IMPE J and DEWIL R (2011) Parameter identification and modelling of the biochemical methane potential of waste activated sludge. *Environ. Sci. Technol.* **45** 4173–4178. https://doi.org/10.1021/es1037113

ANGELIDAKI I, ALVES MM, BOLZONELLA D, BORZACCONI L, CAMPOS JL, GUWY AJ, KALYUZHNYI S, JENICEK P and VAN LIER JB (2009) Defining the biomethane potential (BMP) of solid organic wastes and energy crops: A proposed protocol for batch assays. *Water Sci. Technol.* **59** (5) 927–934. https://doi.org/10.2166/wst.2009.040

BATSTONE DJ, KELLER J, ANGELIDAKI I, KALYUZHNYI SV, PAVLOSTATHIS SG, ROZZI A, SANDERS, WTM, SIEGRIST H and VAVILIN VA (2002) Anaerobic digestion model No 1 (ADM1). Scientific and Technical Report No 9. International Water Association (IWA), London. https://doi.org/10.2166/wst.2002.0292

BATSTONE DJ, TAIT S AND STARRENBURG D (2009) Estimation of hydrolysis parameters in full-scale anaerobic digesters. *Biotechnol. Bioeng.* **102** (5) 1513–1520. https://doi.org/10.1002/bit.22163

BOTHA RF (2015) Characterization of organics for anaerobic digestion by modelling augmented biochemical methane potential test results. MSc (Eng) thesis, Dept of Civil Engineering, University of Cape Town.

BOTHA RF, IKUMI DS and EKAMA GA (2015) Characterization of organics for anaerobic digestion by modelling augmented biochemical methane potential test results. 4th YWP-ZA Biennial Conference, 16–18 Nov 2015, Pretoria.

BROUCKAERT CJ, IKUMI DS and EKAMA GA (2010) A 3 phase anaerobic digestion model. 12th IWA AD conference, 30 Oct–4 Nov 2010, Guadalajara, Mexico.

BROUCKAERT CJ, BROUCKAERT BM and EKAMA GA (2021a) Integration of complete elemental mass-balanced stoichiometry and aqueous-phase chemistry for bioprocess modelling of liquid and solid waste treatment systems – Part 1: The physico-chemical framework *Water SA* **47** (3) 276–288. https://doi.org/10.17159/wsa/2021.v47.i3.11857

BROUCKAERT CJ, EKAMA GA, BROUCKAERT BM and IKUMI DS (2021b) Integration of complete elemental mass-balanced stoichiometry and aqueous-phase chemistry for bioprocess modelling of liquid and solid waste treatment systems – Part 2: Bioprocess stoichiometry. *Water SA* **47** (3) 289–308. https://doi.org/10.17159/wsa/2021.v47.i3.11858

EKAMA GA (2009) Using bioprocess stoichiometry to build a steady state plant wide wastewater treatment plant model. *Water Res.* **43** (8) 2101–2120. https://doi.org/10.1016/j.watres.2009.01.036

EKAMA GA, BROUCKAERT CJ and BROUCKAERT BM (2022) Integration of complete elemental mass-balanced stoichiometry and aqueous-phase chemistry for bioprocess modelling of liquid and solid waste treatment systems – Part 4: Aligning the modelled and measured aqueous phases. *Water SA* **48** (1) 21-31. https://doi.org/10.17159/wsa/2022.v48.i1.3322

GASZYNSKI C (2020) Identification of wastewater primary sludge composition using augmented batch tests and mathematical models. PhD thesis, Dept. of Civil Eng., University of Cape Town.

GHOOR T (2 019) Developments in anaerobic digester modelling. PhD thesis, Dept. of Civil Eng., University of Cape Town.

GRAU P, DE GRACIA M, VANROLLEGHEM PA and AYESA E (2007) A new plant wide methodology for WWTPs. *Water Res.* **41** 4357–4372. https://doi.org/10.1016/j.watres.2007.06.019

IKUMI DS, BROUCKAERT CJ and EKAMA GA (2011) A 3 phase anaerobic digestion model. 8th IWA Watermatex Conference, 20–22 June 2011, San Sebastian, Spain.

IKUMI DS, HARDING TH and EKAMA GA (2014) Biodegradability of wastewater and activated sludge organics in anaerobic digestion. *Water Res.* **56** (1) 267–279. https://doi.org/10.1016/j.watres.2014.02.008

IKUMI DS, HARDING TH, VOGTS M, LAKAY MT, MAFUNGWA HZ, BROUCKAERT CJ and EKAMA GA (2015) Mass balances modelling over wastewater treatment plants III. WRC Report No. 1822/1/14. Water Research Commission, Pretoria.

JENSEN PD, GE H and BATSTONE DJ (2011) Assessing the role of BMP tests in determining anaerobic degradability rate and extent. *Water Sci. Technol.* **64** (4) 880–886. https://doi.org/10.2166/wst.2011.662

LIN J, MA Y, CHAO AC and HUANG C (1999) BMP test on chemically pretreated sludge. *Bioresour. Technol.* **68** 187–192. https://doi.org/10.1016/S0960-8524(98)00126-6

LOEWENTHAL RE, RISTOW NE, SOTEMANN SW, WENTZEL MC and EKAMA GA (2005) Hydrolysis of primary sewage sludge under methanogenic, acidogenic and sulfate-reducing conditions. WRC Report No. 1216/1/05, Water Research Commission, Pretoria.

MikebyDHI (2021) – Modelling and simulation of wastewater treatment plants, URL: www.mikebydhi.com/products/west (Accessed 30 December 2021).

MOODY L, BURNS R, HAAN WW and SPAJIC R (2009) Use of Biochemical methane potential (BMP) assay for predicting and enhancing Anaerobic digester performance. *Proceedings of the 44th Croatian and 4th International Symposium on Agriculture,* 16–20 February 2009, Opatija, Croatia. 930–934.

MOOSBRUGGER RE, WENTZEL MC, LOEWENTHAL RE, EKAMA GA and MARAIS GvR (1993) Alkalinity measurement: Part 3 – A 5 pH point titration method to determine the carbonate and SCFA weak acid/bases in aqueous solution containing also known concentrations of other weak acid/bases. *Water SA* **19** (1) 29–40.

OWEN W, STUCKEY D, HEALY JB Jr, YOUNG L and McCARTY P (1979) Bioassay for monitoring biochemical methane potential and anaerobic toxicity. *Water Res.* **13** 485–492. https://doi.org/10.1016/0043-1354(79)90043-5

POINAPEN J, EKAMA GA and WENTZEL MC (2009) Biological sulphate reduction using primary sewage sludge in a upflow anaerobic sludge bed reactor – Part 2: Modification of simple wet chemistry analytical procedures to achieve COD and S mass balances. *Water SA* **35** (5) 535–542. https://doi.org/10.4314/wsa.v35i5.49179

POINAPEN J and EKAMA GA (2010) Biological sulphate reduction using primary sewage sludge in a upflow anaerobic sludge bed reactor – Part 5: Development of a steady state model. *Water SA* **36** (3) 193–202.

PORGES N and HOOVER SR (1952) Assimilation of dairy waste by activate sludge: II. The equation of synthesis and rate of oxygen utilization. *Sewage Ind. Wastes* **24** (3) 306–312.

RAPOSO F, BANKS CJ, SIEGERT I, HEAVEN S and BORJA R (2006) Influence of inoculum to substrate ratio on the biochemical methane potential of maize in batch tests. *Process Biochem.* **41** 1444–1450. https://doi.org/10.1016/j.procbio.2006.01.012

RAPOSO F, DE LA RUBIA MA, FERNANDEZ-CEGRI F, BORJA R (2011a) Anaerobic digestion of solid organic substrates in batch mode: An overview relating to methane yields and experimental procedures. *Renew. Sustainable Energ. Rev.* **16** 861–877. https://doi.org/10.1016/j.rser.2011.09.008

RAPOSO F, FERNANDEZ-CEGRI V, DE LA RUBIA MA, BORJA R, BELINE F, CAVINATO C, DEMIRER G, FERNANDEZ B, FERNANDEZ-POLANCO M, FRIGON JC, GANESH R, KAPARAJU P, KOUBOVA J, MENDEZ R, MENIN G, PEENE A, SCHERER P, TORRIJOS M, UELLENDAHL H, WIERINCK I and DE WILDE V (2011b) Biochemical methane potential (BMP) of solid organic substrates: evaluation of anaerobic

biodegradability using data from an international inter-laboratory study. *J. Chem. Technol. Biotechnol*. **86** 1088–1098. https://doi.org/10.1002/jctb.2622

SPEECE RE (1996) *Anaerobic Biotechnology for Industrial Wastewaters.* Archae Press, Nashville.

SPEECE RE (2008) Anaerobic biotechnology and odor/corrosion control for municipalities and industries. Archea Press, Nashville. ISBN 1-57843-052-9, pp 586.

SÖTEMANN SW, RISTOW NE, WENTZEL MC and EKAMA GA (2005) A steady-state model for anaerobic digestion of sewage sludges. *Water SA* **31** (4) 511–527. https://doi.org/10.4314/wsa.v31i4.5143

STANDARD METHODS (1998) *Standard Methods for Examination of Water and Wastewater* (20th edn). American Public Health Association, Water Environment Federation and American Water Works Association, Washington DC.

VANNECKE TPW, LAMPENS D, EKAMA GA and VOLCKE EIP (2015) Evaluation of the 5 and 8 pH point titration methods for monitoring alkalinity and VFA in anaerobic digesters treating solid waste. *Environ. Technol.* **36** (7) 681–869. https://doi.org/10.1080/09593330.2014.964334

VAN ZYL PJ, WENTZEL MC, EKAMA GA and RIEDEL K-H (2008) Design and start up of a high rate anaerobic membrane bio-reactor for the treatment of a low pH, high strength dissolved organic wastewater. *Water Sci. Technol.* **57** (2) 291–295. https://doi.org/10.2166/wst.2008.083

VOLCKE EIP, VAN LOOSDRECHT MCM and VANROLLEGHEM PA (2006) Continuity-based model interfacing for plant-wide simulation: A general approach. *Water Res.* **40** (15) 2817–2828. https://doi.org/10.1016/j.watres.2006.05.011

WENTZEL MC, EKAMA GA and LOEWENTHAL RE (2003) Fundamentals of biological behaviour and wastewater strength measurement. Chapter 9. In: Mara D and Horan N (eds) *Handbook of Water and Wastewater Microbiology.* Elsevier Science Ltd. 131–157. ISBN 0-12-470100-0.

WESTERGREEN S, BROUCKAERT CJ and FOXON KM (2012) Modelling of ionic interactions with wastewater treatment biomass. *Water Sci. Technol.* **65** (6) 1014–1020. https://doi.org/10.2166/wst.2012.922

APPENDIX

Derivation of the oxygen (f_O) and hydrogen (f_H) mass ratio equations

Equations 4 and 5 were derived using the $\gamma_{S\text{-COD}}$ (e$^-$/mol) Eq. 11 in Brouckaert et al. (2021b) (Part 2) and the mass balance Eq. 3, i.e.

$$\gamma_{S,COD} = 4x + y - 2z - 3a + 5b + 6c - \text{ch e}^-/\text{mol on the COD basis (i.e. EDC of N excluded)} \quad (A1)$$

In Eq. A1, the COD of the e$^-$ donor $C_xH_yO_zN_aP_bS_c{}^{ch}$ is γ_S e$^-$/mol x 32/4 gO$_2$/e$^-$ or $\gamma_S M_O/2$, where M_O is the atomic mass of oxygen (16). The coefficients of x, y, z, a, b and c in Eq. A1 are simply the oxidation states of the C, H, O, N, P and S products of the COD reaction (viz., $CO_3{}^{2-}$, H_2O, $NH_4{}^+$, $PO_4{}^{3-}$, $SO_4{}^{2-}$) relative to their elemental state (Part 2 – Brouckaert et al., 2021b, Figure 2-1), where the products themselves have zero EDC relative to the COD oxidation reaction. The molecular mass of the e$^-$ donor $C_xH_yO_zN_aP_bS_c{}^{ch}$ (M_{ed}, g/mol) is given by

$$M_{ed} = xM_C + yM_H + zM_O + aM_N + bM_P + cM_S \tag{A2}$$

where M_C, M_H, M_O, M_N, M_P and M_S are the atomic masses of C, H, O, N, P and S. So the COD/mass ratio $f_{cv} = (\gamma_{S,COD} M_O)/(2 M_{ed})$, from which $\gamma_{S,COD} = 2f_{cv}M_{ed}/M_O$. From Eq. 1, the elemental mass ratios are given by $f_C = xM_C/M_{ed}$, $f_H = yM_H/M_{ed}$, $f_O = zM_O/M_{ed}$, $f_N = aM_N/M_{ed}$, $f_P = bM_P/M_{ed}$ and $f_S = cM_S/M_{ed}$, from which $x = f_CM_{ed}/M_C$, $y = f_HM_{ed}/M_H$, $z = f_OM_{ed}/M_O$, $a = f_NM_{ed}/M_N$, $b = f_PM_{ed}/M_P$ and $c = f_S M_{ed}/M_S$ and the charge 'mass' ratio (charge/g e⁻ donor) is $f_{ch} = ch/M_{ed}$ from which $ch = f_{ch}M_{ed}$. Substituting these expressions for x, y, z, a, b, c and ch into Eq. A1 for the COD and dividing through by M_{ed} yields,

$$\frac{2f_{cv}}{M_O} = 4\frac{f_C}{M_C} + 1\frac{f_H}{M_H} - 2\frac{f_O}{M_O} - 3\frac{f_N}{M_N} + 5\frac{f_P}{M_P} + 6\frac{f_S}{M_S} - f_{ch} \tag{A3}$$

Usually the charge (ch) of the unknown organic e⁻ donor is zero so f_{ch} is set to zero. Equation A3 is linear in which all the terms are known except f_H and f_O. It can be solved simultaneously with the mass balance Eq. 3, and if the atomic masses are retained as integer values, the f_O Eq. 4 and f_H Eq. 5 are obtained.

With the charge set as zero ($f_{ch} = 0$), Eqs 4 and 5 can be rewritten as:

$$1 = \frac{8}{12}f_C + \frac{18}{16}f_O + \frac{17}{14}f_N + \frac{26}{31}f_P + \frac{26}{32}f_S + \frac{1}{8}f_{cv} \text{ gVSS/gVSS} \tag{A4}$$

$$1 = \frac{44}{12}f_C + \frac{9}{1}f_H - \frac{10}{14}f_N + \frac{71}{31}f_P + \frac{80}{32}f_S - f_{cv} \quad \text{gVSS/gVSS} \tag{A5}$$

If Eq. A4 is multiplied by 8 and added to Eq. A5 and the resulting equation is divided through by 9, the mass balance for 1 g organics, Eq. 3, is obtained.

While Eqs 4 and 5 and the rewritten Eqs A4 and A5 look complex, the latter follow a specific rule in their make-up. This rule allows the mass ratio equations for f_O and f_H to be written simply from the element atomic masses and the coefficients in the $\gamma_{S,COD}$ (e⁻/mol) equation of the selected elements CHONP or S making up the e⁻ donor. Also, this rule also can be applied if other mass ratios than f_O and f_H are to be determined. Moreover, this rule is independent of the choice of the e⁻ donor reactants and products in the oxidation reaction, e.g., the TOD can also be the basis of the EDC.

Rule for f_O equation

In Eq. A4 for the oxygen mass ratio f_O (in which f_H is absent), the COD/VSS ratio (f_{cv}) is relative to the selected oxidation products of the COD test, i.e., ammonia, phosphate and sulphate. Now in Eq. A4, from which Eq. 4 for f_O is derived, the denominator of the fraction coefficients in front of the mass ratio terms is the atomic mass of its corresponding element, i.e., 12 for f_C, 14 for f_N, and so on. The numerator is the atomic mass of the element minus (1)/(+1) times the element's corresponding coefficient in the EDC/mol ($\gamma_{S,COD}$) equation taking due consideration of its sign, where the (1) in (1)/(+1) is the atomic mass of H and the (+1) is the coefficient of the H in the γ_S equation (Eq. A1). The reason that these values of the H appear here is because the H is the other mass ratio (with the O) not measured (i.e. f_H is absent in Eq. 4). So for γ_S in terms of the COD (Eq. A1), applying this rule, the numerator of the f_C term in Eq. A4 is 12 − (1)/(+1) x (+4) = +8 and the numerator of the f_N term in Eq. A4 is 14 − (1)/(+1) x (−3) = +17, where the +4 and −3 are the coefficients in the γ_S Eq. A1 of the C and N elements, respectively. Following this rule, the fractions of the f_P and f_S terms in Eq. A4 are [31 − (1)/(+1) x (+5)]/31 = +26/31 and [32 − (1)/(+1) x (+6)]/32 = +26/32. The EDC/g $\gamma_{S,COD}$ (= f_{cv} /8 for COD, Eq. 1) also is multiplied by (1)/(+1) = +1, as Eq. A4 shows. If boron, which has an atomic mass of 10, were added to the electron donor composition as B_d, then an additional term +3d is added to

Eq. A1 for the EDC (γ_S) in terms of COD (see Figure 2-1 in Part 2 – Brouckaert et al., 2021b,). This is obtained by balancing the e$^-$ donor reaction of boron in the COD test producing its most oxidized state, H_3BO_3, as the oxidation product, i.e. $-B_d - 3dH_2O + dH_3BO_3 + 3d(H^+ + e^-) = 0$. So the mass ratio term added to the right hand side of Eq. A4 (from which then Eq. 4 for f_O is obtained) is $[10 - (1)/(+1)$ x $(+3)/10] = +7/10f_B$, where f_B is the mass ratio of boron (gB/g) in the electron donor.

Rule for f_H equation

For the hydrogen mass ratio f_H (Eq. 5), the rule is the same as that for Eq. 4, except that now the atomic mass of O and the coefficient of O in the γ_s Eq. A1 are used in Eq. A5 because f_O is absent from it. The denominator of the fraction coefficients in front of the mass ratio terms again is the atomic mass of its corresponding element, i.e., 12 for f_C, 14 for f_N, and so on. The numerator is the atomic mass of the element minus $(16)/(-2)$ times the element's corresponding coefficient in the EDC/mol ($\gamma_{s,COD}$) equation (Eq. A1), taking due consideration of its sign, where the (16) in $(16)/(-2)$ is the atomic mass of O and the (-2) is the coefficient of O in the γ_S equation (Eq. A1). So for γ_S in terms of the COD (Eq. A1), the numerator of the f_C term in Eq. A5 is $12-(16/(-2)$ x $(+4) = +44$, for the f_N term is $14 -(16/(-2)$ x $(-3) = -10$ and for the f_H term is $1-(16)/(-2)$ x $(+1) = 9$. Following this rule, the fraction coefficients of the f_P and f_S terms in Eq. A5 are $[31 - (16)/(-2)$ x $(+5)]/31 = +71/31$ and $[32 - (16/(-2)$ x $(+6)]/32 = +80/32$. The EDC/g γ_S $(= f_{cv}/8$ for COD, Eq. 1), is also multiplied by $(16)/(-2) = -8$ as Eq. A5 shows. If boron were added to the e$^-$ donor, then the fraction coefficient of the f_B term in Eq. A5 would be $[10 - (16/(-2)$ x $(+3)]/10 = +34/10$.

Generalizing the mass ratio equation

Retaining the atomic masses as integer values in the derivation of Eqs 4 and 5 made this rule apparent and allows an overall generalization of Eqs A4 and A5 to be made, i.e.

$$1 = (f_{cv})\frac{M_j}{C_j} + \Sigma_{i=1}^{N}\left[\frac{M_i-C_i\left(\frac{M_j}{C_j}\right)}{M_i}\right]f_i \qquad \text{(A6)}$$

M_i	= atomic mass of element with known (measured) element mass ratio
C_i	= coefficient in γ_S equation of known (measured) element mass ratio
N	= number of elements that make up the component
f_i	= mass ratio of element i
i	= the specific element selected.

Equation A6 shows that when $i = j$, i.e., the selected element and the omitted (non-measured) element are the same, its fraction is zero and is the reason it effectively does not appear in the equation. Tailoring Eq. A6 to f_H, for which $M_j = 1$ and $C_j = +1$ and to f_O for which $M_j = 16$ and $C_j = -2$ yields:

$$1 = (f_{cv})\frac{1}{+1} + \Sigma_{i=1}^{N}\left[\frac{M_i-C_i\left(\frac{1}{+1}\right)}{M_i}\right]f_i \qquad \text{(A7)}$$

$$1 = (f_{cv})\frac{16}{-2} + \Sigma_{i=1}^{N}\left[\frac{M_i-C_i\left(\frac{16}{-2}\right)}{M_i}\right]f_i \qquad \text{(A8)}$$

where f_i (i = 1 to N) are the mass ratios of the N elements that make up the substrate e⁻ donor (or biomass), e.g., f_C, f_H, f_O, f_N, f_P and f_S. Substituting the M_i and C_i values for the individual elements C, N, P and S into Eqs A7 and A8 yields Eqs A4 and A5 from which Eqs 4 and 5 are obtained. Equation A6 is expanded in Table 3-A1 to show the coefficients in the mass ratio equations based on mass balance for any two unknown (non-measured) mass ratios of the possible seven (six elements CHONPS and COD).

Rule for the f_O and f_H equations independent of electron donor products

The rule (Eq. A6) for the f_O (Eq. A4) and f_H (Eq. A5) applies irrespective of the selection of the e⁻ donor oxidation products of the elements. This is because the coefficients in the γ_S equation and the fraction coefficients in the mass ratio equations are related, and compensate for one another. A change in γ_S resulting from choosing different e⁻ donor oxidation products is compensated for by an equal and opposite change in associated mass ratio fraction.

For example, if nitrate is selected as the oxidation product of the N element in the e⁻ donor reaction, then the EDC/mol ($\gamma_{S,TOD}$) is given by Eq. 2 in Brouckaert et al. (2021b) (Part 2), i.e.

$$\gamma_{S,TOD} \quad = 4x + y - 2z + 5a + 5b + 6c - ch \text{ e}^-/\text{mol on the TOD basis (i.e. EDC of N included)} \quad (A9)$$

This $\gamma_{S,TOD}$ is +5 − (−3) = 8a e⁻/mol higher than the $\gamma_{S\text{-COD}}$ of Eq. A1 with ammonia as the oxidation product for N. Dividing this difference $\Delta\gamma_S$ by the molecular mass of the e⁻ donor (M_{ed}) yields $\Delta\gamma'_S$ = 8a/M_{ed} e⁻/g. This is the EDC of ammonia, i.e., 8a e⁻/mol or equivalently 8gO_2/e⁻ x 8a = 64a gO_2/mol ammonia oxidized to nitrate. Noting that the f_{cv} term in Eq. A4 for f_O is multiplied (1)/(+1) (or M_j/C_j in Eq. A6), which is implicit in Eq. A4 as +1, and that 14a/M_{ed} = f_N yields $\Delta\gamma'_S$ = +8/14 f_N. Hence changing the f_{cv} term to f_{tv} in Eq. A4 for f_O increases it by +8/14 f_N. However, the change of the coefficient of the N element in the γ_S equation (from COD, f_{cv}/8 to TOD f_{tv}/8) also causes the coefficient of the f_N term in Eq. A4 to change by the same amount but with opposite sign, to keep the f_O mass ratio of the e⁻ donor unchanged. From Eq. A7, the fraction of the f_N term in the f_O Eq. A4 for the TOD becomes [14 − (1)/(+1) x (+5)]/14 = +9/14. The fraction of the f_N term in Eq. A4 for f_O has therefore changed by (+9/14) − (+17)/14)f_N = −8/14f_N, which is equal but has the opposite sign to the change in the f_{cv} term to f_{tv} in Eq. A4.

The same happens in the f_H Eq. A5, except the f_{cv} term in Eq. A5 for f_H changes by (16)/(−2)x 8a/M_{ed} e⁻/g, which yields $\Delta\gamma'_S$ = −64/14 f_N and the fraction of the f_N term in the f_H Eq. A5 becomes [14 − (16)/(−2) x (+5)]/14 = +54/14. This is a change of (+54/14) − (−10/14) f_N/14 = +64/14f_N. This is also an equal but opposite sign change in changing the f_{cv} term to f_{tv} in Eq. A5.

The same equal and opposite compensation between the coefficients of the γ_S and f_S terms in the f_O and f_H equations takes place if sulphide is selected as the oxidation product of the S element in the e⁻ donor reaction, which changes the coefficient in the e⁻ donor equation γ_S from +6 to −2. The coefficients in the f_H and f_O equations for the different e⁻ donor reaction products of the N (ammonia and nitrate) and S (sulphate and sulphide) elements are given in Table 3-A2.

Table 3-A1. *Coefficient fractions in mass ratio equations in the form of Eqs A6 to determine non-measured mass ratios (Column 1) from measured ones based on mass balance. The numbers in the ( ) are the coefficients in the EDC (γ_S) equation based on COD (ammonia and SO_4^{2-} e⁻ donor reaction products, Eq. A1). The procedure also works for other combinations of e⁻ donor reaction products, e.g. NO_3^- and SO_4^{2-} (TOD), ammonia and sulphide and ammonia and SO_4^{2-} provided the coefficients in the associated EDC (γ_S) equation are selected, e.g. Eq. A9 for TOD. Examples of how the matrix works are given below. (M_i, M_j = element atomic mass; C_i = coefficient in γ_S equation).*

Not measured M_j ; C_j	Carbon: f_C $M_i = 12$	Hydrogen: f_H $M_i = 1$	Oxygen: f_O $M_i = 16$	Nitrogen: f_N $M_i = 14$	Phosphorus: f_P $M_i = 31$	Sulphur: f_S $M_i = 32$	COD: f_{cv}
Carbon: f_C $M_j = 12$, $C_j = 4$	$\frac{12-(4)12/(4)}{12}=0$	$\frac{1-(1)12/(4)}{1}=\frac{-2}{1}$	$\frac{16-(-2)12/(4)}{16}=\frac{22}{16}$	$\frac{14-(-3)^a12/(4)}{16}=\frac{23}{14}$	$\frac{31-(5)12/(4)}{31}=\frac{16}{31}$	$\frac{32-(6)^b12/(4)}{32}=\frac{14}{32}$	$\frac{12}{(4)}$
Hydrogen[1]: f_H $M_j = 1$, $C_j = 1$	$\frac{12-(4)1/(1)}{12}=\frac{8}{12}$	$\frac{1-(1)1/(1)}{1}=0$	$\frac{16-(-2)1/(1)}{16}=\frac{18}{16}$	$\frac{14-(-3)^a1/(1)}{14}=\frac{17}{14}$	$\frac{31-(5)1/(1)}{31}=\frac{26}{31}$	$\frac{32-(6)^b1/(1)}{32}=\frac{26}{32}$	$\frac{1}{(1)}$
Oxygen: f_O $M_j = 16$, $C_j = -2$	$\frac{12-(4)16/(-2)}{12}=\frac{44}{12}$	$\frac{1-(1)16/(-2)}{1}=\frac{9}{1}$	$\frac{16-(-2)16/(-2)}{16}=0$	$\frac{14-(-3)^a16/(-2)}{14}=\frac{-10}{14}$	$\frac{31-(5)16/(-2)}{31}=\frac{71}{32}$	$\frac{32-(6)^b16/(-2)}{32}=\frac{80}{32}$	$\frac{16}{(-2)}$
Nitrogen[2]: f_N $M_j = 14$, $C_j = -3^a$	$\frac{12-(4)14/(-3)^a}{12}=\frac{92}{12\times3}$	$\frac{1-(1)14/(-3)^a}{1}=\frac{17}{3}$	$\frac{16-(-2)14/(-3)^a}{16}=\frac{20}{16\times3}$	$\frac{14-(-3)^a14/(-3)^a}{14}=0$	$\frac{31-(5)14/(-3)^a}{31}=\frac{163}{31\times3}$	$\frac{32-(6)^b14/(-3)^a}{32}=\frac{60}{32}$	$\frac{14}{(-3)^a}$
Phosphorus: f_P $M_j = 31$, $C_j = 5$	$\frac{12-(4)31/(5)}{12}=\frac{-64}{12\times5}$	$\frac{1-(1)31/(5)}{31}=\frac{-26}{5}$	$\frac{16-(-2)31/(5)}{16}=\frac{142}{16\times5}$	$\frac{14-(-3)^a31/(5)}{14}=\frac{163}{14\times5}$	$\frac{31-(5)31/(5)}{31}=0$	$\frac{32-(6)^b31/(5)}{32}=\frac{-26}{32\times5}$	$\frac{31}{(5)}$
Sulphur: f_S $M_j = 32$, $C_j = 6^b$	$\frac{12-(4)32/(6)^b}{12}=\frac{-28}{12\times3}$	$\frac{1-(1)32/(6)^b}{1}=\frac{-26}{6}$	$\frac{16-(-2)32/(6)^b}{16}=\frac{80}{16\times3}$	$\frac{14-(-3)^a32/(6)^b}{14}=\frac{180}{14\times6}$	$\frac{31-(5)32/(6)^b}{31}=\frac{26}{31\times6}$	$\frac{32-(6)^b32/(6)^b}{32}=0$	$\frac{32}{(6)^b}$
COD: f_{cv}	1	1	1	1	1	1	0

[1]For the case where the hydrogen mass ratio (f_H) is one of the two non-measured mass ratios, the Eq. 4A in which it does not appear is obtained by equating to 1 the sum along the hydrogen row of each of the fraction values in the columns with their corresponding mass ratio (column heading), i.e., $8/12f_C + 0f_H + 18/16f_O + 17/14f_N + 26/31f_P + 26/32f_S + 1/1(f_{cv}) = 1$. Then based on mass balance ($f_C + f_H + f_O + f_N + f_P + f_S = 1$), if the oxygen mass ratio (f_O) is the other non-measured mass ratio, Eq. 4 in the paper is obtained by making f_O the subject of the equation.

[2]Similarly, for the case where the nitrogen mass ratio (f_N) is one of the two non-measured mass ratios, the equation in which it does not appear is obtained by equating to 1 the sum along the nitrogen row of each of the fraction values in the columns with their corresponding mass ratio (column heading), i.e., $92/(12 \times 3)f_C + 17/3f_H + 20/(16 \times 3)f_O + 0f_N + 163/(31 \times 3)f_P + 60/32f_S + 14/(-3)(f_{cv}) = 1$. Then based on mass balance ($f_C + f_H + f_O + f_N + f_P + f_S = 1$), if the oxygen mass ratio (f_O) is the other non-measured mass ratio, it is obtained by making f_O the subject of the equation.

[a]Change from −3 (Eq. A1) to +5 (Eq. A9) when the e⁻ donor product of N element changes from ammonia to NO_3^-

[b]Change from +6 (Eq. A1) to −2 when the e⁻ donor product of S element changes from SO_4^{2-} to sulphide

Table 3-A2. *Coefficients in the EDC (γ_S), f_O and f_H mass ratio equations for different e^- donor oxidation reaction products*

Element	C	H	O	N	P	S	B			C	N	P	S	B
	Coefficients of the EDC equation							**Coefficients of the f_o and f_h mass ratio equations**						
Oxidation products	x	y	z	A	b	C	D	Eq.	e^-	f_C	f_N	f_P	f_S	f_B
Nitrate, sulphate (TOD, Eq. A9)	4	1	−2	5	5	6	3	f_O	$-(f_{cv})$	−8/12	−9/14	−26/31	−26/32	−7/10
								f_H	$8(f_{cv})$	−44/12	−54/14	−71/31	−80/32	−34/10
Nitrate, sulphide	4	1	−2	5	5	-2	3	f_O	$-(f_{cv})$	−8/12	−9/14	−26/31	−34/32	−7/10
								f_H	$8(f_{cv})$	−44/12	−54/14	−71/31	−16/32	−34/10
Ammonia, sulphate (COD, Eq. A1)	4	1	−2	−3	5	6	3	f_O	$-(f_{cv})$	−8/12	−17/14	−26/31	−26/32	−7/10
								f_H	$8(f_{cv})$	−44/12	10/14	−71/31	−80/32	−34/10
Ammonia, sulphide	4	1	−2	−3	5	-2	3	f_O	$-(f_{cv})$	−8/12	−17/14	−26/31	−34/32	−7/10
								f_H	$8(f_{cv})$	−44/12	10/14	−71/31	−16/32	−34/10

Appendix B: Integration of complete elemental mass-balanced stoichiometry and aqueous-phase chemistry for bioprocess modelling of liquid and solid waste treatment systems – Part 4: Aligning the modelled and measured aqueous phases

GA Ekama[1], CJ Brouckaert[2] and BM Brouckaert[2]

[1]Water Research Group, Department of Civil Engineering, University of Cape Town, Rondebosch 7700, Cape Town, South Africa

[2]Water, Sanitation and Health Research and Development Centre, School of Chemical Engineering, University of KwaZulu-Natal, Durban, South Africa

ABSTRACT

Completely mass-balanced biological, physical and chemical process stoichiometry ensures that the CHONPS material and charge content entering and exiting bioprocess system models is conserved, which is a requirement for pH prediction in integrated physical, chemical and biological process models. Bioprocesses transform the material content from reactants to products, exchanging material between the aqueous, gaseous and solid phases, which cause pH changes in the aqueous phase. By measuring the material content of the aqueous phase, the progress of bioprocesses can be monitored. Alkalinity is an important aqueous-phase property that can be used to track aqueous-phase changes caused by physical, chemical and biological processes. Alkalinity is a stoichiometry property of the components in solution (i.e., a linear function of the amounts present). Its uptake from, and release to, the aqueous phase can both be modelled with bioprocess stoichiometry, and measured in physical bioprocess systems, and so aid in linking the modelled and measured aqueous-phase compositions. Changes in the concentrations of components containing the elements C,H,O,N,P and S result in changes in six weak acid/bases systems in the aqueous phase, all of which affect the total alkalinity. These are: inorganic carbon (IC), ortho-phosphate (OP), free and saline ammonia (FSA), volatile fatty acids (VFA), free and saline sulphide (FSS) and the water itself. Characterization of the aqueous phase to quantify the material content of the aqueous phase containing these six weak acid/base systems using the 5-point titration method is described. While several alkalinity titration based methods are available for anaerobic digestion bioprocess monitoring, only the 5-point titration is sufficiently accurate for aqueous-phase characterization to quantify the aqueous-material content for pH prediction in bioprocess models.

INTRODUCTION

In Part 3 (Ekama and Brouckaert, 2022) of this series, the alignment of the modelling and measurement frameworks for biochemical processes was discussed in terms of element balances and model components. Components are model constructs that represent material content in the system, but not necessarily the physical forms which the material takes in the system, which is, in turn, represented by species. As pointed out in Part 1 (Brouckaert et al., 2021a), the rate at which biochemical transformations occur typically depends on the species present, both in terms of the availability of reactant species and the presence of inhibitory species. For example, acetogenic methanogenesis (Bioprocess 1 in Table 2-1 of Part 2 – Brouckaert et al., 2021b) in anaerobic digestion is highly sensitive to pH, which is in turn dependent on all the dissolved aqueous species present in the aqueous phase. Note that in this series of papers, species are italicised (e.g. CO_3^{2-}), while their corresponding components are not (e.g. CO_3^{2-}).

This paper, Part 4, discusses the measurements needed to characterize the aqueous phase for modelling purposes, and how to interpret these measurements in terms of components and species. Central to the discussion is the measurement of alkalinity, which was introduced from a modelling perspective in Part 1 (Brouckaert et al., 2021a).

As discussed in Part 1, speciation modelling, which determines dissolved species concentrations from component concentrations, is very well established. Speciation algorithms are discussed in Part 5 (Brouckaert et al., 2022).

In broad conceptual terms, the problem to be addressed is that the composition of a solution is best expressed in terms of components for modelling purposes, but not all available measurements are directly related to components. Specifically, pH and electrical conductivity (which can be used to infer ionic strength) are related to the composition in terms of species. The speciated composition is completely determined by the component composition; however, to translate component concentrations into species concentrations requires a speciation model. The same speciation model can therefore be used to map a combination of component-related and species-related measurements into a complete specification of the composition, which includes all the component concentrations and all the species concentrations.

The weak acid/base system components are CO_3^{2-}, NH_4^+, $PO4^{3-}$, HS^- and Ac^- (CH_3COO^-). (The interactions of other VFAs are so similar to acetate that they cannot be distinguished by titration.) The corresponding measurements are IC, FSA, OrthoP, FSS and VFA. Total hydrogen ions cannot be measured directly. OrthoP and FSA are standard measurements at treatment plants. FSS measurements are less common, but can be obtained using standard titrimetric methods. Direct measurement of VFA requires gas chromatography (GC), while direct IC measurement also requires an expensive inorganic carbon analyser, with which it is difficult to prevent errors due to CO_2 loss. In practice, alkalinity measurements, along with pH, can be used in combination with other analytic measurements to characterise the weak acid/base content of the aqueous phase fully.

138

Alkalinity

Alkalinity has the following useful characteristics:

- It is easy to measure.
- It is a summary property that is a linear function of all the weak acid/base components present. It can also be simply expressed as a linear function of the weak acid/base component concentrations (Eqs 19a and 19b in Part 1 – Brouckaert et al., 2021a).
- As discussed in Parts 1 and 2, the changes in aqueous-phase alkalinity as a specific reaction proceeds can be calculated directly from the reaction stoichiometry. Alkalinity measurements can therefore be used to link the modelling and measurement frameworks at specific points in time, as well as to track changes in the aqueous phase over time.
- Since alkalinity is also related to pH buffer capacity, it has direct application as a control parameter for pH-sensitive processes such as anaerobic digestion.

Bioprocesses change the protonated states of aqueous species

The energy change resulting from e^- transfer between the e^- donor and e^- acceptor drives the bioprocess. The changes in e^- donating capacity (EDC) of bioprocess reactants and products also result in changes in the number of protons associated with some of the components, which affects the speciation of the aqueous phase and hence the pH. For example, in autotrophic denitrification (Bioprocess 5a in Table 2-1 of Part 2 – Brouckaert et al., 2021b), sulphide is the e^- donor, and is transformed to sulphate; and nitrate is the e^- acceptor, and is transformed to nitrogen gas. Sulphate and nitrate are strong acids, and so are almost completely dissociated in the aqueous phase – almost all are in the un-protonated NO_3^- or SO_4^{2-} form. The free (H_2S) and saline (HS^-, S^{2-}) sulphide (FSS) and free (NH_3) and saline (NH_4^+) ammonia (FSA) are weak acid/bases and so are partially dissociated. Hence, fully protonated (NH_4^+, H_2S) and partially protonated (HS^-, S^{2-}, NH_3) forms co-exist in the aqueous phase. Because each of these species has a different protonated state, bioprocesses such as sulphate reduction (sulphate to sulphide), nitrification (ammonia to nitrate) and autotrophic denitrification (sulphide to sulphate and nitrate to nitrogen gas), cause a change in the aqueous H^+ concentration and hence pH. In integrated biological, chemical and physical process modelling, these changes in H^+ concentration are tracked, so that pH can be calculated.

Aqueous-phase concentrations have a non-linear effect on speciation and pH

To predict pH within bioprocess models, completely element-balanced stoichiometry is necessary. This requires modelling both the bioprocesses and the speciation of the aqueous phase in which they take place. Bioprocess kinetics are generally dependent on the concentration of the biomass that mediates the bioprocess – doubling the biomass concentrations approximately doubles the reaction rates. A reaction rate is largely dependent on the concentrations of just those species that take part in the specific reaction, whereas equilibrium reactions are affected, to a greater or lesser extent, by all species present in the solution. Thus, how a reaction affects something like pH depends on the whole solution composition, not just the species taking part in that reaction. Therefore, not only do the bioprocesses

themselves affect the pH, but the bulk liquid concentrations at which they take place also affect the aqueous-phase speciation, and hence pH.

Aqueous-phase equilibrium reactions are modelled with algebraic equations
The relative concentrations of the different protonated states of the species of a weak acid/base are determined by the dissociation equilibrium constant(s) (K_d) of the weak acid/base. Because the dissociation and association rates are extremely fast, they reach equilibrium virtually instantaneously relative to the bioprocess rates. Equilibrium states are determined by reaction equilibrium constants (K_d), rather than reaction rates. Two advantages arise: (i) equilibrium reactions seldom require calibration, because equilibrium constant values are well known (unlike the bioprocesses, which are usually held in a non-equilibrium state by kinetic factors which require calibration for different reactor conditions), and (ii) they can be represented by a set of algebraic equations. This avoids combining very fast aqueous speciation reactions with the much slower bioprocess and physico-chemical process reactions (gas stripping and mineral precipitation), which leads to greater numerical stability and shorter simulation times for the integrated biological, chemical and physical process models (Batstone et al., 2002; Brouckaert et al., 2010, Ikumi et al., 2011; Lizarralde et al., 2015; Part 5 – Brouckaert et al., 2022).

Measuring and modelling the aqueous-phases concentrations
Bioprocesses change the organic and inorganic component concentrations representing the material content entering a bioprocess system from one form (reactants) to another (products) without changing the material content leaving the system in the solid, aqueous or gaseous phases. This means that, if the correct measurements can be made to quantify the material entering and leaving the system, the progress and performance of the bioprocess(es) can be monitored. In Part 3 (Ekama and Brouckaert, 2022) this flux/mass balance principle was applied to characterise the influent electron (e^-) donor organics and biomass. In this paper, the characterisation of the aqueous phase through measuring the material content entering and exiting bioprocesses, and inferring solution composition in terms of model components, is considered.

LINKING THE MODELLING AND MEASUREMENT FRAMEWORKS
To predict pH correctly, the entire ionic composition in which the bioprocesses take place needs to be established. This is because the ionic strength, often estimated from electrical conductivity (EC) or total dissolved solids (TDS), affects the speciation of the aqueous phase. To measure and model all the ions in the aqueous phase of biological treatment systems is neither practically feasible nor computationally efficient. Therefore, the ions that have the greatest impact on the speciation of the aqueous phase and pH are selected for modelling (Part 1 – Brouckaert et al., 2021a,) and require measurement. These are the ions of (i) the weak acid/bases that change as a result of the reactions of the bioprocesses, (ii) the minerals that can precipitate or dissolve, and (iii) the ion-pairs that can form to significant extents. The ionic strength resulting from the selected (or modelled), and therefore measured, ions is usually lower than the ionic strength calculated from measured concentrations. To make up the ionic strength deficit, Na^+ and Cl^- can be added to the modelled aqueous-phase composition to represent the unmeasured ions in the solution. Na^+ and Cl^- are usually present and have particularly weak interactions with other

ions, so normally do not need to be accurately reflected in the model. Details of the component selection is outlined in Part 5 (Brouckaert et al., 2022). The measurement of the weak acid/bases, in particular the inorganic carbon (IC) system via the H_2CO_3 alkalinity, aligned with determining the material content of the aqueous phase and the calculation procedure for converting the measured aqueous concentrations to model components, are considered below.

CHARACTERIZING THE AQUEOUS PHASE: MEASUREMENT OF ALKALINITY IN MIXED WEAK ACID/BASE ENVIRONMENTS

As mentioned in Part 1 (Brouckaert et al., 2021a), alkalinity is the remaining capacity of weak acid anions in a solution to bind protons, and is measured by titration with a strong acid. Where there are number of weak acids, it is possible to divide the overall solution alkalinity into contributions from each weak acid/base system, which we term the **speciated alkalinities**. Thus, we will refer to carbonate alkalinity (H_2CO_3 *alk*), phosphate alkalinity ($H_2PO_4^-$ *alk*), sulphide alkalinity (H_2S *alk*), etc. Note that $H_2CO_3, H_2PO_4^-, H_2S$ are the reference species of their respective systems, as discussed in Part 1 (Brouckaert et al., 2021a). Although the speciated alkalinities sum to the total alkalinity, which is a linear function of component concentrations, they are complex non-linear functions of the solution pH, and cannot be easily related to measurements without a speciation model of the solution. This means that they have limited practical application in solution models, although they can be useful concepts for explaining solution phenomena (as in the following sections).

Characterizing mixed weak acid/base samples

In aqueous samples with a mixture of *n* (say 6) weak acid/bases (including water), *n* (6) measurements are required to characterize it, one for each weak acid/base system, including the water itself. **Characterization** here means to quantify all individual component concentrations of all the weak acid/base systems. So in a water sample with a mixture of six weak acid/bases, viz. (i) IC, (ii) FSA, (iii) OP, (iv) FSS, (v) VFA (represented as acetic acid HAc) and (vi) the water itself, at least six measurements are required to characterize it. These six measurements could be (i) the pH and the total concentrations of the (ii) FSA (N_T), (iii) OP (P_T), (iv) FSS (S_T), (v) VFA (A_T) and (vi) IC (C_T). As discussed in the introduction, direct measurements of inorganic carbon (IC) and VFA are not available in many wastewater laboratories, and direct measurement of H$^+$ is not possible at all. However, it is possible to change the H$^+$ concentration by a known amount by adding a strong acid or strong base. Titration can therefore be used, together with some form of speciation model, to infer the unmeasured concentrations. This is an unusually complex version of the 'standard addition method', used in analytic chemistry to compensate for matrix effects that influence the measurement of concentration. The response of the measurement to the addition of known amounts of the substance in question provides information for establishing its concentration in the original sample. The usual case is that there is a single substance of interest, the measurement response is assumed linear, and no specific information about the matrix is sought. In the titration methods described here, the response is decidedly non-linear, and some form of speciation model is required to interpret it. The availability of detailed and accurate models of solution behaviour also make it possible to infer the concentrations of substances other than H$^+$, in particular, carbonate and acetate.

There are three ways that titration with acid has been used to estimate the carbonate alkalinity, and hence the carbonate concentration (C_T):

- Determining the total alkalinity from a single titration to a pH endpoint, which can be either a fixed value of 3.7, or to the point of minimum buffer capacity, which will deviate slightly from 3.7 depending on the solution composition. H_2CO_3 alk is then determined by subtracting the alkalinity contributions of other weak acid components, which have to be analysed separately (including VFA).
- A two-point titration with pH end-points 5.75 and 4.3, to measure the partial alkalinity (PA) and total alkalinity (TA). This provides approximate values of the C_T and VFA concentrations; other weak acid concentrations have to be analysed separately.
- The 5-point titration that provides more accurate values for the C_T and VFA concentrations; the other weak acid components still have to be analysed independently.

The following sections describe and compare these three procedures, using the solution specified in Table 4-1 as an example.

Table 4-1. *Characteristics of the example AD liquor before and after gas loss (electrical conductivity EC = 1 778 mS/m or ionic strength IS = 0.128 mol/L). The relationship between EC and IS from Bhuiyan et al. (2009)*

Reference species	All alks in mg/L as CaCO₃	C_T	P_T		S_T	A_T	N_T	Total Alk **
		H_2CO_3 alk	H_3PO_4 alk	$H_2PO_4^-$ alk	H_2S alk	HAc alk	NH_4^+ alk	
Before gas loss (low pH = 7.00)	mg/L*	1 048	500	500	300	240	1 000	-
	mg/L as CaCO₃	3 812	1 375	567	267	199	17	4 862
After gas loss (high pH = 8.02)	mg/L*	870	500	500	50	240	1 000	-
	mg/L as CaCO₃	3 642	1 564	776	73	171	73	4 862
Difference (mg/L*)		−178	0	0	−250	0	0	-
Difference (mg/L as CaCO₃)		−17	169	169	−208	0	55	0

*mg element/L except for A_T which is mgHAc/L

**$H_2CO_3/NH_4^+/H_2PO_4^-/H_2S/HAc$ alkalinity (Alk_t)

Speciated alkalinity and buffer capacity vs. pH curves for the solution in Table 4-1 appear in Figures 4-1, 4-2a and 4-2b. The loss of volatile components during the preparation of the sample for titration is an inevitable complication. Its effect on the alkalinities is shown in Figure 4-1.
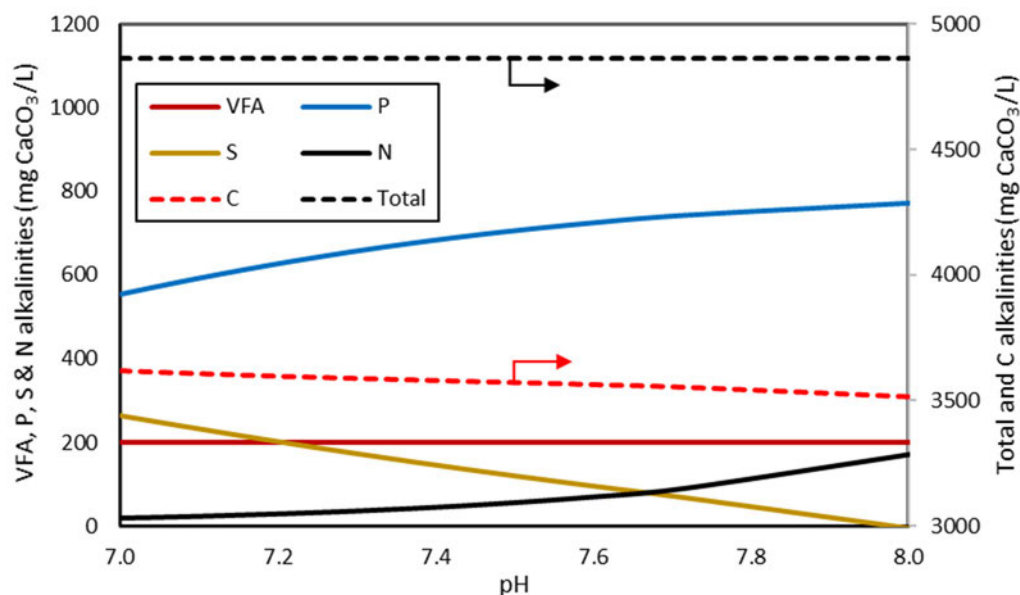

Figure 4-1. *Speciated alkalinities during loss of CO_2 and H_2S before titration for the example AD liquor (Table 4-1), showing how changes due to individual ions compensate for one another to result in an unchanged total alkalinity*.

Figures 4-2a and 4-2b represent the subsequent titration. The right-hand axis of Figure 4-2a gives the H^+ added, showing how alkalinity is directly related to H^+. The units customarily applied to alkalinity (mg/L as $CaCO_3$) can be misleading, since alkalinity is not necessarily related to $CaCO_3$, or even to CO_3^{2-}; however, it is always related negatively to H^+. The pH end-points for the various titration methods are shown for reference.
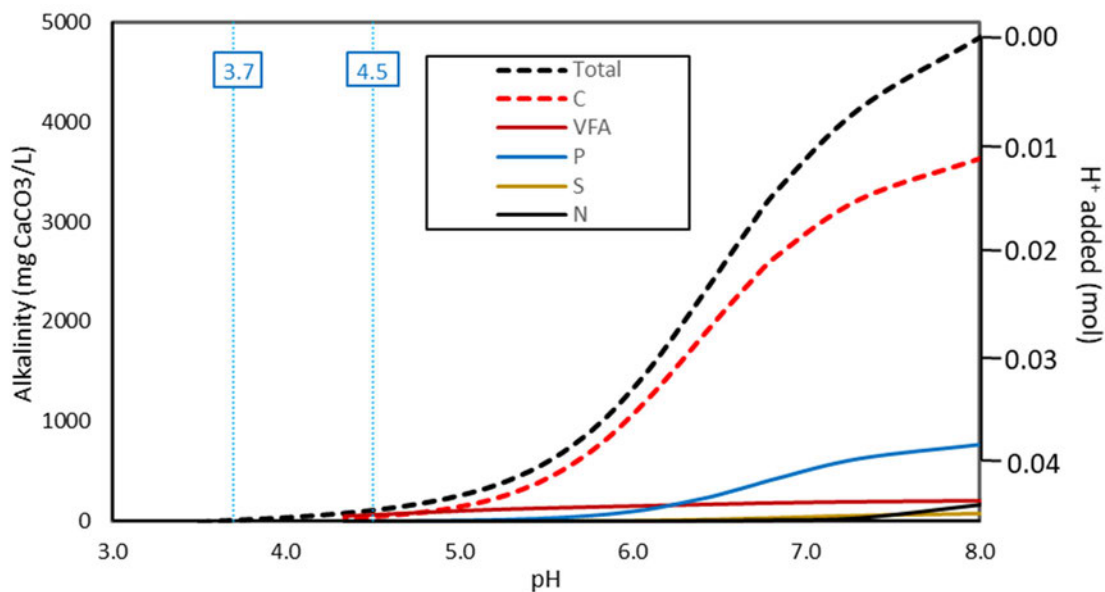
Figure 4-2a. *Speciated alkalinities during titration of the example AD liquor (Table 4-1 – after loss of CO_2 and H_2S). The right-hand axis shows the H^+ added during the titration.*
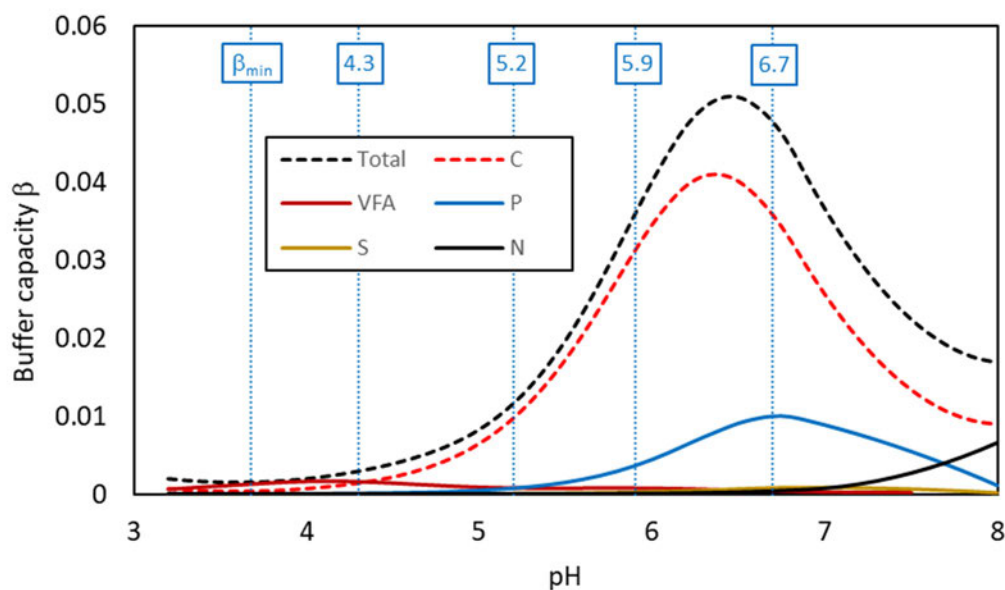
Figure 4-2b. *Buffer capacity diagram corresponding to Figure 4-2a (Table 4-1 – after loss of CO_2 and H_2S). Buffer capacity is the derivate of the pH-alkalinity curve, in H^+ molal units rather than alkalinity units. Titration pH values are shown in the blue text boxes.*

Titrating to the minimum buffer capacity pH point

When the IC system is the only weak acid/base present in a water sample or the contribution of other weak acid/base systems is very small, as is the case in most natural waters (Stumm and Morgan, 1996), total alkalinity $Alk_T \approx Alk_t \approx H_2CO_3\,alk$ and can be determined by titrating to the H_2CO_3 equivalent solution

at pH of around 4.5. However, in mixed weak acid/base systems such as anaerobic digestate, the other weak acids/bases not only bind protons, contributing to the alkalinity, but also affect the end-point of the titration. This is illustrated in Figures 4-2a and 4-2b, which show that zero alkalinity and minimum buffer capacity (β_{min}) occur at pH ~ 3.7.
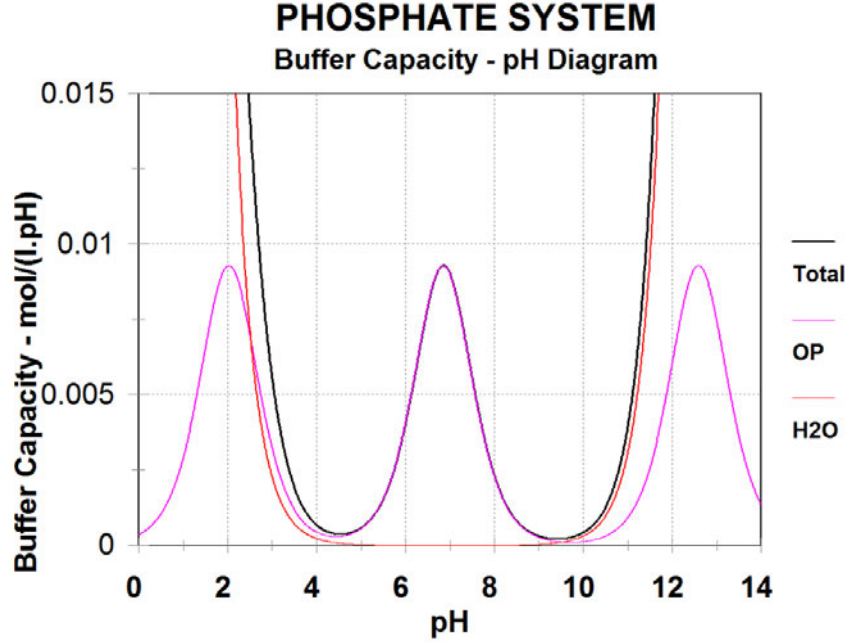

Figure 4-3. *Buffer capacity (β) curve of the triprotic ortho-phosphate (OP) weak acid/base system. Note the peak buffer capacity at the 1st (pH = pKp1~2) and 3rd (pH = pKp3~12) are masked by the buffer capacity of the H$^+$ and OH$^-$, respectively.*

Figure 4-3 shows that titration to the minimum β at around pH 3.7 excludes the first pK_{p1} of the phosphate system. This is because, although $H_2PO_4^-$ and HPO_4^{2-} are weak acids, H_3PO_4 is a strong acid. Its buffer capacity is masked by the buffer capacity of H_2O for pH below 3. Therefore, while all the weak acid/bases have been titrated to their most protonated state at the pH of the minimum β, the OP system has not. At the pH for minimum β, the OP system is mostly in its $H_2PO_4^-$ form; therefore, $H_2PO_4^-$ is the appropriate reference species. Thus, the alkalinity obtained by titrating to the minimum β at pH~3.7 is approximately the Alk_t defined by Eq. 19b in Part 1 (Brouckaert et al., 2021a), i.e., the $H_2CO_3/NH_4^+/H_2PO_4^-/H_2S/HAc$ alkalinity.

With the $H_2CO_3/NH_4^+/H_2PO_4^-/H_2S/HAc$ alkalinity (Alk_t) determined by titrating to the minimum β, the H_2CO_3 alkalinity for the sample can be calculated by subtracting the subsystem alkalinities from Alk_t, i.e.:

$$H_2CO_3 \ alk = Alk_t - NH_4^+ \ alk - H_2PO_4^- \ alk - H_2S \ alk - HAc \ alk \tag{1}$$

where the subsystem alkalinities can be calculated from the sample 'in-situ' pH (7.00 in Table 4-1) and the measured total species concentrations of the FSA, OP, FSS and VFA weak acid/base systems (Loewenthal et al., 1989, 1991).

The pH at the minimum β in the alkalinity titration changes with H_2CO_3 alk (or C_T), decreasing as C_T increases but, from a theoretical sensitivity analysis, the error in the H_2CO_3 alk due to this change is quite small (Moosbrugger et al., 1993). Figure 4-4a shows the pH of the minimum β versus theoretical H_2CO_3 alk corresponding to solution compositions with the same P_T, S_T, A_T and N_T as the example AD liquor in Table 4-1 before gas loss but with varying C_T. Figure 4-4b shows the % error with respect to the theoretical H_2CO_3 alk of the measured H_2CO_3 alk, as determined by titration to the minimum β, or titration to fixed pH of 3.7. From Figure 4-4b, if the H_2CO_3 alk is more than 50% of the Alk_t the error in H_2CO_3 alk is less than 0.5% ((from Table 4-1, Alk_t = 4 862 mg/L as $CaCO_3$ and does not change if C_T is added or removed as H_2CO_3).
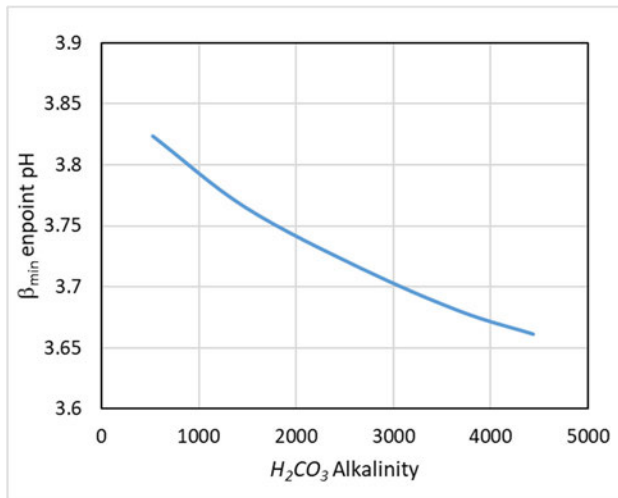
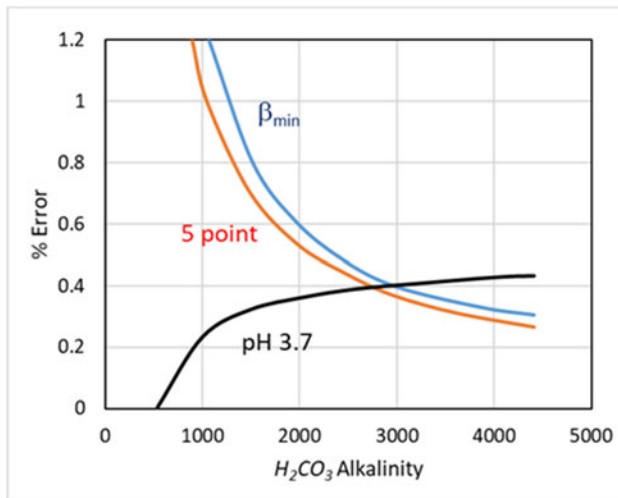**Figure 4-4a.** *Titration end-point pH at minimum buffer capacity (β_{min})*

Figure 4-4b. *% error of the H_2CO_3 alk from its theoretical value, as measured by titration to β_{min} ; titration to fixed pH of 3.7, or 5-point titration.*

Partial (PA) and total (TA) alkalinity titration

A titration method developed by Ripley et al. (1986) for control of ADs yields the partial (PA), intermediate (IA) and total (TA) alkalinities. A detailed review of alkalinity measurement in AD liquor is given by Moosbrugger et al. (1993a, b). The PA is obtained by titrating a sample from the in-situ pH to 5.75 and the TA was obtained by titrating further to 4.30. The PA and IA are proxies for the H_2CO_3 alkalinity and VFA concentrations, respectively, where IA = TA − PA. Ripley et al. (1986) used the IA/PA ratio, which has become known as the Ripley ratio, as an indication of approaching AD failure – a ratio > 0.30 means that the VFA concentration is too high relative to the H_2CO_3 alk concentration. The advantage of the PA and IA is that, aside from in-situ AD pH, no other measurements are required to assess that AD operating condition. However, the PA and IA are only approximate proxies for the actual H_2CO_3 alk and VFA concentrations. Figure 4-5 shows the PA versus the actual H_2CO_3 alk concentration from 50 to 4 400 mg/L as $CaCO_3$ (C_T from 140 to 1 250 mgC/L) with P_T, S_T, A_T and N_T as given in Table 4-1 (before gas loss), while Figure 4-6 shows the IA versus the actual VFA concentration (Figure 4-6) for fixed C_T = 1 048 mgC/L and varying VFA from 50 to 1 500 mgHAc/L. Therefore, while the PA and IA are useful control parameters for AD, they cannot be used for characterizing the aqueous phase of mixed weak acid/base systems for modelling purposes. Modelling the AD system with pH prediction requires accurate characterization of the AD influent and liquor (effluent) aqueous phases.
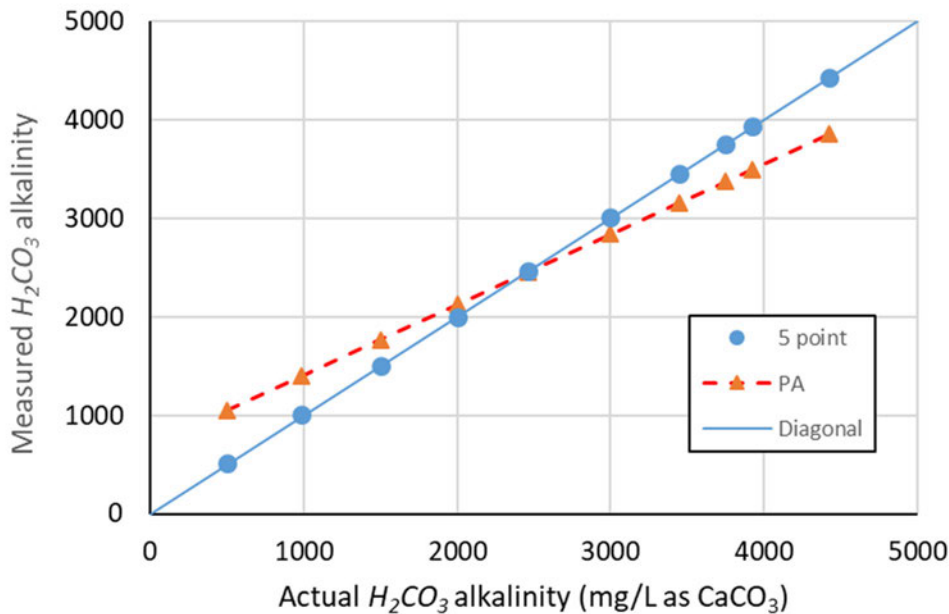

Figure 4-5. *Partial alkalinity (PA) and H_2CO_3 alkalinity as determined by the 5-point titration versus actual H_2CO_3 alkalinity for an AD liquor containing a mixture of ortho-P (OP, P_T) = 500 mgP/L, ammonia (FSA, N_T) = 1 000 mgN/L, sulphide (H_2S, S_T) = 300 mgS/L and volatile fatty acids (VFA, represented by acetate, HAc, A_T) = 240 mgHAc/L and varying inorganic carbon (IC, C_T) from 138 to 1 242 mgC/L (which yield H_2CO_3 alk from 490 to 4 417 mg/L as $CaCO_3$).*
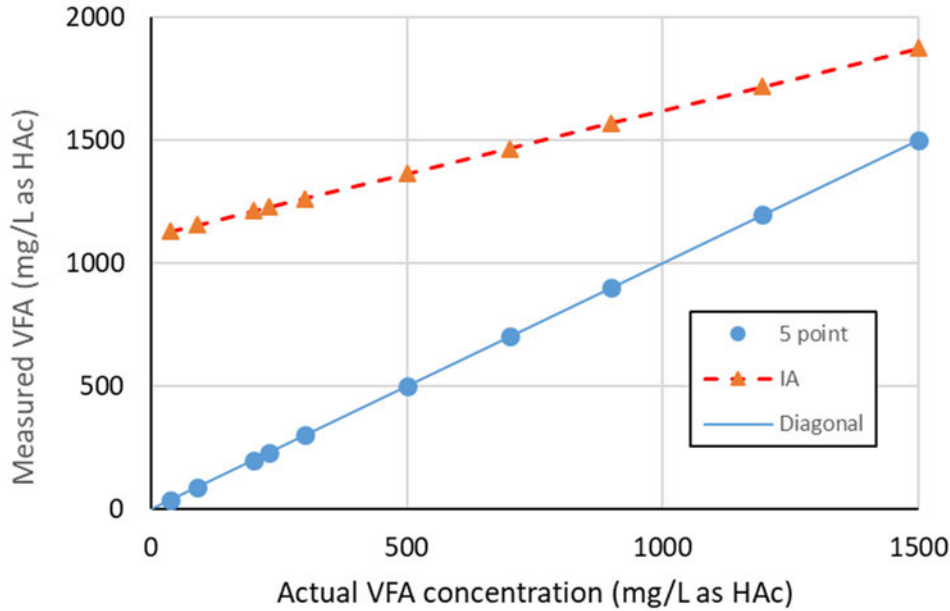
Figure 4-6. *Intermediate alkalinity (IA) and VFA concentration as determined by the 5-point titration versus actual VFA concentration for an AD liquor containing a mixture of ortho-P (OP, P_T) = 500 mgP/L, ammonia (FSA, N_T) = 1 000 mgN/L, sulphide (FSS, S_T) = 300 mgS/L, inorganic carbon (IC, C_T) = 1 048 mgC/L and varying volatile fatty acids concentration (VFA, represented by acetate, HAc) from 50 to 1 500 mgHAc/L*

THE 5-POINT TITRATION METHOD

The five-pH-point titration method of Moosbrugger et al. (1992, 1993a,b) (Lahav and Loewenthal, 2002; Lahav et al., 2002; Lahav and Morgan, 2004; Vannecke et al., 2015) is a better method, not only for control of ADs, but also for characterizing water samples with mixtures of weak acid/bases for aqueous-phase modelling and pH prediction purposes. This method can be applied to water samples containing the five (six counting water) weak acid/bases mentioned above (IC, FSA, OP, FSS, HAc, or $[CO_3^{2-}]$, $[NH_4^+]$, $PO_3^{3-}]$, $[HS^-]$, $[Ac^-]$) and requires total species concentrations for the FSA, OP and FSS ($[NH_4^+]$, $PO_3^{3-}]$, $[HS^-]$) to be known. It gives as output the H_2CO_3 alk (in mg/L as $CaCO_3$) and the VFA concentration as *HAc* (in mgHAc/L). The five pH points of the titration are the sample 'in-situ' pH, two pH points centred around the pK_{c1} ($\approx$6.3) of the IC system, i.e., pH $\approx$ 6.3 + 0.4 = 6.7 and 6.3 − 0.4 $\approx$ 5.9 and two pH points centred around the pK_a ($\approx$4.8) of the HAc system, i.e., pH $\approx$ 4.8 + 0.5 = 5.2 and 4.8 − 0.5 $\approx$ 4.3 (see Figure 4-2b). These four pH points do not have to be titrated to exactly – however, the cumulative volume added and the actual pH points reached for the volume added **near** to the four pH points have to recorded as accurately and precisely as possible and entered into the 5-point titration companion

computer programs (available from https://washcentre.ukzn.ac.za/bio-process-models/). Also entered are the measured N_T, P_T and S_T concentrations and temperature and electrical conductivity (EC, mS/m, in lieu of ionic strength, IS) for pK value correction. For the inputted data, the program searches for the best C_T and A_T concentrations to account for the measured buffer capacity represented by the volume of acid added from the 'in-situ' pH to the four pH points (Moosbrugger et al., 1993a,b).

5-point titration programmes
The 5-point titration method requires the measured data to be fitted to a speciation model, which includes all the relevant weak acid/base systems, in order to be able to extract the VFA and carbonate concentrations. Moosbrugger et al. (1992) developed the original algorithm. Equations for the differences in speciated composition at the titration points (see Figure 4-2b) are solved simultaneously for the un-measured component concentrations, i.e. $[CO_3^{2-}]$, $[Ac^-]$, $[H^+]$. The equations are formulated in terms of speciated alkalinities, and use a simplified speciation model, which accounts for non-ideal activity coefficients, but not ion pairs. This allows an analytic solution to the equations. Because the original programme was written in Turbo-Pascal, which is no longer supported by modern computers, a number of other versions have been published that implement the same algorithm in different programming languages (see Appendix).

The above description does not exactly reflect the original approach of Moosbrugger et al. (1993a), but is a re-interpretation in terms of the concepts advanced in this series of papers: specifically, the distinction between components and species. The key concept linking components and species is provided by 'Duhem's theorem', discussed in Part 1 (Brouckaert et al., 2021a). Its implication is that a solution's composition in terms of species is completely specified by its composition in terms of components (together with temperature and pressure). A speciation routine, such as the one described in Part 5 (Brouckaert et al., 2022), simulates the effect of Duhem's theorem by calculating the species concentrations that correspond to the specified component concentrations. Having such a routine available suggests an alternative algorithm for solving the 5-point titration system that is conceptually (but not computationally) simpler. This involves setting up the compositions of initial solution and the titration points in terms of components (i.e. $[PO_3^{3-}]$, $[NH_4^+]$, $[HS^-]$ plus estimates of $[CO_3^{2-}]$, $[Ac^-]$, $[H^+]$), and using the speciation routine to calculate the corresponding pH values. The unknown component concentrations ($[CO_3^{2-}]$, $[Ac^-]$, $[H^+]$) are then adjusted to obtain the closest fit to the measured pH values. This approach has been implemented in Microsoft Excel as VBSpeciation6_1.xlsm, with the speciation routine programmed as a spreadsheet function using Visual Basic, and the component adjustments effected using the Excel Solver (see Appendix). All the complex computations are hidden in the speciation function and the solver, leaving only the very straightforward material balance calculations to complete the application. This makes the program very flexible – for example, it is easy to add more titration points, or fit more unknown components (although any such extension should be subjected to an error analysis similar to the one described in the next sections). The speciation spreadsheet has many other uses beside the 5-point titration; for example, it was used to prepare Figures 4-1, 4-2a and 4-2b.

Errors in 5-point titration results

Any error in the N_T, P_T and S_T concentrations entered into the 5-point titration programme will be assigned to the H_2CO_3 *alk* and HAc (A_T) concentrations, resulting in errors in these concentrations (Poinapen et al., 2009). However, the relative impact of errors in N_T, P_T and S_T depends on the solution conditions. If the pH of the AD liquor is <7.5, the alkalinity of the ammonia system is very low (see Table 4-1), and zero or an estimated concentration could be entered for FSA (N_T) with low error in the H_2CO_3 *alk* and HAc concentrations. Also, if the FSS (S_T) and OP (P_T) concentrations are low, their contribution to the Alk_t is low, and zeros or estimated concentrations could also be entered into the programme for these concentrations. For example, if in the case of the AD liquor in Table 4-1 before gas loss (pH = 7.0), half the actual FSA, OP and FSS concentrations were separately entered into the programme, then the maximum errors in the H_2CO_3 alk and HAc concentrations are +5.8% and +3.5%, respectively (Table 4-2). This arises because in AD liquor, with the high partial pressure of CO_2 in the AD head space, the H_2CO_3 *alk* makes up the greater part (>50%) of the Alk_t.

Table 4-2. *H_2CO_3 alk and HAc concentration differences obtained from the 5-point titration programme for half the actual FSA, OP and FSS concentrations (IS = 0.124 mol/L or EC = 1 778 mS/m using the IS-EC equation of Bhuiyan et al., 2009)*

	H_2CO_3 *alk* mg/L as CaCO$_3$	% Error	HAc mg/L	% Error	FSA mgN/L	OP mgP/L	FSS mgS/L
Actual conc.	3 730	0.0	240.0	0.0	1 000	500	300
5-point titration results							
Correct FSA, OP and FSS	3 719	−0.3	242.2	+0.1	1 000	500	300
Halve FSA	3 725	+0.2	248.7	+2.7	500	500	300
Halve OP	3 938	+5.8	250.7	+3.5	1 000	250	300
Halve FSS	3 843	+3.3	248.0	+2.4	1 000	500	150

The 5-point titration for AD control

Unlike the PA and TA titration method, the 5-point titration programme requires input values for N_T, P_T and S_T and errors in these values will result in errors in the calculated H_2CO_3 *alk* and *HAc* concentrations and the Ripley ratio. However, for AD control even quite large errors may be tolerable. Figures 4-5 and 4-6 show the 5-point titration is much more accurate for predicting the H_2CO_3 *alk* (Figure 4-5) and especially *HAc* (Figure 4-6) concentrations compared to the IA/TA method. Furthermore, Table 4-2

shows that relatively large errors (50%) in N_T, P_T or S_T have a relatively small impact on the calculated *H₂CO₃ alk* and *HAc* concentrations (<6%) for low sulphide liquors. Therefore, for AD control, the 5-point titration requires no more effort than the PA and TA, and can be automated, provided that reasonable estimates of FSA, OP and FSS concentrations are entered into the programme.

The 5-point titration for aqueous-phase characterization

The 5-point titration is also a good method for aqueous-phase characterization for mass-balanced modelling purposes, and organic composition determination (Part 3 – Ekama and Brouckaert, 2022); however, in this case accurate determination of N_T, P_T and S_T is essential. The aqueous OP and FSA usually are quite stable because transfer to gas or solid phases is negligible at the neutral pH of bio-systems – no P gas can form and the pH is too low for significant mineral precipitation and ammonia gas evolution. This is not the case for the sulphide – sulphide readily escapes to the gas phase at neutral pH. Entering inaccurate total sulphide species concentration into the 5-point titration programme results in inaccurate *H₂CO₃* alk (and hence C_T) and HAc concentrations and hence incorrect characterization of the water sample (Poinapen et al., 2009).

The 5-point titration method for samples with pH < 6.7

If the AD sample has a pH below the pH of the first pH titration point <6.7, then an appropriate quantity of NaOH can be added to the sample to raise the pH, after which the 5-point titration is conducted as usual. Although the addition of the strong base increases the total alkalinity of the sample, it does not change the C_T, A_T, N_T, P_T and S_T total species concentrations. Therefore, the same C_T and A_T results are obtained.

Effect of H₂S and CO₂ loss on 5-point titration results

Loss of CO_2 and H_2S from the sample do not change the Alk_t (see Figure 4-1). This can be explained by noting that they leave the solution in their reference forms, which contribute zero alkalinity, or by considering the evolution reactions, for which ΔAlk_t values are zero, i.e.

$2H^+ + CO_3^{2-} \rightarrow CO_{2(g)} + H_2O$ and $H^+ + HS^- \rightarrow H_2S_{(g)}$
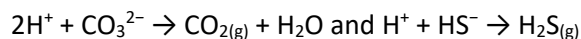
However, these reactions **do** cause the sample pH to increase due to the loss of acid species. In the case of a pure carbonate or sulphide system, the loss of CO_2 or H_2S from the original solution can be calculated from the change in pH. However, in a mixed system, from which both gases are escaping, one must be measured directly in order to calculate the other.

Poinapen et al. (2009) investigated the loss of sulphide from samples between collection and analysis and different methods to prevent it, and recommended the following: (i) measuring the in-situ pH, i.e. directly in the reactor (rather than in samples extracted from the reactor, from which gases can readily escape); and (ii) taking two samples from the reactor, one as is, the other collected with 2 drops of 1 N NaOH to immediately raise its pH above 11. This second sample can be filtered without loss of H₂S (even using vacuum), and the FSS determined by difference between COD tests on samples with organics and FSS and organics only (sulphide removed by precipitation with $ZnSO_4$ and filtration). The first sample is used for FSA and OP determination and for the 5-point titration. The FSA, OP, FSS obtained from the

COD tests, and in-situ pH are used as inputs to the 5-point titration programme, as are the volumes of acid added to reach the four pH points. This procedure provided accurate *H₂CO₃ alk* and mixed weak acid/base speciation results, from which good C balances could be obtained over sulphidogenic systems fed primary sewage sludge; (see also the discussion of sulphidogenesis in Part 2 – Brouckaert et al., 2021b).

The 5-point titration has been demonstrated in several studies to be an accurate method for determining the *H₂CO₃ alk* and VFA concentrations in mixed weak acid/base samples (Lahav et al., 2002, Hey et al., 2013; Vannecke et al., 2015). It is convenient because it does not require the VFA (A$_T$) total species concentration, which requires a gas chromatograph for its measurement. The 5-point titration is therefore a simple and useful test not only for monitoring ADs via the VFA/*Alk$_t$* ratio (Moosbrugger et al., 1993a,b) but also for characterizing the aqueous phase for complete mass modelling.

CALCULATION OF COMPONENT CONCENTRATIONS FOR MODEL INPUT

The characterization of the aqueous-phase composition in terms of components is required in order to be able to model and track changes in the aqueous phase due to bioprocesses. The measurements that are used in the 5-point titration methodology, pH and electrical conductivity, reflect species concentrations, which must be translated to the component concentrations required for modelling. This translation is essentially what the 5-point titration program does; however, the output of TITRA5.exe, the original Moosbrugger version, did not provide the component concentrations (although they figured in the internal calculations). This required a post-calculation to reconstruct the concentrations of H$^+$ and the weak acid anions, using the speciation equations of Loewenthal et al. (1991), which are the same as used by TITRA5.exe. This is not an issue with subsequent implementations of the algorithm, which include these component concentrations in the output (see Appendix).

However, there are components that are considered implicitly, but not explicitly, by the algorithm, and a bioprocess model needs these as inputs also. The following section explains how these can be estimated.

Aligning modelled and measured ionic strength

To predict pH correctly, the entire ionic composition in which the bioprocesses take place needs to be established. This is because the ionic strength, a measure of the total concentration of charged species in solution, affects the speciation of the aqueous phase. The ionic strength is given by:

$$IS = \frac{1}{2} \sum Z_i^2 C_i \qquad (2)$$

where Z_j and C_j are the charge and concentrations in mol/kg of ionic species *i*.

To measure and model all the ions in the aqueous phase of biological treatment systems is neither practically feasible nor computationally efficient. Therefore, the ions that have the greatest impact on the speciation of the aqueous phase and pH are selected for modelling (Part 1 – Brouckaert et al., 2021a) and require measurement. These are the ions of (i) the weak acid/bases that change as a result of the reactions of the bioprocesses, i.e., the IC, VFA, OP, FSA and sulphide systems as well as H$^+$, (ii) the ions involved in bioprocesses, especially nutrient removal, and mineral precipitation, which include Ca^{2+},

Mg^{2+}, K^+, Fe^{3+}, Fe^{2+}, NO_3^-, NO_2^- and SO_4^{2-}, and (iii) any ion-pairs that can form to significant extents such that they affect (i) and (ii). The sum of contributions of the selected (or modelled), and therefore measured, ions is typically lower than the total ionic strength which may include less important, unmeasured ionic species.

Furthermore, the total ionic strength of a wastewater sample cannot be measured directly and is calculated instead from measurements of either electrical conductivity (EC) or total dissolved solids (TDS). For example, the later versions of the 5-point titration program listed in the Appendix calculate IS_{meas} using the equation of Bhuiyan et al. (2009):

$$IS_{meas} = \frac{7.22 \times 10^{-5}\ EC_T}{[1+0.0198(T-25)]}$$ (3)

where EC_T is the EC at $T°C$ in mS/m and T = temperature in °C.

In real wastewaters, IS_{meas} calculated using Eq. 3 is usually significantly higher than IS calculated from Eq. 2 using available direct and indirect measurements of specific species. To make up the deficit in ionic strength (IS), Na^+ and Cl^- can be added as components in the speciation model, such that (i) the IS of the positively charged ions (IS_{+ve}) and negatively charged ions (IS_{-ve}) are equal and (ii) add up to the measured IS_{meas} obtained from the EC_T (Eq. 3). Na^+ and Cl^- are typically used to represent the unmeasured ions in the aqueous phase because they are ubiquitous in aqueous environments, have particularly weak interactions with other ions and are not involved in the bioprocesses typical modelled, so normally do not need to be accurately reflected in the model.

Ionic strength is a function of all the charged species in solution while most of the available measurements, e.g., C_T, N_T, P_T, S_T, and A_T, represent total component concentrations (discussed in Part 1 – Brouckaert et al., 2021a); therefore a speciation model is required to relate the available measurements to the total ionic strength.

To determine all the measured species concentrations requires the pH, the total species concentrations (C_T, N_T, P_T, S_T, and A_T in mol/kg), and the dissociation constants corrected for ionic strength (pK'). The activity coefficients (γ_m, γ_d, γ_t for monovalent, divalent and trivalent ions respectively) used for pK' correction are calculated using the Davies equation with IS_{meas} (Eq. 3) and temperature ($T°C$) (Loewenthal et al., 1989). The IS_{+ve} is the ionic strength contribution of all the cationic species, such as Ca^{2+}, Mg^{2+}, K^+, NH_4^+ and H^+ (where $[H^+] = 10^{-pH}/\gamma_m$), and IS_{-ve} is the ionic strength contribution of all the anions, such as HCO_3^- and HPO_4^-.

Hence, IS_{+ve} and IS_{-ve} are calculated from:

$$IS_{+ve} = \frac{1}{2}\sum_{i=1}^{m} Z_i^2 C_i$$ (4a)

$$IS_{-ve} = \frac{1}{2}\sum_{j=1}^{n} Z_j^2 C_j$$ (4b)

where m and n are the number of measured cations and anions, respectively, and Z_i and C_i and Z_j and C_j the charge and concentrations in mol/kg of the cation i and anion j.

With IS_{+ve} and IS_{-ve} known, the concentrations of Na^+ and Cl^- in mol/L to be included in the aqueous phase to achieve the IS_{meas} are obtained from:

$$IS_{+ve} + \frac{1}{2}[Na^+] = IS_{-ve} + \frac{1}{2}[Cl^-] \tag{5a}$$

and

$$IS_{+ve} + \frac{1}{2}[Na^+] + IS_{-ve} + \frac{1}{2}[Cl^-] = IS_{meas} \tag{5b}$$

from which

$$[Na^+] = IS_{meas} - 2\,IS_{+ve} \tag{6c}$$

and

$$[Cl^-] = IS_{meas} - 2\,IS_{-ve} \tag{6d}$$

CONCLUSIONS

To predict pH with bioprocess models requires (i) complete integration of biological, chemical and physical processes, (ii) complete CHONPS element mass- and charge-balanced stoichiometry, and (iii) complete aqueous-phase ionic speciation. Integrating biological, chemical and physical processes and including complete CHONPS element mass- and charge-balanced bioprocess stoichiometry pose little difficulty, but modelling the entire aqueous-phase ionic content is both inefficient computationally and impractical analytically. To obviate this, only the components that have a significant influence on the aqueous-phase speciation and pH are measured and modelled. Depending on the selection of the bioprocesses to be modelled, these are the two virtually completely dissociated strong acids H_2SO_4 and HNO_3 (and any other strong acids that may be necessary for the particular model), the six partially dissociated weak acids and bases, viz. the inorganic carbon (IC), ortho-phosphate (OP), free and saline ammonia (FSA), volatile fatty acids (VFA, represented by acetate HAc), free and saline sulphide (FSS) and the water itself, and ions like Ca^{2+}, Mg^{2+}, Na^+ and K^+ that are involved in the physical, chemical and biological processes of interest in the model such as precipitation and ion pairing.

The aqueous-phase ionic strength (IS) of these modelled and measured total species and ion concentrations is lower than the ionic strength calculated from electrical conductivity measurements IS_{meas}. To adjust the modelled IS to match IS_{meas}, Na^+ and Cl^- are added to the modelled aqueous mix. This ensures that the ionic strength of the aqueous phase is correct, so that the dissociation constants (pK) of the weak acids and bases are correctly adjusted for ionic strength.

Any changes to the aqueous-phase ion mix, including the $[H^+]$ or pH, due to the biological, chemical or physical processes, are calculated by the model relative to this initial state. This approach requires accurate speciation of the initial and final aqueous phases, which in turn requires accurate measurement of the total species concentrations of the five weak acids and bases arising from the CHONPS element content of the electron donor. Accurate speciation can be accomplished with the in-situ pH, FSA, OP and FSS analyses, and the 5-point titration for measuring the VFA and carbonate

component concentrations (A_T and C_T).

The papers in this series frequently refer to speciated alkalinities for two reasons: to aid understanding of the complex interactions between solution species, and when referring to previously published results that used them (e.g. Loewenthal et al., 1989; Moosbrugger et al., 1993b; Poinapen et al., 2009). However, we do not recommend their use in practice. Referring to Figure 4-1, only the total alkalinity/pH curve is measurable – all the others are derived from a speciation model. It is a recurring theme of this series of papers that component concentrations provide a more compact and efficient representation of solution composition, given that the species concentrations can always be obtained from the component concentrations via a speciation model.

ABBREVIATIONS

alk   alkalinity

COD   chemical oxygen demand

EC   electrical conductivity

EDC   electron donating capacity

FSA   free and saline ammonia

FSS   free and saline sulphide

HAc   acetic acid (CH_3COOH)

IC   inorganic carbon

IS   ionic strength

mol   moles

OP   ortho-phosphate

pH   negative log of the hydrogen ion activity

TDS   total dissolved solids

VFA   volatile fatty acids

SYMBOLS

A_T total acetate species concentration (mgHAc/L)

Alk_T total alkalinity referenced to $H_2CO_3/H_3PO_4/NH_4^+/H_2S/HAc$

Alk_t total alkalinity referenced to $H_2CO_3/H_2PO_4^-/NH_4^+/H_2S/HAc$

C   carbon

C_T total inorganic carbon species concentration (mgC/L)

e^- electron

H   hydrogen

IS   ionic strength

IS_{meas} ionic strength estimated from the measured electrical conductivity (EC)

IS_{+ve} ionic strength contributed by positive ions

IS_{-ve}	ionic strength contributed by negative ions
K_d	dissociation constant
L	litre
m	milli (10^{-3}) or metre
N	nitrogen
N_T	total ammonia species concentration (mgN/L)
O	oxygen
P	phosphorus
pK	negative log of dissociation constant. Subscripts a, c1, c2, n, p1, p2, p3, s1 and s2 refer to the dissociation constants of the acetate, inorganic carbon, ammonia, 1st 2nd and 3rd ortho-phosphate and the sulphide weak acid/base systems respectively. 1,2,3 refer to the number if protons lost relative to the most protonated species.
P_T	total ortho phosphate species concentration (mgP/L)
S	sulphide or Siemens
S_T	total sulphide species concentration (mgS/L)
β	buffer capacity [mol/(L·pH)]
γ_m	activity coefficient for monovalent ions, divalent and trivalent ions respectively
γ_d	activity coefficient for divalent ions
γ_t	activity coefficient for trivalent ions

REFERENCES

ANDREWS JF and GRAEF SP (1971) Dynamic modelling of the anaerobic digestion process. Anaerobic biological treatment processes. *Advances in Chemistry Series No. 105*. 126–162. American Chemical Society, Washington D.C. https://doi.org/10.1021/ba-1971-0105.ch008

BATSTONE DJ, KELLER J, ANGELIDAKI I, KALYUZHNYI SV, PAVLOSTATHIS SG, ROZZI A, SANDERS WTM, SIEGRIST H and VAVILIN VA (2002) Anaerobic digestion model No 1 (ADM1). Scientific and Technical Report No 9. International Water Association (IWA), London. https://doi.org/10.2166/wst.2002.0292

BHUIYAN IH, MAVINIC DS and BECKIE RD (2009) Determination of temperature dependence of electrical conductivity and its relationship with ionic strength of anaerobic digester supernatant for struvite precipitation. *J. Environ. Eng.* **135** 1221–1226. https://doi.org/10.1061/(ASCE)0733-9372(2009)135:11(1221)

BROUCKAERT CJ, IKUMI DS and EKAMA GA (2010) A 3 phase anaerobic digestion model. *12th IWA AD Conference*, Guadalajara, Mexico, 30 Oct–4 Nov 2010.

BROUCKAERT CJ, BROUCKAERT BM and EKAMA GA (2021a) Integration of complete elemental mass-balanced stoichiometry and aqueous-phase chemistry for bioprocess modelling of liquid and solid waste treatment systems – Part 1: The physico-chemical framework. *Water SA* **47** (3) 276–288. https://doi.org/10.17159/wsa/2021.v47.i3.11857

BROUCKAERT CJ, EKAMA GA and BROUCKAERT BM (2021b) Integration of complete elemental mass-balanced stoichiometry and aqueous-phase chemistry for bioprocess modelling of liquid and solid waste treatment systems − Part 2: Bioprocess stoichiometry. *Water SA* **47** (3) 289–308. https://doi.org/10.17159/wsa/2021.v47.i3.11858

BROUCKAERT CJ, BROUCKAERT BM and EKAMA GA (2022) Integration of complete elemental mass-balanced stoichiometry and aqueous-phase chemistry for bioprocess modelling of liquid and solid waste treatment systems: Part 5 – Aqueous-phase speciation. Water SA 48(1) 32–39. https://doi.org/10.17159/wsa/2022.v48.i1.3738

CAPRI MG and MARAIS GvR (1975) pH adjustment in anaerobic digestion. *Water Res.* (3) 307–314. https://doi.org/10.1016/0043-1354(75)90052-4

EKAMA GA and BROUCKAERT CJ (2022) Integration of complete elemental mass-balanced stoichiometry and aqueous-phase chemistry for bioprocess modelling of liquid and solid waste treatment systems: Part 3 – Measuring the organics composition. *Water SA* 48(1) 21–31. https://doi.org/10.17159/wsa/2022.v48.i1.3322

HARDING TH, IKUMI DS and EKAMA GA (2011) Incorporating phosphorus into plant wide wastewater treatment plant modelling – Anaerobic digestion. *8th IWA Watermatex Conference*, San Sebastian, Spain, 20–22 June 2011.

HEY T, SANDSTRÖM D, IBRAHIM V and JÖNSSON K (2013) Evaluating 5 and 8 pH-point titrations for measuring VFA in full-scale primary sludge hydrolysate. *Water SA* **39** (1) 17–22. https://doi.org/10.4314/wsa.v39i1.3

IKUMI DS, BROUCKAERT CJ and EKAMA GA (2011) A 3 phase anaerobic digestion model. *8th IWA Watermatex Conference*, San Sebastian, Spain, 20–22 June 2011.

LAHAV O and LOEWENTHAL RE (2000) Measurement of VFA in anaerobic digestion: The 5 point titration method revisited. *Water SA* **26** (3) 389–392.

LAHAV O, MORGAN BE and LOEWENTHAL RE (2002) Rapid, simple, and accurate method for measurement of VFA and carbonate alkalinity in anaerobic reactors. *Environ. Sci. Technol.* **36** (12) 2736–2741. https://doi.org/10.1021/es011169v

LAHAV O and MORGAN BE (2004) Titration methodologies for monitoring of anaerobic digestion in developing countries – a review. *J. Chem. Technol. Biotechnol.* **79** (17) 1331–1341. https://doi.org/10.1002/jctb.1143

LIZARRALDE I, BROUCKAERT CJ, VANROLLEGHEM P, IKUMI D, EKAMA GA AYESA E and GRAU P (2015) A general methodology for incorporating physical-chemical transformations into multi-phase wastewater treatment process models. *Water Res.* **74** 239–256. https://doi.org/10.1016/j.watres.2015.01.031

LOEWENTHAL RE and MARAIS GvR (1976) *Carbonate Chemistry of Aquatic Systems: Theory and Applications*. Ann Arbor Science Publishers Inc, Ann Arbor, Michigan.

LOEWENTHAL RE, EKAMA GA and MARAIS GvR (1989) Mixed weak acid/base systems Part I – Mixture

characterization. *Water SA* **15** (1) 3–24.

LOEWENTHAL RE, WENTZEL MC, EKAMA GA and MARAIS GvR (1991) Mixed weak acid/base systems Part II: Dosing estimation, aqueous phase. *Water SA* **17** (2) 107–122.

McCARTY PL (1974) Anaerobic processes. Presented at: International Association for Water Pollution Research (IAWPR, now IWA) short course on "Design aspects of biological treatment", Birmingham, UK, 18 Sept 1974.

MOOSBRUGGER RE, WENTZEL MC, EKAMA GA and MARAIS GvR (1992) Simple titration procedures to determine H_2CO_3*alkalinity and short chain fatty acids in aqueous solutions containing known concentrations of ammonium, phosphate and sulphide weak acid bases. WRC Report No. TT 57/92, Water Research Commission, Pretoria. ISBN 1 874858 54 3.

MOOSBRUGGER RE, WENTZEL MC, LOEWENTHAL RE, EKAMA GA and MARAIS GvR (1993a) Alkalinity measurement: Part 3 – A 5 pH point titration method to determine the carbonate and SCFA weak acid/bases in aqueous solution containing also known concentrations of other weak acid/bases. *Water SA* **19** (1) 29–40.

MOOSBRUGGER RE, WENTZEL MC, EKAMA GA and MARAIS GvR (1993b) A 5 pH point titration method for determining the carbonate and SCFA weak acid bases in anaerobic systems. *Water Sci. Technol.* **28** (2) 237–245. https://doi.org/10.2166/wst.1993.0112

MUSVOTO EV, WENTZEL MC, LOEWENTHAL RE and EKAMA GA (1997) Kinetic based model for mixed weak acid/base systems. *Water SA* **23** (4) 311–321.

MUSVOTO EV, EKAMA GA, WENTZEL MC and LOEWENTHAL RE (2000) Extension and application of the three phase weak acid/base kinetic model to the aeration treatment of anaerobic digester liquors. *Water SA* **26** (4) 417–438.

POINAPEN J, EKAMA GA and WENTZEL MC (2009) Biological sulphate reduction using primary sewage sludge in a upflow anaerobic sludge bed reactor – Part 2: Modification of simple wet chemistry analytical procedures to achieve COD and S mass balances. *Water SA* **35** (5) 535–542. https://doi.org/10.4314/wsa.v35i5.49179

RIPLEY LE, BOYLE JC and CONVERSE JC (1986) Improved alkalimetric monitoring for anaerobic digestion of high-strength wastes. *J. WPCF* **58** 406–411.

SÖTEMANN SW, RISTOW NE, WENTZEL MC and EKAMA GA (2005) A steady-state model for anaerobic digestion of sewage sludges. *Water SA* **31** (4) 511–527. https://doi.org/10.4314/wsa.v31i4.5143

STUMM W and MORGAN J (1996) *Aquatic Chemistry* (3rd edn). Wiley, New York. ISBN 9781118591482

TAIT S, SOLON K, VOLCKE EIP and BATSTONE DJ (2012) A unified approach to modelling wastewater Chemistry: Model Corrections. *Proc. WWTmod2012 Conference*, Mont-Sainte-Anne, Québec, Canada, 26–28 February 2012.

VANNECKE TPW, LAMPENS D, EKAMA GA and VOLCKE EIP (2015) Evaluation of the 5 and 8 pH point titration methods for monitoring alkalinity and VFA in anaerobic digesters treating solid waste. *Environ. Technol.* **36** (7) 681–869. https://doi.org/10.1080/09593330.2014.964334

VAN ZYL PJ, WENTZEL MC, EKAMA GA and RIEDEL K-H (2008) Design and start up of a high rate anaerobic membrane bio-reactor for the treatment of a low pH, high strength dissolved organic wastewater. *Water Sci. Technol.* **57** (2) 291–295. https://doi.org/10.2166/wst.2008.083

APPENDIX

5-point titration software

The following programs can be downloaded from https://washcentre.ukzn.ac.za/bio-process-models/

Table 4-A1. *5-point titration software*

Version	Programme	Language/software	Speciation model
1	Titra5	TurboPascal 4.0*	Moosbrugger et al. (1992)
2	Titra5_IStr.xlsm	MS Excel	Moosbrugger et al. (1992)
3	VBSpeciation6_1	MS Excel	Part 5 – Brouckaert et al. (2022)

*can be run on 64 bit computers within DosBox 0.74-3 (2019)

In the 5-point titration method, it is recommended to dilute the sample to C_T less than 500 mg/L as $CaCO_3$ to avoid undue loss of CO_2 during titration (Moosbrugger et al., 1992). As a result, the titration takes place at lower ionic strengths than if the sample was undiluted. Version 1 does not account for this, and uses the undiluted sample ionic strength to calculate the pK corrections resulting in a small error in the H_2CO_3 alk and HAc concentrations calculated from the 5-point titration. This is corrected in Version 2 which calculates the pKs at the diluted ionic strengths.

A minor improvement introduced in Version 2 concerns the calculation of the ionic strength from the measured conductivity. The earlier version used a general correlation for natural waters; this was replaced by the correlation of Bhuiyan et al. (2009), which was developed for AD liquors.

The simplified speciation model used in Versions 1 and 2 does not include ion-pairing, however, the difference between including and excluding ion-pairing is very small provided the ionic strength is <0.2 mol/L (EC = 2 770 mS/m) (Tait et al., 2012).

Version 3 uses the more rigorous approach to speciation modelling outlined in Part 5 (Brouckaert et al., 2022) and includes ion-pairing in the speciation calculations. The Microsoft Excel-based VBSpeciation6_1.xlsm has a set of ionic speciation routines, implemented as spreadsheet functions that take their inputs from ranges of cells. It includes a worksheet that implements the 5-point titration concept. For the 5-point titration, the solution concentrations corresponding to the five titration points are calculated by mass balance using standard Excel formulae, from which the corresponding pH values

are calculated using the speciation functions. The calculated pH values are then fitted to the measured values in the least-squares sense by adjusting the H^+, CO_3^{2-} and Ac^- component concentrations in the initial solution composition (i.e. before titrant addition), using the Excel Solver. The Na^+ and Cl^- concentration in the initial solution can optionally be adjusted to match ionic strength and charge balance. This version has the advantages that the differences between all the calculated and measured pH values are visible to the user, ion pairing is taken into account, and other ion measurements that might influence the pH calculations (such as SO_3^- or Ac^-) can be entered where available. It is also straightforward to insert further titration points if desired.

Appendix C: Modelling mesophilic-thermophilic temperature transitions experienced by an aerobic membrane bioreactor treating furfural plant effluent

LG Kay[1], CJ Brouckaert[1] and RC Sindall[1]

[1]Pollution Research Group, Department of Chemical Engineering, University of KwaZulu-Natal, King George V Avenue, Durban, 4041, South Africa

ABSTRACT

A mathematical model was developed of an aerobic membrane bioreactor (MBR) treating effluent from a by-products facility at a sugar mill producing furfural, based on measurements of microbial kinetics and stoichiometry at different temperatures. The model was calibrated and validated against plant data using volumetric flow into the MBR and volumetric sludge wasting from the MBR as inputs. The model is able to predict steady-state and unsteady-state operation of the MBR under both mesophilic and thermophilic conditions, and the transitions between the two regimes. Comparison of model simulations and plant data suggests that thermophilic operation is advantageous, but it is less stable than mesophilic operation and frequent feed disruptions can have detrimental effects on MBR operation.

KEYWORDS: WASTEWATER TREATMENT MODELLING, FURFURAL PROCESS EFFLUENT, THERMOPHILIC, PHYSICO-CHEMICAL FRAMEWORK

INTRODUCTION

The Sezela Mill Complex, operated by the Illovo Group, consists of a sugar mill with an attached downstream products facility. The downstream site includes a furfural production plant and a range of smaller plants that produce derivatives of furfural. The furfural plant generates an effluent as a by-product of the furfural production process, which is acidic in nature and has a high chemical oxygen demand (COD). The COD consists primarily of acetic acid, with minor amounts of formic acid and intermittent furfural contamination (Judd, 2011). The discharge of the effluent has a negative effect on the mill's water balance. Possible treatment of the effluent therefore provides an opportunity for water recovery, attractive for financial and environmental reasons. This prompted the construction of a pilot-scale aerobic membrane bioreactor (MBR).

The MBR has a hydraulic design capacity of 1 200 $m^3 \cdot d^{-1}$ but in practice treats a feed flow rate of no more than 1 000 $m^3 \cdot d^{-1}$. The MBR is a 4 600 m^3 (29 m diameter, 7 m depth) open cylindrical tank and air is supplied to the mixed liquor through diffusers distributed along the bottom of the tank. It is fitted with a bank of 12 EK400 Kubota flat sheet modules, with a total membrane area of 2 840 m^2, submerged within the tank. Two 224 kW blowers, rated at 7 060 $Nm^3 \cdot h^{-1}$ at 740 mbar, supply air via the fine bubble diffusers along the floor of the tank. A third 61.5 kW blower, rated at 2 880 $Nm^3 \cdot h^{-1}$ at 500 mbar, also supplies air as coarse bubbles to scour and clean the membranes. MBR technology was selected due to the suspected presence of an unknown trace toxin in the process effluent that is thought to inhibit conventional aerobic or anaerobic treatment (Judd, 2011). The high (12 to 14 g/L) mixed liquor suspended solids (MLSS) achieved by the MBR is thought to overcome this limitation.

When a steady high feed rate can be sustained, the temperature rises to around 50°C (thermophilic operation), and at a steady low feed rate it operates at around 40°C (mesophilic operation). During mesophilic operation the hydraulic retention time (HRT) is approximately 13 days, and the sludge retention time (SRT) approximately 105 days. For thermophilic operation, the HRT and SRT are about 6 days and 55 days, respectively.

Feed fluctuations to the MBR occur frequently, due to both external and internal operational factors. During these fluctuations, the temperature of the MBR shifts, which often results in a transition between mesophilic and thermophilic temperature regimes. The transition to lower temperature is marked by a dramatically reduced biomass activity, which leads to operational instability.

Thermophilic operation has the advantages of specific reaction rates several times higher than those for mesophilic operation, and lower sludge production. However, more aeration is required, there is an increased tendency for foaming, and the sludge may have poor settling characteristics (LaPara and Alleman, 1999).

It was proposed that an integrated model capable of predicting temperature, pH and biomass activity (via oxygen utilization rate) would be a useful tool to explore design options and to devise operational strategies that best mitigate feed fluctuations and keep the process as stable as possible.

There has recently been a coordinated effort to establish a comprehensive modelling framework for bio-processes, extending the representation of the biologically mediated reactions to include other physico-

chemical phenomena which interact with them (e.g. Batstone et al., 2012; Lizarralde et al., 2015; Solon et al., 2017). Although the energy balance is a logical part of such a framework, it has not received much attention up to now, as few bio-processes involve sufficiently large energy transfers to cause significant interactions with the material transformations taking place. The Illovo MBR model provided an opportunity to demonstrate the incorporation of the energy balance into the framework in a particularly uncomplicated example. It has only one rate-limited biological reaction, four ionic equilibrium systems (acetate, carbonate, ammonia and phosphate), two phase transfer processes (evolution of carbon dioxide and evaporation of water), and one energy balance. Although the energy balance contains a number of terms, those representing transfers to or from the environment turned out to be minor compared to those originating within the process itself.

This study describes the development of a mathematical model of the mass and energy balances over the MBR, based on measurements of the microbial kinetics and stoichiometry at different temperatures. The model was used to simulate the dynamic operation of the MBR under mesophilic and thermophilic modes of operation and the transition between the two temperature regimes.

METHODS
The investigation involved a combination of experimental work and model development.

Experimental methods
Influent to the MBR was sampled daily and used to produce weekly composite samples. The composite samples were tested for COD using the standard closed reflux, colorimetric method (5220 D) and for total acidity using a titrimetric method using 0.1 N sodium hydroxide (2310 B) (Bridgewater et al., 2012).

The mixed liquor was sampled near the MBR surface when the blowers were running to ensure adequate homogeneity, and transported immediately to the respirometer to ensure negligible thermal shock. The MBR operating temperature was between 40 and 50°C; the temperature of the sample dropped by no more than 5°C during transportation to the respirometer. The temperature was then increased by the respirometer to the original sampling temperature.

The MLSS concentration of the MBR was obtained daily, following standard methods for total suspended solids (TSS) determination (2540 D) (Bridgewater et al., 2012).

A BM-EVO respirometer (Surcis, 2019) was used to carry out oxygen uptake rate (OUR) tests. This is essentially a 1 L, 2 compartment, mixed reaction vessel, equipped with aeration in one compartment, a circulating pump and a dissolved oxygen (DO) probe in the un-aerated compartment.

The endogenous respiration rate of the MBR mixed liquor was measured by a cyclic OUR test, in which intermittent aeration is used to drive the DO concentration between set limits, and the rate of decline of the oxygen concentration is measured while the aeration is off.

Exogenous respiration rate was measured using a dynamic oxygen uptake response test. After continuous aeration until conditions of endogenous respiration were achieved (about 24 h), the sample was circulated between the aerated and non-aerated compartments, with the DO electrode located in

the non-aerated compartment. The drop in DO concentration when substrate is added is a measure of the increased rate of respiration caused by the uptake of the substrate. The relationship between the drop in DO and the reaction rate was established by calibrating the apparatus with a substance with a known chemical oxygen demand (sodium sulphite), and one with a known biological oxygen demand (sodium acetate).

Model development

The model of the Illovo MBR was an assembly of features taken from literature models to match the particular aspects of the system. The biological reactions were formulated following the IWA ASM1 (International Water Association Activated Sludge Model No 1) (Henze et al., 1987), simplified as acetic acid was the only substrate under consideration. ASM1 does not consider energy balances, so the energy balance model of Sedory and Stenstrom (1995) was selected due to its ability to give a complete breakdown of the heat exchange mechanisms occurring, and its extensive use by various authors (LaPara and Alleman, 1999; Gillot and Vanrolleghem, 2003; Makinia et al., 2005).

The development of the model was carried out over the following series of steps:

- A mass balance over the MBR was formulated with a suitable description of the pertinent kinetic processes, and an ionic speciation subroutine was added for prediction of pH
- An energy balance over the MBR was formulated to predict temperature
- A temperature-dependent description of the kinetic parameters in the mass balance was obtained from laboratory tests at mesophilic (40°C) and thermophilic (50°C) temperatures
- The combined mass and energy balance were calibrated using parameters obtained from the experimental work and the literature
- The dynamic model was validated against an independent set of plant data
- A sensitivity analysis was carried out to determine the effects of various parameters in the energy balance on temperature
- The model was used to simulate both mesophilic and thermophilic operation of the MBR and the results used to assess how process operation could be improved

Model components and reactions

The model was formulated in two stages. Initially it only considered biological reactions, using a formulation similar to ASM1. Later, when it was realised that pH was important, because the plant operators used it to regulate the feed to the reactor, equilibrium ionic reactions were added to the model for pH prediction, which required some additional components, and some additional detail in the representation of the existing components.

The biological reactions included only growth and decay of heterotrophic microorganisms as the feed contained only soluble, readily biodegradable organic substrate (assumed to be acetic acid). Nitrification was not included in the model, as just sufficient nitrogen and phosphorus were dosed in to satisfy the biomass nutrient requirements. Table C-1 lists the components involved in the biological reactions; the stoichiometry and kinetics of the biological reactions are represented as a Gujer matrix in Table C-2; the ionic model components are listed in Table C-3; the transformed Gujer matrix including ionic components appears in Table C-4.

Table C-1. *Biological model components*

S_S	Soluble readily biodegradable substrate
X_H	Active heterotrophic biomass (assumed to be $C_5H_7O_2N$)
X_P	Un-biodegradable particulate material resulting from cell death
S_O	Dissolved oxygen

Table C-2. *Gujer matrix for the biological reactions (in COD units)*

i Components	1	2	3	4	Rate
j Processes ↓	S_S	X_H	X_P	S_O	expression
1 Aerobic growth of biomass	$-1/Y$	1		$(1-Y)/Y$	$\dfrac{\mu_m S_S X_H}{K_S + S_S}$
2 Biomass decay		-1	f_P	$(1-f_P)$	$k_d X_H k_d X_H$
	Biodegradable substrate	Active biomass	Inert matter	Dissolved oxygen	

Y: yield coefficient in biomass growth; μ_m: maximum specific growth rate; K_S: half saturation coefficient; f_P: yield of inert residue; k_d: specific death rate constant

Including pH prediction requires a transformation that is characteristic of the physico-chemical framework: adding relevant ionic components and assigning atomic content to the biological reaction components, so that the interaction between the biological and ionic reactions can be represented. Thus S_S was assumed to be acetic acid $C_2H_4O_2$, and X_H and X_p were assigned the same elemental formula $C_5H_7O_2N$.

Table C-3. *Ionic model components*

H^+	Hydrogen ion
$C_2H_3O_2^-$	Acetate ion (assumed to be ionised S_S)
NH_4^+	Ammonium ion
$CO_3^=$	Carbonate ion
PO_4^{-3}	Phosphate ion

Table C-4. *Gujer matrix, transformed according to the physico-chemical modelling framework*

I	1	2	3	4	5	6	7	8	Rate
J	S_S	X_H	X_P	S_O	H^+	$CO_3^=$	NH_4^+	H_2O	expression
1	$-2.5/Y$	1		$\dfrac{5(1-Y)}{Y}$	$\dfrac{(7.5-9Y)}{Y}$	$\dfrac{5(1-Y)}{Y}$	-1	3	$\dfrac{\mu_m S_S X_H}{K_S + S_S}$
2		-1	f_P	$-5(1-f_P)$	$9(1-f_P)$	$5(1-f_P)$	$(1-f_P)$	$3(1-f_P)$	$K_d X_H$
	$C_2H_3O_2^-$	$C_5H_7O_2N$	$C_5H_7O_2N$	O_2	H^+	$CO_3^=$	NH_4^+	H_2O	

The stoichiometric coefficients in Table C-4 are expressed in molal units rather than COD units as in Table C-2, and reflect balances over the reactions on the elements C,H,O,N and electrons. The COD of each component is inherent in its elemental formula, and the unit conversions are 64 g COD·mol^{-1} for $C_2H_3O_2^-$ and 160 g COD·mol^{-1} for $C_5H_7O_2N$. The parameter Y is not affected by the change in units. The rate expressions continue to use COD units.

Mass balance

The mass of fluid within the MBR (i.e. liquid level) fluctuates depending on the feed rate into the MBR as well as the sludge and permeate withdrawal rates; these are all independent of one another. To simplify the mass balance, the mass content of the MBR was assumed constant, as plant data shows only small fluctuations in liquid level during operation, ±0.1 m in 6.5 m.

The overall mass balance was therefore represented as:

$$m_o = m_e + m_{sw} + m_p \tag{1}$$

Where:

m_o is the mass flow rate of the furfural plant effluent fed into the MBR (kg·s^{-1})
m_e is the mass flow rate of evaporation from the MBR (kg·s^{-1})
m_{sw} is the mass flow rate of sludge wasting from the MBR (kg·s^{-1})
m_p is the mass flow rate of the permeate from the MBR (kg·s^{-1})

Assuming a uniform density throughout the reactor, and of the feed, evaporated water, sludge wasting and permeate streams, the mass balance is written in volumetric terms as follows:

$$q_o = q_e + q_{sw} + q_p \tag{2}$$

Where:

q_o is the volumetric flow rate of the furfural plant effluent fed into the MBR (m^3·s^{-1})
q_e is the volumetric flow rate of evaporation from the MBR (m^3·s^{-1})
q_{sw} is the volumetric flow rate of sludge wasting from the MBR (m^3·s^{-1})
q_p is the volumetric flow rate of the permeate from the MBR (m^3·s^{-1})
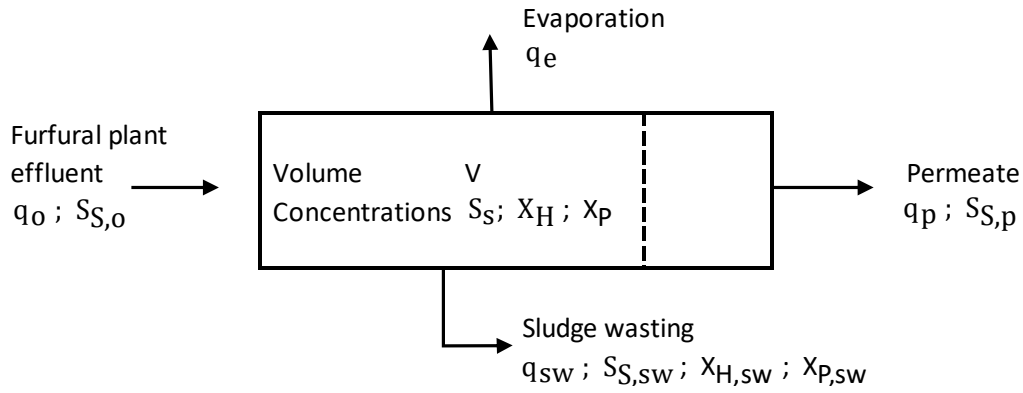
This is illustrated in Figure C-1.

Figure C-1. *MBR mass balance (modified from Gent, 2012)*

Component mass balances

Complete mixing of the MBR contents was assumed for the mass balance model; therefore the soluble concentrations of each of the components in the outlet streams (permeate and sludge wasting) were taken as equal to the concentrations of each component within the MBR. It was assumed that no solids pass through the membranes; consequently, the solids concentration of the waste sludge stream is the same as that in the MBR.

Readily biodegradable substrate, S_S

S_S enters the MBR with the feed, exits through the sludge wasting and permeate streams, and is consumed by reaction. It was assumed that soluble S_S can pass through the membrane. The furfural plant effluent is primarily acetic acid; S_S is assumed to consist entirely of acetic acid. The mass balance for the substrate is:

$$\frac{d(VS_S)}{dt} = q_o S_{S,o} - q_{sw} S_{S,sw} - q_p S_{S,p} + r_{S_S} V \tag{3}$$

Where:

$S_{S,o}$ is the concentration of the substrate in the furfural plant effluent stream ($kg·m^{-3}$)
$S_{S,sw}$ is the concentration of the substrate in the sludge wasting stream (equal to residual substrate concentration S_S) ($kg·m^{-3}$)
$S_{S,p}$ is the concentration of substrate in the permeate (equal to residual substrate concentration S_S) ($kg·m^{-3}$)
r_{S_S} is the rate of consumption of the substrate ($kg·m^{-3}·s^{-1}$)
V is the volume of the mixed liquor within the MBR (m^3)

Active heterotrophic biomass, X_H

The model assumes no biomass enters the MBR with the feed; it is only generated from growth on S_S. Sludge dosing from the neighbouring conventional activated sludge (CAS) plant was not considered, which occasionally occurs in practice to boost the microbial population. The biomass was modelled with

complete retention by the membranes; it was assumed that particulate material can only be removed through sludge wasting. The mass balance for active biomass is:

$$\frac{d(VX_H)}{dt} = -q_{sw}X_{H,sw} + r_{X_H}V \tag{4}$$

Where:

$X_{H,sw}$ is the concentration of the biomass in the sludge wasting stream (equal to residual biomass concentration X_H) (kg·m^{-3})
r_{X_H} is the biomass growth rate (kg·m^{-3}·s^{-1})

Inert organic matter from decay, X_P

X_P is particulate material generated during the decay of biomass, and is only removed through sludge wasting. The mass balance for X_P within the MBR is:

$$\frac{d(VX_P)}{dt} = -q_{sw}X_{P,sw} + r_{X_P}V \tag{5}$$

Where:

$X_{P,sw}$ is the concentration of inert organic matter from decay (equal to residual inert organic matter concentration X_P) (kg·m^{-3})
r_{X_P} is the rate of inert organic matter from decay formation (kg·m^{-3}·s^{-1})

Energy balance

The energy balance model of Sedory and Stenstrom (1995) was selected due to its detailed set of heat exchange mechanisms, and its extensive use by several authors (LaPara and Alleman, 1999; Gillot and Vanrolleghem, 2003; Makinia et al., 2005). The assumption of complete mixing implies a uniform temperature in the MBR, equal to the outlet stream temperature.

The overall energy balance is represented by:

$$V\rho C_p \frac{dT}{dt} = Input(H_{liq}) - Output(H_{liq}) + Q \tag{6}$$

Where Q is the sum of the various heat transfer terms illustrated in Figure C-2:

$$Q = Q_{SR} + Q_{AR} + Q_C + Q_{EV} + Q_A + Q_{TW,l} + Q_{RX} + Q_P \tag{7}$$

Where:

Q_{SR} is the heat gain from solar radiation (W)
Q_{AR} is the heat loss from atmospheric radiation (W)
Q_C is the heat loss due to surface convection (W)
Q_{EV} is the heat loss due to surface evaporation (W)
Q_A is the heat loss due to aeration (W)
Q_{TW} is the heat loss due to convection from the tank sides and floor (W)
Q_{RX} is the heat gain from the exothermic reaction (W)
Q_P is the heat gain from the compressors (W)

Input(H_{liq}) and Output(H_{liq}) are the enthalpy input and output terms respectively (W).
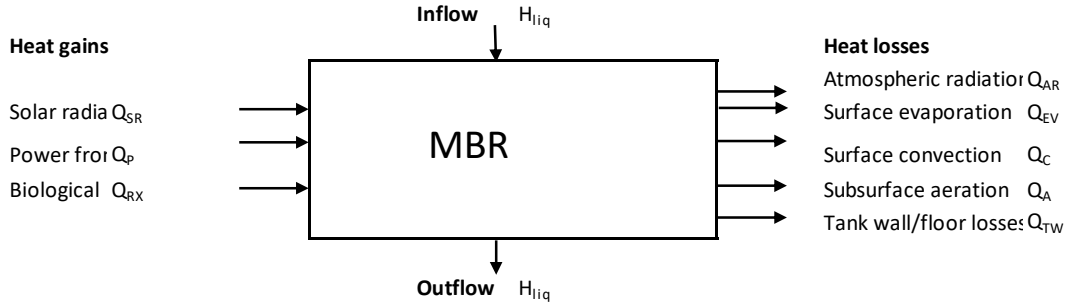

Figure C-2. *MBR heat exchange components (after Talati and Stenstrom, 1990)*

Enthalpy flows

The enthalpy terms consider the heat provided or lost by the liquid streams entering and leaving the MBR. They do not include enthalpy lost due to evaporation of water from the MBR, which is accounted for separately through the surface evaporation and aeration heat transfer terms.

The enthalpy terms are defined as follows:

$$Input\left(H_{liq}\right) = q_o \rho_l C_{p.l} T_i \tag{8}$$

$$Output\left(H_{liq}\right) = \left(q_{sw} + q_p\right)\rho_l C_{p.l} T \tag{9}$$

Where:

ρ_l is the density of the MBR inlet and outlet streams, assumed equal to water (kg·m^{-3})
T_i is the influent temperature (°C)
T is the MBR temperature (°C)
$C_{p.l}$ is the liquid heat capacity, assumed to be constant at 4 170 J·kg^{-1}·K^{-1}

Solar radiation

Radiation from the sun is an important factor due to the open surface of the MBR. A correlation was developed by Raphael (1962) to predict the contribution from solar radiation to the energy balance:

$$Q_{SR} = H_{SR,0}(1 - 0.0071 C_c^2)A_s \tag{10}$$

Where:

C_C is the cloud cover (tenths)
A_S is the surface area of the reactor contents in direct contact with the environment (m^2)
$H_{SR,0}$ is the average daily absorbed solar radiation for clear sky conditions (W·m^{-2})
This is dependent on meteorological conditions, site latitude, and the time of year. The average daily absorbed solar radiation may be calculated from a simplified form presented by Talati and Stenstrom (1990):

$$H_{SR,0} = a - b.sin\left(\frac{2\pi(d+183)}{366} + c\right) \tag{11}$$

Where:

d is the day of the year (out of 366)

The values for a, b and c are obtained from the following correlations:

$a = (4.843 \times 10^{-5})(95.1892 - 0.3591l - 8.4537 \times 10^{-3}l^2)$

$b = (4.843 \times 10^{-5})(-6.2484 + 1.6645l - 1.1648 \times 10^{-2}l^2)$

$c = 1.4451 + 1.434 \times 10^{-2}l - 1.745 \times 10^{-4}l^2$

Where:

l is the latitude of the reactor (°)

This correlation is valid between 26° and 46° latitude and must be adjusted by adding 183 days for use in the Southern Hemisphere.

Atmospheric radiation

The heat exchange that results from atmospheric radiation is based on Stefan Boltzmann's radiation law. This is expressed as the difference between the incoming and back radiation as follows:

$$Q_{AR} = [\epsilon\sigma(T + 273.15)^4 A_s] - [(1 - \lambda)\beta\sigma(T_a + 273.15)^4 A_s] \qquad (12)$$

Where:

ϵ is the water-surface emissivity
σ is the Stefan-Boltzmann constant (W·m^{-2}·K^{-4})
λ is the water-surface reflectivity
β is the atmospheric radiation factor
T_a is the ambient temperature (°C)

The atmospheric radiation factor β ranges between 0.75 and 0.85 for most conditions. Previous research has found that 0.97 and 0.03 are good estimates for the emissivity and reflectivity of water (ϵ and λ), respectively (Talati and Stenstrom, 1990).

Surface convection

The temperature difference between the air and the water surface provides the driving force for heat loss by surface convection. The following was obtained from Novotny and Krenkel (1973):

$$Q_C = \rho_g C_{p,g} h_v A_s (T - T_a) \qquad (13)$$

Where:

ρ_g is the density of air (kg·m^{-3})
$C_{p,g}$ is the specific heat of air at constant pressure (J·kg^{-1}·K^{-1})
h_v is the convective transfer coefficient (m·s^{-1})

The rate of convective heat loss is affected by the vapour transfer coefficient, which is dependent on the wind velocity. The following equation was developed by Novotny and Krenkel (1973):

$$h_v = (4.537 \times 10^{-3})A_s^{-0.05}WS \qquad (14)$$

Where WS is the wind speed (m·s^{-1})

Surface evaporation

The calculation of the heat loss due to evaporation from the MBR mixed liquor surface developed by Novotny and Krenkel (1973) is dependent on wind velocity, relative humidity, and temperature:

$$Q_{EV} = \left[55.448 \left(1 - \frac{r_h}{100} \right) + 3.322(T - T_a) \right] e^{0.0604T_a} \cdot WS \cdot A_s^{0.95} \tag{15}$$

Where:

r_h is the relative humidity of ambient air (%).

Aeration

Evaporation of water occurs in the course of contact between air from aerators and water in the tank. Air bubbles are assumed to enter the MBR at ambient temperature and humidity, and leave the system at the MBR operating temperature, saturated with water vapour (Novotny and Krenkel, 1973). The amount of water transferred depends on the air flowrate, tank temperature, ambient air temperature, and relative humidity.

The evaporative heat losses are dependent on the difference in the vapour pressure between the water and air. The equation was developed by Novotny and Krenkel (1973) and modified to this final form by Talati (1988):

$$Q_{AL} = \frac{MM_w q_g \Delta H_{vap}}{100R} \left\{ \frac{v_w [r_h + h_f (100 - r_h)]}{(T + 273.15)} - \frac{v_a r_h}{(T_a + 273.15)} \right\} \tag{16}$$

Where:

Q_{AL} is the evaporative heat loss due to aeration (W)
R is the universal gas constant (8.314 J·mol^{-1}·K^{-1})
v_a is the vapour pressure of water at air temperature (Pa)
v_w is the vapour pressure of water at reactor temperature (Pa)
h_f is the exit air humidity factor – assumed to be 1, as air is assumed to be saturated at exit
MM_w is the molar mass of water (kg·mol^{-1})
ΔH_{vap} is the latent heat of evaporation (J·kg^{-1})

Tank wall and floor conduction/convection

Heat losses from the aeration tank walls and floor depend upon the material of construction, the heat transfer area, and its thickness. Heat transfer coefficients for the tank material to air and the tank material to earth are different. Therefore, this model includes two terms: one for the MBR tank wall area exposed to air and one for the MBR tank area exposed to the ground.

The governing equation is as follows:

$$Q_{TW} = U_{a/g} A_l \left(T - T_{a/g} \right) \tag{17}$$

Where:

$U_{a/g}$ is the overall heat transfer coefficient for conduction from liquid phase through the reactor walls to air/ground (W·m^{-2}·K^{-1})

A_l is the area of the reactor that surrounds the liquid phase (m^2)

$T_{a/g}$ is the temperature of the air/ground (°C)

The overall heat transfer coefficient is given by:

$$U = \frac{1}{\frac{1}{K_i} + \frac{x_1}{k_1} + \frac{x_2}{k_2} \ldots\ldots + \frac{1}{K_0}}$$ (18)

Where:

x_i is the thickness of materials (m)

k_1 is the thermal conductivity of materials (W·m^{-1}·K^{-1})

K_i is the surface conductance at the air-surface area inside the tank (W·m^{-2}·K^{-1})

K_o is the surface conductance at the air-surface area outside the tank (W·m^{-2}·K^{-1})

The factor $1/K_i$ becomes zero if liquid is in contact with the surface of the wall. If the outside wall is in contact with air, an approximate value of K_0 is taken as 33.90 W·m^{-2}·K^{-1}. If the wall is surrounded by an earth embankment greater than 3 m thick, K_0 becomes 0.285 W·m^{-2}·K^{-1} (Sedory and Stenstrom, 1995).

Heat of reaction

The heat generated from reaction is calculated for the two principle reactions, the growth of biomass and the subsequent oxidation of decaying biomass:

$$Q_{RX} = \left[\frac{\mu_m S_S X_H}{K_S + S_S} \Delta H_{rxn,X_H} + (1 - f_P) k_d X_H \Delta H_{rxn,d} \right] V$$ (19)

Where:

$\Delta H_{rxn,X_H}$ is the heat of reaction for the growth reaction (J·mol X^{-1})

$\Delta H_{rxn,d}$ is heat of reaction for the endogenous respiration reaction (J·mol X^{-1})

V is the reactor volume (m^3)

The reaction rate expressions in Eq. 19 were previously defined in Table C-2, and were assumed to be independent of temperature, and calculated at standard conditions. The heat of reaction for growth (ΔH_{rxn}) is dependent on the biological yield (Y).

Mechanical power

In diffused aeration systems, the air stream is heated by compression. The heat input to the system is dependent upon the efficiency of the compressor. A fraction of the temperature increase during compression is lost as the bubbles expand when they rise through the medium.

$$Q_P = B(1 - \eta/100)$$ (20)

Where:

B is the power of the aerator/compressor (W)

η is the efficiency of the aerator/compressor (%)

Implementation in MATLAB

The mass balance, energy balance, and speciation routine for the prediction of pH were simulated using MATLAB R2010a.

The mass and energy balances form a set of linked ordinary differential equations (ODE's). Their solution was found by numerical integration using the MATLAB function 'ode23t'.

RESULTS

The results from the laboratory investigation were values and temperature dependence of the reaction kinetic parameters. These were then combined with several sets of historical plant data to calibrate and validate the whole model.

Reaction kinetic parameters

Specific death rate constant, k_d

To determine k_d of the activated sludge, cyclic OUR tests were performed using the respirometer. The mixed liquor sample was aerated for 24 h prior to the test to ensure any external substrate present in the sample was consumed, and endogenous respiration reached. A plot of the natural logarithm of the OUR during endogenous respiration, as a function of time, describes the exponential decay of biomass as a straight line with slope k_d. For an exponential decay, the relationship between OUR and active biomass concentration does not need to be known, since it does not affect the slope of the logarithmic plot. Three samples were tested at 40°C (mesophilic) and two samples were tested at 50°C (thermophilic). The results of these tests and the average values for each temperature of study are shown in Table C-5.

Table C-5. *Summary of specific death rate for mesophilic and thermophilic temperatures*.

Temperature (°C)	k_d (h^{-1})
40	0.0123 ± 0.0053
50	0.0249 ± 0.0069

Table C-5 shows a two-fold increase in k_d between mesophilic and thermophilic operation. This is within the range expected based on other related studies (Vogelaar et al., 2003; Abeynayaka, 2009).

Aerobic yield of heterotrophic biomass, Y

Y was estimated using the dynamic response test performed on the respirometer. Six tests were performed at 40°C, and four tests were carried out at 50°C.

The integral of the respirogram gives the oxygen consumed during the test.

Y was determined from the ratio of the oxygen consumed to the COD of the added substrate.

The calculated Y values are shown in Table C-6 and it can be seen that it is significantly lower at the higher temperature.

Table C-6. *Summary of yield results for mesophilic and thermophilic temperatures*

Temperature (°C)	Y (units)
40	0.620 ± 0.031
50	0.512 ± 0.013

Heterotrophic maximum growth rate μm and half saturation coefficient KS

μ_m and K_s were determined by fitting a mass balance model of the respirometer to the OUR data. The experimentally determined values for k_d and Y were fixed, and μ_m and K_S were found by regression.

The active biomass concentration was estimated as a fraction of the MLSS concentration. A MLSS to MLVSS (mixed liquor volatile suspended solids) ratio of 0.75, and an active biomass concentration (XH) to MLVSS ratio of 0.35 was used (Casey, 2006; Ubisi et al., 1997).

Four respirograms were used for the mesophilic kinetic regression and three respirograms were used for the thermophilic kinetic regression. The average parameter values for each of the temperatures were found and the standard deviation calculated. These results are summarised in Table C-7.

Table C-7. *Summary of maximum growth rate and half saturation coefficient results for mesophilic and thermophilic temperatures*

Temperature (°C)	μ_m (h^{-1})	K_S (g·L^{-1})
40	0.0209 ± 0.0032	0.895 ± 0.187
50	0.0407 ± 0.0072	1.00 ± 0.47

Temperature dependence

The effect of temperature on the reaction rate of biological processes was expressed empirically as $r(T) = r(T_{ref}) \cdot \theta^{(T - T_{ref})}$ (Eddy et al., 2003). Estimates of the temperature dependence of these parameter values were derived from values at 40 and 50°C. The values of θ for the various kinetic parameters are shown in Table C-8. These experimentally obtained parameters were used as initial estimates in the calibration of the combined MBR model.

Table C-8. *Temperature dependence of mass balance parameters, with T_{ref} = 40°C.*

	μ_m	K_S	Y	k_d
θ	1.07	1.01	0.981	1.07

pH model

In the physico-chemical modelling approach, the concentrations of ionic components are inputs to an ionic speciation subroutine at each interation step (Brouckaert et al., 2010). The variables of interest that the speciation routine calculates are the pH of the solution, the activity coefficients (γ), the concentrations of the species (c), and the dissolved CO_2 concentration. The driving force for CO_2 transfer depends on the dissolved CO_2 concentration and the partial pressure of CO_2 in air bubbles in contact with the liquid. The rate of CO_2 evolution to the bubbles controls the accumulation of dissolved CO_2, and therefore strongly influences the system pH.

The molar concentration of hydrogen ions entering the MBR was assumed to be the same as the molar concentration of acetic acid, as determined from the measured COD. Urea and phosphoric acid are dosed daily into the MBR to maintain a healthy microbial community. A nutrient dosing ratio of nitrogen and phosphorus was assumed from literature, as COD:N:P of 100:11:2 on a mass basis (1:0.25:0.021 on a molar basis) (Milenko and Vrtovsek, 2004). The pH of the feed stream was matched to plant data by adjusting the carbonate concentration.

The effect of the pH on the biomass activity in the Illovo MBR had been investigated by Kennedy and Young (2006). Their data were incorporated into the model to simulate the effect of lowered pH on the MBR microbial system. The biomass activities were normalised as percentages, and piecewise linear interpolation between the values was used, as shown in Figure C-3. The biomass activity factor was applied to the growth rate parameter μ_m.
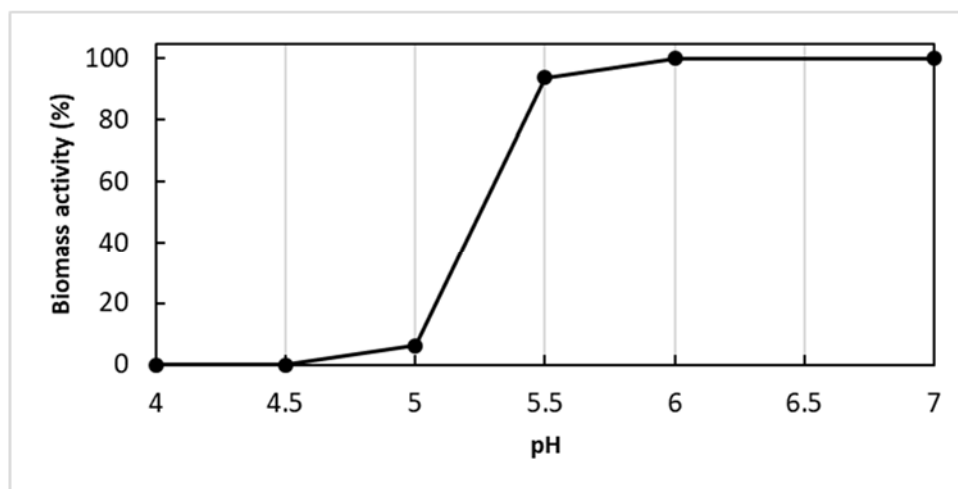

Figure C-3. *Biomass activity as a function of pH*

Model calibration

Calibration of the model against data from the full-scale plant was necessary in order to test the applicability of the kinetic parameters obtained from the laboratory tests, and to establish parameters related to the plant operation. Unfortunately, the reactor was not operating normally during the laboratory and modelling investigation. A fault in a distillation unit in the furfural process resulted in a reduced effluent supply, with the result that thermophilic operation was not achieved during that year (2013), and historical data from 2012 had to be used for the calibration. This had the disadvantages that

the biomass used in the laboratory tests might not have been fully representative of the biomass present at the previous time, and that it was not possible to check conditions that had not been recorded, such as wind speed or cloud cover. Furthermore, certain online measurements, notably the temperature of the feed to the reactor, had been overwritten, due to the limited storage capacity of the SCADA control system. In the calibration regression these unknown variables were treated as constant parameters, constrained to fall within their known ranges.

The calibration was carried out in several stages, using different selected sets of plant data from 2012 and 2013. Firstly, 5 periods of relatively steady operation, in which the feed rate, sludge wasting rate and operating temperature remained fairly constant, were selected for steady state calibrations at temperatures between 40°C and 50°C. Then a period was selected during which varying feed rates resulting in a fluctuating temperature for dynamic calibration.

Recorded furfural plant effluent feed rates (q_o), and sludge wasting rates (q_{sw}) were used as model inputs for the calibrations. All other input parameters were assumed constant (feed temperature, feed COD concentration, weather conditions, etc.; the final values for these parameters are listed in the Appendix). The regressed parameters were adjusted to fit the measured reactor temperature and sludge concentration, the effluent COD, and, in the final calibration stage, the reactor pH.

The calibration procedure was able to match the measured temperatures, sludge concentrations and effluent CODs satisfactorily, with parameter values that fell within their expected ranges. For example, the calibrated fit of the reactor temperature is shown in Figure C-4. The reasonable correspondence between simulation and measurements is an indication that the heat transfer terms that were represented by fixed parameter values, although these must have varied considerably over the time period, had relatively little influence on the energy balance.
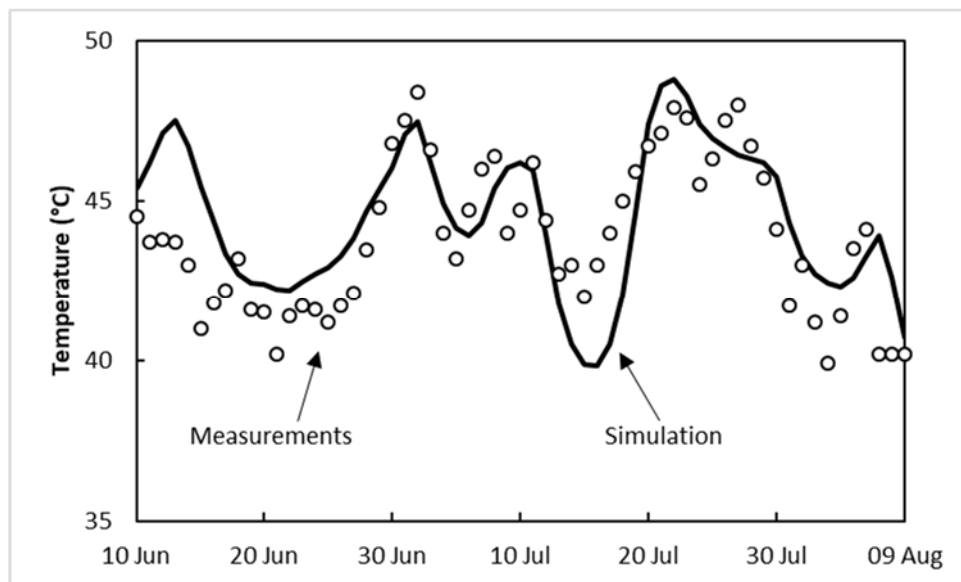

Figure C-4. *Comparison of measured and simulated temperatures after dynamic calibration*

However, the simulated pH was much less satisfactory, exhibiting much larger fluctuations than observed on the plant (Figure C-5, before re-calibration). The reason was found to be that the active biomass population in the model responded too slowly to changes in the loading rate of acetic acid, to which the reactor pH is very sensitive; i.e., the maximum growth rate μ_m had been set too low. This had been based on the laboratory data, together with an assumed X_H to MLVSS ratio of 0.35 (see Table C-7), which was clearly not appropriate for this particular system. It is a recurring problem of such biological reaction models that the growth rates are based on the concentration of live biomass: a modelling construct that is not directly measurable. When a reaction rate is represented as $\frac{\mu_m S_S X_H}{K_S + S_S}$, μ_m and X_H cannot both be inferred from just a measured reaction rate: all that can be inferred is the product (μ_m X_H).

The dynamic calibration was re-run, including μ_m as a regression parameter. The pH simulation in Figure C-5 shows the substantial improvement between the initial and final calibrations with the root mean squared difference (RMSD) decreasing from 1.14 to 0.47. The decreased fluctuations are a direct result of the increased μ_m value. This higher value of μ_m corresponds to lower, but more rapidly varying, concentrations of active biomass (on average 2.5 g/L compared to 3.7 g/L before recalibration). The re-calibration had only marginal effects on the other variables; for example, the RMSD for the temperature decreased very slightly from the 1.66°C of Figure C-4 to 1.61°C.

Even where it is not strictly correct for the biomass being tested, an assumed value for the active biomass concentration should usually be good enough for most purposes, and indeed proved to be good enough for the steady-state calibration of the model. It was even good enough for most aspects of the dynamic calibration; its limitation was only revealed by the poor prediction of the dynamic pH behaviour. So, the dynamic re-calibration raised μ_m to increase the responsiveness of the reaction rate, while reducing the average X_H to maintain the same average reaction rate.
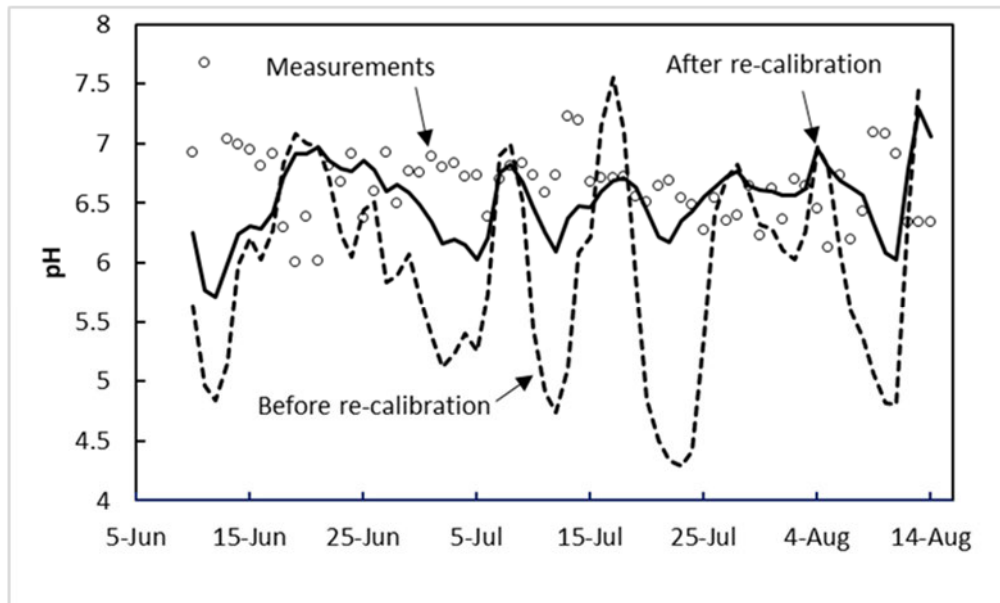

Figure C-5. *pH comparison for 2012 period before and after dynamic re-calibration*

Validation

The final validation of the model was carried out using plant data from 2010, a different period from that of the calibration data. Only q_o and q_{sw} were used as variable model inputs, all other parameters were considered to be constant, and fixed at the values determined by the calibration (see Appendix).

Mesophilic-thermophilic temperature transition

The overall objective of the model was the ability to simulate the transition from mesophilic to thermophilic temperature. To test this, a period of data was found from 2010 that showed a clear transition from under 40°C to above 50°C, with no process upsets and minimal external sludge dosing during the transition. Only q_o and q_{sw} obtained from the plant data were used as model input variables.
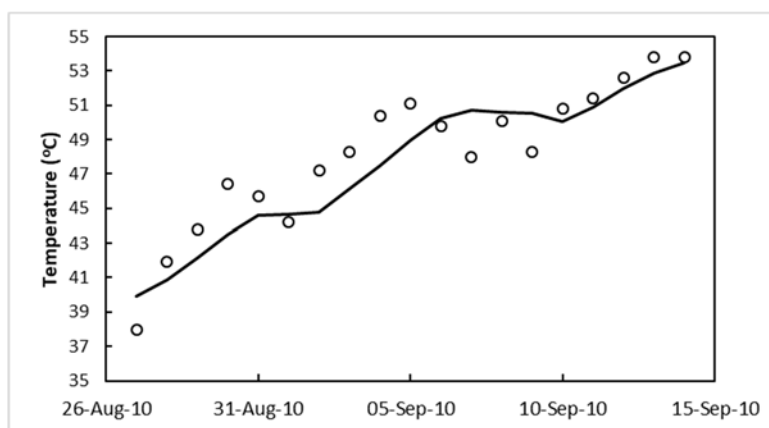

Figure C-6. *Mesophilic to thermophilic temperature transition during 2010*

The model was able to describe the temperature transition between mesophilic and thermophilic regimes as shown in Figure C-6, with RMSD of 1.7°C, following the trends of the data during the transition; thus meeting the primary objective of the model.

Sensitivity analysis

A sensitivity analysis was performed on the final calibrated model to determine the parameters that had the most significant effect on the MBR temperature.

There was a small effect on the MBR temperature for the observed feed temperature range of 36 to 40°C. The effect was more significant for thermophilic operation than for mesophilic, the lowest feed temperature bringing the MBR temperature down to 45°C. The operation of blowers did not have a significant effect on the MBR temperature, with temperature changes of no more than 1°C.

A wind speed of 2 m·s^{-1} increases the MBR temperature by around 5°C for mesophilic and thermophilic operation, while a wind speed of 8 m·s^{-1} reduces the temperature by around 4°C for both thermophilic and mesophilic operation. The MBR operating temperature is sensitive to changes in the ambient temperature, between 10 and 40°C. Mesophilic operation is more sensitive, with temperatures varying by ± 9°C while thermophilic temperatures vary by ± 6°C.

The assumption of an average wind speed and the ambient temperature throughout the energy balance calibration will therefore cause some error; these parameters vary considerably in reality. Rainfall by itself does not have a significant effect on the steady-state MBR temperature; however, it is the conditions that tend to come with rainfall, i.e., high wind speeds and low ambient temperatures, which affect the MBR temperature.

The aeration rate and the relative humidity have a significant effect on the evaporation rate from the MBR. As expected, the evaporation rate increases with an increase in aeration, and increases with a decrease in relative humidity. The evaporation rate is always greater at a higher temperature. However, a greater amount of water is evaporated per volume of feed for mesophilic temperatures, approximately double that for thermophilic operation. This is due to the longer hydraulic residence time (HRT) experienced for mesophilic operation.

DISCUSSION AND APPLICATION OF THE MODEL

The model has been shown to be capable of steady-state and dynamic prediction of temperature and pH within the required range for the design and operational model predictions.

The temperature can be accurately predicted to within 2°C during a dynamic simulation over an extended period of time (over 60 days), with only the feed rate (q_o) and the sludge wasting rate (q_{sw}) required as inputs. The model is also capable of pH predictions to within 0.5 pH units.

Both temperature regimes are adequately represented by a single biomass population with temperature-dependent kinetic parameters. This does not necessarily mean that microorganism population does not change, merely that it was not necessary for the model to represent a change to match the available experimental data.

The heat generated by reaction is the largest energy term for both modes of operation, constituting 25% and 36% for mesophilic and thermophilic regimes, respectively. There is a significant difference between the heats of reaction for the regimes, as at thermophilic operation higher microorganism death rates occur, leading to higher heat generation from the exothermic biomass decay.

After final calibration of the model the influent flow rate at mesophilic (40°C) and thermophilic (50°C) operation was determined to be 12.9 $m^3 \cdot h^{-1}$ and 29.3 $m^3 \cdot h^{-1}$ each, respectively. Thus, for the same furfural plant effluent feed rate to the MBR, mesophilic operation would require a reactor working volume that is 2.2 times larger than thermophilic operation.

Operational predictions

The model was used to simulate a number of process upset scenarios that the MBR would typically encounter during a season of operation.

Thermophilic-mesophilic/mesophilic-thermophilic process transitions

The feed rate to the MBR was altered following steady-state operation to cause the operating regime to shift from mesophilic to thermophilic, and from thermophilic to mesophilic.

The model was run for 100 simulated hours at the thermophilic flow rate of 29.3 m$^3 \cdot$h^{-1} to ensure steady conditions, then the feed rate was reduced to 12.9 m$^3 \cdot$h^{-1} or vice versa, corresponding to HRTs of 5.8 and 13.1 days, respectively. The sludge wasting flow rate was simultaneously switched between the corresponding values of 3.1 and 1.6 m$^3 \cdot$h^{-1}, with corresponding SRTs of 105.7 and 54.6 days, respectively.

Feed flow decrease

The temperature, pH and biomass responses caused by this transition are shown in Figures C-7 and C-8. As the feed rate is cut the pH of the MBR initially rises rapidly as a result of the rapid depletion of acetic acid at the lower feed rate. The lower S_S leads to lower X_H growth rates and to an initial decrease in X_H. However, as the temperature in the MBR decreases, the X_H death rate decreases, which leads to an increase in X_H above that observed for thermophilic operation.
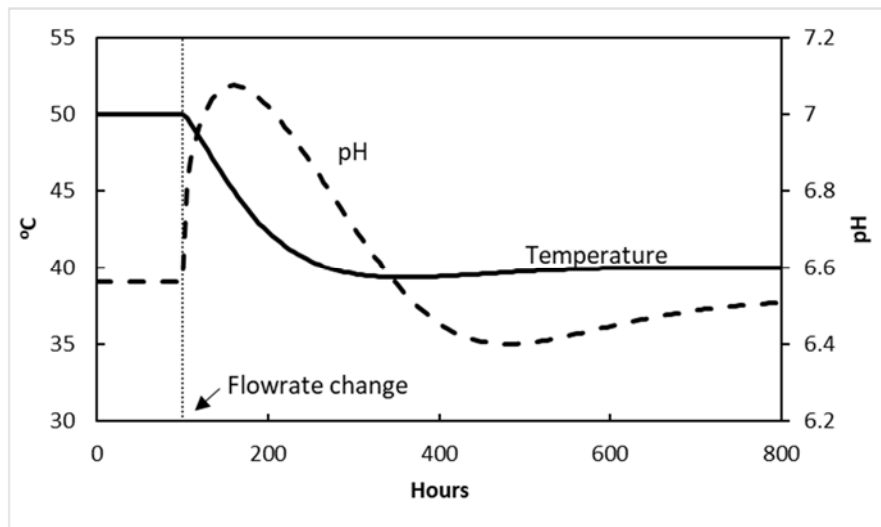

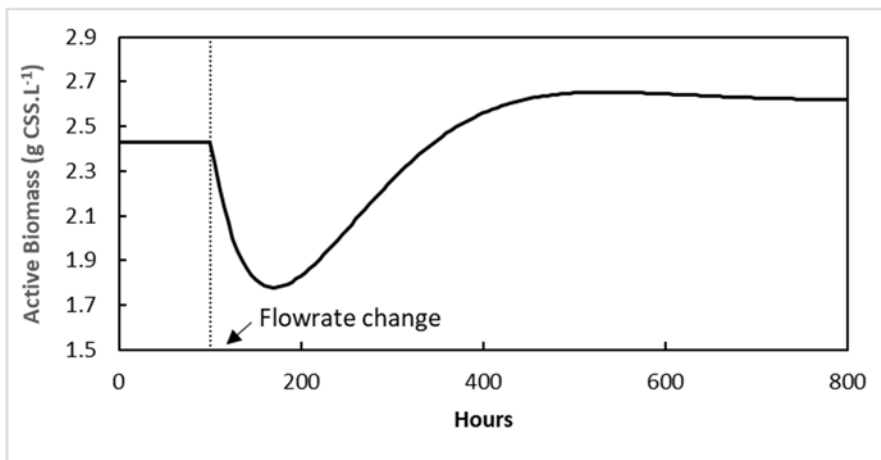**Figure C-7.** *Simulated temperature and pH responses to a decrease in feed flowrate*

Figure C-8. *Simulated active biomass response to a decrease in feed flowrate*

A trial-and-error search was performed on the model to determine the heating required to maintain the temperature at 50°C at the lower feed rate. The power required to maintain thermophilic operation for a mesophilic feed rate was found to be 790 kW.

Feed flow increase

The model predicts that an abrupt increase in feed rate has an adverse effect, as the pH rapidly drops below 5, inhibiting the biological reaction as shown in Figure C-3. Figure C-9 shows the modelled pH and temperature responses. The process is unable to recover from this condition without intervention.
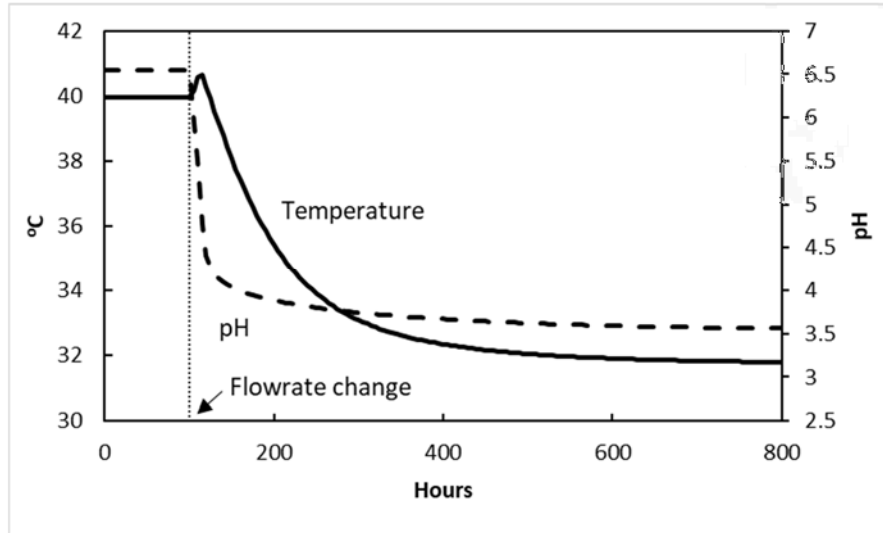

Figure C-9. *Simulated temperature and pH responses to an abrupt increase in feed flowrate*

To avoid the sharp pH drop, the abrupt increases in feed and sludge wasting rates were replaced by a gradual transition. The simulated transition from mesophilic to thermophilic operation in this way takes about 400 h (17 days) as seen in Figure C-10.

X_H initially increases due to an increased S_S concentration, leading to increased X_H growth rates. An increase in temperature leads to an increased death rate, which decreases X_H, as well as an increase in μ_m which brings SS back to a steady-state value.

To determine the amount of cooling required to maintain mesophilic operation for a thermophilic feed rate, cooling was applied. It was found by trial that 920 kW is required to maintain a mesophilic temperature for a thermophilic feed rate.

It is time consuming to increase the operating temperature by controlling the feed only, due to its low pH. Temperature drops can occur considerably faster, as there is no pH limitation. It is critical to keep the MBR pH above 6 to maintain biomass activity. For mesophilic operation the feed rate is tightly constrained; any sudden increase results in a detrimental drop in pH.
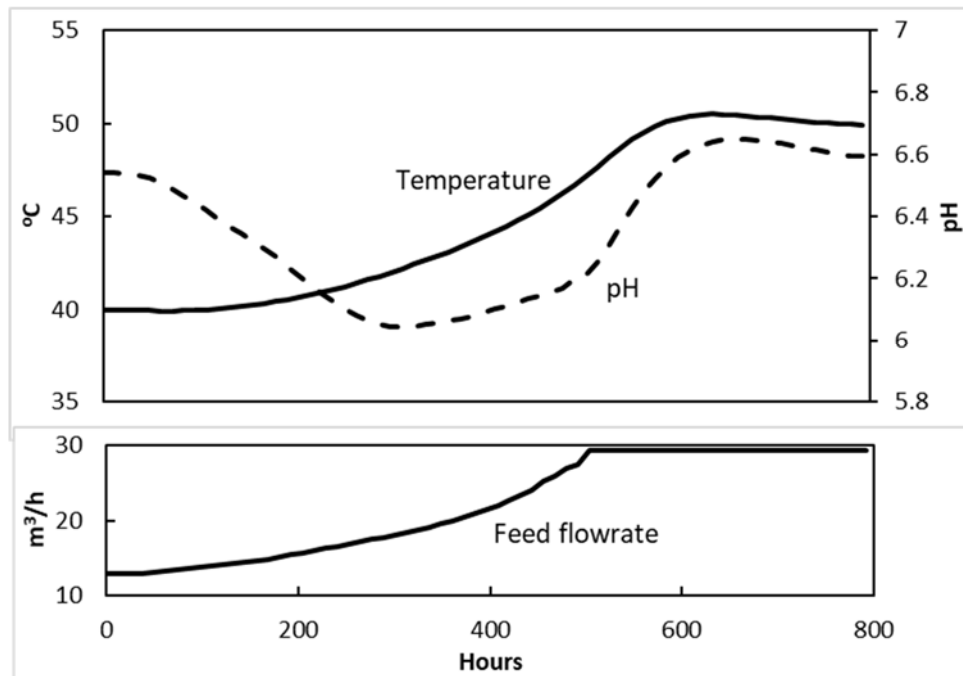
Figure C-10. *Simulated temperature and pH responses to a controlled increase in flowrate*

MBR instability (feed – no feed – feed)

The transitions described in the previous sections, and illustrated in Figures C-6 to C-9, provide a pattern for understanding various process disturbances. If feed to the MBR is cut for a significant amount of time, the lack of substrate leads to a depletion of biomass. When the feed is subsequently increased, there is insufficient biomass to assimilate the additional acetic acid load: the pH drops, inhibiting the biological reaction and causing failure of the process if there is no intervention.

When operating in the mesophilic regime (around 40°C) the maximum time for a feed interruption without causing instability was found by trial to be 98 h (4.1 days).

If, after such an incident, the feed flow is increased under pH control (as illustrated in Figure C-10), the temperature gradually climbs back to 40°C, taking over 300 h (12.5 days) to fully recover.

When operating in the thermophilic regime (around 50°C), the situation is similar, except that the maximum duration of a feed interruption is only 30 h before instability will ensue. During the recovery, the temperature drops to below 42°C in the first 44 h, then starts to increase again. The total recovery time back to a thermophilic temperature of 50°C is again approximately 300 h (12.5 days).

In order to obtain a clear answer as to which temperature regime to design for, a full technical and economic analysis in the context of the entire process design is required, which takes into account the nature and frequency of process upsets. Under steady operating conditions, thermophilic operation can handle more than double the effluent load for a given reactor size. If a method were found to reduce instability under thermophilic operation, this would be the preferred solution. The primary cause of the observed instability is frequent feed fluctuations, and the time taken to recover normal operation.

One of the possible solutions to reduce feed fluctuations to the MBR may be a buffer tank. This would increase the capital costs involved with thermophilic operation, but would likely be less than the capital costs involved with constructing the larger MBR required for mesophilic operation.

CONCLUSIONS

The dynamic mass and energy balance model is successful in predicting steady-state and unsteady-state operation of the MBR under both mesophilic and thermophilic conditions. The temperature can be predicted within 2°C, and the pH within 0.5 units over a period greater than 60 days, using only the daily furfural feeding and sludge wasting rates as model inputs. A single biomass population can be used to model the MBR by including temperature dependencies in the kinetic and stoichiometric parameters.

There are advantages and disadvantages associated with both mesophilic and thermophilic operation of the MBR. A detailed economic analysis would be required to determine which regime is optimal. Both the model simulations and plant data suggest that thermophilic operation could be advantageous, but it is less stable than mesophilic operation, and frequent feed disruptions will have serious adverse effects.

ACKNOWLEDGEMENTS

REFERENCES

ABEYNAYAKA A (2009) Thermophilic aerobic membrane bioreactor for industrial wastewater treatment. Master of Engineering, Asian Institute of Technology.

BATSTONE DJ, AMERLINCK Y, EKAMA GA, GOEL R, GRAU P, JOHNSON B, KAYA I, STEYER JP, TAIT S, TAKACS I, VANROLLEGHEM PA, BROUCKAERT CJ and VOLKE E (2012) Towards a generalized physicochemical framework. *Water Sci. Technol.* **66** (6) 1147–1161.

BRIDGEWATER L, RICE EW, BAIRD RB, EATON AD and CLESCERI LS (eds) (2012) *Standard Methods for the Examination of Water and Wastewater*. APHA-AWWA-WEF, Washington D.C.

BROUCKAERT CJ, IKUMI D and EKAMA GA (2010) Modelling of anaerobic digestion for incorporation into a plant-wide wastewater treatment model. *WISA Biennial Conference*, 18–22 April 2010, Durban, South Africa.

CASEY TJ (2006) *Unit Treatment Processes in Water and Wastewater Engineering.* Aquavarra Research Limited, Blackrock, Dublin.

TCHOBANAGLOUS G, BURTON FL and STENSEL HD (2003) *Wastewater Engineering: Treatment and Reuse*. McGraw Hill Education, New York.

GENT RD (2012) Experimental effluent treatment at Sezela. *Proceedings of the South African Sugar Technologists' Association* **85** 267–277.

GILLOT S and VANROLLEGHEM PA (2003) Equilibrium temperature in aerated basins—comparison of two prediction models. *Water Res.* **37** 3742–3748.

HENZE M, GRADY CPL (Jnr), GUJER W, MARAIS GVR and MATSUO T (1987) Activated sludge model No 1. *IWA Scientific and Technical Report No 1*. International Water Association, London. ISSN 1010-707X.

JUDD S (2001) *The MBR Book: Principles and Applications of Membrane Bioreactors for Water and Wastewater Treatment*. Elsevier Ltd, Oxford, UK.

KENNEDY S and YOUNG T (2006) *Membrane bioreactors for water re-use in Southern Africa*. URL: http://www.kubotafreeair.com/files/S_%20Kennedy%20&%20T_%20Young%20(2007) _%20Membrane%20Bioreactors%20for%20Water%20ReUse%20in%20Southern%20Africa.pdf (Accessed 22 March 2013).

LAPARA TM and ALLEMAN JE (1999) Thermophilic aerobic biological wastewater treatment. *Water Res.* **33** 895–908.

LIZARRALDE I, FERNANDEZ-AREVALO T, BROUCKAERT CJ, VANROLLEGHEM PA, IKUMI DS, EKAMA GA, AYESA E and GRAU P (2015) A new general methodology for incorporating physico-chemical transformations into multiphase wastewater treatment process models. *Water Res.* **74** 239–256.

MAKINIA J, WELLS SA and JIMA P (2005) Temperature modeling in activated sludge systems: A case study. *Water Environ. Res.* **77** 8.

MILENKO R and VRTOVSEK J (2004) The study of nutrient balance in sequencing batch reactor wastewater treatment. *Acta Chim. Slovenika* **51** 779–785.

NOVOTNY V and KRENKEL PA (1973) Simplified mathematical model of temperature changes in rivers. *Water Pollut. Control Fed.* **45** 240–248.

SEDORY PE and STENSTROM MK (1995) Dynamic prediction of wastewater aeration basin temperature. *J. Environ. Eng.* **121** 609–618.

SOLON K, FLORES-ALSINA X, KAZADI MBAMBA C, VOLKE EIP, TAIT S, BATSTONE DJ, GERNAEY KV and JEPPSSON U (2015) Effects of ionic strength and ion pairing on (plant-wide) modelling of anaerobic digestion. *Water Res.* **70** 235–245.

SURCIS SL (2019) Multifunctional respirometry systems.
URL: http://www.surcis.com/en/products_362 [Accessed 8 January 2019]

RAPHAEL JM (1962) Prediction of temperature in rivers and reservoirs. *J. Power Div.* **88** 157–188.

TALATI SN (1988) *Heat Loss in Aeration Tanks.* MSc Civil Engineering, University of California.

TALATI SN and STENSTROM MK (1990) Aeration-basin heat loss. *J. Environ. Eng.* **116** 70–86.

UBISI MF, JOOD TW, WENTZEL MC and EKAMA GA (1997) Activated sludge mixed liquor heterotrophic active biomass. *Water SA* **23** 239–248.

VOGELAAR JC, KLAPWIJK B, TEMINK H and VAN LIER JB (2003) Kinetic comparisons of mesophilic and thermophilic aerobic biomass. *J. Ind. Microbiol. Biotechnol.* **30** 81–88.

APPENDIX

Table C-A1. *Model parameters*

Symbol	Description	Value	Units
A_l	Area of the reactor that surrounds the liquid phase	624.6	m²
A_S	Surface area of the reactor contents in direct contact with the environment	575.9	m²
B	Power of the aerator/compressor	288.5	kW
C_C	Fractional cloud cover	0.45	-
f_P	Fraction of inert COD generated by cell lysis	0.15	kg·kg⁻¹
h_f	Exit air humidity factor	1	-
K_i	Surface conductance at the air-surface inside reactor	33.91	W·m⁻².K⁻¹
K_o	Surface conductance at the air-surface outside reactor	0.285	W·m⁻².K⁻¹
K_S	Half saturation constant	See Table C-4	kg·m⁻³
k_d	Specific death rate constant	See Table C-2	h⁻¹
l	Latitude of the reactor	30	°
P	Pressure	101 325	Pa
$S_{S,O}$	Soluble substrate (assumed acetic acid) in feed stream.	17 800	mgCOD·kg⁻¹
r_h	Relative humidity percentage	83	%
T_a	Ambient temperature	25	°C
T_e	Earth temperature	25	°C
V_r	Volume of the reactor	4 060	m³
WS	Wind velocity	5	m·s⁻¹
Y	Biological yield	See Table C-3	-
β	Atmospheric radiation factor	0.85	-
ϵ	Water-surface emissivity	0.97	-
η	Efficiency of the aerator/compressor	0.6	-
θ	Reaction rate temperature coefficient	See Table C-6	-
λ	Water-surface reflectivity	0.03	-
μ_m	Maximum specific growth rate	0.0763 at 40°C	h⁻¹